Building the Crust at the Mid-Atlantic Ridge

RRS Charles Darwin
Cruise 65 Report

February, 1992

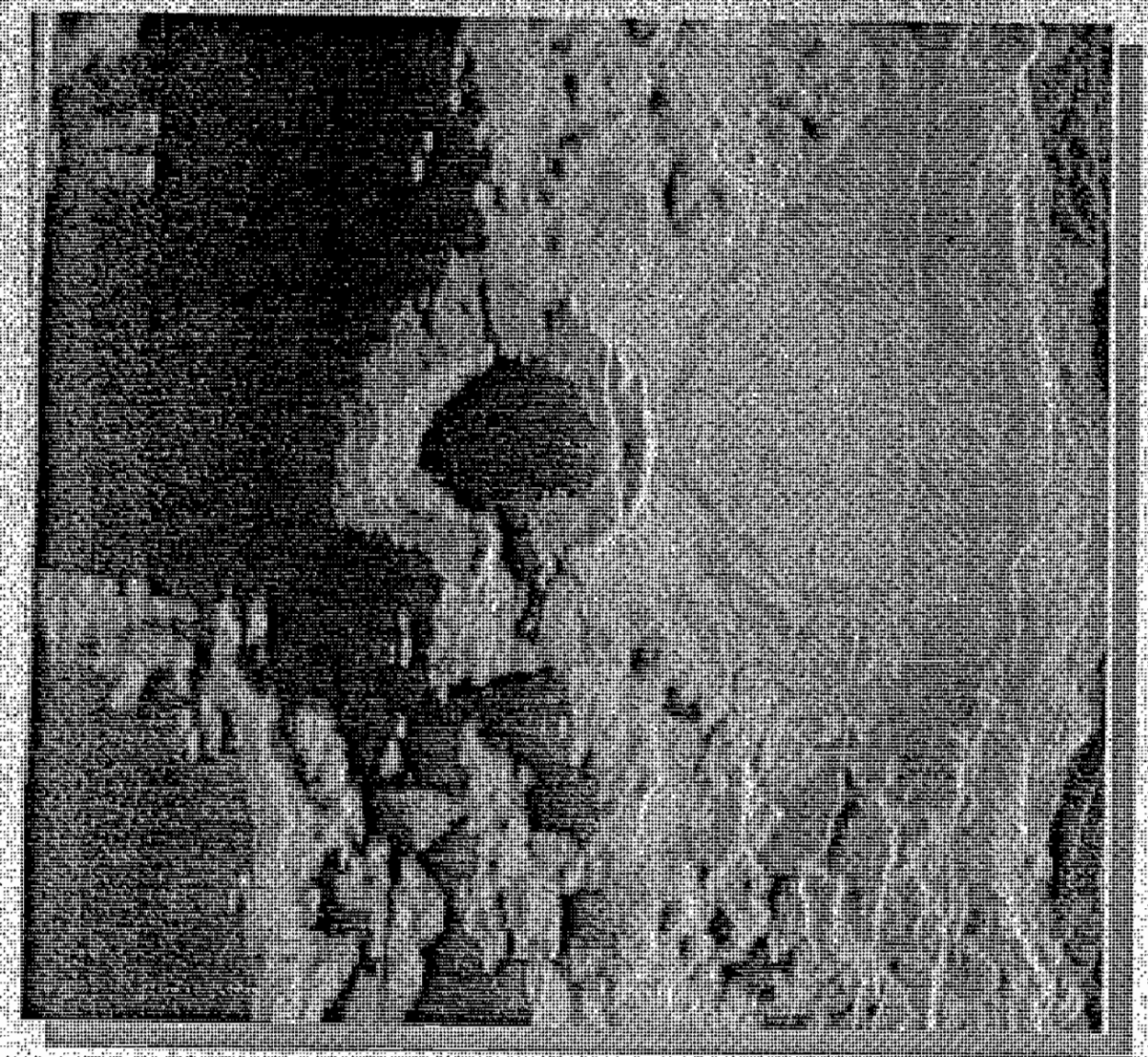

This document reports work conducted at sea during Cruise 65 of RRS Charles Darwin. It may not be used until 1 March, 1993 for scientific research, except with permission from J.R.Cann (Dept. of Earth Sciences, University of Leeds, UK) or D.K.Smith (Woods Hole Oceanographic Institution, USA).

The cruise was funded by the Natural Environment Research Council, with additional contributions from the Office of Naval Research (USA), the National Science Foundation (USA), the University of Leeds and the Royal Society. Cruise participants are happy to acknowledge their gratitude for this support.

Joe Cann, PI	University of Leeds
Deborah Smith, Co-PI	Woods Hole Oceanographic Institution
Martin Dougherty	Boise State University
Jian Lin	Woods Hole Oceanographic Institution
Sara Spencer	Geologisches Institute
Christopher MacLeod	Institute of Oceanographic Sciences
Eddie McAllister	University of Leeds
Jane Keeton	Science Laboratories
Scott Garland	Boise State University
Ben Brooks	University of California, Santa Cruz
Rachel Pascoe	University of Leeds
Nick Millard	Institute of Oceanographic Sciences
Chris Flewellen	Institute of Oceanographic Sciences
Robert Lloyd	Research Vessel Services
Mike Sampson	Research Vessel Services
Dave Booth	Research Vessel Services
John Wynar	Research Vessel Services
Andy Hill	Research Vessel Services

Cover illustration. TOBI image of W Seamount. This prosaically named edifice is a cratered, flat-topped seamount in Segment 17 on the Mid Atlantic Ridge. The crater is simple, and has a diameter more than half of that of the top of the seamount (diameter of the rim of the seamount is approximately 1200 meters, its height approximately 250 meters). The lip of the crater may have fed hummocky flows running south from the seamount. The smooth surfaces east and west of the seamount may be smooth lava flows or else talus slopes.

Table of Contents

List of Figures

I. Overview

1.1 Summary of Results

The main scientific objective of Cruise 65 of RRS Charles Darwin from 28 January to 1 March 1992 was to improve our understanding of the volcanic and tectonic processes that produce the distinctive topography of the Mid-Atlantic Ridge between 24 N and 30 N. The inner valley floor of the slow spreading (12-14 mm/yr) Mid-Atlantic Ridge (MAR) is covered with small volcanoes (50-650m in relief). Many of these volcanoes are associated with axial volcanic ridges, most of which are nearly centrally located on the valley floor. From Sea Beam swath bathymetry we inferred that the ridges are composed of piled up seamounts and hummocky flows, and we interpreted them to be the sites of crustal construction. This style of volcanism is dramatically different from that observed at the fast-spreading East Pacific Rise (EPR) where the rise crest is dominated by fissure-fed eruptions which may flow for tens of kilometers from the rise axis. We set out to use side scan sonar imagery, dredging and camera tows to test this model.

To accomplish our principal objective we chose four areas of interest along the ridge axis. In three of them we surveyed first with the IOSDL TOBI deep-towed side scan sonar vehicle and then conducted detailed dredging to obtain basalt samples to determine magmatic relationships. In the fourth area we had time only for a TOBI survey. One of the areas was the site of three successful runs of the Bathysnap camera system. Underway gravity and magnetics (the latter measured both at the surface and on TOBI) were collected for shipboard and shore-based analysis. TOBI runs occupied 14 of the 23 days of science time. During that time the vehicle experienced only two small faults.

Of the 18 spreading segments between the Kane and Atlantis Fracture zones, our four areas included substantial parts of eight, and we extended one TOBI track to cover a good part of a ninth. In the eight primary segments we insonified most of the median valley floor from two directions, and also covered parts of the bounding faults as well as the first fault block of the median valley wall on one or other side.

Area 1 covers the southern half of Segment 17, with its long narrow median valley containing a straight axial volcanic ridge decorated with excellent seamounts, and much of Segment 16, a broad short segment with a highly asymmetric axial volcanic ridge. The two segments are separated by a high, narrow oblique septum. The area runs from 28° 40' N, 43° 30' W to 29° 10' N, 43° 10' W. Within the area we undertook a four day TOBI survey, including three lines along the median valley and a double line into the crestal mountains and back, 15 dredge stations and three successful camera runs.

Area 2 consists of the southern half of Segment 11 and the northern half of segment 10, and runs from 26° 20'N, 44° 40'W to 27° 05'N, 44° 32'W. These two segments were chosen because they contain medium sized axial volcanic ridges and overlap in a simple relationship similar to that often seen on the East Pacific Rise. Most of the median valley of this area was covered by three TOBI tracks, and a line through the crestal mountains was also included. Nine dredge hauls were made here.

Area 3 contains the southern part of Segment 6, a large part of the major non-transform offset

that runs west from its southern end, and the northern part of Segment 5. It runs from 24° 50'N, 45° 50'W to 25° 15'N, 45° 25'W. Segment 6 was chosen for study because it is one of only two segments in the Kane-Atlantis area with no axial volcanic ridge. The non-transform offset is the largest in the region. Part of this area was covered with four TOBI swaths and part with two. Ten dredge stations were attempted here, though one failed to bring anything back and at another a dredge was lost.

Area 4 lies only a few miles north of Area 3. It includes all of Segment 7 and a large part of Segment 8, separated by a septum. Both segments have unusually large axial volcanic ridges, that of Segment 8 supporting especially large seamounts. The area runs from 25° 20'N 45° 25'W to 25° 50'N, 45° 05"W. Three long TOBI tracks were run in this area, one of which was extended to reach into Segment 9 far enough to image the TAG hydrothermal field. No dredges or camera stations were attempted here.

The cruise produced a wide range of scientific results. It was possible to distinguish six main types of volcanic building blocks from which the topography of the median valley and the axial volcanic ridges are built: (1) flat-topped seamounts (2) hat-shaped seamounts (3) hummocky seamounts (4) hummocky ridges (5) hummocky patches (6) sheet flows. Each segment has its own volcanic character, some having more seamounts or others more hummocky ridges, for example, but the basic components are the same.

In Segment 6 units of all kinds have been erupted on a basement of sheet flows, which makes it possible to calculate their individual volumes, and hence to estimate the size of the associated magma chambers.

Some of the seamounts are impressive features on their own, especially two tall flat-topped seamounts in Segment 17 of Area 1, Sumpter and W, and Possum Peak in the major offset south of Segment 6. The hat shaped seamounts have a wide brim of flows around the seamount crown. Some of the larger hummocky seamounts form major topographic units on top of large axial volcanic ridges.

Fault patterns within the median valley are complex, but most faults are axis parallel. Even in offset zones and on septa there are few oblique faults. Most offset occurs through fault blocks plunging while faults die out. The simple overlap offset of Area 2 is not marked by faulting or fracturing, and is hard to see on TOBI images.

In nine different places we imaged major landslides on the walls of the walls of the median valley. Landslide deposits must make a substantial contribution to the MAR crust. These landslides show complex and varied landforms. From one we dredged serpentinite, basalt and blue-grey muddy breccia.

Gravity lines along the ridge axis were reduced on board ship, and show that each segment has an associated mantle Bouguer gravity low, though these vary greatly in magnitude. Those of Segment 17 in Area 1 and Segment 6 in Area 3 are particularly large, while those of Segment 7, 8 and 9 in Area 4 are much smaller.

Images of the first fault block above the median valley floor show excellent preservation of median valley volcanic features, including hummocky ridges and flat-topped seamounts. On some

blocks an entire axial volcanic ridge has been split off and uplifted from the median valley floor.

Further out in the crestal mountains a very regular pattern is seen, with a succession of large faults throwing down towards the spreading axis, and back-tilted volcanic surfaces progressively more covered in sediment with distance from the axis.

On the technical side, a considerable achievement was the development of software that enables the shipboard processing of TOBI images, allowing selection of segments of images (such as are displayed in many places in this report) and also application of standard methods of image analysis. The means for doing this will be made freely available to future users.

Finally we completed the manuscript of a paper to be submitted to Nature on the volcanology of the median valley floor in this region.

This is only a brief summary of the results of what was an exceptionally successful cruise, both in terms of the work achieved and also the nature of the insights gained into ridge crest processes. We have assembled this unusually complete cruise report both for our own use and for the information of others. It contains, after an introduction, an account of each area in detail, together with chapters on transit work, gravity and magnetics and on TOBI data processing.

1.2 Personnel

The personnel listed below formed the scientific party on Leg 65 in the North Atlantic.

1.2.1 Scientific personnel

Johnson R. Cann
Dept. of Earth Sciences
University of Leeds
Leeds LS2 9JT
0532-335200 (w)
0532-786771 (h)
0670-512789 (h)
0532-335259 (fax)
cannj@earth.leeds.ac.uk

Deborah K. Smith
Dept. of Geology and Geophysics
Woods Hole Oceanographic Institution
Woods Hole, MA 02543
(508)-548-1400 x2472
(508)-457-2187 (fax)
dsmith@aqua.whoi.edu

Jian Lin
Dept. of Geology and Geophysics
Woods Hole Oceanographic Institution
Woods Hole, MA 02543

(508)-548-1400
(508)-457-2187 (fax)
jlin@aqua.whoi.edu

Martin E. Dougherty
Dept. of Geosciences
Boise State University
Boise, Idaho 83725
(208)-385-4003
(208)-385-4061 (fax)
md@kanaha.idbsu.edu

Sara Spencer
Geologisches Institute
ETH Zentrum
CH 8092 Zurich, Switzerland
010-411-256-3690
010-411-252-20819 (fax)
sara@erdw.ethz.ch

Scott Garland
Dept. of Geosciences
Boise State University
Boise, Idaho 83725
(208)-385-1166
(208)-385-4061 (fax)
scg@kanaha.idbsu.edu

Eddie McAllister
Dept. of Earth Sciences
University of Leeds
Leeds LS2 9JT
0532-335241
0532-335259 (fax)
eddie@earth.leeds.ac.uk

Rachel Pascoe
Dept. of Earth Sciences
University of Leeds
Leeds LS2 9JT
0532-335241
0532-335259 (fax)

Chris MacLeod
Institute of Oceanographic Sciences, Deacon Laboratory
Brook Road
Wormley, Godalming
Surrey GU8 5UB

0428-684141
0428-683066 (fax)

Ben Brooks
University of California Santa Cruz
Santa Cruz, CA 95064

Jane Keeton
Dept. of Geological Sciences
Science Laboratories
South Road
Durham City DH1 3LE
091-374-2532
j.a.keeton@durham.ac.uk

1.2.2 Support personnel

Nick Millard
Chris Flewellen
Institute of Oceanographic Sciences
Deacon Laboratory
Brook Road
Wormley, Godalming
Surrey GU8 5UB
0428-684141
0428-683066 (fax)

Dave Booth
Andy Hill
John Wynar
Mike Sampson
Robert Lloyd
NERC Scientific Services
Research Vessel Services
No. 1 Dock
Barry
South Glamorgan CG6 6UZ
0446-737451
0446-720562 (fax)

1.3 Scientific Objectives

The primary scientific objectives of Leg 65 were:

1) Test the morphological inferences made from previously collected Sea Beam swath bathymetry of the median valley. For example, are seamounts identified on the Sea Beam maps identifiable as individual volcanoes on the TOBI images?

2) Define the different morphological styles of volcanism on the TOBI scale. Can the different styles and their associated textures be related to features observed at larger scales on Sea Beam maps and smaller scales on camera images?

3) Distinguish the differences between edifices generated by eruptions through pipes, and those generated by sustained fissure eruptions.

4) Infer the volcanic history of the inner valley floor from the stratigraphic relationships. For example, assess the degree of fracturing in neighboring structures.

5) Determine how axial volcanic ridges are constructed. For example, are they composed of piled up seamounts and fissure-fed flows?

6) Obtain rock samples from neighboring seamounts for geochemical analyses. Determine if they are derived from the same crustal magma body, and infer the magmatic plumbing system below the ridge.

7) Determine the relationship between volcanism and faulting. Do volcanism and faulting occur simultaneously?

8) Investigate the location and generation of new median valley fault scarps on the inner valley floor. Are axial volcanic ridges cut by median valley faults?

9) Survey an axial volcanic ridge that has been carried into the crestal mountains. Does the fossil axial volcanic ridge have the same morphology typical of a ridge currently observed on the inner valley floor?

10) Determine the nature of the septa that divide separate magmatic segments.

11) Determine the extent and nature of small-scale magmatic segmentation.

1.4 Instrumentation

1.4.1 TOBI

TOBI (Towed Ocean Bottom Instrument).

TOBI is a deep-tow stable platform designed primarily to carry high resolution sidescan, a sub-bottom profiler and a triaxial magnetometer. An additional 100Kg. of buoyancy allows a variety of extra instruments to be installed and included in the data stream sent up the armored conducting tow cable. The vehicle has an open aluminium frame under syntactic foam buoyancy blocks. It is a little over 4 meters long and weighs 2 tonnes in air, although when correctly ballasted it is slightly positively buoyant in water. Stability is improved by tethering it to a depressor weight on the end of the towing cable by a 200 mere neutrally buoyant umbilical. Maximum operating depth is 6000 meters and it requires a towing cable length of about 1.5 times the water depth to achieve a survey speed of 1.5 - 2 knts. The sidescan has a total swath width of 6000 meters. Resolution is dependent on range; close in to the ship track the insonified footprint has an along track dimension of 2 m. with an across track dimension of 7m. At far range these dimensions change to 20m. x 2m. Data logging and on-line displays are controlled by two PS/2s and data is stored on 600

M byte magneto optical cartridges, each containing about 24 hours of data.

Vehicle construction.

Main frame.	Welded aluminium open frame. 4.2 x 1.1 x 1.1 m., c. 200Kg.
Buoyancy.	Syntactic foam. Density 0.66. 1.8 cubic meters (600Kg. buoyancy).
Payload	400Kg.

Instrument package. (Darwin 65).

Sidescan	Frequency. 30Khz. Pulse length. 2.8ms. (2m. res. far range) Beam angle. 0.8 X 45 degrees. Pulse rep. 4 sec. Swath width. 6000 meters. Power. 500 watts/side.
Profiler.	Frequency. 7.5Khz. Pulse length. 0.28ms. (0.2 m. res.) Beam angle. 25 degrees. Power. 600 watts.
Magnetometer.	Type Tri-axial fluxgate. Resolution. 10nT.
Vehicle monitoring	Pressure 0.1% water depth. pitch/roll 0.13 degree. compass 0.3 degrees.
Emergency location beacon	Frequency 10 Khz. Range 6 miles Duration 3 months (acoustically switchable)

Depressor. 600Kg. cast steel. 300mm.dia. x 1.4m.

1.4.2 Camera

Bathysnap

1.4.3 Dredging

Dredging was conducted with a standard RVS dredge with a wire mesh or chain dredge bag an inner polypropylene net bag. A pipe dredge was towed behind the dredge net, and a 10 m length of chain was towed in front to help keep the dredge on the bottom. A series of weak links allowed the dredge first to pivot on its arms, and then to come free, throttled by a wire strap, before the whole dredge assembly was lost if the final 5 ton weak link failed. The dredge was run with a pinger 100 m above the dredge, and was lowered until the pinger came to 50 m above the bottom.

Dredge sites were selected from Sea Beam maps of the area, using information from TOBI images in addition. The ship was held stationary at the chosen start point until the dredge had reached the bottom. The ship was then moved at 0.5 kt about 1-1.5 km away from the start point, paying out wire as the ship moved to keep the pinger about 50 m above the bottom. After about 45 minutes on the bottom, when the ship had moved 1-1.5 km, the dredge was hauled in. It was at this stage that most bites occurred. Simulation with graph paper suggested that the dredge did not move more than 300 m on the bottom, so that the position of dredged samples are well located. Use of this technique, coupled with correlation of TOBI and Sea Beam maps, gave us confidence that specific features were in fact being dredged. Most of our targets were greater than 300 m in diameter, and we consider errors in positioning to be less than that.

Of the 35 dredge stations, 32 recovered useful amounts of rock, one a few glass fragments, one came up empty, and another dredge was lost (on Possum Peak).

1.4.4 Computing/processing network

See Chapter 8 for summary of scientific computer systems and TOBI data analysis.

1.4.5 Underway geophysical equipment

Instruments logged by shipboard ABC computer system

1. Navigation

a. GPS: Trimble 40000SX, including a Rb clock to allow fixes from two satellites. The system for data logging and display was most efficient in providing exercise for the scientists when the communications link crapped out (very frequent).

b. Transit: Magnavox MX 1107RS using Arma Brown MK10 gyros and CID EM log for dead reckoning between fixes. (the output from gyros and EM log were also recorded)

2. Echosounder

Simrad EA5000 with V3 software, operating in a continuous single ping/await return pulse mode. Bottom detected automatically and logged every ping.

3. Magnetometer

Varian proton magnetometer V75 towed 150 m behind ship, sampled every 6 seconds. During TOBI runs at low speed we towed the same instrument with its cable made buoyant by plastic foam pipe logging.

4. Gravimeters

a. LaCoste and Romberg analogue S40 averaged over 6 minutes.

b. LaCoste and Romberg digital S84 with a 4 minute damping applied.

These were tied into the gravity base station at Ponta Delgada with a Texas Instruments Worden portable land gravimeter.

5. Time reference

DMW IRIG B clock system.

Instruments not logged by ABC computer system

1. 3.5 kHz echosounder

IOSDL design with 3-4 kHz chirped signal

All equipment was supplied, maintained, and operated by NERC RVS.

1.5 Scientific Responsibilities

1.5.1 Underway Science

Supervision of underway data collection and logging: Dave Booth and John Wynar

Collection and interpretation of magnetics and gravity data: Jian Lin

1.5.2 Towed Ocean Bottom Instrument (TOBI)

Care and maintenance of the TOBI instrument package: Nick Millard and Chris Fluellin

Logging of TOBI surveys: Eddie McAllister

Curation of TOBI data: Jane Keeton

Post-processing of and development of analysis techniques for application to TOBI data: Marty Dougherty and Scott Garland

1.5.3 Dredging

Logging of dredge stations: Sara Spencer

Curation of dredged rocks: Ben Brooks

Curation of dredged animals: Rachel Pascoe

Slabbing and thin sections: Eddie McAllister

1.5.4 Photography

Setting up camera system: Chris MacLeod

Logging camera runs: Chris MacLeod

Developing photographs: Chris MacLeod and Sara Spencer

1.5.5 Computer Systems

Shipboard computers: Rob Lloyd

Scientific computing system: Scott Garland

1.5.6 Scientific Interactions

Seminars and meeting organization: Jian Lin

1.5.7 Mechanical Maintenance of Instruments

RVS mechanical technicians: Mike Sampson and Andy HIll

1.6 Seminar summaries

1.6.1 Chris MacLeod

Study of oceanic spreading axis segmentation in the Troodos and Oman ophiolites.

Recent marine studies of marginal basins have revealed well-organized spreading centres that are segmented by transform faults, overlapping spreading centres, propagating rifts, etc. This strongly suggests that, whatever their geochemical differences, the physical processes of seafloor spreading and spreading axis segmentation in marginal basins are comparable to those at open ocean mid-ocean ridges. Although ophiolites are widely regarded as analogues of marginal basin oceanic lithosphere, identification and detailed field investigation of ridge axial discontinuities fossilized within them can nevertheless reveal much about the mechanisms, and ultimately the causes, of segmentation at mid-ocean ridges in general. I have been engaged in such study in Cyprus and in Oman, where the two most well-preserved ophiolites in the world are to be found. In the Troodos ophiolite I have studied transform fault processes and the relationship between tectonism and magnetism at ridge-transform intersections. In Oman I have looked at spatial variations of the sheeted dike-gabbro transition (seismic layer 2-3 boundary) in order to identify along-strike terminations of axial magma chambers. I am attempting to characterize the axial discontinuities thus identified and relate them to spatial variations in the lower crust and upper mantle, in order to build up a three-dimensional picture of the way spreading cells function and inter-relate.

1.6.2 Sara Spencer and Eddie McAllister

Spatial And Temporal Distribution Of Faults Within The Axial Valley Of The Reykjanes Ridge: An Interpretation Of TOBI Images.

Three faulting styles have been recognized within the axial zone of the obliquely spreading Reykjanes Ridge. These are 1: Faults and fractures that act as conduits and feeders for volcanic edifices (oriented 015, subparallel to the spreading normal direction); 2: Thermal and gravity collapse faults found in association with the axial volcanic ridges (of varied orientation); and 3: Median valley (or "escalator") faults (oriented 036 parallel to the main ridge trend). The Reykjanes is unique in that its obliquity allows these different fault categories to be analyzed separately, something that is impossible on the more common orthogonal spreading ridges. Furthermore the rift to non-rift transition (at 60 N) gives new insight into the generation of median valleys which cannot purely be spreading rate dependant.

1.6.3 Marty Dougherty

Seismo/Acoustic Wave Propagation

Seismic methods have often been employed by marine geologists and geophysicists to investigate the structure of the oceanic crust. Inherent in much of this work has been the assumption that

the seismic velocity structure of the crust is simple and laterally homogeneous. Seismo/acoustic wave propagation through this type of crustal model is simple and predictable. However, more recent higher resolution geological and geophysical surveys have demonstrated that on a finer scale, the oceanic crust is anything but laterally homogeneous. Seismic methods are still very useful in these types of media but we must first understand the physics of wave propagation through complex, three-dimensional media. Knowledge of the effect of laterally heterogeneous structure on seismo/acoustic wave propagation has been applied to some widely different marine problems. Examples of these include the anisotropy in oceanic crust, the generation and propagation of low-frequency seafloor noise, crustal evolution, low-angle acoustic backscatter from the seafloor, and the detection and delineation of axial magma chambers beneath mid-ocean ridges.

1.6.4 Jian Lin

The Control of Segmentation on Three-dimensional Mid-Atlantic Ridge Rifting

Increasing evidence in the last decade has indicated that the rifting process of slow-spreading ridges, such as the Mid-Atlantic Ridge, varies dramatically along-axis. Recently my colleagues and I have studied in detail the segmentation processes of the Mid-Atlantic Ridge between the Kane and Atlantis transforms (24-31N). From analysis of gravity, seismicity, fine-scale Sea Beam bathymetry, and numerical modeling, we found that: (1) The MAR axis is broken into a series of spreading segments by either transform or non-transform offsets. At non-transform offsets, the rift valleys overlap by a substantial distance. (2) The crustal thickness is considerably greater at segment mid-points than at the distal ends. This might reflect focusing of magma supply at segment mid-points. (3) The style of rifting varies systematically along a spreading segment. For example, rift topography is more symmetric and tectonic faults have smaller displacements at segment mid-points than at the distal ends. These observations, as well as additional evidence from teleseismic activity, suggest that the brittle lithosphere (thermal boundary layer) might be thinnest at the segment mid-point and increase consistently towards the segment boundaries. This expedition is a continuation of our effort in understanding the segmentation and rifting processes of the MAR. By participating in the cruise and working with the PIs and other scientists, I would like to achieve two primary objectives: (1) To understand how MAR volcanic structures are rifted and rafted away from the inner rift valley. This objective will be achieved by identifying tectonic and volcanic features on the TOBI images and by comparing the TOBI results with our previously collected Sea Beam data. (2) To determine the geophysical characteristics of fine-scale ridge-axis tectonic and volcanic features identifiable on the TOBI data. We will first collect and analyze shipboard gravity and magnetic data, as well as the deep-towed TOBI magnetic data. The results will then be carefully compared with TOBI side-scan features.

1.6.5 Rachel Pascoe

Three-Dimensional Euler Interpretation of Gravity and Magnetics

The 3-D Euler method gives a semi-automatic interpretation of gravity and magnetics data. It uses damped least squares linear inverse theory to solve for the source position and depth using Euler's equation of homogeneity. An important part of the 3-D Euler method is the interpretation of maps of solutions generated using different structural indices. The structural index can be inter-

preted as the rate of fall off of the potential field away from the source and hence an indication of the nature of the source. For example, a steeply dipping fault would have a structural index of 1. This method was used to interpret gravity and magnetics data from the Luangwa Valley in north-eastern Zambia. This northeast-southwest striking rift is composed of three half-grabens connected by accommodation zones. The major border fault complex of the two southern sub-basins is to the west and is marked by the Muchinga Escarpment which rises over 300 m above the valley floor. The data used only covers this southern-most area. The results from the 3-D Euler interpretation were compared with the seismic interpretation and geological map. The major border fault complex was clearly picked out in both the gravity and magnetics data, and some of the smaller faults were also delineated.

1.6.6 Ben Brooks

We have analyzed the shape and distribution characteristics of 175 small seamounts from nearly complete Sea Beam bathymetry over >2500 sq. km. near the Galapagos 95*W propagator system on the Cocos-Nazca spreading axis. In conjunction with data from seamount studies at the Mid-Atlantic Ridge and East Pacific Rise our data suggest that there are certain fundamental controls on the nature of seamount volcanism. Seamounts' heights at the Galapagos propagator are exponentially distributed according to Jordan and Smith's (1988) model, the average height/basal radius ratio of 0.16+/-0.05 is very near the well-correlated average of 0.21, We do not find any significant difference in number of seamounts between different crustal age bins and thus conclude that on-axis formation of seamounts is most likely.while flatness (the ratio of a seamount's top to basal diameter) range from 0-0.6 and average slope angle of 13+/-4 deg. also agree very well with previous studies.

Seamount occurrence at the Galapagos propagator can vary with magmato-tectonic region. There are roughly two times as many seamounts on "normal" crust created at the doomed axis as on crust in the zone of material transferred from the Cocos to the Nazca plates reflecting the destructive nature of lithospheric transferral in this zone. The number of seamounts on propagator-created crust is also significantly lower than for any other region suggesting that, although the propagator is believed to be well-supplied with magma, not as much of its magma goes into seamount production as in other regions. We do not find any significant difference in number of seamounts between different crustal age bins and thus conclude that on-axis formation of seamounts is most likely.

1.6.7 Jane Keeton

The detection of circular features using the Hough transform

The Hough transform remaps edge points from (x,y) space into parameter space. In the case of a circle, the Cartesian equation is $r^2=(x-a)^2+(y-b)^2$, where r is the radius of the circle and (a,b) is the centre of the circle. The transform therefore projects edge points into 3 dimensional parameter space (r,a,b). An edge point transforms to produce a circular locus for each possible radius; these loci represent circles of which the edge points may be part.

A typical Hough transform procedure, written by A.M. Cross, utilizes a Sobel derived edge strength image and edge orientation image. The parameter space is quantized into discrete bins; called the 'accumulator array', and an edge point 'votes' for all those circles of which it may be

part. In order to reduce the memory required by the accumulator array, the circle radii are limited to a number of discrete values, producing a 2-dimensional array (a,b), where the maximum counts from all the radii are stored in each cell. A threshold value is set for the edge strength image and the transform is applied. The edge orientation information can be employed if a specific contrast is only required, e.g. 'dark pixels on light'. At this stage, an arc length can be applied and adjusted according to the quality of the data. A threshold or a second pass of the Hough transform is then used to identify the highest cell counts in the accumulator array. The application of the Hough transform procedure subsequently outputs circle centre locations (a,b), together with the radii responsible for the maximum counts in the accumulator array.

The viability of the technique for the detection of circular seamounts from TOBI high resolution sidescan sonar data shall be investigated.

II. Area 1, Segment 16/17

2.1 Area 1: Segment 17/16

Area 1 includes the southern half of the long narrow Segment 17 and a large part of the short broad Segment 16. These segments lie towards the northern end of the Kane - Atlantis Sea Beam survey area, separated by a gap of four segments from the almost complete coverage of the ridge axis in Areas 2, 3 and 4.

Segment 17 was chosen for study because it has many characteristics of a classic segment. It has a long, narrow median valley with a straight, continuous, moderate sized axial volcanic ridge in it. The longitudinal profile of the segment is gently and continuously arched from one end to the other, and the associated mantle Bouguer gravity anomaly is the largest of any between the Kane and Atlantis fracture zones. It contains some very well defined seamounts, including the second highest in the whole Kane - Atlantis area, which are found both on and off the axial volcanic ridge.

Segment 16 is very different. The median valley in 16 is short and very broad. It contains three separate ridges, of which it is impossible to say on bathymetric grounds which might be the currently active site of volcanism. The mantle Bouguer anomaly is small. The two segments are separated by a narrow, high septum.

In Area 1 we undertook a major TOBI survey, with three long lines covering the entire median valley floor and the first fault block of the median valley to the east. We continued the TOBI survey with a line from the centre of Segment 17 diagonally out through the crestal mountains and back, thus giving a view of the off axis development of volcanic morphology, faulting and sedimentation. In addition we made 15 dredge stations and 4 camera stations.

The axial volcanic ridge in Segment 17 is constructed unconformably on previously fractured volcanic terrain. It is narrow, and composed of hummocky patches and caterpillar ridges, with a variety of seamounts, including large, flat-topped edifices, hummocky heaps and small, smooth seamounts. There is only one possible hat seamount, and that is partly buried under other flows.

Two major seamounts are especially conspicuous, W Seamount and Sumpter Seamount, both of similar shape. Both have flat summit regions and steeply sloping sides, and both are squarely centered on the axial volcanic ridge. Sumpter has a number of shallow craters intersecting on its summit, while W has one major crater that occupies more than half of the summit diameter. In both cases flows appear to originate at the summit and run along the axial volcanic ridge as hummocky ridges, though it is possible that the hummocky ridges are later than the seamounts. Dredges of basalts from both tops and flanks of both seamounts will help resolve this question.

Our TOBI lines across Segment 16 showed that the most recent volcanism is on the westernmost of the three topographic ridges in the broad median valley, as suggested by the location of the crustal magnetization high in the segment. This was confirmed by the dredging of very fresh basalt from two seamounts on that ridge. The axial volcanic ridge is thus very asymmetrically placed in the segment, and may have jumped there recently.

We made eleven dredge hauls on the axial volcanic ridge of Segment 17, designed to test whether there are volcanic connections along the segment, whether seamounts and fissure erup-

tions have different origins, whether the off-ridge seamounts are related to neighboring on-axis seamounts and whether the flows surrounding large seamounts have been fed from those edifices or from separate fissure eruptions. The answers to those questions must await shore based geochemical analysis.

As with the other septa that we imaged with TOBI, the one between Segments 16 and 17 does not show evidence of special tectonic features associated with it. There is a steep scarp towards Segment 16 which may have a particular association with the septum, but other structures crossing the septum seem to have an origin as normal ridge-parallel faults. A dredge on the septum brought back somewhat weathered lavas.

On the western side of the axial valley of Segment 17, at its southern end, is a major landslide. It appears to have originated at a large fault scarp, and has give rise to a range of slide and flow morphologies. At one point there is a dome in the middle of the slide area, and other parts have a TOBI texture like crumpled paper. A flow from the landslide has spread across the median valley floor to the edge of the axial volcanic ridge.

We made a dredge station on the upper surface of the landslide, which contained angular clasts of serpentinite, pillow lava, metabasalts and gabbro, set in a matrix of blue-grey mud made up of crushed material of the same lithologies. We interpret this as the product of serpentinite diapirism associated with the major fault along which the collapse has occurred. The landslide may have been triggered by that diapirism.

The TOBI lines into the crestal mountains showed a very orderly array of faults, downthrowing towards the median valley, with backtilted surfaces of volcanic terrain partly covered with sediment. Where the volcanic terrain can be seen through the sediment, it is made up of the same components as the that of the present median valley, including flat-topped seamounts, hummocky piles and hummocky ridges.

2.2 Waypoints

Waypoints and actual ship track for the TOBI survey in Area 1 are presented in Figure 2.1. Also in the figure are seamounts which have been previously identified from Sea Beam bathymetry (Smith and Cann, 1990, 1991), axial valley highs, and historical earthquakes in the region (relocated by Lin and Bergman, 1990).

The following way points define the TOBI survey of Segment 17/16:

A0) 28°40.7'N, 43°29.3'W - launch TOBI

A1) 28°42.0'N 43°27.7'W

A2) 28°55.3'N 43°11.1'W

A3) 29°10.0'N 43°07.8'W

A4) 29°10.0'N 43°09.5'W

A5) 28°56.1'N 43°12.7'W

A6) 28°43.0'N 43°29.0'W

A7) 28°44.1'N 43°30.3'W

A8) 28°56.9'N 43°14.3'W

A9) 29°10.0'N 43°11.3'W

In addition to the waypoints above a transect of the crestal mountains was added to the end of the survey of Area 1. The following way points define this transect:

S1) 29°13.5'N, 43°10.4'W

S2) 29°9.7'N, 43°30.0'W

S3) 29°6.5'N, 43°30.0'W

S4) 29°10.0'N, 43°12.0'W

S5) 29°11.73'N, 43°2.42'N

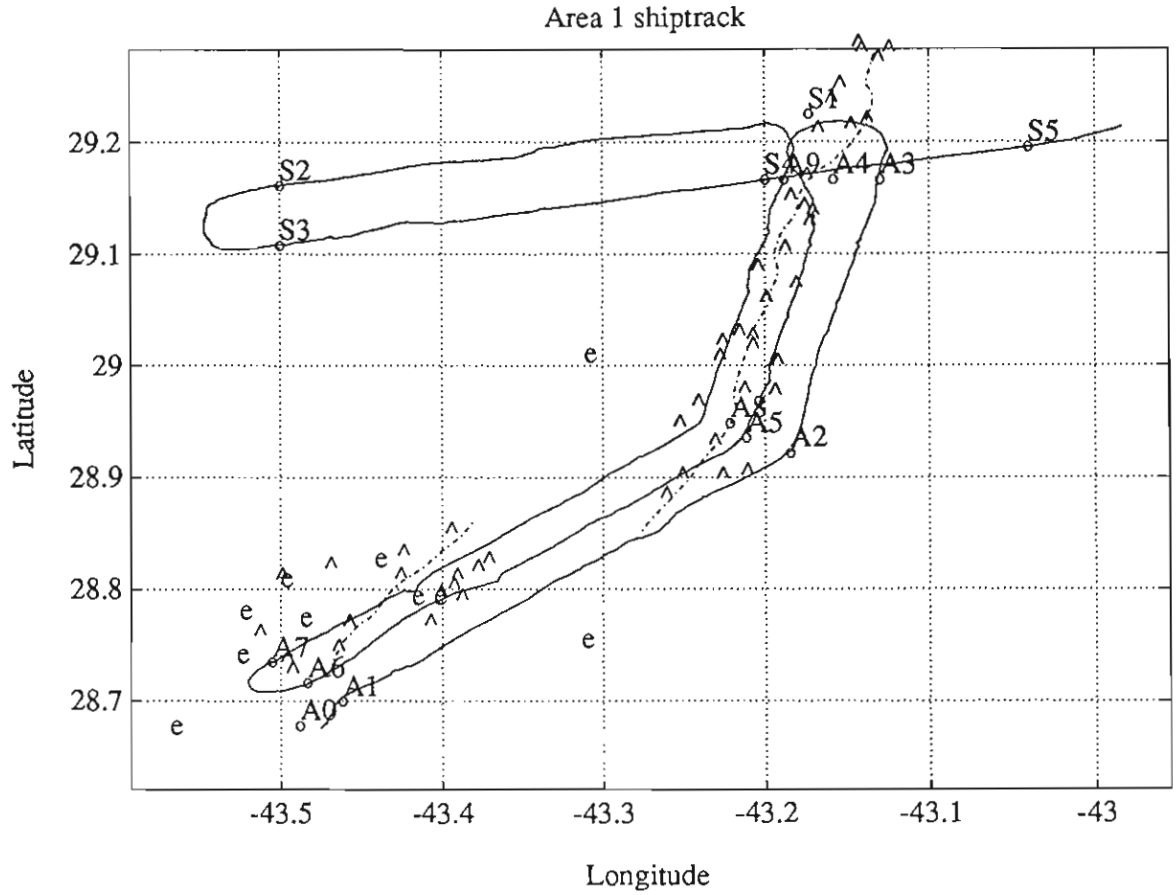

Figure 2.1 Area1 shiptrack

Waypoints (text labels), shiptrack (solid line) axial volcanic highs (dashed lines), earthquakes (e's), and Sea Beam identified seamounts (^'s) for Area 1.

2.3TOBI Run, Track line images

TOBI images for the entire Area 1 survey are shown in Figures 2.2 through 2.6. The images presented on these pages have been severely downsized from the original data. Each scanline of data (across track) in its original form contains 8000 pixels of information, 4000 to port and 4000 to starboard. Each pixel in the original data covers 0.75 meters of the seafloor. Distance from the TOBI sled and TOBI altitude affect this coverage so the 0.75 meter value should be taken as approximate. Along the ship track the original data contains a ping every 4 seconds for an along track pixel size of 4.0 meters. Again, as ship speed, distance from TOBI, and TOBI altitude affect

this coverage, the 4.0 meter valued should be used as an approximation. In total, TOBI produces 8000 pixels of information every 4 seconds or 900 scanlines of 8000 pixels every hour.

The images in Figures 2.2 through 2.6 each represent approximately 4 hours, 27 minutes of information (4000 scanlines of 8000 pixels each in the original data) with time progressing from the top down in each frame. The original data has been reduced to 800 scanlines of 200 pixels each of the strips in the figures. Detailed images of certain interesting regions are outlined in white boxes and are presented in the next section. Rock dredge sites are also indicated on the images.

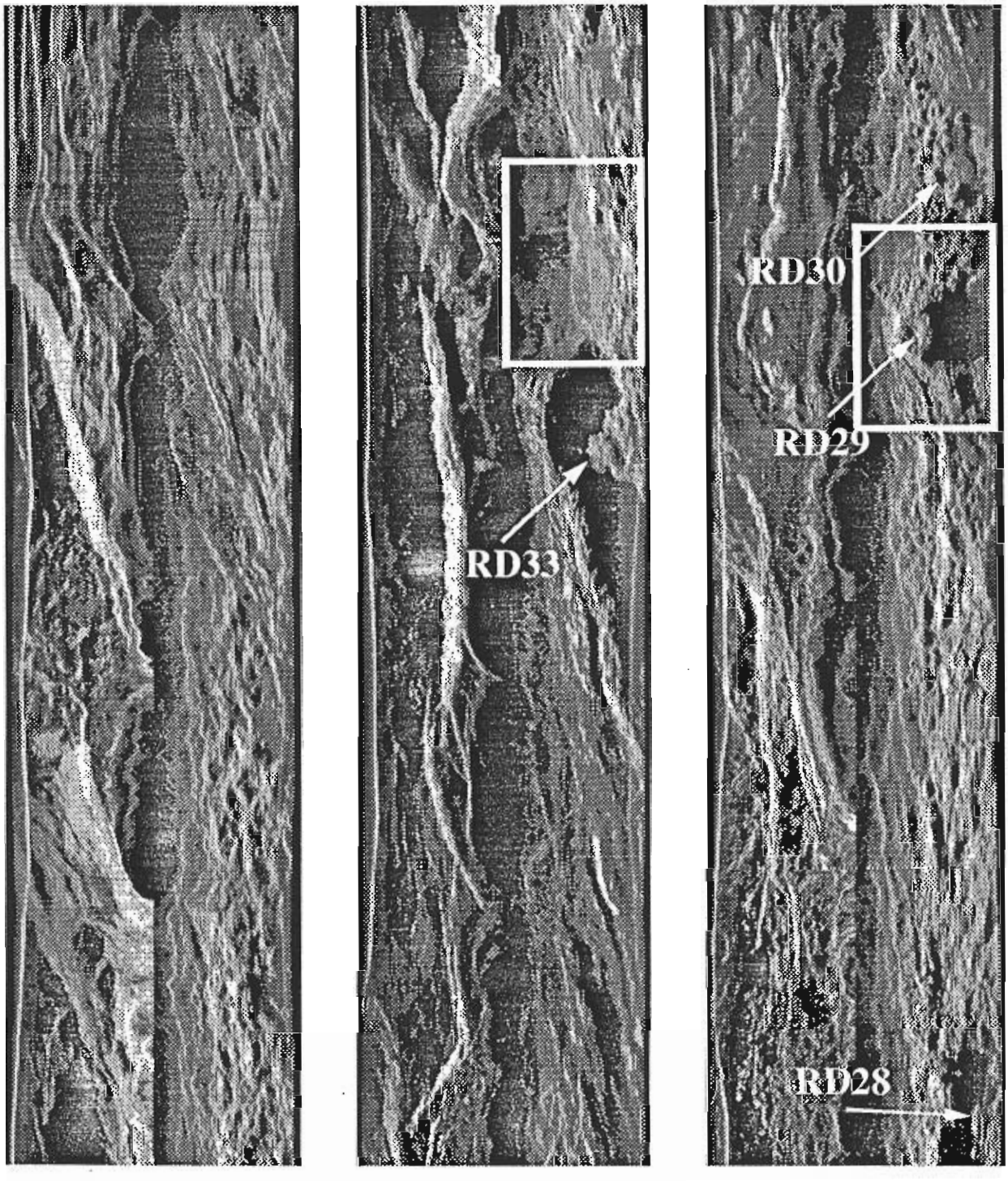

Figure 2.2 TOBI images starting 1530/048 Z.

Time progresses from left to right and from the top down in each frame. Each strip contains approximately 4000 TOBI pings for a total time of approximately 4.44 hours per strip. A ponded flow area and Sumpter Seamount are outlined in white boxes and described in detail below. Rock dredge sites area also indicated and described below.

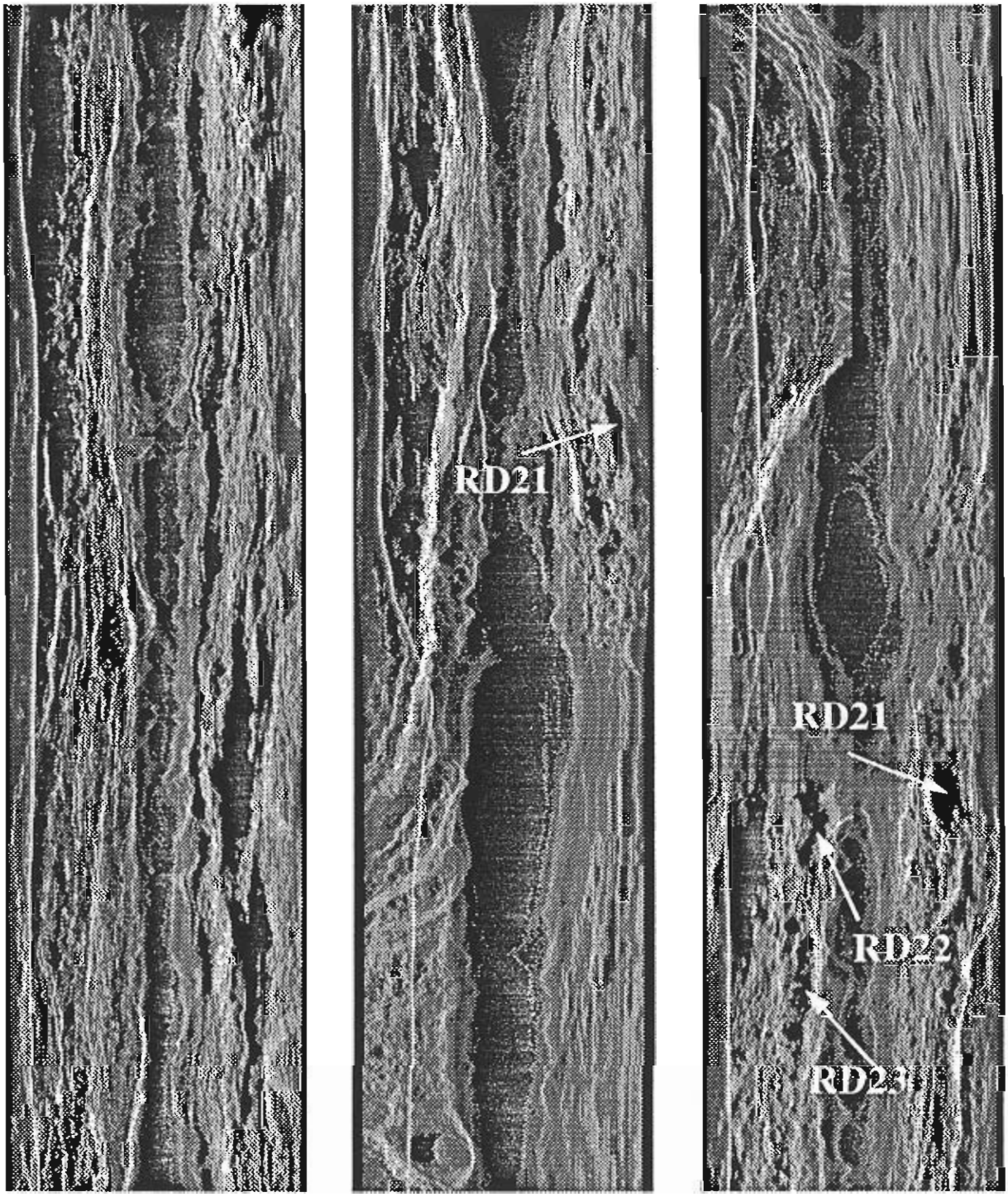

Figure 2.3 TOBI images starting 2250/049 Z.

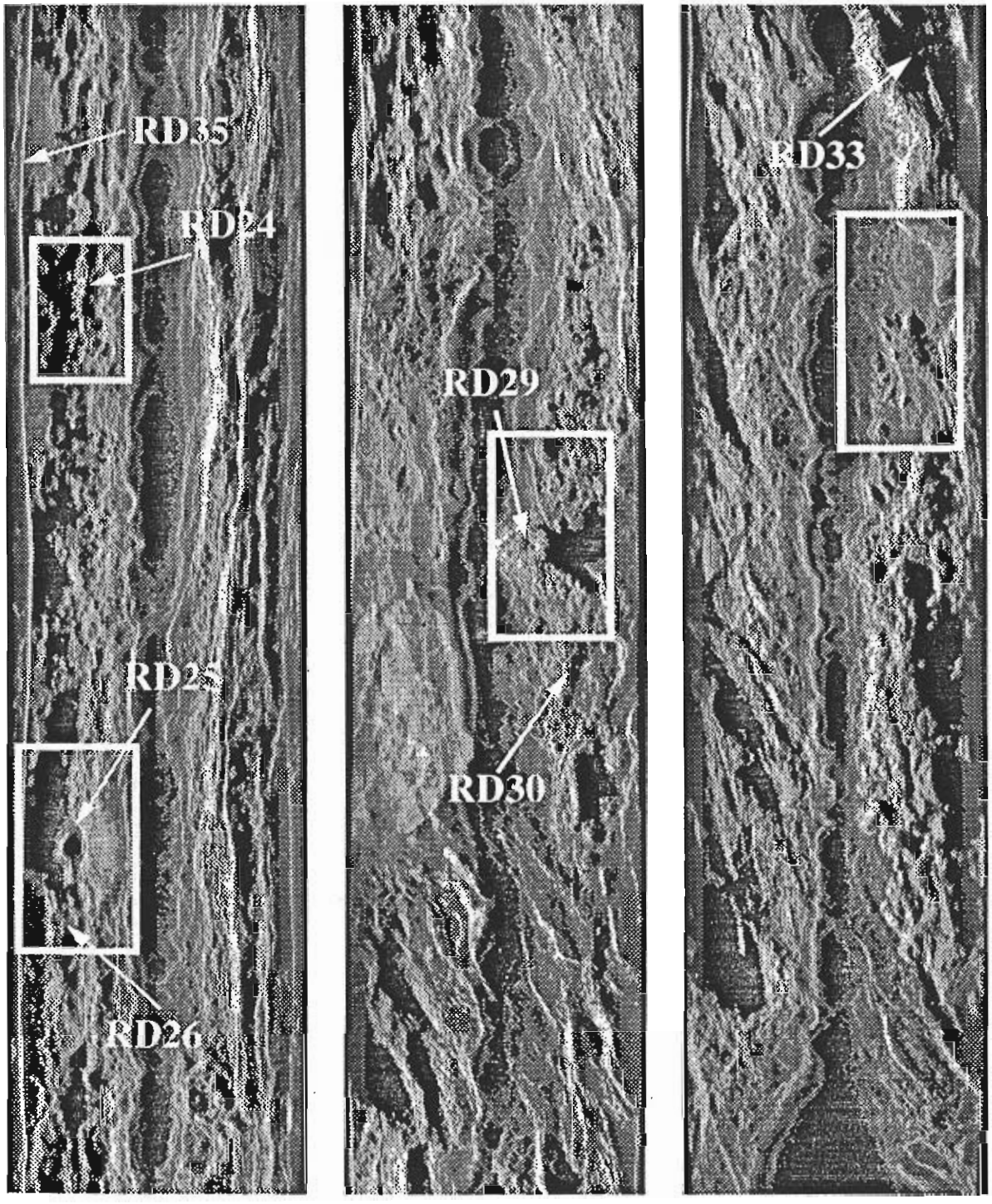

Figure 2.4 TOBI images starting 1200/050 Z.

Rock dredge sites are indicated and described in detail below. The caterpillar area, W Seamount, Sumpter Seamount, and the ponded sheet flow area are outlined in white boxes and presented in detail below.

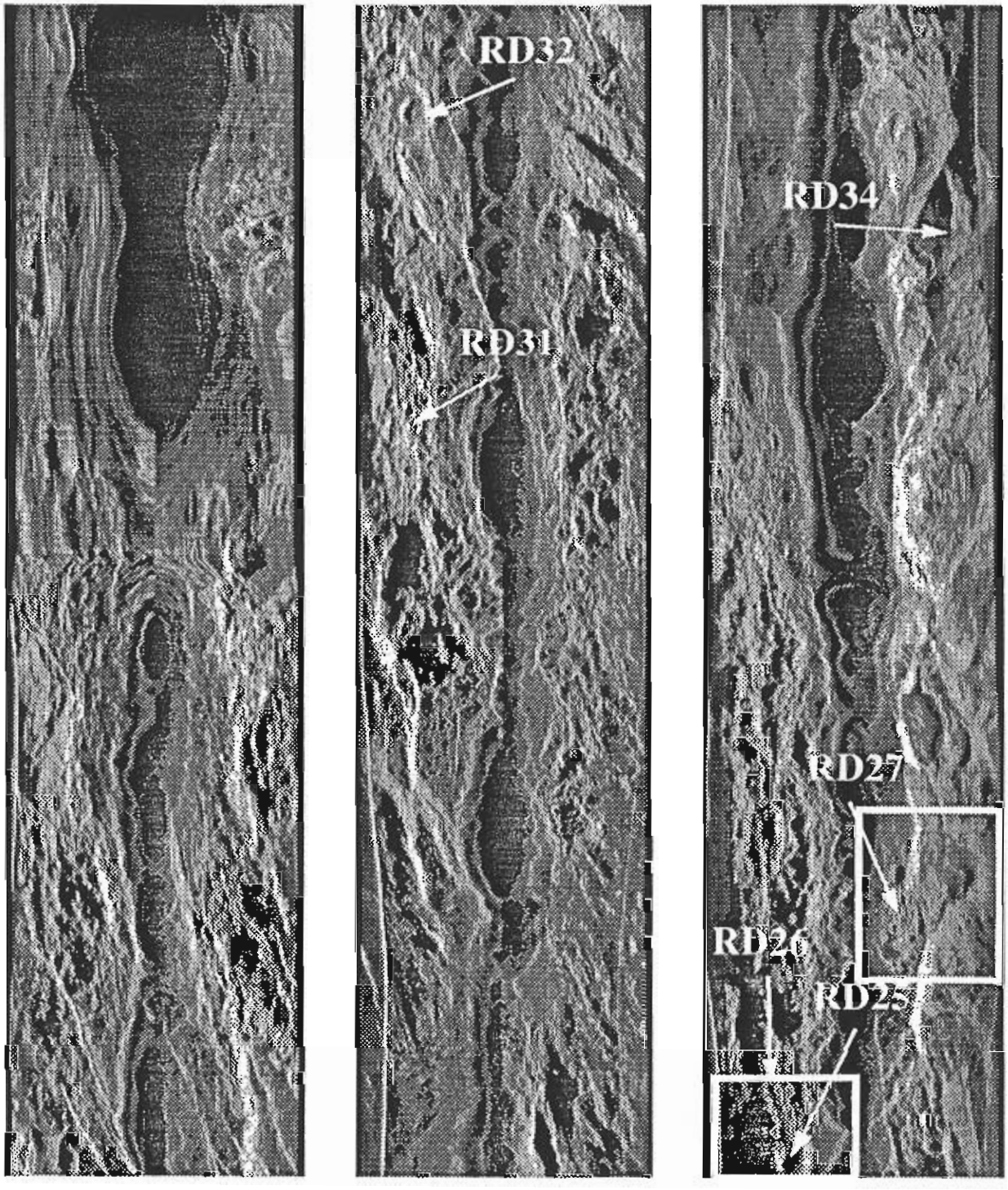

Figure 2.5 TOBI images starting 0130/051 Z.

Rock dredge sites are indicated and described in detail below. The landslide area and a second view of W Seamount is outlined in the white box and described in detail below.

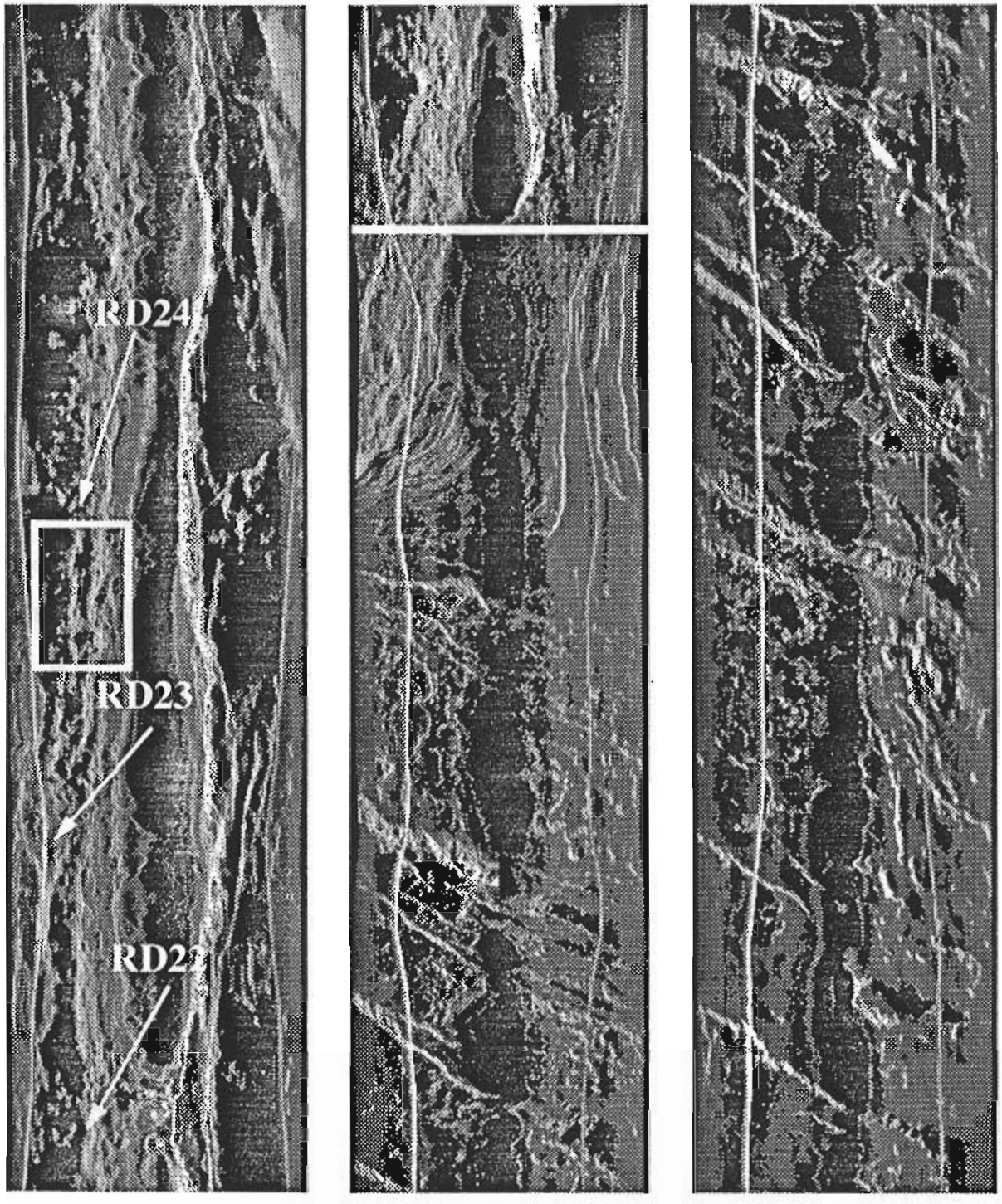

Figure 2.6 TOBI images starting 1445/051 Z.

Rock dredge sites are indicated and described in detail below. The caterpillar area is outlined in white and is also described in detail below. The start of the crestal mountains transect (to the west of the inner valley) is indicated on the center image (see figure 2.1 for trackline).

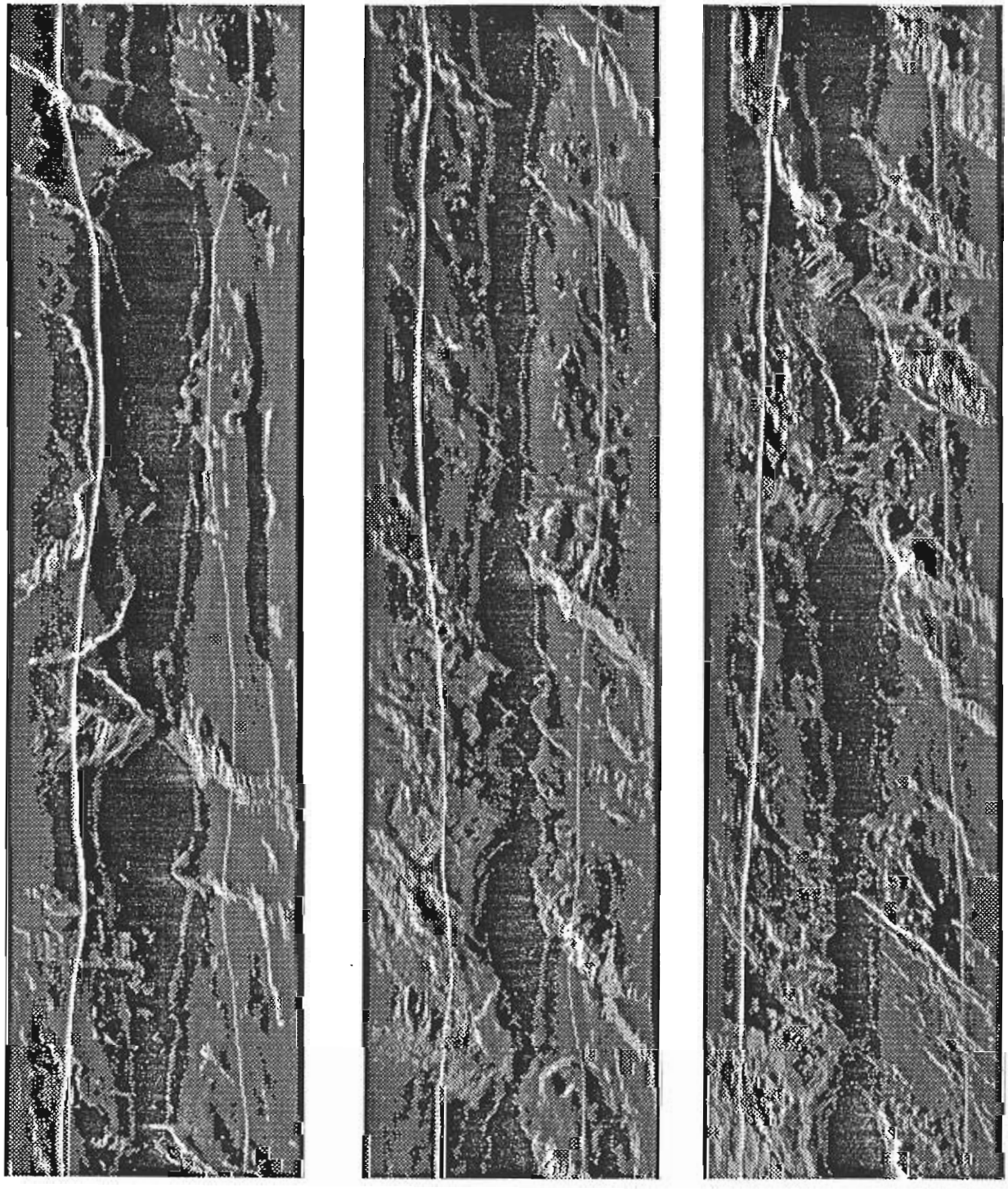

Figure 2.7 TOBI images starting 0400/052 Z.
Crestal mountains to the west of the inner valley.

Figure 2.8 TOBI images starting 1730/052 Z.

The inner valley is crossed obliquely in the top half of the image. Crestal mountains to the east of the inner valley are shown in the bottom of the image.

2.4 TOBI Run, detailed images

2.4.1 Sumpter Seamount

Sumpter is the larger of two flat-topped, cratered seamounts in Segment 17. These are the tallest flat-topped seamounts imaged anywhere in our survey. Sumpter has a complete crater, with signs of multiple subsidence, giving an irregular outline. The flanks are covered with variably smooth or hummocky lava. Whether the hummocky lava flowed from the seamount will be tested by analysis of dredges RD29 and RD30. from the top and southern flank of the seamount.

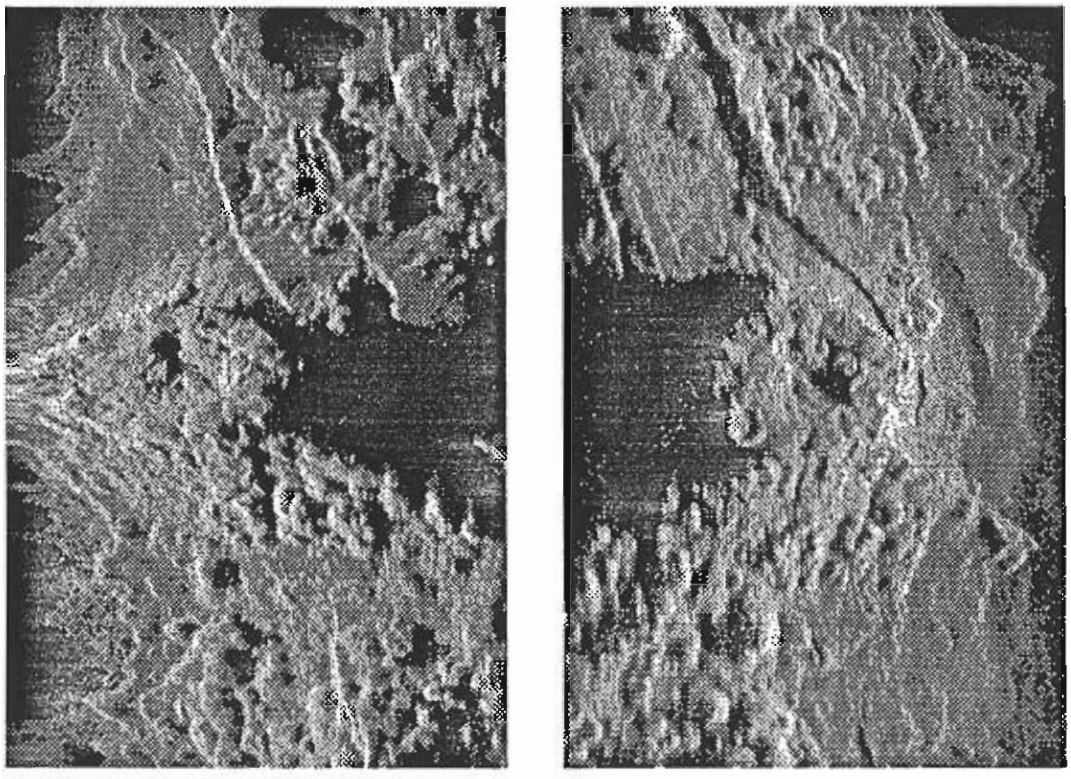

Figure 2.9 Doubly insonified Sumpter Seamount

Two views of Sumpter Seamount, the largest flat-topped seamount present on the Sea Beam and/or TOBI surveys. Possum Peak, in Segment 5 is the largest volcanic edifice in the Sea Beam survey area.

2.4.2 W Seamount

This prosaically named edifice is the second cratered flat-topped seamount in Segment 17. The crater is simple, and has a diameter more than half of that of the top of the seamount. The lip of the crater may have fed hummocky flows running south from the seamount, and again this will be tested by analysis of dredged basalt. The smooth surfaces east and west of the seamount may be smooth lava flows or else talus slopes.

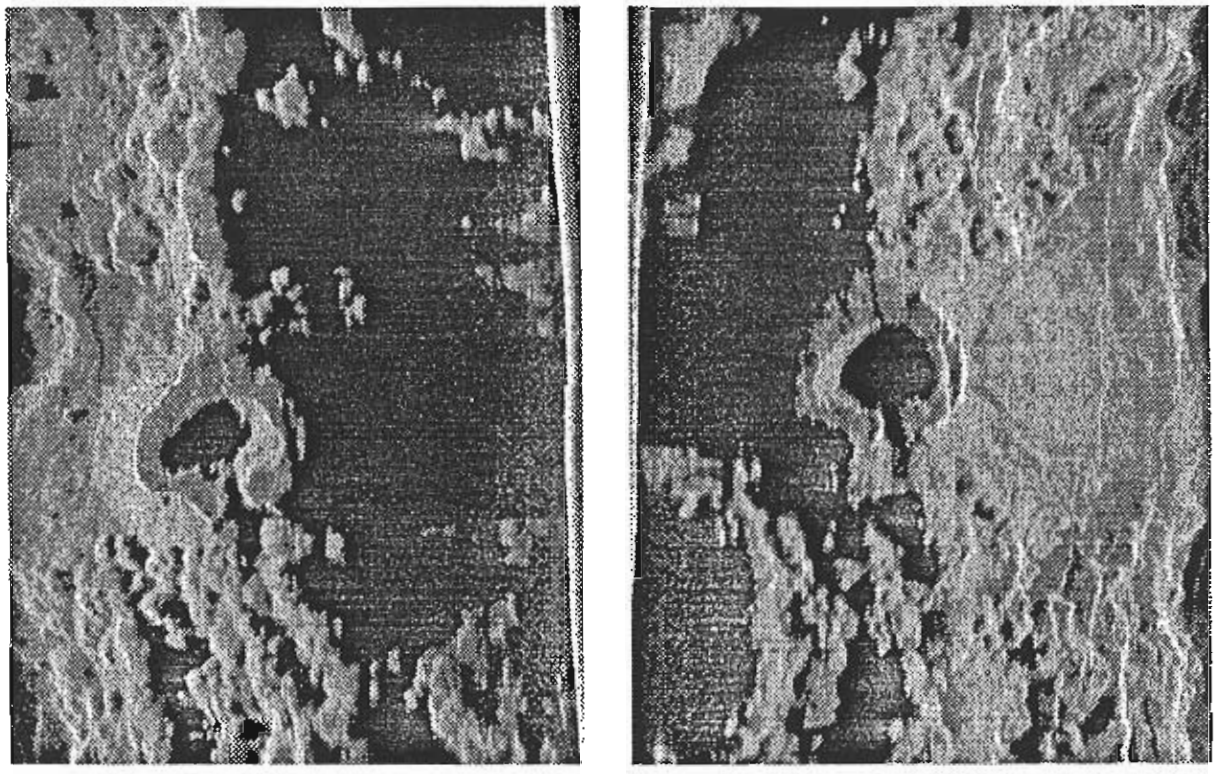

Figure 2.10 Doubly insonified W Seamount

2.4.3 Ponded sheet flow

The axial volcanic ridge of Segment 16 is close to the septum that separates Segments 16 and 17. Here a sheet flow (or perhaps the brim of a hat seamount) emerges from the axial volcanic ridge and is ponded against the base of the steep wall that forms the septum. A circular structure that may be the center of a hat is seen to the left hand side. Morphology shows that this volcanism is recent, and thus that the AVR of Segment 16 is placed very asymmetrically within its broad inner valley.

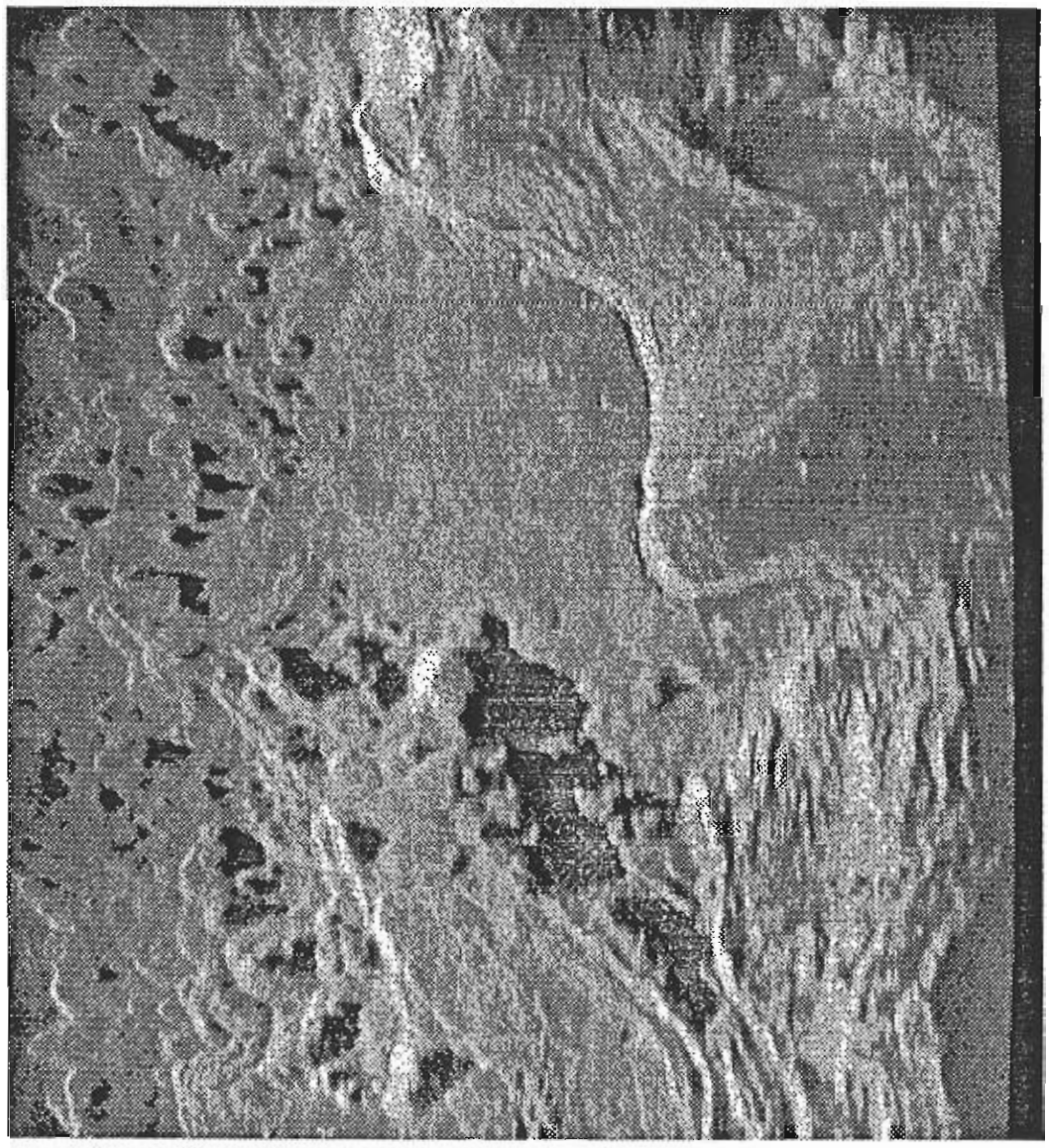

Figure 2.11 Ponded flow area detailed image.

2.4.4 Caterpillar Ridges

The central part of Segment 17 has a fine display of caterpillar ridges, running parallel to the axial volcanic ridge. These ridges are up to 3 km long and have the now classic knobby shape. Such ridges form over short eruptive fissures, probably rising from small magma chambers at depth, and erupting relatively small quantities of magma.

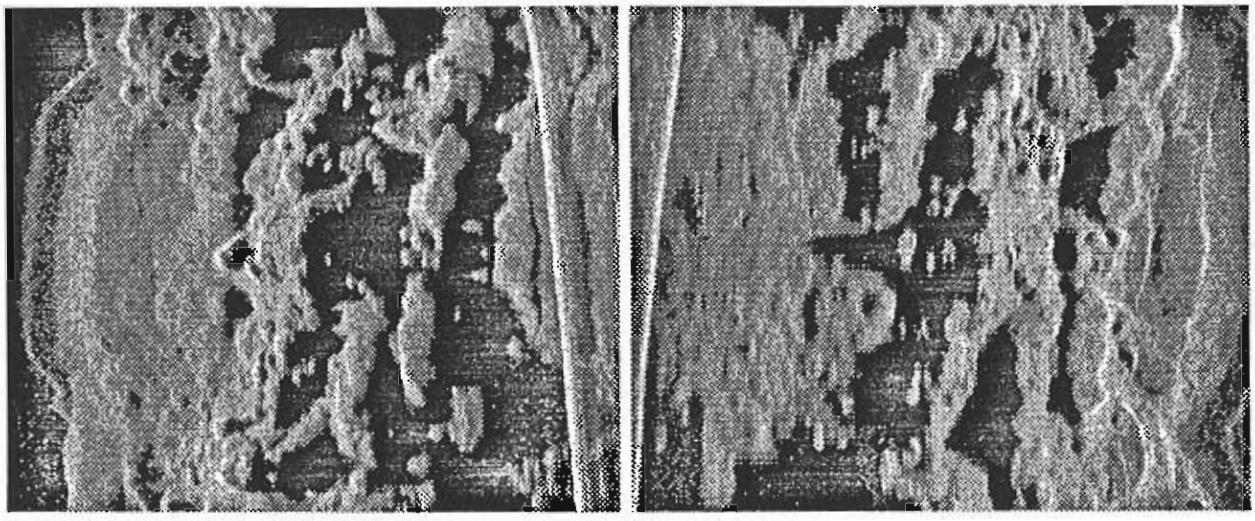

Figure 2.12 Dual-insonified Caterpillar Ridges detailed images.

2.4.5 Landslide

The southern end of the western wall of Segment 17 is the site of a large and complex landslide. Morphologies include domes, large flat flows and a terrain with a texture like crumpled paper. A dredge from the crumpled paper terrain produced serpentinites, basalts and masses of blue-gray, mud-matrix breccia. The image shows the toe of part of the landslides as it covers typical volcanic

terrain.

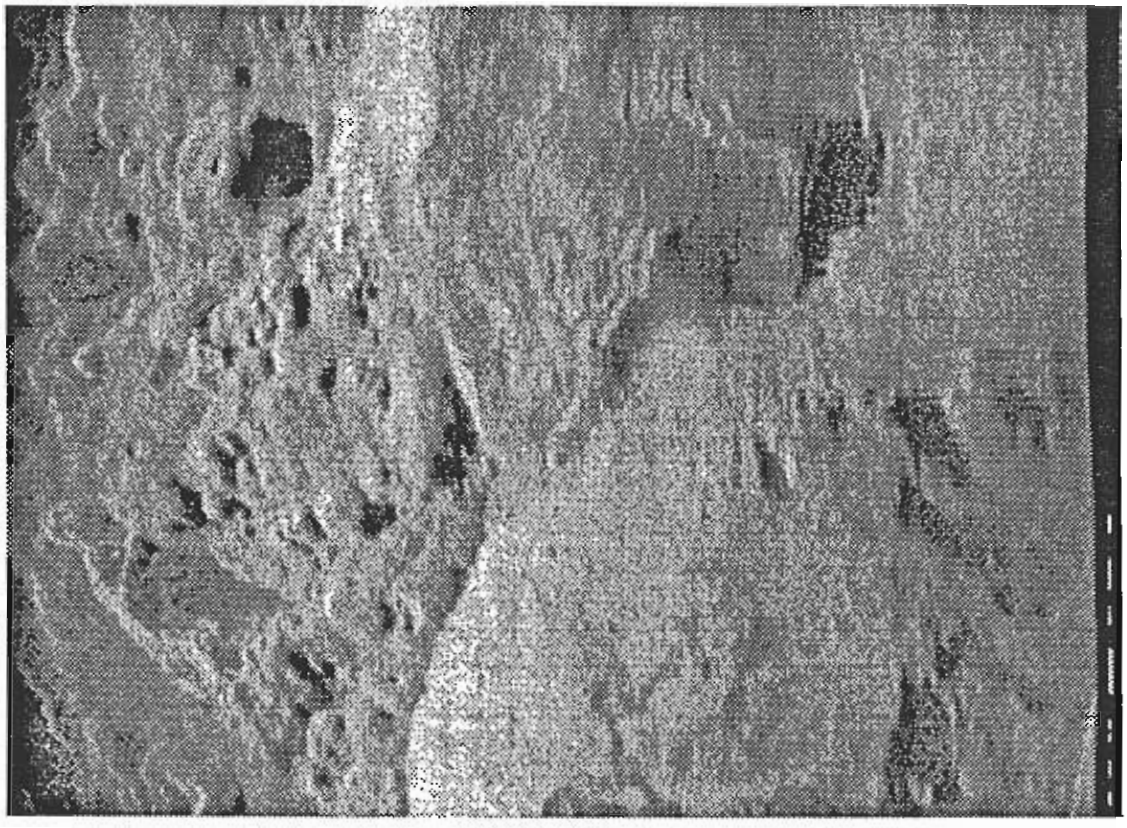

Figure 2.13 Landslide area detailed image.

2.5Geological map description

Detailed interpretation of the TOBI images of each area included the production of a geological map found in the back pocket of this volume. These maps, although only preliminary interpretations and lacking bathymetric data, have been useful in underlining the spatial distribution of the volcanic edifices, faults and landslides that have been imaged. Description of individual features has already been included in the summaries, so the discussion here will be limited to the interaction observed between the different processes.

Area 1 focuses on the offset between segments 16 and 17. On the bathymetric data the segments are seen as axial highs within the median valley and are separated by a septum (central high). On the geological map each of these segments is characterized by robust AVRs in which hummocky terrain appears to be the dominant volcanic form. The hummocks occur in a variety of sizes with diameters ranging from 250m to 45m (the smallest imaged hummock). These hummocks are arranged in hummocky heaps (one type of seamount) but more often in a series of linear ridges (caterpillars). Although these in some areas maintain an orientation parallel to the axial valley, elsewhere they cross-cut one another to create a lattice pattern. Smooth seamounts are also seen at outcrop either sitting on top of the hummocks or more often partially buried beneath them.

Faulting within the neo-volcanic zone is limited; though a variety of large and small en-ech-

elon faults are found parallel to the ridge off-axis. The larger faults (typically tens of km in length) are curvilinear in outcrop and often terminate in a splay of more minor off-sets. This pattern changes towards the end of the segments where faults are linked by a series of lateral ramps which parallel the off-set.

Smaller en-echelon faults (typically a few km in length) are also common off-axis, tending to form dense concentrations creating a stepped (terraced) geometry. This is particularly apparent along the eastern margin of segment 17 where the faults are seen dissecting hummocky terrain. Further off-axis both faults and hummocks become progressively buried under pelagic sediment (seen as low back scatter on the TOBI images).

The septum comprises a network of back-tilted blocks bounded by cross cutting faults orientated sub-parallel and sub-perpendicular to the ridge axis. These blocks comprise fine scale hummocky terrain upon which there is no significant sedimentation within the central zone, although pelagic sediments occur off-axis. The northern end of the septum is partially buried beneath a large landslip which is characterized by bright reflectors on the TOBI image. The landslip is made up of a combination of debris flows and coherent blocks. Elsewhere sedimentation is pelagic and is restricted to the off-axis zones.

2.6 Dredging

The sites chosen for dredging in Area 1 are

RD 21) 29° 09.03' N, 43° 9.27' W, Depth 3131 m, 32 rocks + gravel

hummocky flow on a linkage from the axial volcanic wall to the inner valley bounding scarp

Hand specimens. Moderately altered (palagonitic patches on glassy exterior rind), moderately porphyritic (~10% plagioclase, <1% olivine phenocrysts), dark grey sheet flow/pillow basalt. Rocks have subangular shapes, are decimeter-sized and occasionally have white worm casts on their surfaces.

Thin section. Porphyritic pillow basalt (RD21.19). This section was taken from the variolitic margin. The groundmass consists of flow orientated plagioclase microlites, glass plus subordinate olivine. Plagioclases have a rail track morphology, typical of rapid chilling. The olivines are small rounded to acicular and tend to cluster together. The phenocrysts represent around 10% of the whole rock, of which 90% are plagioclases. Maximum size of the plagioclases is 2 mm. Three types of plagioclases were identified: (i) euhedral laths with multiple twins, these have an extinction angle of 20 degrees, which corresponds to An40; (ii) anhedral to subhedral simple to complexly twinned plagioclases with a sieve texture containing glass inclusions. These have an extinction angle of 30-34 degrees corresponding to An60; (iii) rounded (due to resorption) oscillatory zoned plagioclases. Epitaxial growth around the crystal boundary is common. The olivine phenocrysts are anhedral and form complex intergrowths with plagioclase. They have a maximum size of 0.3mm and represent less then 5% of the phenocrysts.

RD 22) 29° 8.78' N, 43° 10.27' W, Depth 3085 m, 10 rocks + gravel

caterpillar ridge on the axial volcanic ridge adjacent to RD 21.

Hand specimens. Highly altered (widespread palagonitic alteration), moderately porphyritic (<10% plagioclase phenocrysts), black /dark grey glassy pillow basalt. Rocks are gravel to decimeter-sized and angular in shape.

Thin section. Sparsely porphyritic pillow basalt (RD22.10). Thin section taken from the glassy margin and variolitic margin. The groundmass is completely isotropic brown glass displaying a variolitic texture. The phenocrysts are composed of 70% plagioclase and 30% olivine. The plagioclases have a typical rail track form with subordinate hollow box basal sections. One section shows oscillatory zonations, having a more calcic outer edge. The rest of the plagioclases display simple to complex twinning and commonly have glass inclusions. The olivines all have a rapid growth form, with 'space-ship' and 'fish bone' acicular being common. All the olivines contain glass inclusions. A complex inter-relationship between the olivines and the plagioclases is displayed.

RD 23) 29° 7.01' N, 43° 11.11' W, Depth 3187 m, 17 rocks + gravel

fissure ridge on the axial volcanic ridge

Hand specimens. Highly altered (extensive palagonitic coating and "weathering"), sparsely porphyritic (<3% plagioclase phenocrysts), black/light grey glassy pillow basalt. Rocks are decimeter-sized (max. 25 cm long) and angular to pillow-shaped.

Very sparsely porphyritic pillow basalt (RD23.8). Thin section taken from the variolitic margin. Minor acicular plagioclase microlites and rare subrounded olivines are set in a glass matrix to form the groundmass. The plagioclases are all rail track type. The phenocrysts are all less then 0.5mm with olivine forming the largest and most abundant phase. These are commonly rounded to acicular with glass and chrome spinel inclusions. The plagioclases are less than 0.4 mm in length. They are acicular anhedral laths and commonly contain glass inclusions. Twinning is dominantly simple.

Thin section. Porphyritic basalt (RD23.12).Thin section from the variolitic margin. Glass is the dominant phase in the groundmass with subordinate acicular plagioclase microlites and equant to acicular olivines. The phenocrysts are split 50:50 between the plagioclase and olivine phases. The plagioclases are subhedral laths with simple to complex twinning, and commonly show acicular projections at the lath corners. The larger plagioclases (1 mm) have a partial sieve, and occasional epitaxial growth around the crystal boundaries. The olivines are euhedral to subhedral with glass inclusions found around the crystal boundary. They have a maximum size of 0.8 mm.

RD 24) 29° 4.38' N, 43° 11.74' W, Depth 3140 m, 24 rocks + gravel

hummocky fissure flows on the axial volcanic ridge

Hand specimens.

a) 21 rocks. Slightly altered (some palagonite in cracks, some Fe-staining), highly porphyritic (~30% plagioclase megacrysts), light grey pillow basalt. Rocks are decimeter to gravel-sized (max. 30cm long), rounded/tubular in

shape and are slightly vesicular.
b) 3 rocks. Moderately altered (palagonitic coating), sparsely porphyritic (<2% plagioclase phenocrysts on glassy margin), light grey basalt. Rocks are decimeter to gravel-sized (max. 20 cm long) and angular-shaped.

Thin section. Porphyritic basalt (RD24.7 & RD24.9). Thin section taken from the interior of a pillow basalt. The groundmass is 70% acicular plagioclase microlites plus acicular to rounded olivines in felted mat texture. Both rail track and hollow box plagioclases are present, with the former forming radiating laths. A preferred flow orientation of the microlites is found in RD24.9. Olivine is the dominant phenocryst representing 60% of all phases. They are euhedral (equant) to anhedral and have a maximum size of 1.5 mm. Some of the olivines show signs of resorption with further regrowth in cracks and along the boundary. Inclusions of chrome spinel plus an anisotropic phase have been found. The most prominent feature of this section is the resorption and regrowth textures of the olivine crystals. Plagioclases are present both as simple twinned and untwinned crystals. The former having an extinction angle of 22 degrees (An40). Their form is subhedral laths to equant, and are up to 1.2 mm in length. The untwinned plagioclases have an oblique cleavage plane, occasional with ghost twins. The cleavage plane sometimes contains a twin.

RD 25) 29° 0.16' N, 43° 12.75' W, Depth 3058 m, 12 rocks + gravel + coarse sand

summit of W seamount

Hand specimens.

a) 10 rocks. Highly altered (extensive palagonite coating), highly porphyritic (~25% plagioclase phenocrysts (5-8mm)), black basalt. Rocks are decimeter to gravel-sized, subangular shaped and have worm casts on their surfaces.
b) 2 rocks. Highly altered (extensive palagonite coating), sparsely porphyritic (~1% plagioclase phenocrysts) though some portions have more dense phenocryst concentrations than others, black basalt. Rocks are decimeter to gravel-sized (max. 10cm long), angular-shaped and slightly vesicular.

Thin section. Porphyritic basalt (RD25.1). Section taken from the variolitic margin. Glass dominates the groundmass with plagioclase microlites representing 10%. These are acicular and display rail track and hollow box morphologies and are flow orientated. No olivine was found in the groundmass. Phenocrysts are plagioclase and olivine. The plagioclase (80%) have aspect ratios from 1 to 5 and are subhedral. They display simple to complex twinning with an extinction angle of 33 degrees (An60) Complexly twinned plagioclase do not have sections perpendicular to x and hence no extinction angle was measured. Resorption and alteration of complexly zoned plagioclase are suggested by the anhedral crystals, they also contain glass inclusions. The olivines have a maximum size of 0.4 mm are subhedral and equant, and commonly contain chrome spinel inclusions.

RD 26) 28° 59.49' N, 43° 12.85' W, Depth 3652 m, 7 rocks + gravel

flows on the southern flank of W seamount

Hand specimens.

a) 6 rocks + gravel. Moderately to slightly altered (palagonitic coating in

patches), aphyric, pale/dark grey basalt. Rocks are gravel-sized (max. 8cm long), subrounded/subangular-shaped and have an aphanitic groundmass.
b) 1 rock. Highly altered (extensive palagonite coating), highly porphyritic (~25% plagioclase phenocrysts (2-5mm)), black basalt. The rock is decimeter-sized and subangular-shaped.

Thin section. Sparsely porphyritic glassy basalt (RD26.6). The groundmass is dominated glass with acicular plagioclases and olivines representing 20% of the total. The phenocrysts form 10% of the rock, with plagioclases being the most ubiquitous. The majority of them are untwinned and subhedral and both lath and equant in shape, while the twinned minerals tend to be subhedral to anhedral laths. No extinction angle was measured. Olivines are small (0.3 mm) equant subhedral crystals which tend to be isolated. Chrome spinel is a common inclusion mineral.

RD 27) 28° 57.96' N, 43° 12.61' W, Depth 3243 m, 12 rocks + gravel + mud

seamount #532, a hummocky seamount on the axial volcanic ridge

Hand specimens. Moderately altered (palagonite coating in patches), aphyric, black/dark grey pillow basalt. Rocks are decimeter to gravel-sized (max. 30 cm long), pillow-shaped and have an aphanitic groundmass surrounded by a glassy rind.

Thin section. Sparsely porphyritic glassy basalt (RD27.6). Section from the pillow margin. The groundmass is 100% variolitic glass. The phenocrysts are all olivine phases. They are acicular with central boss to sieve textured equant crystals. Alteration of the olivine boundaries is developed with inclusions of both chrome spinel and glass. The maximum size of the olivines is 0.4 mm. It is one of very few basalts sampled that are free of plagioclases.

RD 28) 28° 57.8' N, 43° 11.37' W, Depth 3343 m, 7 rocks + gravel + mud

seamount #533 on the linkage from the axial volcanic ridge to the inner valley wall bounding fault

Hand specimens. Moderately altered (palagonite coating in patches), aphyric, black/grey basalt. Rocks are gravel-sized (max. 5cm long), subangular-shaped and have an aphanitic groundmass with devitrification spherules. There are examples of life on these rocks: worm casts and a small white, fuzzy sponge which uses the pale brown mud-patches for a substrate and looks not-unlike a two-day old growth on Ben's chin were his hair color white.

Thin section. Sparsely porphyritic basalt (RD28.2). No microlites were found in the groundmass, it being completely composed of variolitic glass. The phenocrysts are all olivine crystals. These are perfectly euhedral crystals (1 mm) which are arranged in clusters, although isolated crystals are observed. Both chrome spinel and glass inclusions found.

RD 29) 28° 53.26' N, 43° 15.17' W, Depth 3333 m, 8 rocks + gravel

SUMPTER SEAMOUNT
top of Sumpter seamount (#526)

Hand specimens. Highly altered (extensive palagonite coating), moderately porphyritic

(~20% plagioclase, <5% olivine megacrysts), dark grey sheet flow basalt. Rocks are decimeter-sized (max. 30 cm long), angular-shaped and slightly vesicular.

Thin section. Highly porphyritic basalt (RD29.1). This holocrystalline rock has a 50:50 ratio of plagioclase to olivine in the groundmass. The olivines are dendritic laths forming a feathery matted texture. The plagioclases are acicular rail track to hollow box forms. The phenocrysts are plagioclase and olivine (just for a change!!!). The plagioclases are up to 3 mm in length and have a range of twinning styles from completely untwinned to complexly twinned. The latter also have glass inclusions. A couple of oscillatory zoned crystals were also found, these are subhedral with alteration at the crystal boundary. The olivines are subhedral to subrounded with chrome spinel inclusions. Little to no alteration was identified.

RD 30) 28° 52.48' N, 43° 15.31' W, Depth 3685 m, 10 rocks + gravel

flows on the southwest flank of Sumpter

Hand specimens. Highly altered (extensive palagonite coating which reaches a few mm below the surface), moderately porphyritic (15-20% plagioclase, <1% olivine megacrysts), black sheet flow basalt. Rocks are decimeter-sized (max. 15 cm long), subangular-shaped, slightly vesicular in places. Worm casts occur on the surfaces of these rocks, and in one pitted out portion a collection of forams with no surrounding mud is nestled.

Thin section. Highly porphyritic basalt (RD30.1). The groundmass is dominated glass with some submicroscopic inclusions which may be olivine. The phenocrysts represent 30% of the whole rock. These are large (4 mm) simple to multiple twinned plagioclase laths and small (0.5 mm) equant subrounded olivines. The plagioclases are split into the larger anhedral complexly twinned crystals that show evidence of alteration, and the smaller simple twinned euhedral crystals. Olivines are generally isolated in the groundmass, and are equant to lath shaped. No inclusions found.

RD 31) 28° 48.21' N, 43° 22.56' W, Depth 3520 m, 28 rocks + gravel

seamount in segment 17

Hand specimens. Moderately altered (some palagonite coating in patches), aphyric, black glassy sheet flow basalt. Rocks are gravel to decimeter-sized (max. 10 cm long), angular-shaped, slightly vesicular, and many of the rocks are very smooth, showing a ropy texture which might be a first glimpse of Hyperbarian pottery, if, indeed, these abyssal beings had need of such utilities.

RD32) 28° 46.98' N, 43° 24.54' W, Depth 3688 m, glassy bits

flat-topped keyhole, seamount 516 in Segment 16

Hand specimens. Slightly altered (palagonite in cracks), aphyric, pale blue-grey/black sheet flow/pillow basalt. Rocks are decimeter-sized (max. 10cm long), subangular, and often have planar, gently creased surfaces. They are very slightly vesicular.

RD 33) 28° 49.14' N, 43° 20.6' W, Depth 3252 m, 18 rocks + gravel

septum between segments 16 and 17, dredge 1 towards the east

Hand specimens. Highly altered (extensive palagonite coating), aphyric, grey basalt. Rocks are decimeter-sized (max. 20cm long), subangular to rounded in shape, 25% vesicles, and harbored a sponge and a "plant like thing."

RD 34) 28° 55.2' N, 43° 17.39' W, Depth 3668-3726 m, ~200 rocks + gravel + sediment

landslide dredge

Hand specimens. The rocks from this dredge (that surely must be considered for immediate inductance into the oceanographic Hall of Fame) are numerous and of various kinds.

a) 54 rocks- pillow lava Slightly altered (some Fe-oxide weathering), aphyric, grey/brown pillow basalt. Rocks are decimeter-sized (max. 50cm long), sub-angular with rounded glassy margins and some have up to 3% vesicularity. 1 worm was in this haul.

b) 19 rocks- rodingitised gabbro decimeter-sized (max. 20cm long), sub-angular to sub-rounded, light grey/speckled gabbros that have been variably mylonitised.

c) 10 rocks- highly weathered serpentinite Up to decimeter-sized (max. 50 cm long), subangular, brown/greenish brown/grey, highly friable serpentinized harzburgites.

d) 7 bags of assorted samples- melange matrix Samples range in color from browns to greys and contain angular clasts of serpentine set in a muddy matrix. There is also some "sand-grade sedimentary stuff" in this haul.

e) 20 rocks- highly sheared serpentinites Up to decimeter-sized (max. 20cm long), angular, greenish-grey/blue-grey, highly sheared serpentinized harzburgites with abundant slickenside surfaces.

f) 15 rocks - tectonised harzburgite Up to decimeter-sized (max. 30 cm long), angular, green to brown, penetratively deformed harzburgite with a strong tectonite fabric.

g) 5 rocks - pyroxene rich ultramafics decimeter-sized (max. 40cm long), sub-rounded, brown to green-grey, peridotites with more than 30% pyroxene. This haul contains one pyroxenitic sample.

h) 9 rocks - serpentinite breccias decimeter-sized (max. 40cm long), sub-rounded, brown to grey, breccias with angular serpentinite fragments in a crushed serpentinite matrix.

i) 73 rocks - serpentinised harzburgite decimeter-sized (max. 50 cm long), angular to subrounded, brown/blue/green-grey, serpentinised harzburgite with 30% bastite crystals and a weak tectonic fabric.

j) 27 rocks - mesh-textured harzburgites/serpentinite decimeter-sized (max. 20 cm long), sub-angular to sub-rounded, pale green-grey, harzburgites and dunites with a fine mesh texture replacing olivine.

k) 12 rocks - serpentinized dunite Up to decimeter-sized (max. 20 cm long), sub-angular, brown-grey/grey, potential dunites with very little or no bastite crystals.

l) 54 rocks - others Up to decimeter-sized (max. 20cm long), sub-angular to sub-rounded, grey to brown variety of rocks including metabasalts, indurated sediment, and some ultramafics.

RD 35) 29° 5.45' N, 41° 12.16' W, Depth 3187 m, glassy bits

flat-topped seamount west of the axial volcanic ridge in the northern part of the survey of Segment 17

Hand specimens. Moderately altered (palagonite coating in patches), moderately porphyritic (~15% plagioclase phenocrysts), dark grey glassy sheet flow basalt. Rocks are decimeter-sized (max. 20 cm long), subangular to subrounded, and ~10% vesicles.

Thin section. Highly porphyritic glassy basalt (RD35.2). Section cut from the glassy margin. The groundmass is 90% glass and 10% plagioclase microlites and acicular olivines. The phenocrysts are dominated by plagioclase, with 70% of the whole. There maximum size is 3 mm and they have forms ranging from rapid growth morphologies to euhedral. Twinning is from untwinned to complex, with an extinction angle of 29 degrees (An55). Glass inclusions are found within simple and multiply twinned crystals but not in the complexly twinned ones Two oscillatory plagioclases were found, these had more calcic rims. The olivines are much smaller, 0.5 mm maximum. Their form is typically euhedral and equant. They are either isolated or associated with simply twinned plagioclases. Some contain chrome spinel inclusions.

2.7 Underway Geophysics

See Chapter 7 for summary of overall gravity and magnetics results.

2.8 Camera Runs

Camera station 4: Sumpter Seamount lat: 28° 53.25' N long: 43° 15.15' W

Operations. Because of the electrical problems encountered on previous runs an immersion test was carried out on the camera prior to deployment proper. The system was found to be working perfectly. The camera was deployed for real at 2120/054 Z, and reached the bottom at 2247Z. At 2259 we ripped the weight off, but continued flying the camera, using the echo-sounder trace alone, until 0015/055Z when the run was aborted. On reaching the surface at 0118 (minus bob) both camera and flash were found to be completely discharged, even though they had been fully charged immediately prior to deployment. The battery charger to the flash unit was found subsequently to be defective.

Results. No photographs of the bottom were obtained, although we got some quite nice pictures of the bob. These had obviously been taken upon descent, implying once again that some electrical failure and short circuiting had occurred at high pressure.

Camera station 5: Caterpillar Ridge lat: 29° 04.30' N long: 43° 12.00' W

Operations. In the hope of improving the lamentable reliability of the BATHYSNAP system, for station 5 we replaced the RVS two-probe switch by the more robust single-probe IOS switch, and modified the circuitry of the camera and pinger to allow the camera to trigger the pinger directly. We also replaced the wire to the bob by chain, in order to reduce the likeli-

hood of it becoming tangled in the camera frame. However, although deck tests showed the new switchgear to function perfectly, it once more failed in operation. The camera was deployed at 0552/056Z, but steadfastly refused to trigger upon reaching the bottom (at 0713). Eventually the run was aborted at 0754. The barrel of the switch was found to have twisted and jammed.

Results. No photographs were obtained from station 5; however, camera station 8 was sited at the same place and was successful. The results of this station are described below.

Camera station 6: Flat-topped Seamount lat: 29° 04.30' N long: 43° 12.40' W

Operations. The camera was initially lowered at 1523/056Z; however, at 1540 double pinging (implying a short circuit) was noticed and the camera brought back to the surface. The fault in the camera pressure housing cap was repaired and the system was redeployed, with a fresh load of film, at 1720. It reached the bottom (approximately 3150m water depth) at 1906, at which stage we had 3209m of wire out. The system operated perfectly, and we estimate from the echosounder records that 140 photographs were taken up until 2046 (3098m wire out), when the decision was made to haul up. The camera reached the surface at 2212, complete with bob but with the main arm holding the switch and flash bent by 20?.

Results and interpretation. By some miracle 138 images were found upon processing of the film. Frame numbers 009-082 show the seafloor to be composed predominantly of subangular to subrounded decimeter-sized talus. At the time these photographs were taken, the ship had moved from a point 500m northeast of the waypoint directly onto it, and the echosounder was indicating that the ground was rising; hence we surmise that the camera was mounting a flank of the seamount.

Frame numbers 084-146 show a partly sedimented, rather subdued terrain. Most images suggest undulose, flattish flow tops more compatible with a sheet flow-type morphology. In many instances unidentifiable lava blocks stick up through a blanket of sediment. Pillowed lava flows are visible at the end of the run, appearing at the same time as the echosounder was indicating that the ground was dropping away. It is possible that far edge of the seamount was being reached just as the run finished.

These images suggest that the flat top to this seamount is composed predominantly of sheet flows that are partly blanketed by sediment, and that the steep sides to the seamount are formed by lava talus slopes. It is possible that the sheet flows give way to pillowed flows at the edge of the seamount's flat top.

Camera station 7: Hummocky Seamount lat: 29° 05.4' N long: 43° 11.4' W

Operations. The camera was deployed at 2320/056Z, and reached the bottom at 0044/057Z. We pogoed successfully until 0115, at which point the system started double pinging continuously. After this we flew the camera using the echosounder trace alone until 0202, when we aborted the run. The camera was retrieved at 0320, minus bob but otherwise intact.

Results. Images were recognized on the negatives up until frame number 229. The bob was lost on frame number 044; after this point the camera was taking pictures every 15 seconds regardless, hence there are many gaps and out of focus images on the succeeding negatives.

Nevertheless, it is possible to delineate five domains of differing seafloor morphology: (i) frames 014-044: pillow lava and pillow debris, slightly sedimented; (ii) 045-074: lava talus, decimeter scale; (iii) 083-156: heavily sedimented seafloor with lumps of lava debris and occasional pillow lobes sticking out; (iv) 182-195: fresh unsedimented pillow lavas; and (v) 227-229: slightly sedimented pillows. The echosounder indicated that the seafloor started to slope downwards at about frame 152, and a steep rise was detected at the equivalent of frame 184. This suggests that the fresh pillow lavas of domain (iv) may have formed a distinct mound or ridge. Overall, it can be deduced that the terrain around the hummocky seamount is more irregular and variable than the flat-topped seamount, and is dominated by pillowed rather than sheeted flows.

A white galatheid crab called Reggie is visible on frame 155. These types of crabs are common and do not indicate proximity to any hydrothermal vents or anything wacky like that.

Camera station 8: Caterpillar Ridge lat: 29° 04.5' N long: 43° 11.3' W

Operations. The camera system was deployed at 0420/057Z, and on the bottom and operating at 0612. It pogoed without problems until 0816, at which stage it started to double ping continuously. We flew the camera by the echosounder alone until 0845, when we aborted the run and hauled the camera to the surface. It was recovered at 1000, minus bob, chain and IOS switch, which had been ripped bodily from its mounting.

Results. Image were recognizable between frame numbers 008 and 226. The bob, chain and switch were left under a pillow at frame 110. The character of the seafloor over which the camera was dragged changed during the run, and we recognize nine different 'domains': (i) frames 008-032: unsedimented angular to sub-angular decimeter-sized talus; (ii) 033-043: some fresh pillows and other less distinctive extrusive forms, also talus and some fine sediment protruding blocks; (iii) 044-058: unsedimented angular to sub-angular decimeter-sized talus; (iv) 059-086: pillow lavas, some very fresh, some slightly sedimented; (v) 087-090; massive, blocky lava; (vi) 091-097: unsedimented angular to sub-angular decimeter-sized talus; (vii) 098-110: very fresh pillows; interstitial sediment minor; (viii) 119-203: lava debris, with some fine interstitial sediment; and (ix) 209-226: fine sediment with some pillows and blocks of lava protruding.

These photographs suggest that this caterpillar ridge is a relatively young feature: many of the lavas are very fresh, and are not much blanketed by pelagic sediment, and the talus deposits are apparently texturally quite immature. As with the hummocky seamount, lavas appear to be extruded predominantly in the form of pillowed flows, doubtless giving rise to the rough 'cauliflower' type of texture that characterizes the hummocky heaps common on the TOBI images.

2.9 Daily Log

February 18 (JD 49)

We arrived on site at approximately 0400 to begin the survey of Area 1. TOBI was launched at about 0500. The first TOBI line began at the southern end of Segment 16 insonifying the southeastern border of the inner valley floor. The septum between Segments 16 and 17 was crossed at approximately 1500, and we began our first northward track into Segment 17 running along the

eastern bounding fault. Sediment cover was extensive just north of the septum, but decreased sharply as we reached the axial volcanic ridge in Segment 17. Seamount #526 a large volcano (about 320 m in relief) was one of several seamounts insonified to the west of the track on the axial volcanic ridge. Seamount 526 has a smooth flat top. Hummocky flows cover the southern flank. To the east, the topography on the first fault block was sedimented with the tips of hummocks sticking through the cover. At the end of the day we approached the turn from A3 to A4 to begin the southward survey of the center of the inner valley floor.

Gossip abounds about the replacement of Joe the steward in the Saloon. Ping Pong is very popular.

February 19 (JD 50)

The turn from A3 to A4 took longer than expected, and we were finally back on the line at about 0800. This southward line is centered just to the east of the asymmetrically located axial volcanic ridge. Seamount 537 was imaged on the crest of the volcanic ridge. It is approximately 220 m high with a large crater that makes up most of the flat top. It has a seemingly smooth texture, with what appears to be a debris flow on the eastern slope. At the southern end of Segment 17 seamount 526 was insonified a second time. As the septum was approached sediment cover increased. In addition, a debris flow from the bounding inner valley wall covered a large portion of the western deep. We crossed the septum into Segment 16 late in the day, insonifying the axial volcanic ridge which is asymmetrically located to the west.

It was decided to add the crestal mountain transit to the end of the current TOBI survey, thereby saving recovery and launching times. A track to the east out over the crestal mountains and back was laid out and way points picked. Two tracks will be run with only a slight overlap in the TOBI records, providing a nearly 12 km wide swath for obtaining information on how the crust is carried away from the ridge.

Popular activities include hacky sack (still), and ping pong. Unpopular activities include keeping up to date with the cruise report.

February 20 (JD 51)

At the start of the day the turn between way points A6 to A7 was completed. The last TOBI line was begun heading north along the western edges of Segments 16 an 17. Transverse ridges with a northeasterly strike were crossed in Segment 16, as well as Keyhole Seamount. The western end of the septum was crossed at approximately 0900 and the TOBI images showed a large debris flow extending down slope into the deep at the end of Segment 17. At way point A8 the tracked turned north to head up Segment 17. The slump continued to the north along the western edge of the inner valley floor draping the volcanics for about 9 miles. W Seamount (#537) on the top of the axial volcanic ridge was insonified from the west. Way point A9 was reached at approximately 1900, and we began to make the turn to Way point S1, the start of the crestal mountain transect. At 2200 the survey of the crestal mountains had begun and we were imaging sedimented step faults of the median valley wall.

A solemn mood has taken over as people realize that we have 4 days left over for dredging and camera work.

February 21 (JD 52)

Julian Day 51 started one third of the way between way points S1 and S2 in the crestal mountains. Most of the faults imaged have throws facing inward towards the inner valley floor. There is some evidence for mass wasting on the major faults. Sediment cover appears to increase after the crest of the mountains has been reached. Volcanic hummocky topography sticks up through the sediment, and some seamounts are recognizable. At 0400 the turn was begun to way point S3. The turn was complete by 0730, and an adjacent line back towards the spreading axis was run. It was decided to continue the line across the inner valley floor into the crestal mountains on the eastern side. There appear to be differences in faulting: the fault on the western side is much steeper; and differences in sediment cover: the returns are brighter on the eastern side.TOBI surveying stopped at 0830, and the instrument was on deck at about 02030. At 2330 the ship arrived at the first dredge - a hummocky flow linking the axial volcanic ridge to the bounding scarp wall.

The meeting today discussed the scientific interest of the cruise participants. Joe led the discussion and people outlined their plans for analyzing and writing up the data.

February 22 (JD 53)

Rock dredging of Segment 17 began in earnest on Julian Day 53. Our first dredge site (RD1) was located on a hummocky flow that links the axial volcanic ridge to the bounding scarp of the inner valley floor. Although the dredge was throttled a large sample of rocks was brought back. They appeared to be sparsely porphyritic basalts, somewhat weathered. Some glass shards were obtained, also. We then moved on to RD2 a caterpillar ridge on the axial volcanic ridge adjacent to RD1. Jane led this effort and dredge came back with a sufficient rocks for study, yet not an overwhelming number to label. The ship steamed south for a few miles to RD3 located in a fissure region of the axial volcanic ridge. Scott led this dredge. Although it appeared that the dredge was lost because of the high loads recorded on the tensiometer all was well in the end. The dredge came back throttled, but carrying a commendable sampling of basalt and gravel. AD4 was located on hummocky fissure flows on the axial volcanic ridge. The dredge came back with a fine haul of porphyritic basalt (including pillow tubes), and aphyric basalt and glassy gravel. The assault on W seamount began at 1815. AD5 was located at the top of the seamount and it was hoped that the dredge would sample in the summit crater. A small but fine selection of glassy phyric basalts with glass shards with ropy texture was returned. A mud/glass sand mixture most of which got hosed over the side was in the pipe dredge. At 2340 we were on site for AD6 on the southern flanks of W Seamount.

Today had no highlights to report.

February 23 (JD 54)

The dredge from site AD6 on the flanks of W seamount came back to the surface at about 0300. Three small bags of rocks were collected from this site. These included glassy aphyric basalts with one small phyric sample. The dredge started down at AD7, a hummocky heap seamount (#532) on the axial volcanic ridge about 0330. At about 0830 the dredge was on deck and contained one large basalt piece, gravel, and mud. At 0752 the dredge was over the side again on its way to sample a hummocky pile next to AD7. Contents of the haul from AD8 included several pieces of flow top with pattering. It was decided by the captain and the pso that swim call was the

next order of the day. Roger went over the side in the Zodiak, and within an hour had the motor started with a little help from Steve. Shortly afterwards bodies started flying from the Bridge in spectacular fashion. All scientists participated (from various level decks and the ladder as well, and in various attire), and spirits were raised measurably.

After swimming it was back to business as usual. We steamed to Sumpter Seamount (AD9) and the dredge went over at about 1600. Sumpter was successfully dredged giving up one large fragment and some flow pieces. It was then decided to have a camera station at Sumpter. The day ended with the camera on its way back up and with hopes that this run would turn out successfully.

The crews bar was closed until science ends on Wednesday. The officer's bar remains open with a notice to not give alcoholic beverages to any crew member.

February 24 (JD 55)

The camera run begun the previous day did not work. There were problems with the battery discharging before it reached the seafloor, and no pictures of the bottom were taken. In addition, the weight was missing; there was no apparent damage to the camera. At 0130 we arrived at dredge site AD10, the southwest flank of Sumpter Seamount. At 0600 the dredge was back on board along with several small pieces of lava crust, including a fine piece of ropy lava. At 0730 we were at dredge site AD11 on seamount 516 in Segment 16. The dredge was back at 1132. The haul contained a fine moderate haul of platy basalt pieces with glassy tops and lustrous bottoms. At 1310 we arrived at dredge site AD12, Keyhole Seamount (# 605) in Segment 16. Numerous pieces of fresh glassy basalt were recovered. At 1830, the septum between Segments 16 and 17 (Site AD 13) was dredged. At 2243 the dredge returned with large angular manganese coated, palagonite sedimented, fracturized basalt. Some critters were also found. At 2330 the dredge started down to sample the landslide on the west side of Segment 17 (AD1 5). Site AD 14 also on the land slip was skipped.

The science meeting today focussed on the science to be done in our final days. It was decided to dredge the septum and the landslide and then to attempt another camera run on hummocky ridges on the axial volcanic ridge of Segment 17. Jimmy was fired, and moral is low with the crew.

February 25 (JD 56)

The dredge from site AD 15 arrived with a large load of rocks and sediments. Abundant serpentine and some gabbro were observed. After this a camera run was attempted on the axial volcanic ridge of Segment 17. After the camera reached the bottom it did not seem to be triggering, so it was pulled up after 15 minutes or so. When the camera reached the surface we steamed off to dredge site AD 16 a flat topped seamount on the west side of the axial volcanic ridge. The dredge was on its way down at 1000. A fine haul of glassy sheet flows with some palagonite was brought back. This was our last dredge site, and we turned our attention to obtaining bottom photographs. Apparently some of the connections had been leaking and they were packed with sealant. The camera was lowered at our last dredge site at 1523. The camera seemed to work and it was hauled back in at 2046. The total number of photographs taken was 140. When the camera arrived on deck it was seen that the main arm to the switch was bent slightly, and the flash partly knocked from its retaining clips, but otherwise it was undamaged. The switch was working fine, and all was bolted

back together again. The film had advanced the expected amount. The next camera site was on a hummocky seamount. The camera went over the side at 2320.

There was no scientific meeting today. Most (all) of the afternoon was spent labeling rocks from the landslip dredge. This day marked the last watch of some of the scientists

February 26 (JD57)

The last day of science has arrived. This has been a very successful cruise in terms of science for all participants. A second successful camera run was completed at 0320. The camera came on board slightly scratch and dented but surprisingly ok. At 0420 the camera was again over the side to photograph the caterpillar ridge at AD4. At 0622 the photo taking began. One hundred and six pictures were taken between the start and 0815 when the pinger began double pinging continuously. At 0845, we started hauling the camera in.

END OF SCIENCE.

III. Area 2, Segments 10/11

3.1 Summary

Area 2 consists of the southern end of Segment 11 and the northern end of Segment 10. These are the only two segments in the region covered by Sea Beam data between the Kane and Atlantis transform faults in which the volcanic ridges overlap as commonly seen on the East Pacific Rise. Large half graben bounding faults are observed on the western side of Segment 11 and the eastern side of Segment 10. Each of the segments has a well developed axial volcanic ridge. On the eastern side of Segment 10 south of the overlap is a major land slide (Tucholke, 1992) the front of which now marks the inner bounding scarp of the inner valley floor. To the north of the overlap in Segment 11 two volcanic ridges occupy the inner valley floor. Crustal magnetization highs are located on the western most of these.

Our work in Area 2 fell into two phases, a TOBI survey of three days followed by dredging for two days. The TOBI survey yielded images that could be given a preliminary analysis on board ship.

The features interpreted from Sea Beam as small volcanoes fall into two categories on the TOBI records. Some are round flat-topped features, sometimes with a summit crater ranging from a few tens to a few hundreds of meters in diameter. Others are irregular piles of hummocky lava. The former group has a very distinctive appearance on TOBI records, both from the characteristic regular morphology and from the surface texture, which is uniform and medium grey. The second group can only be distinguished from the surrounding abundant hummocky flow material by its topographic form.

One of the seamounts (#325, named 'That's All Seamount') on the median valley floor is especially well imaged. It is seen from both east and wes t at high resolution. From the Sea Beam swaths, it is about 1600 m in diameter, and 70 m in relief. The flat top is estimated at 1100 m wide. The TOBI images show the feature as having steep sides and a flat top cut by a large irregular crater which may be two craters coalesced. The crater has clearly formed by subsidence, and there has been some reactivation of volcanism in its centre, forming two hummocks there. The high resolution of TOBI allows imaging of small pits in the flat top only a few meters across.

Both hummocky and smooth-textured types of seamounts form isolated topographic highs, not associated with any linear features, and probably are fed from short fissures. Within the area we were able to identify other styles of volcanism, including rows of hummocks, aligned parallel to the spreading axis, and hence presumably fed by fissures, and ridges composed entirely of hummocks, which are probably the result of more copious fissure eruptions.

Area 2 contains the overlap zone between Segments 10 and 11, as interpreted from Sea Beam maps. The offset between the two segments is small, and the separate identity of the two segments is not obvious on morphological grounds. Gravity measurements were made during the TOBI surveys, and interpretations by Jian Lin on board suggest that each segment has a separate mantle Bouguer anomaly low ("bull's-eye") indicating that they are in fact separate mantle/magmatic systems.

TOBI images of the overlap zone show no first order differences between the segments. Each is characterized by a moderately sized axial volcanic ridge with abundant hummocky surface and some smooth seamounts, there are few faults imaged on the ridges. The boundary between the seg-

ments show no surface structural break, nor any simple sign of changing stress fields. Dredges were made on each side of the boundary to investigate magmatic relationships between the segments.

A diagonal TOBI line through the crestal mountains, and images from other lines of the edges of the median valley gives evidence of the evolution of the crust during transport out of the median valley. Large and small scale mass wasting is evident in most of the images of the median valley walls. The spectacular landslip of Tanner's Toe is clearly seen to overlap on the volcanic forms of the median valley floor, and is uniformly bright in back scatter. The smooth front surface of the slip contains bright solid blocks tens of meters across. Rocks dredged from Tanner's Toe are angular, even-sized decimetric blocks, with no finer material.

On the opposite side of the valley is a smaller but more complex landslip area, containing deep rotational blocks, flows of disaggregated material and slides of more coherent rock. Talus fans are very common and are seen especially well off axis. They are smooth in TOBI images, with varied shades of grey, apparently depending on the age of reworking of the surface. Active stone chutes are lighter than adjacent inactive parts of the fans.

In the crestal mountains all of the faults have the same polarity, throwing down towards the median valley. Steep slopes dipping away from the valley, which from Sea Beam maps alone might have been interpreted as outward-throwing faults, can be seen on TOBI images to be outward tilted segments of volcanic sea floor. These slopes show the hummocky volcanic texture, dotted with seamounts, characteristic of the modern median valley floor.

At the start of the inward track, some of the major faults of the crestal mountains curve from a ridge parallel direction towards an E-W trend, probably indicating a past position of the Segment 11/12 boundary.

3.2 Waypoints

The following way points define the TOBI survey of Segment 10/11. They include a 20 mile transit across the crestal mountains of the median valley (B1-B4). Waypoints and actual ship track for the TOBI survey in Area 2 are presented in Figure 3.1. Also in the figure are seamounts which have been previously identified from Sea Beam bathymetry (Smith and Cann, 1990, 1991), axial valley highs, and historical earthquakes in the region (relocated by Lin and Bergman, 1990).

B1) 27° 08.5'N 44° 07'W -Deploy TOBI; start crestal mountain transit

B2) 26° 54'N 44° 22'W

B3) 26° 49.8'N 44° 26'W

B4) 26° 48'N 44° 31'W- Start inner valley floor survey

B5) 26° 35.6'N 44° 34'W

B6) 26° 26.2'N 44° 39.2'W

B7) 26° 26.5'N 44° 40.5'W

B8) 26° 36.2'N 44° 35.2'W

B9) 26° 55.5'N 44° 31.4'W

B10) 26° 55.5'N 44° 32.7'W

B11) 26° 43.5'N 44° 35.2'W

B12) 26° 27'N 44° 42 0.0'W- Pull TOBI

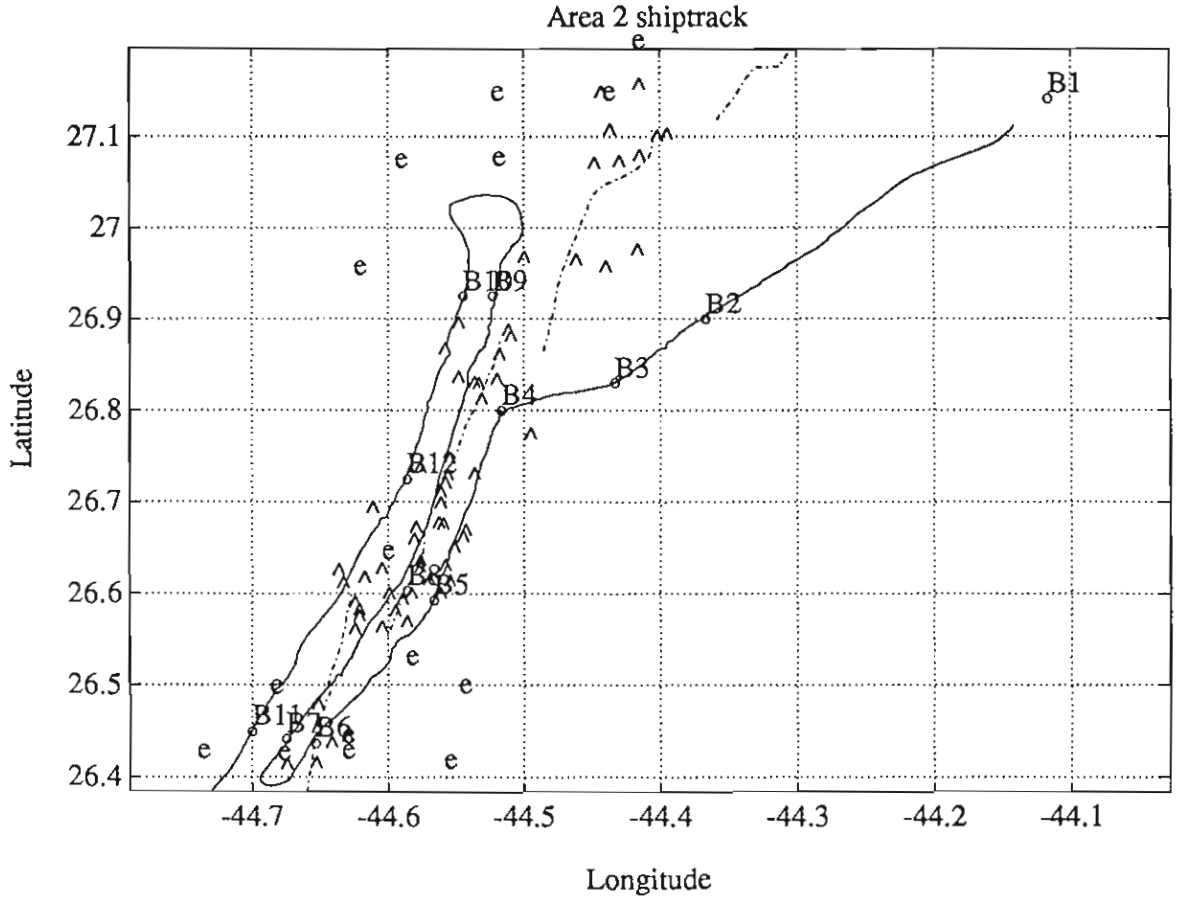

Figure 3.1 Area 2 ship track

Waypoints (text labels), shiptrack (solid line), axial volcanic highs (dashed lines), earthquakes (e's), and Sea Beam identified seamounts (^'s) for Area 2.

3.3 TOBI Run, Track line images

TOBI images for the entire Area 2 survey are shown in Figures 3.2 through 3.6. The images presented on these pages have been severely downsized from the original data. Each scanline of data (across track) in its original form contains 8000 pixels of information, 4000 to port and 4000

to starboard. Each pixel in the original data covers 0.75 meters of the seafloor. Distance from the TOBI sled and TOBI altitude affect this coverage so the 0.75 meter value should be taken as approximate. Along the ship track the original data contains a ping every 4 seconds for an along track pixel size of 4.0 meters. Again, as ship speed, distance from TOBI, and TOBI altitude affect this coverage, the 4.0 meter valued should be used as an approximation. In total, TOBI produces 8000 pixels of information every 4 seconds or 900 scanlines of 8000 pixels every hour.

The images in Figures 3.2 through 3.6 each represent approximately 4 hours, 27 minutes of information (4000 scanlines of 8000 pixels each in the original data) with time progressing from the top down in each frame. The original data has been reduced to 800 scanlines of 200 pixels each of the strips in the figures. Detailed images of certain interesting regions are outlined in white boxes and are presented in the next section. Rock dredge sites are also indicated on the images.

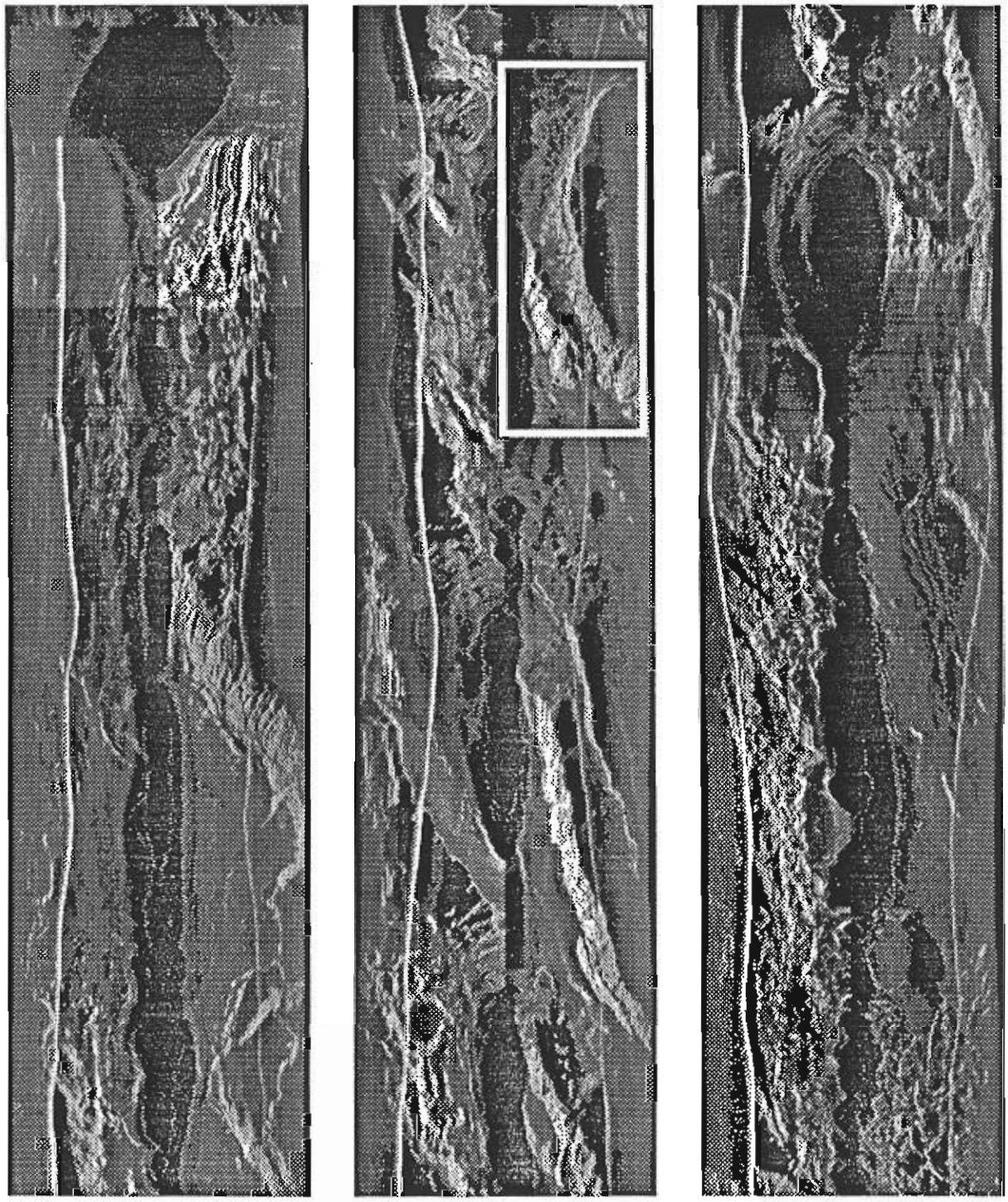

Figure 3.2 TOBI images starting 1840/032 Z.

Time progresses from left to right frame by frame and from the top down in each frame. Each strip contains approximately 4000 TOBI pings for a total time of approximately 4.44 hours per strip. This run came down crestal mountains into the median valley floor. The Texas Two Step Fault outlined in white box is described in detail below.

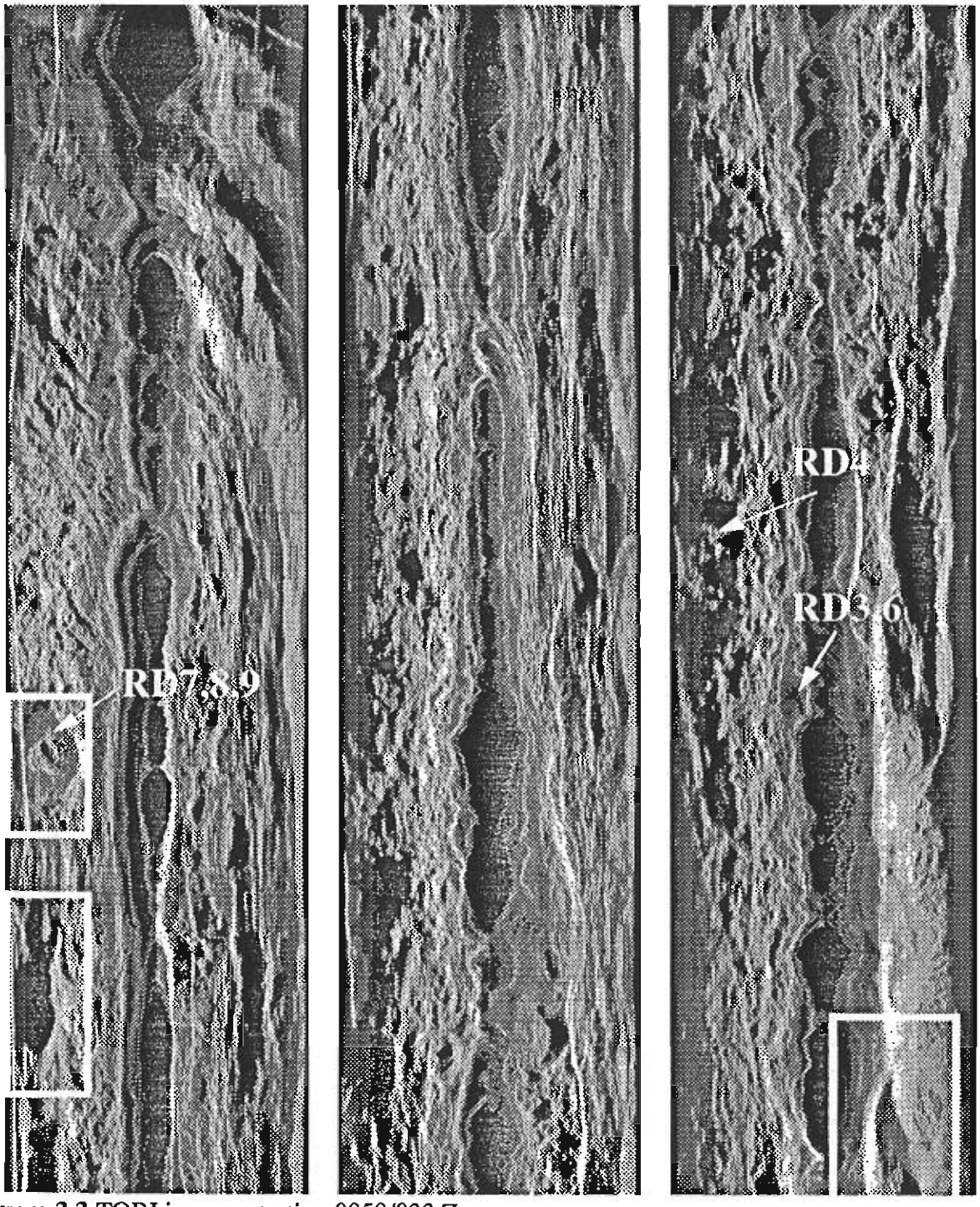

Figure 3.3 TOBI images starting 0858/033 Z.

That's All Seamount, the hummocky volcanic ridge, and Tanner's Toe are outlined in white boxes and described in detail below.

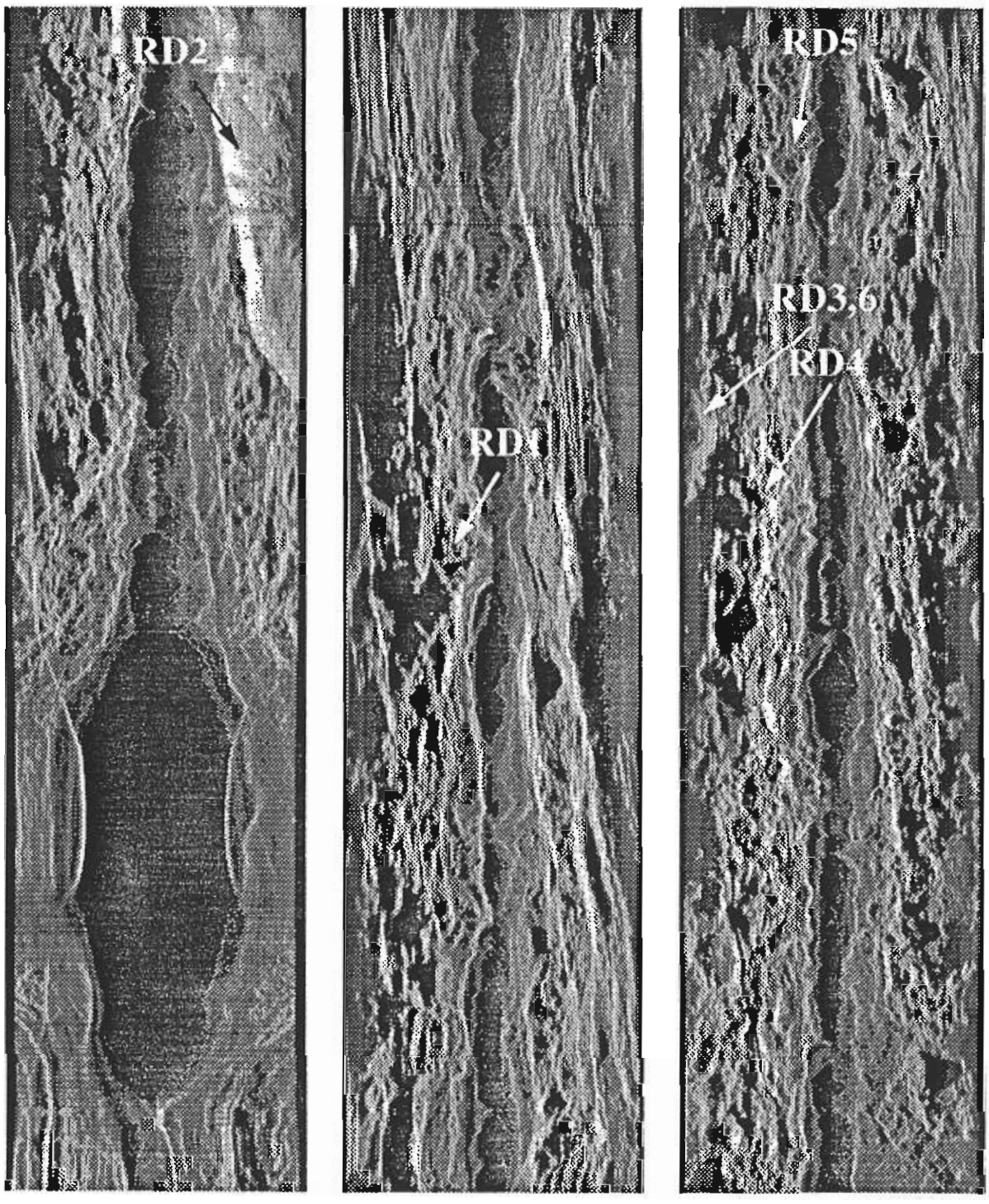

Figure 3.4 TOBI images starting 2222/033 Z.

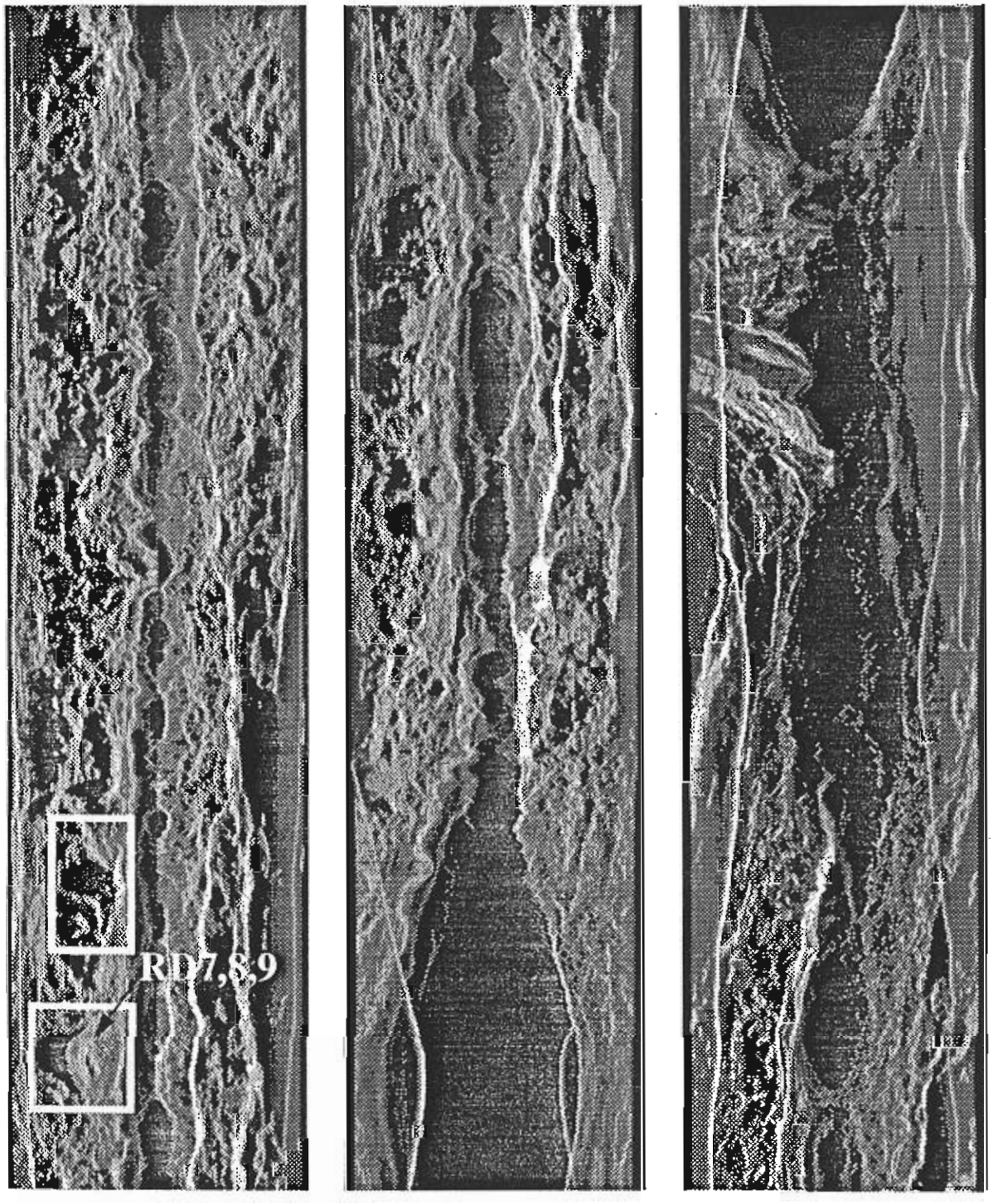

Figure 3.5 TOBI images starting 1147/034 Z.

That's All Seamount and the hummocky volcanic ridge outlined in white boxes and described in detail below.

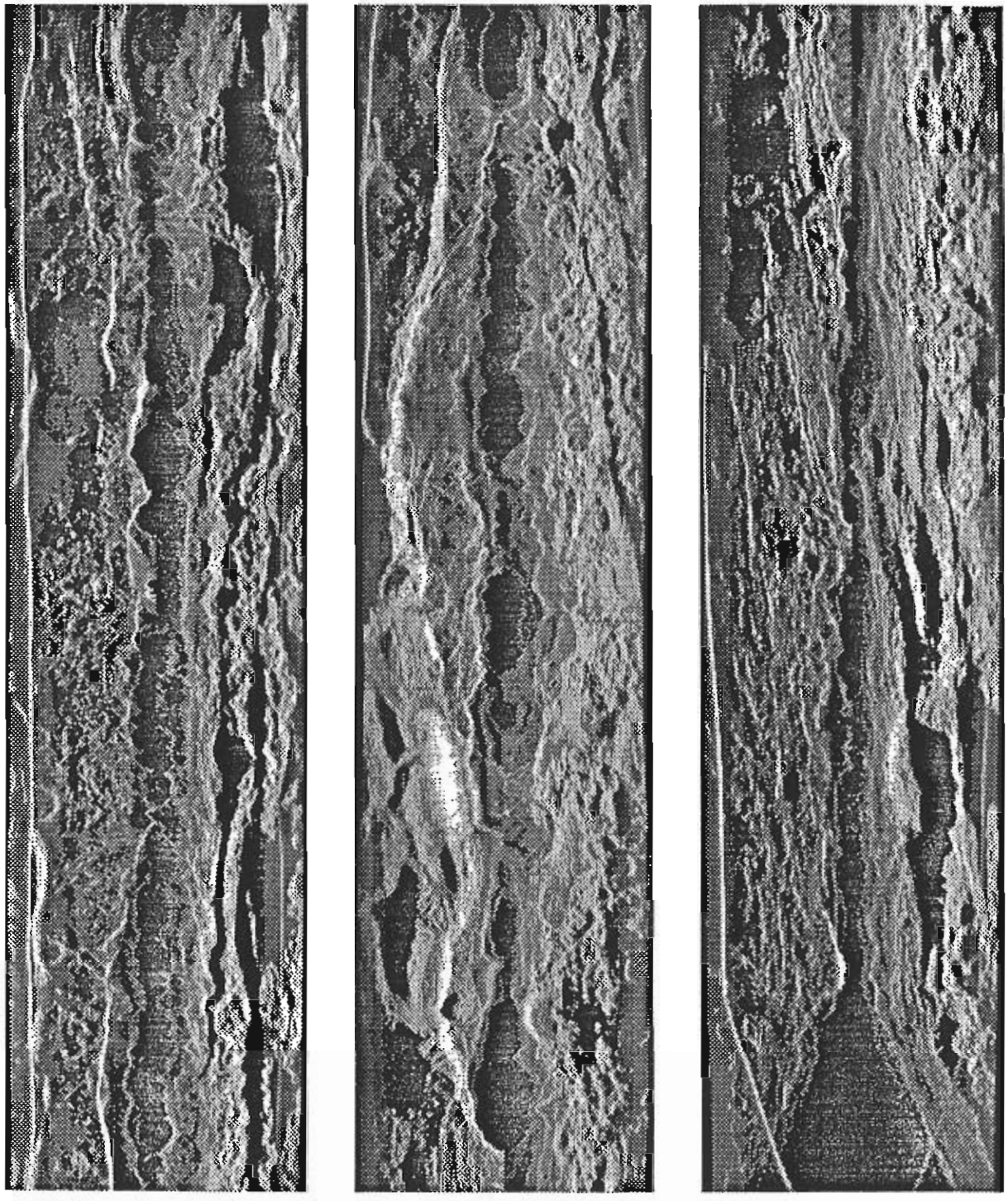

Figure 3.6 TOBI images starting 0103/035 Z2.

3.4 TOBI Run, Detailed images

A number of sections of Area 2 TOBI images were chosen for detailed image analysis.These are presented below in Figures 3.7 through 3.11.

3.4.1 Texas Two Step Fault

This is located on the transect down through the crestal mountains into the median valley (see Figure 3.2). The TOBI images shown here are dominated by extensional faults (oriented 210°, and dipping towards 300°) and associated tilted blocks offset by a lateral ramp (oriented 100°). The faults both show evidence suggesting the development of talus slopes which are in turn draped by pelagic sediment.

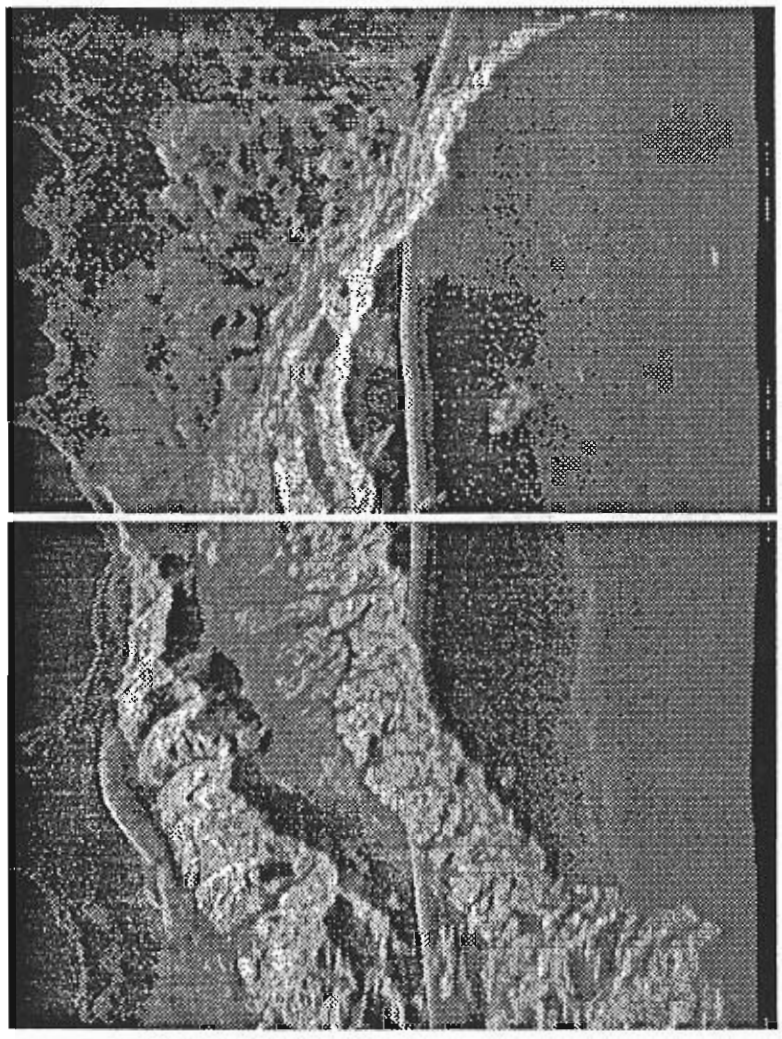

Figure 3.7 Texas Two Step Fault

Lateral ramp transferring the extensional deformation onto the Texas Two Step Fault. Note sediment covered hummocky terrain at the base of the lateral ramp. Note also the well developed, partially sediment covered talus flows.

3.4.2 That's All Seamount

About 1 kilometer in diameter, That's All seamount is characteristic of a group of seamounts with smooth, flat tops and large central craters. The sides of the seamount are apparently talus on the east though flows from the summit have spilled over the edge to the north and south. The crater shows arcuate fractures near its western rim indicating that the crater originated by collapse. Subsequent to the collapse, two small cones formed within the crater during a resurgent phase. Other seamounts of this class have larger resurgent mounds in their craters which sometimes spill over the rim of the crater itself.

The two images in Figure 3.8 are at different slant ranges from the TOBI vehicle so that the left hand image, further from the track, has a lower resolution than the right hand image. On the higher resolution, right hand image, a number of small pits and mounds can be seen on the otherwise entirely flat top of the rim surrounding the crater.

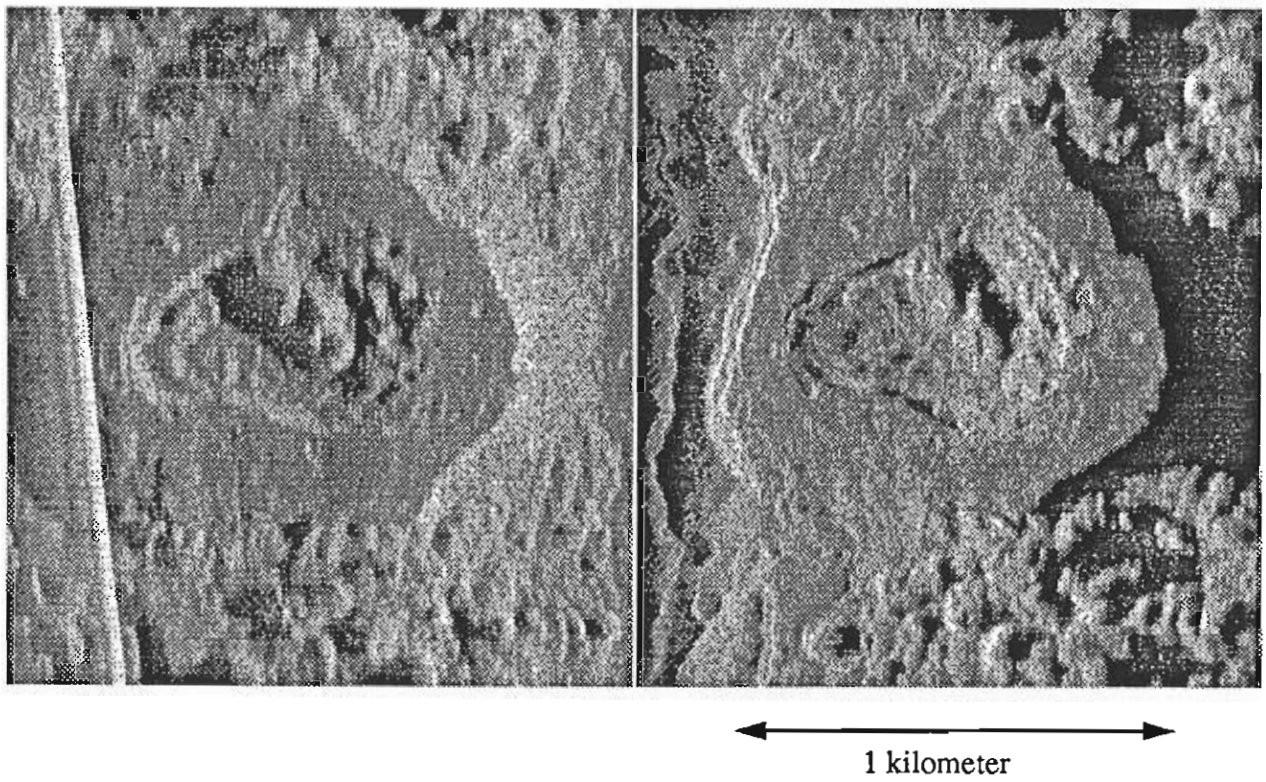

Figure 3.8 Doubly insonified That's All Seamount.

The image on the left has been insonified from the east and is near the edge of the TOBI swath. The right hand image has been insonified from the west and is very near the inside edge of the TOBI swath, hence its higher resolution

3.4.3 Hummocky Volcanic Ridge

Just south of That's All seamount is a ridge constructed from hummocky flow units. These two images show the same ridge insonified from east and west. It is difficult at first to realize that

the feature is the same one, but careful examination of details on the images enables a good correlation to be made. Note that the insonification from the east suggest that the ridge has the form of a simple whale back, while that from the west reveals it to be a more irregular pile of hummocks. Such elongate hummocky forms are probably fed from rather substantial fissures rather than from the pipes or short fissures which appear to feed seamounts.

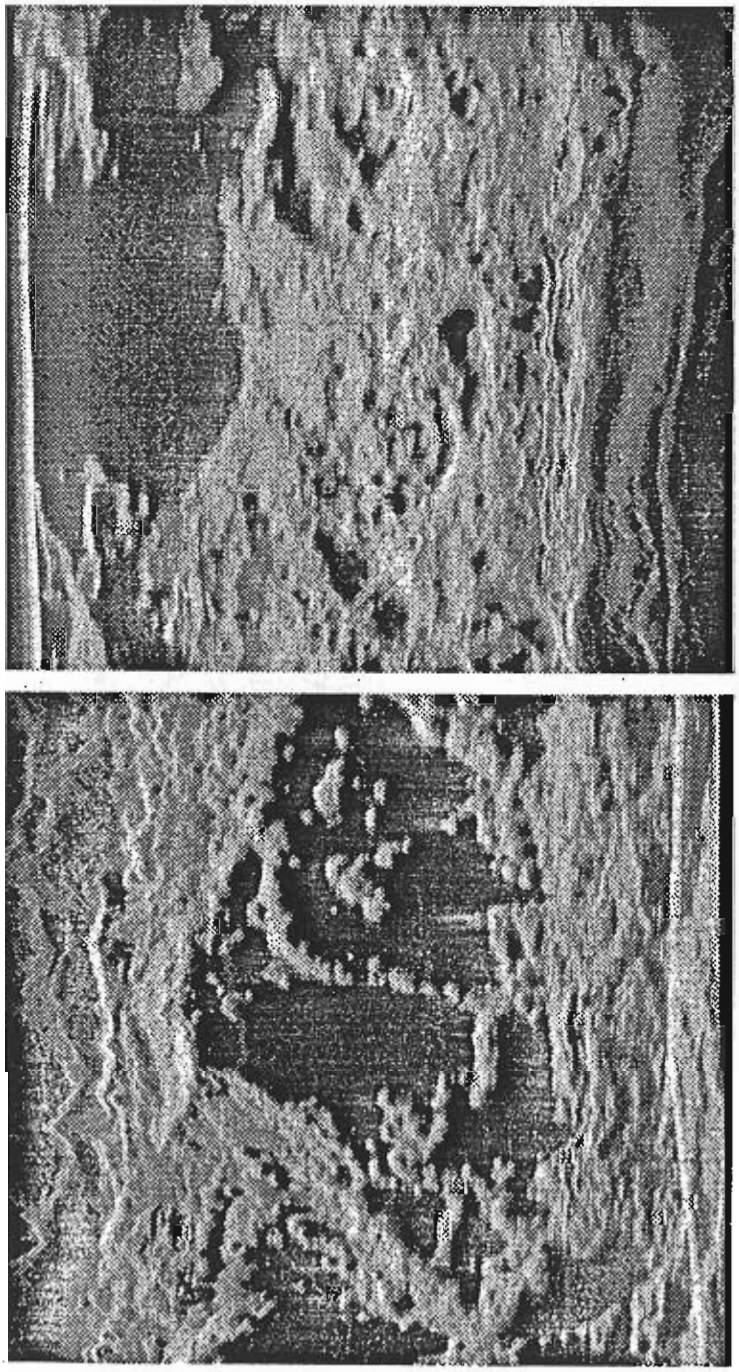

Figure 3.9 Doubly insonified volcanic constructional ridge

3.4.4 Tanner's Toe

Sea Beam morphology suggests that the hammer-headed projection into Segment 10 is a major slope failure of the median valley wall (Tucholke, 1992). These images show the front of the feature, here named Tanner's Toe, as it overlaps on to the constructional volcanic morphology of the median valley.

The image on the left shows the northern end of the front of this landslide overriding the hummocky volcanic morphology of the median valley floor and also a fault block at the edge of the median valley. The right image adjoins the left hand image to the south. On both images, the front of the debris flow is steep and a very bright scatterer. The lower part of the slope has probably been reworked by downslope mass wasting. On the upper part of the slope outcrops of what appear to be major blocks transported in the slide can be seen.

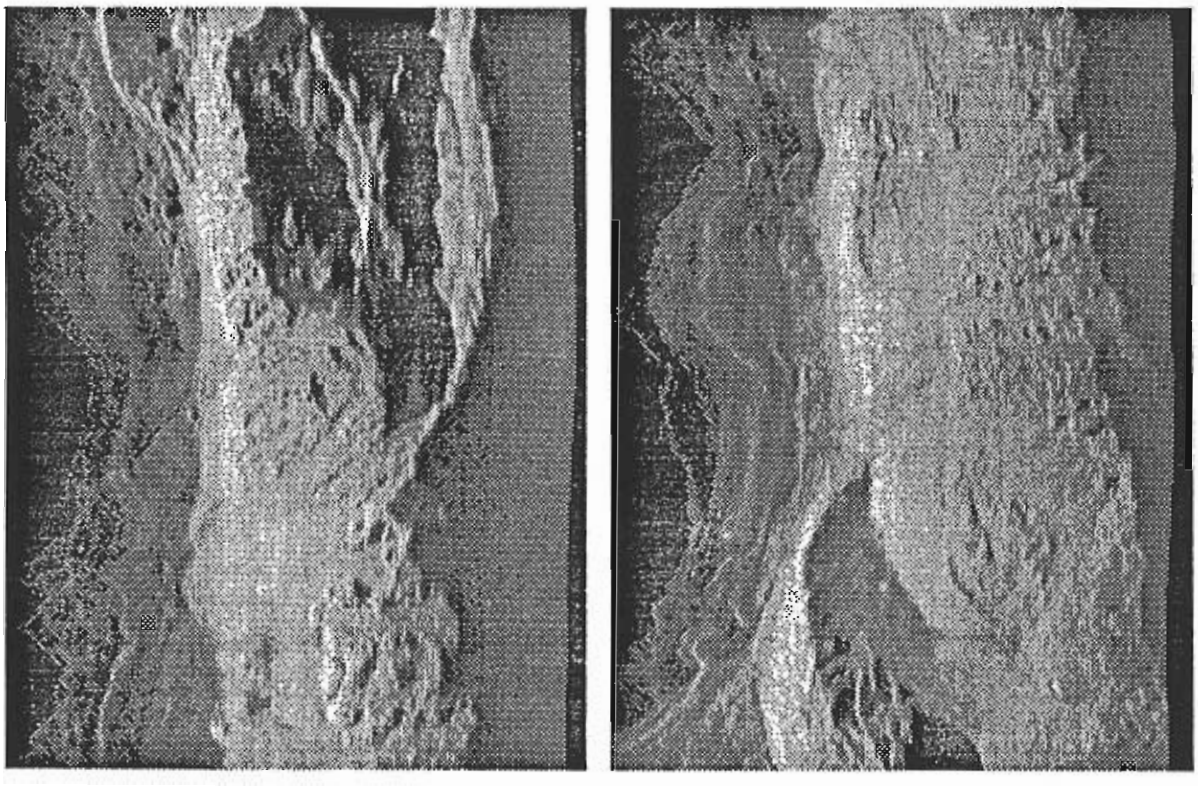

Figure 3.10 Tanner's Toe

Two views of Tanner's Toe, the image on the left being located immediately to the north of the right hand image. Tanner's Toe is a submarine landslide which displays a combination of large fault blocks and debris flows.

3.4.5 Kingdome Seamounts

The westernmost TOBI track in this area imaged the surface of the first fault block up from the western median valley floor. A large proportion of this fault block is covered with hummocky lava flows, itself blanketed in sediment. In a number of places, however, small, sediment-covered seamounts can be seen and this image shows two of these. The low backscatter from the surface of these seamounts is a result of their sediment cover. The northernmost seamount of the pair shows an unusual dome shaped cross-section with a small pit crater at the center.

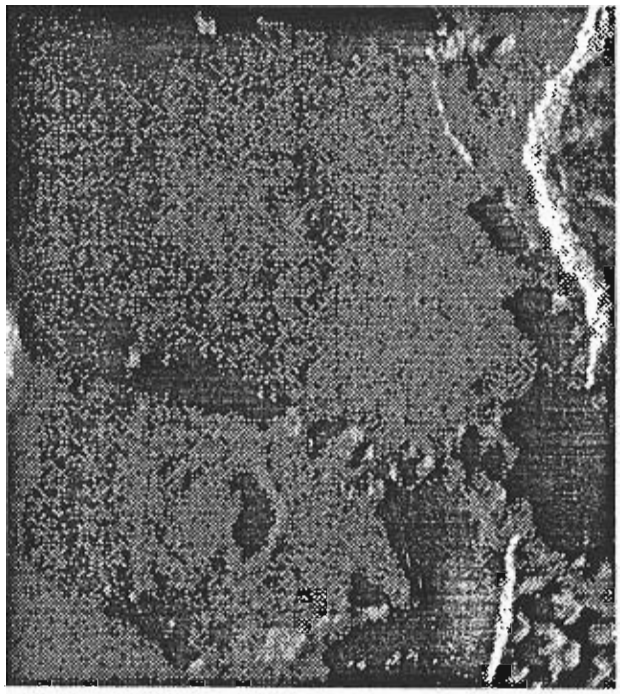

Figure 3.11 The Kingdome seamounts.
These features are located on the first, off-axis fault block to the west of the median valley. The low backscatter amplitude is because these are partially buried by pelagic sedimentation.

3.5 Geological map description

Detailed interpretation of the TOBI images of each area included the production of a geological map. These maps, although only preliminary interpretations and lacking bathymetric data, have been useful in underlining the spatial distribution of the volcanic edifices, faults and landslides that have been imaged. Description of individual features has already been included in the summaries, so the discussion here will be limited to the interaction observed between the different processes.

Area 2 focuses on the overlap of the two segments, 10 & 11. Although this segmentation is obvious from the bathymetric data there is no apparent change in the volcanic style across segments nor any obvious tectonic break shown on the geological map. Both segments are characterized by robust axial volcanic ridges comprising hummocks and isolated, often partially buried seamounts. These seamounts show their greatest concentration on the periphery of the AVRs whilst hummocky terrain dominates along the axis. It is as yet uncertain as to whether this spatial distribution is a function of an initial intrusive pattern of seamounts relative to hummocks or if the seamounts on axis are buried.

The lack of an obvious tectonic break along the axis between segments suggests that either the present configuration of AVRs is relatively new (so that insufficient time has elapsed to create the inevitable space problems) and/or that magmatic production is such that any faults that existed have subsequently been buried. The fact that very few faults are illuminated within the neovolcanic zone together with the overall lack of sediment supports the second view. The only faults that do occur on axis are small in outcrop and tend to be associated with the termination of larger off-axis faults. Outside the neovolcanic zone the fault population increases. The first faults occur at a distance of 2-4km from the central axis, which they parallel. These are en echelon, curvilinear in outcrop and show a consistent throw towards the axis. Their size and distribution varies along the length of the axis relative to the segmentation. Large faults (those extending for several tens of kilometers) are characteristically found adjacent to the central parts of the segment. These usually display a half graben geometry with associated back rotated tilt-blocks. The faults either terminate in a splay of minor faults or show a decline in outcrop accompanied by a rotation towards the neovolcanic zone.

Erosion of the fault scarps is common as shown by the development of gullies and extensive talus slopes. Sedimentation on the back-tilted blocks is mainly pelagic (showing low back-scatter). Smaller faults (up to a kilometer in length) are common throughout but show their maximum concentration at the outer edges of the median valley adjacent to the segment ends. These create a multi-stepped (terraced) geometry reminiscent of those seen on continental hillsides. Along the western edge of the axis this concentration of faults gives way to a landslide. This is characterized by debris flows (bright reflectors) which appear to partially bury a large fault. A similar pattern is seen at the eastern edge of the median valley where a series of large faults are also partially buried beneath a landslip. The position of both landslides corresponds to the tip of the segments.

3.6 Dredging

The following sites were dredged in Area 2. On deck observations, hand sample descriptions, and thin section descriptions are given. Rock dredge locations are also shown in Section 3.3.

RD1) 26°27.7'N, 44°39.4'W, Depth 3375 m, 58 rocks + gravel

Seamount 284 located on the axial volcanic ridge of Segment 10. Lots of glassy basalts were obtained - sheet flows, pillow buds, and lots of fresh shining basalt glass shards. No animals were found although a few worm tubes were evident.

Hand specimens. Very fresh, sparsely porphyritic (< 1% plagioclase phenocrysts, < 1cm in diameter), glassy basalt with black glass exterior rind (0.5-4.5cm thick) and pale grey aphanitic interior. Rocks have angular and pillow shapes, range from decimeter to gravel-size, show minimal vesicularity, have cracks occasionally lined with pale brown mud, and show some alteration to palagonite. A few worm tubes are present on the rock surfaces.

Thin sections. All the sections displayed a similar mineralogy and crystallinity. The groundmass consists of a felted mat of acicular plagioclases and acicular olivines. These form 40-50% of the mode. The remainder of the groundmass is composed of isotropic brown glass. Plagioclase dominates over olivine within the groundmass, forming hollow box like basal sections. An aspect ratio of 10:1 is the common form of plagioclase. Olivines typically form a chain morphology with a subrounded nucleus. These textures are indicative of rapid growth, probably as a result of quenching. The phenocrysts represent approximately 5-10%

of the total rock. Plagioclase was the only phenocryst phase found. It commonly had an anhedral form, with epitaxial growth around the crystal boundary of a more sodic chemistry. An extinction angle in the range 31-35 (bytownite/labradorite) was measured in the phenocrysts. The presence of phenocrysts throughout the basalts implies plagioclase nucleated and grew pre-eruptively. RD2.1 contains unequivocal evidence for communist infiltration into the Hyperbarian community.

RD2) 26°28.8'N, 44°36.2'W, Depth 3930, 29 rocks

Tanner's Toe, the end of a large land slide. The dredge contained a collection of heterogeneous blocks (10-50 cm in diameter) One rock appeared to be a dolerite (from a dike).

Hand specimens. Slightly altered, sparsely porphyritic (< 5% plagioclase phenocrysts, < 1cm diam.), green-grey pillow basalt. Rust-brown, palagonitic alteration is seen on the (~1cm. thick) glassy rind and in cracks. Rocks are angular and range in size from decimeter to gravel size

Thin sections 1. Olivine and plagioclase exist both as phenocrysts and in the groundmass. The latter is composed of acicular plagioclase and subrounded, glass enclosing, olivines. Both are anhedral and lie in a isotropic glassy back ground. The phenocrysts are dominantly plagioclase (70:30), and all subhedral. The extinction angle of the plagioclase is in the range 32-40.

2. Holocrystalline rock with a 60:40 ratio of plagioclase to olivine in the groundmass. Olivines are subhedral to anhedral while plagioclase is euhedral Cubic opaques are ubiquitous and commonly associated with both the plagioclases and the olivines. The phenocrysts have 80:20 plagioclase to olivine ratio. The extinction angle of the plagioclases are in the range 30-34, with some displaying more calcium rich cores.

RD3: 26°32.9'N, 44°35.4'W, Depth 3790 m, 4 rocks

Seamount 290, seamount with smooth texture located in Segment 11 just to the north of the overlapper. Only 4 small fragments were returned in the pipe dredge. The net dredge was empty. The fragments (maximum size 30 cm) were fresh plagioclase.

Hand specimens. Slightly altered (patchy palagonitic coatings on glassy rind), moderately porphyritic (<25% plagioclase phenocrysts), angular, gravel-sized, black glassy basalt

RD4: 26°33.52'N, 44°35.71'W, Depth 3744 m, 136 rocks

Seamount 293, rubbly heap of hummocks just west of Seamount 290 (RD3) in Segment 11. Blocks 5-20 cm in diameter were obtained, as well as gravel. The pillows are not very fresh. The basalt is aphyric and has a thin manganese coating. Two small bits of pelagic mud were seen.

Hand specimens.

a) 1 rock. Moderately altered (patchy palagonitic coatings on glassy rind), moderately porphyritic (~25% glomerocrystic (?) plagioclase, <1% olivine phenocrysts), black pillow basalt with glassy rind and aphanitic interior groundmass. The rock is angular, decimeter-

sized, and anomalous in this dredge.

b) 135 rocks. Highly altered (palagonitic coating on dull-lustered glassy rind), aphyric blue-grey basalt with glassy rind and aphanitic interior. Rocks range from angular to pillow-shaped and decimeter to gravel-sized. Some samples show circular (~1mm diam.) devitrification spheres while others show rust-brown devitrification (?) lineations near the exterior rind.

Thin sections.

Microporphyritic pillow basalt RD 4.1

Thin section of variolitic margin. Acicular plagioclase, olivine plus glass are the dominant groundmass constituents. Both the plagioclases and olivine forms are typical of rapid quenching. The plagioclase microlites are up to 0.2mm in length and display simple Albite twins. Olivine are acicular and subrounded with a maximum size of 0.1mm.The phenocrysts are plagioclase with subordinate olivine, maximum size is 3mm. The plagioclase shows both a sieve texture and a uniform subrounded texture with a length of 10mm. The largest extinction angle found was 38 degrees. Olivines tend to from in small clusters of subrounded anhedral crystals.

Aphyric pillow basalt RD 4.5, 4.17, 4.29, 4.54, 4.75.

Thin sections taken from glassy rind to variolitic margin. Sections vary from almost holocrystalline to 60:40 glass to microlitic plagioclase and olivine. The plagioclase is acicular and subhedral to anhedral, displaying hollow box and rail track forms. Largest plagioclases are 0.5 mm in length, with a 10:1 aspect ratio. Olivines are subordinate and subrounded with sizes in the range 0.1 to 0.2 mm. Section 4.29 have acicular olivines with a central boss. Section 4.54 is the only one to display preferred orientations of microlites.

RD5) 26°32.0'N, 44°37.4'W, Depth 3679 m, 1 rock + gravel

Hummocky terrain next to Seamount 288 located in Segment 10, south of the overlapper. About 1 kg of glassy shards of basalt were recovered. The rocks were porphyritic with plagioclase megacrysts. One piece of aphyric holocrystalline basalt was also in the dredge.

Hand specimens.

a) ~1kg. of gravel shards. Slightly altered (patchy palagonitic coating on rock surfaces), sparsely porphyritic (~5% plagioclase megacrysts), angular, gravel-sized, black glassy basalt.

b) 1 rock. Aphyric, angular, large gravel-sized, black basalt. Rock shows "strange white weathering pattern on one side."

RD6) 26°33.0'N, 44°35.4'W, Depth 3884 m, 23 rocks + gravel

Seamount 290, revisited (see RD3). This was a very successful dredge this time with 6 large blocks of basalt recovered.

Hand specimens. Manganese-coated, moderately porphyritic (~15-20% plagioclase phenocrysts), dark grey, angular, decimeter-sized, pillow basalt

Thin sections.

Porphyritic pillow basalts RD6.3, 6.5 & 6.22.

The groundmass contains flow banded plagioclase microlites and olivine. The plagioclase microlites are acicular some with a sieve texture on the least acicular crystals. The olivines are anhedral with acicular tips. Maximum size of the plagioclases is 0.4mm while the olivines are 0.1 mm. The phenocrysts are sieve textured plagioclase laths and subrounded olivines. Plagioclase to olivine ratio is 60:40. The sieve textured plagioclases contain glass inclusions, and show multiple twinning. Some subrounded plagioclase basal section have no inclusions and show a different extinction angle for the last growth phase. An extinction angle of up to 33 degrees was found. The olivines are seen to cluster into groups, and are subrounded with a maximum size of 1 mm

RD7, RD8, RD9) 26°47.5'N, 44°32.6'W, Depth 3505 m

Seamount 325, located in the northern part of the survey. It was imaged first as we turned into the median valley floor from the transit line in, and then on the survey line heading north. It is a classic flat-topped seamount with smooth texture. In RD7 eight chips of basalt glass were recovered in the pipe dredge. We repositioned and lowered the dredge for RD8. This time several small glassy fragments were recovered and one micro pillow lobe. The glass is very vitreous, with little or no devitrification. Some orange palagonite in pillow rinds was observed. The glass is aphyric to sparsely plagioclase-phyric. RD9 again was lowered on the top of Seamount 325 for a final try for rocks before commencing with the camera runs. RD10 returned with no rocks and a pipe dredge filled with beige mud. Some of the mud formed clumps with a high density of shells. Small glass shards were also observed.

Hand specimens, RD7. 10 gravel shards. Slightly altered (patchy palagonitic coating on rock surface), aphyric, glassy, angular, gravel-sized, black basaltic rind shards.

Hand specimens, RD8. 1 rock +gravel. Sparsely porphyritic (~1 cm plagioclase phenocrysts), angular to rounded, large gravel-sized, black basaltic glass.

Hand specimens, RD9. mud. Beige pelagic mud, ~0.5 cubic meters in volume, which contains fine white shell fragments and fine black shards

3.7 Underway Geophysics

See Chapter 7 for a summary of overall gravity and magnetics work.

3.8 Camera Run

Camera station 1: SE edge of 'That's All' Seamount lat: 26° 47.3'N long: 44° 31.7'W

Operations. The BATHYSNAP camera was deployed at 1000/037, using the CTD wire from the starboard winch. Winching was found to be very difficult because of the extremely light weight of the camera system; accordingly wire had to be paid out very slowly, and the bottom

was only reached at 1520 Z. We detected our first 2 Hz return signals (indicating that the camera was operating) at 1524 Z for approximately two minutes. At this point it became clear that the 6-8 second cycle time set on the Simrad echosounder display gave us insufficient time to raise or lower the camera with the precision needed to get the camera to its 1-4 m operating altitude, without serious risk of our piling it into the bottom with some force. Nevertheless, we were able to detect two further series of two-second returns, of the order of 1-2 minutes duration each, at 1534 Z and 1548 Z, respectively. However, after this latter sequence the 2 Hz signal continued after we raised the camera clear of the bottom. This suggested to us that the weight had probably been torn off and, since we had no reliable means of maintaining the camera 1-4 m from the seabed, we decided (at 1556 Z) to abort the run. The camera system reached the surface at 1812 Z, and found to have the bob line wrapped around the frame.

Results. Upon processing some 28 images were obtained. They cluster in three groups on the negatives, presumably corresponding to the three double ping 'events' that we were able to detect on the echosounder. These clusters of images, however, were separated by blank frames and lay almost half way through the 15m roll of film. This implies that the camera had been firing continuously for approximately 40 minutes before we hit the bottom, and therefore that the reed probe from the switch to the camera had short-circuited at some stage in the water column upon descent.

(i) Negative frame nos. 177-186 (1524z, ship's position 26° 47.33'N 44° 31.71'W): slightly sedimented flat to slightly bumpy lava surfaces, possibly with some magma drainage/collapse structures; probably sheet flow tops.

(ii) Negative frame nos. 203-217 (1534z, ship's position 26° 47.31'N 44° 31.73'W): well-developed fresh pillow lavas, with minimal amounts of pale sediment at pillow interstices. Magma inflation lineations visible on pillow surfaces; hyperbarian grazing trails common.

(iii) Negative frame nos. 274-279 (1548z, ship's position 26° 47.37'N 44° 31.74'W to 26° 47.36'N 44° 31.72'W): slightly sedimented flattish lava surface, sometimes blocky; hyperbarian trails abundant. Probably sheet flow tops.

3.9 Daily Log

February 01 (Julian Day 32)

By the morning of 01 February the wind had shifted from southeast to southwest. The ship arrived at way point, 27° 08.5'N, 44° 07.0'W at approximately 1800. Weather improved remarkably to allow for TOBI deployment. TOBI was over the side and wire paying out at 1846. The winch was stopped at 1954 with 2924 m of wire out. TOBI surveying began on a heading of 221 and a speed of 1.5-2.0 kts. The new flotation magnetometer was deployed at 2015. A bird was seen flying around the ship. Sargasso sea weed began to get more dense. Joe saw a flying fish! Hacky-sackers lose three balls over the side thanks to Eddie M.

TOBI surveying began at 2000. This portion of the survey was chosen for its relevance to the ARSRP (Acoustic Reverberation Special Research Project). It will give an indication of how young, newly created seafloor is faulted and carried away from the median valley to become 'generic' seafloor scatterers.

February 02 (JD 33)

The TOBI transit line that was begun on Julian day 32 (Way Points B1-B4) took a straight line diagonally across the crestal mountains and down the staircase of faults into the floor of the median valley. The diagonal orientation was designed to insonify structures both parallel and perpendicular to the MAR axis. The structure revealed by the swath is essentially simple. Over the 50 kms of swath there are six major faults, all throwing down to the median valley. Between the faults are tilted surfaces of hummocky volcanic terrain with occasional seamounts, identical to that being formed currently within the median valley. The surfaces are tilted away from the median valley, suggesting rotation during faulting. The block nearest to the median valley has a morphology suggesting that it is a large portion of an axial volcanic ridge from the median valley floor, recently upfaulted. The faults are not simple straight features, but are linked by transfer faults into lozenge shaped blocks. The fault scarps show a variety of erosional features and often develop large talus fans at their bases. Sediment covers much of the surfaces of the fault blocks, and is especially thick in local basins. It fills in hollows between lava hummocks, and partially drapes some of the fault surfaces.

At waypoint B4 we dropped into the median valley graben, and turned south-southeast towards waypoint B6 and began surveying along the axis. Soon after the turn seamount #325 was observed. Faulted and fissured topography as well as part of the major graben bounding fault was imaged to port. Remnants of the hummocky topography typical of an axial volcanic ridge were identified in the faulted terrain. In addition, a few fissured and faulted seamounts were found. It was seen that fine scale fissuring grades into 1 or 2 larger scarps along the strike of the axis. Across axis, faults increase in throw towards the edge of the inner valley floor.

The axial volcanic ridge was imaged to starboard. The axial volcanic ridge consists of hummocky topography with small wavelength highs superimposed. A few scattered seamounts distinguished by their flat-tops, circular outline, and especially their smooth texture were noted. The axial volcanic ridge along this survey is primarily unfissured and unfaulted. In one section the hummocky axial volcanic ridge topography extends eastward and links the volcanic ridge with the graben bounding fault.

Near the end of this section of TOBI data the toe of a major landslide identified by Tucholke (1992) was imaged. The day ended about 1.5 miles north of way point B6.

February 03 (JD 34)

The day began at the end of the first TOBI line in Area 2 just north of waypoint B6. The ship took a simple approach to the 180^{0} turn between way points B6 and B7. It took three and one half hours between passing way point B6 with TOBI and B7 on the way back heading north, though some useful records were obtained before way point B7 was reached. On the beginning of the run north the track followed the axial volcanic ridge of Segment 10, and at approximately 0900 crossed the boundary between segments 10 and 11 as defined by the volcanic topography. There was no large scale evidence in the topography for this boundary in the TOBI images, The seafloor is covered in uniform hummocky flows. As the track followed the axial volcanic ridge of Segment 11, more seamounts appeared in the record than had been seen on the previously run track from points

B4-B6. A good image was obtained of seamount 325 with its flat top and crater containing some hummocks. Some seamounts were partly buried and fractured (and not identified as seamounts on the Sea Beam data), but many other volcanic knobs from the Sea Beam map proved to be heaps of hummocks rather than distinctive flat topped, smooth-textured seamounts.

On the track continuing through way points B8 to B9, a small fault paralleling the track to the west gradually grows larger until it becomes the southern end of the western median valley fault of Segment 12. The northern turn from B9 to B10 was extended approximately 3 miles north to include the survey of the faulted block at the edge of the inner scarp. The turn began at about 1900 hours, and was hampered by the strengthening southerly wind, giving a large component of northerly drift.

This area was officially christened the Pet Cemetery. The landslide was named after Ben Brooks' dead cat: Tanner's Toe. The axial volcanic ridge was named after Chris MacLeod's dead cat: Whiskey Ridge; and the large deep just north of the overlapper on the west side of the valley floor was named after Rachel Pascoe's dead cat: Bailey's Bottom. No more dead cat names will be allowed, only dogs.

February 04 (JD 35)

Way point B10 was reached at approximately 0100. It took about 6 hours to complete the turn. Upon obtaining our southerly course, the survey followed a volcanic ridge (through way point B 11) located in the first fault block up in the crestal mountains (presumably a fossil axial volcanic ridge). The ridge dead-ended in a large deep. The survey line continued to the south along another fossil ridge which began just south of the deep. At approximately 0900 when trying to bring in TOBI wire, the winch took a loose turn and hauling the wire had to be stopped. Because we were just coming out of the deep over an escarpment and had to decrease the depth of TOBI, the ships speed was increased to 2 knots. Problems with the winch were sorted out at 0933, we began hauling in, and the ships speed was decreased to 1.5 knots. Another land slide was spotted in the deep at the south end of the last survey line. The ship continued south running along another fossil ridge

The TOBI survey for Area 2 was completed at way point B12 at 1330. At 1420 the depressor weight was on the deck. After TOBI was secured we proceeded to dredge station RD1. Seamount 284. The dredge was put over the side at 1731. It was on the bottom at 1928 and we began to dredge across the top of the seamount which appears to be a pile of hummocks rather than the smoother texture observed on some isolated seamounts. The dredge was back on board at 2040. It was biologically disappointing, just a few worm tubes that we did not curate, but very successful in obtaining rocks. The rocks appeared to be mostly glassy basalts - sheet flows, pillow buds and lots of fresh shining basalt glass. Because GPS was down when the dredging was finished at site RD1 we did not begin dredging immediately at the next site.

We began lowering the dredge at approximately 2340 at site RD2. This site is on the front of Tanner's Toe.

February 05 (JD 36)

The day started with the dredge being lowered at site RD2 on Tanner's Toe. At 0130 the dredge was on the bottom. It was back on deck at 0225. This dredge contained a heterogenous collection of blocks 10-50 cm in diameter. One appeared to be a piece of dike. There was no glassy

basalts in this dredge.

We proceeded to dredge site RD3, seamount 290, a smooth-textured conical edifice with a small flat top. The dredge was lowered over the side at 0410, and was on the bottom at 0538. The dredge was pulled up after 40 minutes on the bottom. The net dredge was completely empty, the pipe dredge contained only small fragments (max 3 cm) of fresh plagioclase-phyric basalt with phyric glassy chilled margins. No animals were observed.

The ship arrived at RD4 at 0819. This site is Seamount 293, a rubbly heap of hummocks just west of Seamount 290 (RD3) in Segment 11. The dredge haul was about one half blocks 5-20 cm in size, and one half gravel. Not very fresh pillow fragments with manganese crust, and some brown pelagic mud were recovered. The basalts are aphyric and altered. RD5 was located just south of RD4 in hummocky terrain next to Seamount 288. About 1 kg of glassy shards were recovered, and one piece of aphyric holocrystalline basalt.

The ship returned to dredge site 3 to try to obtain a larger sample of rocks from seamount 290. RD6 was a success with 6 large blocks in the net dredge. RD7 was at Seamount 325, located in the northern part of the survey. It was first imaged as we turned into the median valley floor from the transit line in, and then on the survey line heading north. It is a classic flat-topped seamount with smooth texture. The dredge contained eight chips of basalt glass in the pipe dredge, the net dredge was empty.

February 06 (JD37)

A second attempt at dredging rocks from seamount 290 was made as day 37 began. It appeared this time from the ship's track and depths under the ship that we dredged for just a short time on the top of the seamount, and then fell off the side. The dredge returned several dozen small glassy fragments (~ 1 cm on a side), 4 fragments about 1.5 cm on a side, and one micropillow lobe. The glass was black and very vitreous with few signs of devitrification. At the same time, traces of orange palagonite were found in the glass rinds.

This second attempt at dredging ended at approximately 0600. Because camera runs could not begin until after sunrise, a third attempt was made on this site. This time the position was determined so that the dredge would cross the central crater. The dredge returned empty of rocks. However the pipe dredge was full of beige mud.

After dredging was complete, the wire was shifted to the starboard side for a camera deployment. There were several problems during the day. First one of the blocks in the run of the coring wire had to be removed to allow the CTD winch to operate. There was also trouble with the spooling of the CTD winch, which required sanding down of the axle that one of the blocks runs on. There were problems with finding the bottom/pinger echoes. The Simrad could only be made to cycle at eight seconds, and that gave too long a gap to respond by hauling up on the wire to move the camera from the seafloor. There was trouble with the winch brake, and finally the camera started pinging on half second pings even though the camera was off the bottom. The station was abandoned and on return to the surface it was found that the camera trigger string had wrapped itself around its supporting arm, so that the weight was pulling on the switch. After assessing the situation it was decided that the ship should abandon the site and move to Area 3 for TOBI surveying.

We began our transit along the rise axis at about 1900. Before we left the wire was rerun through the block to the stern for TOBI towing.

The seminar series continued today with talks by Nick Millard ('TOBI Vehicles'), Chris Flewellen ('TOBI Logging System'), and Jane Keeton ('Recognition of Circular Features Using Hough Transforms'). Jian Lin presented his preliminary gravity data analysis showing that a gravity anomaly high occurs at the boundary between Segment 10 and 11.

IV. Area 3, Segments 5/6

4.1 Summary

Segments 5 and 6 are at the east end of a major zone of dextral offset beginning at the terminus of Segment 2. Segment 5 is short with numerous ridges. Crustal magnetization highs run along one of these ridges. At the northern edge of Segment 5 the largest identified seamount, Possum Peak (630 m.), is found. Segment 6 is one of two segments out of eighteen that has no axial volcanic ridge. Abundant seamounts occur on the valley floor; some form east-west chains.

Segment 6 was identified from Sea Beam maps as being of potential interest, since it is one of only two segments out of the eighteen between the Kane and Atlantis fracture zones to lack an axial volcanic ridge within the median valley floor. The lack of an axial volcanic ridge does not imply a lack of seamounts. There are a large number in this segment. The Sea Beam maps show that the floor of the median valley is unusually flat, and is cut by axis-parallel faults.

The major non-transform offset is one of the most intriguing features of the region, since normally an offset of this size would be taken up by a transform fault. Here there is no morphological evidence for such a structure. Instead there are spreading axis parallel ridges in the generally deep offset zone, some of which appear to be small axial volcanic ridges (those of Segments 3, 4 and 5), and some tectonic blocks. Also in this zone is the largest seamount in the area, Possum Peak. Our survey showed the area to be as interesting as we had anticipated.

The volcanology of Segment 6 is particularly well displayed in TOBI images. In the center of the segment much of the floor of the median valley is covered by smooth, uniformly mid-grey material which we interpret as sheet flows. Slight variations in shades of grey on the surface outline lobate forms that we interpret to be flow fronts. Dredges on the sheet flows recovered good hauls of aphyric glassy basalt. The sheet flows are cut by small faults that define a shallow axial graben within the median valley about 3 km. wide, within which is a swarm of fissures and small faults. Surrounded by the sheet flows are a number of isolated volcanic forms, some of which are clearly later than the flows, though others may be earlier. These forms include an isolated hummocky seamount (Mount Doom), and several rows of hummocks each with a fissure along the summit of the row, representing small fissure fed units. One of these is apparently linked to a small seamount. Because of their isolation by sheet flows from other volcanic forms, the size of these features can be used to deduce the volume of individual hummocky flow units.

Further south from the center of Segment 6, sheet flows are gradually replaced by hummocky flows and seamounts, with textural relations that suggest that the sheet flows are earlier. The seamounts are especially interesting. Many are similar to those observed in Area 2, including many small flat-topped seamounts with central craters, and hummocky mounds, including some of considerable size. The new form found here is the hat shaped seamount, a smooth round, flat-topped seamount, with a broad brim of lava around it of similar texture to that of the top, and apparently having formed at the same time as the mound at the center, either by overspill from the top or by eruption from the base.

Rocks were dredged, with some difficulty, from four of the seamounts in Segment 6, two of the hat shape (Sombrero and Cloche) and two hummocky seamounts (Mount Doom and Hummocky Heaps). All of the samples from the seamounts are strongly plagioclase phyric, and several have olivine phenocrysts as well. A similar relation was seen further south in Segment 1 (Lawson,

pers. comm.). The reason for the contrast between the aphyric lavas of the sheet flows and the phyric lavas of the seamounts is at present enigmatic.

Patterns of faulting in Segment 6 are complex. All major faults imaged throw down towards the median valley axis, but the myriad minor faults may throw either way. Faults take sinuous paths across the median valley floor, often apparently at random, but the faults that define the edges of the shallow axial graben are parallel to each other over most of their distance, though far from straight.

The TOBI images in the offset zone are complex and difficult to interpret. The zone contains axis parallel ridges of young constructional volcanics, such as the ridge of Segment 5, and older sediment covered volcanic material. Major faults run oblique to the axial direction, oriented to suggest that they are oblique extensional faults in a broadly strike slip environment. There is no sign on the images of any transform parallel faults, so the zone cannot be classified as a transform fault zone. Further detailed study is required if its nature is to be understood.

Possum Peak, a 650 m high feature in Segment 5, was imaged from both north and south. The surfaces of the seamount are uniformly bright in the TOBI images, and may be mostly disaggregated blocks. Some outcrops are seen near the base. The crest of the seamount is a knife edge ridge, oriented obliquely to surrounding structures. Two dredges were attempted on Possum Peak. One brought back pillow fragments from the northern slopes, and on the southern slopes the dredge was lost. The nature of this major feature is still unclear.

Mass wasting of slopes, in many different forms, is as striking here as in Area 2. There appears to have been large scale collapse of material from the north into the offset zone on the western side of the valley. The western median valley wall fault shows a large slip in one place, and evidence for downslope flow in another.

One line was run on the first fault block above the median valley floor on the east side of Segment 6, to image an apparent fossil axial volcanic ridge on top of the fault block. The images showed that the block is surprisingly thickly sedimented, but lava hummocks and small seamounts can be seen protruding through the sediment cover. Talus ramps are very clear on the inward facing slope of the ridge, with evidence from variations in brightness of recent downslope flow.

4.2 Waypoints

Waypoints and actual ship track for the TOBI survey in Area 3 are presented in Figure 4.1. Also in the figure are seamounts which have been previously identified from Sea Beam bathymetry (Smith and Cann, 1990, 1991), axial valley highs, and historical earthquakes in the region (relocated by Lin and Bergman, 1990).

The following way points define the TOBI survey of Segments 5 and 6.

C1) 25°13.0'N, 45°27.3'W - Stop to launch TOBI

C2) 25°10.0N, 45°28.2'W - Begin TOBI survey

C3) 24°56.6'N, 45°32.0'W

C4) 24°54.4'N, 45°44.2'W

C5) 24°51.8'N, 45°44.0'W

C6) 24°54.4'N, 45°29.9'W

C7) 25°10.0'N, 45°25.5'W

C8) 25°10.0'N, 45°24.2'W

C9) 24°53.0'N, 45°28.7'W

C10) 24°53.0'N, 45°26.0'W

C11) 25°01.9'N, 45°23.6'W - End TOBI survey.

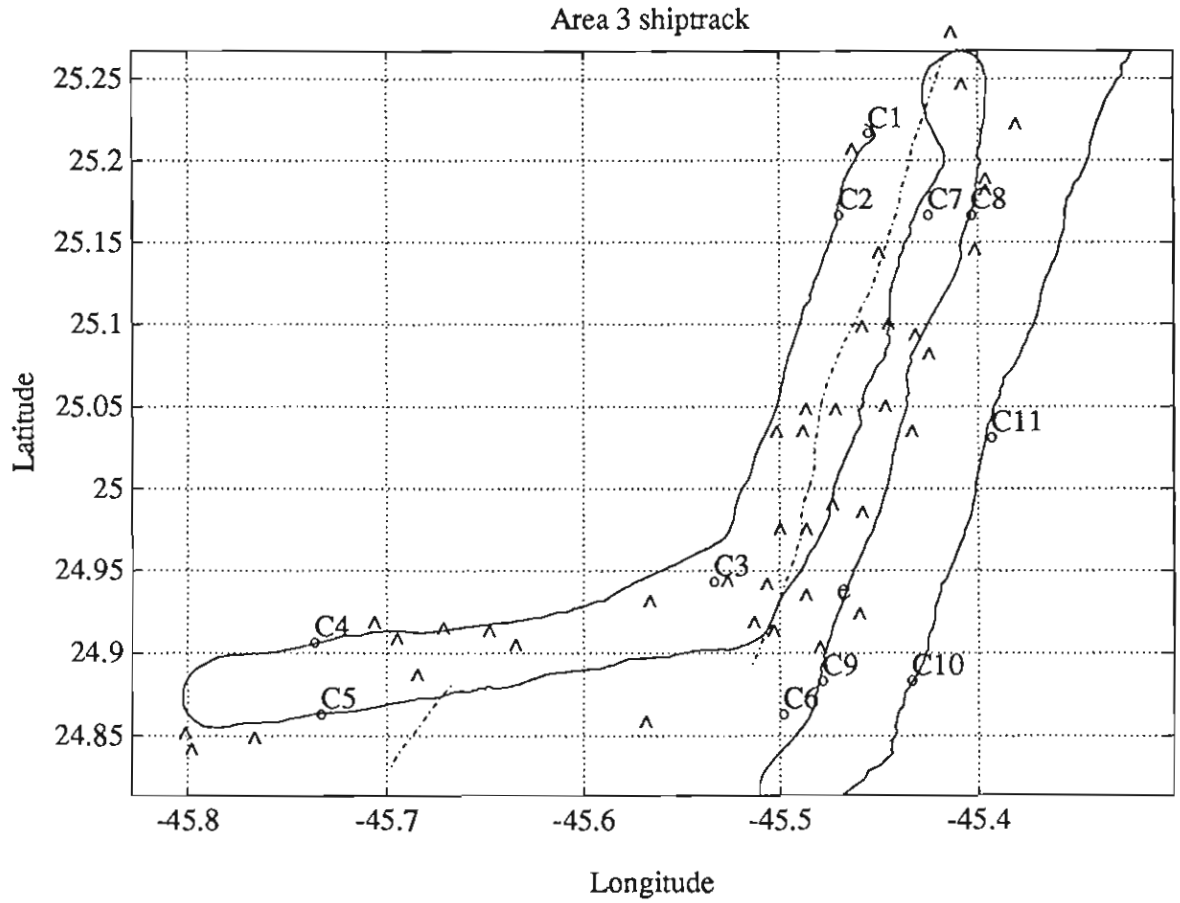

Figure 4.1 Area 3 shiptrack

Waypoints (text labels), shiptrack (solid line), axial volcanic highs (dashed lines), earthquakes (e's), and seabeam identified seamounts (^'s) for Area 3.

4.3 TOBI Run, Track line images

TOBI images for the entire Area 3 survey are shown in Figures 4.2 through 4.7. The images presented on these pages have been severely downsized from the original data. Each scanline of data (across track) in its original form contains 8000 pixels of information, 4000 to port and 4000 to starboard. Each pixel in the original data covers 0.75 meters of the seafloor. Distance from the TOBI sled and TOBI altitude affect this coverage so the 0.75 meter value should be taken as approximate. Along the ship track the original data contains a ping every 4 seconds for an along track pixel size of 4.0 meters. Again, as ship speed, distance from TOBI, and TOBI altitude affect this coverage, the 4.0 meter valued should be used as an approximation. In total, TOBI produces 8000 pixels of information every 4 seconds or 900 scanlines of 8000 pixels every hour.

The images in Figures 4.2 through 4.7 each represent approximately 4 hours, 27 minutes of information (4000 scanlines of 8000 pixels each in the original data) with time progressing from the top down in each frame. The original data has been reduced to 800 scanlines of 200 pixels each of the strips in the figures. Detailed images of certain interesting regions are outlined in white boxes and are presented in the next section. Rock dredge sites are also indicated on the images.

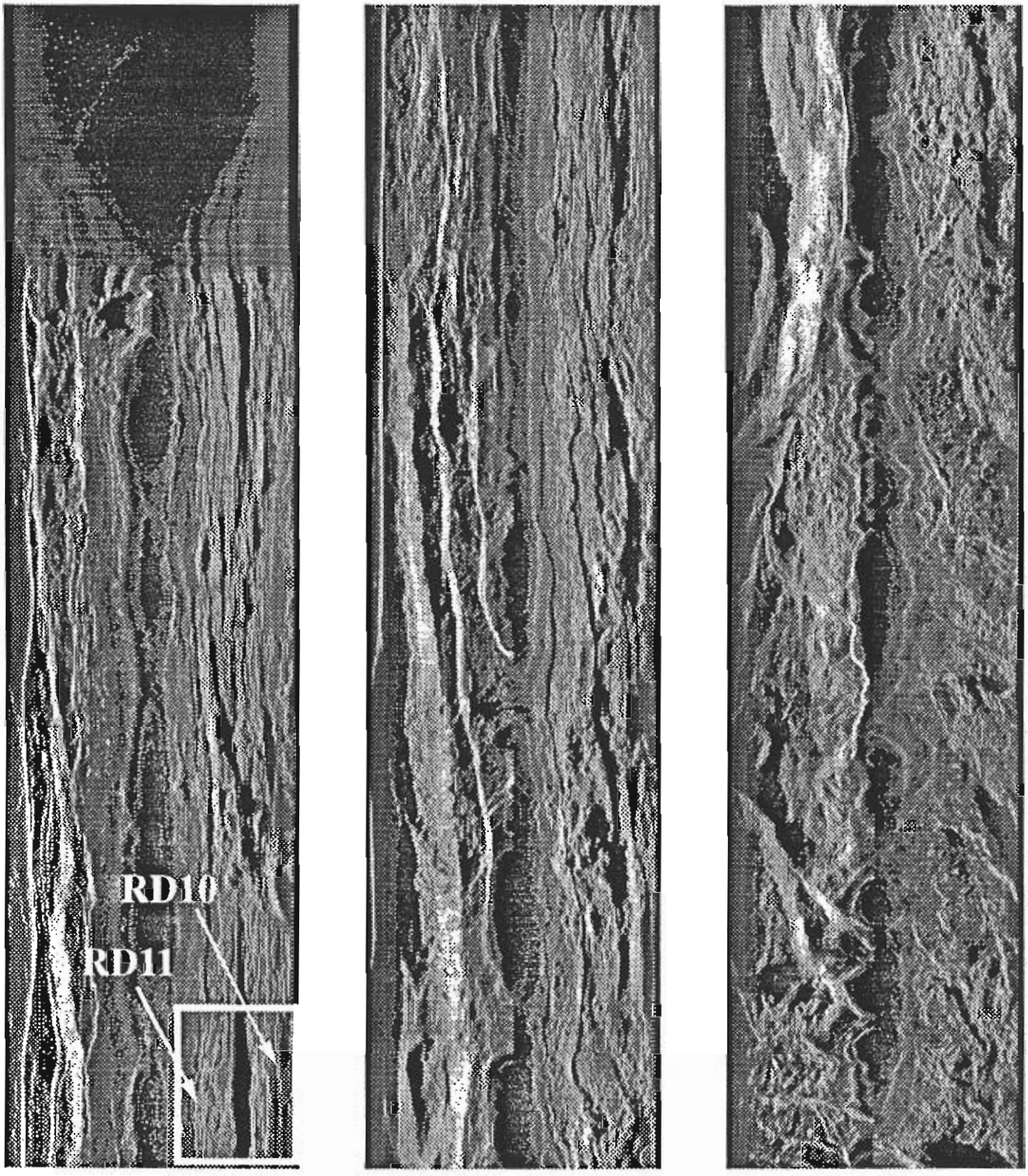

Figure 4.2 TOBI images starting 0635/038 Z

Time progresses from left to right and from the top down in each frame. Each strip contains approximately 4000 TOBI pings for a total time of approximately 4.44 hours per strip. The fault/ flow area enclosed in the white box is presented below in detail.

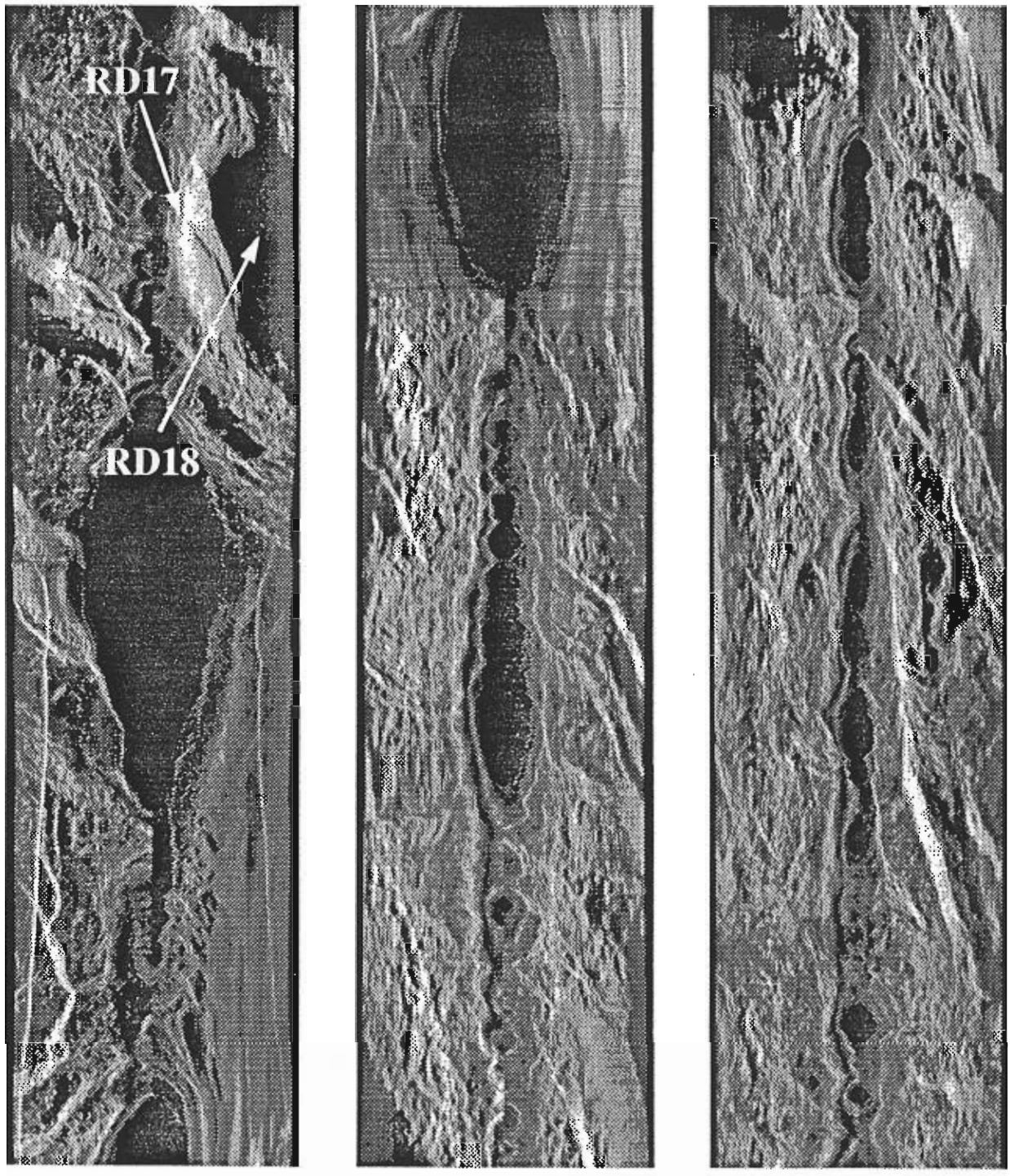

Figure 4.3 TOBI images starting 2000/038 Z
Possum Peak dredge site is indicated. The dredge came back on this one.

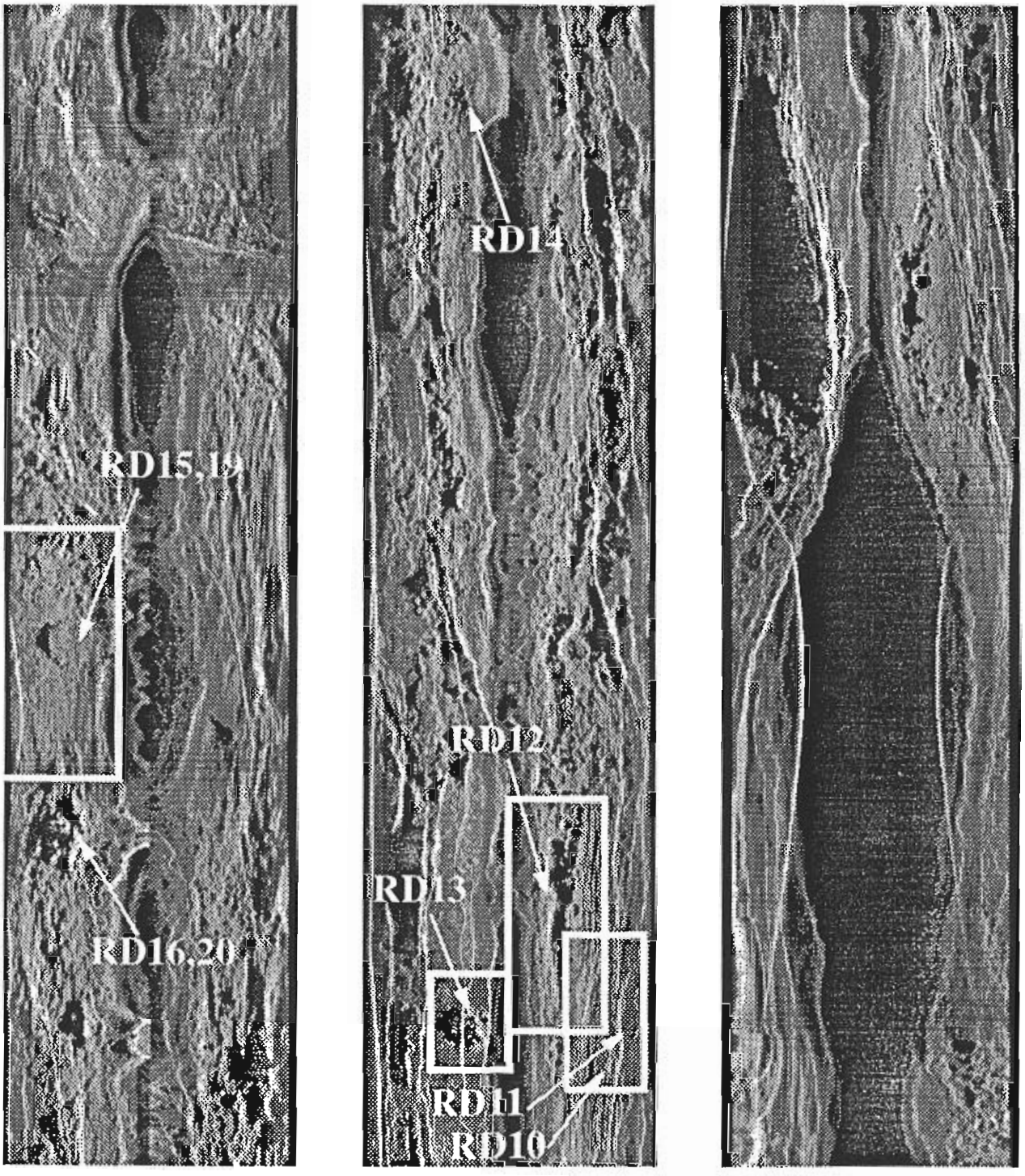

Figure 4.4 TOBI images starting 1005/039 Z

Sombrero Seamount, Mt. Doom, Tadpole Ridge, and the fault/flow area (all enclosed in white boxes) are presented below in detail.

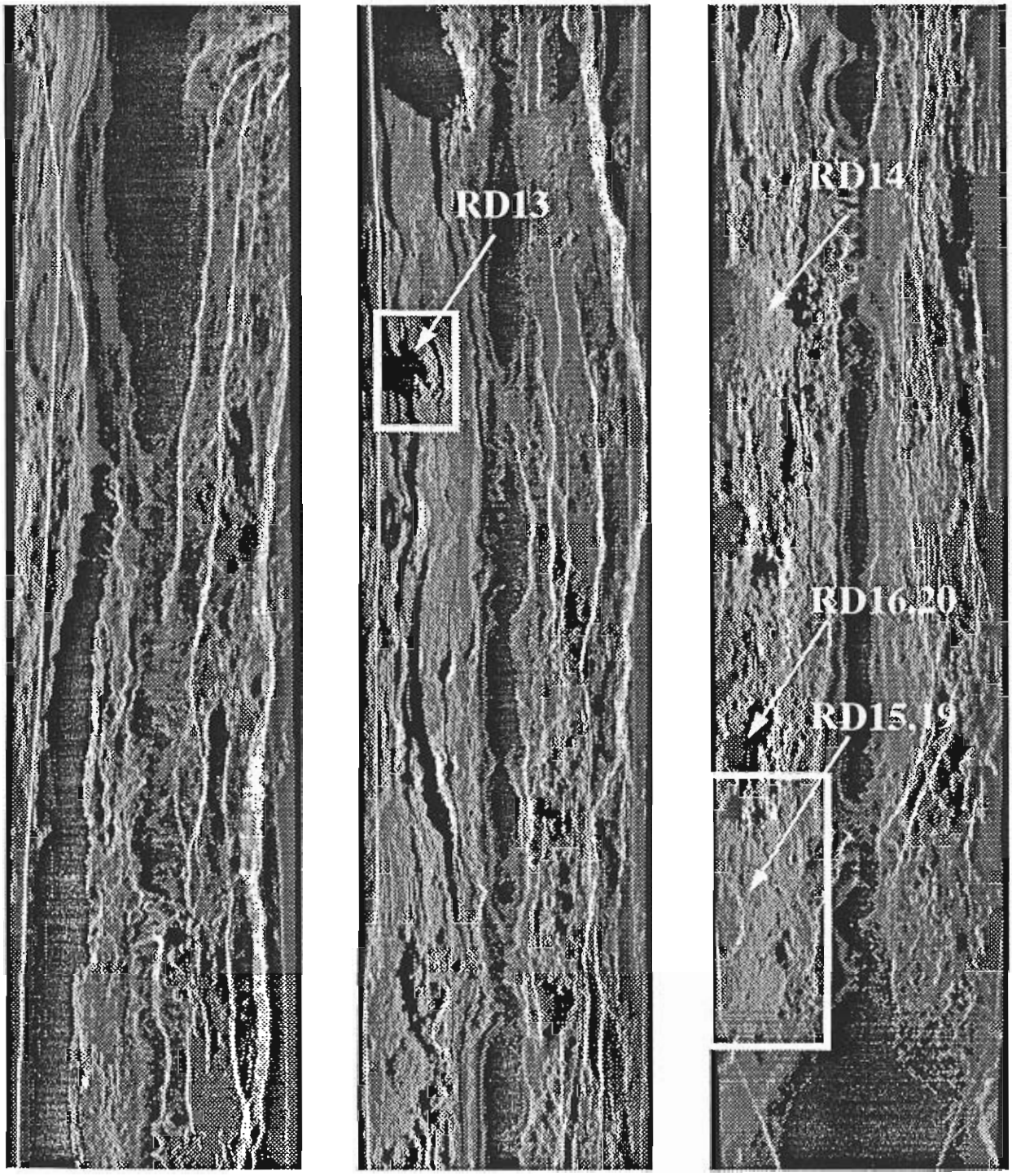

Figure 4.5 TOBI images starting 2324/039 Z

Mt. Doom and Sombrero Seamount (enclosed in white boxes) are presented below in detail.

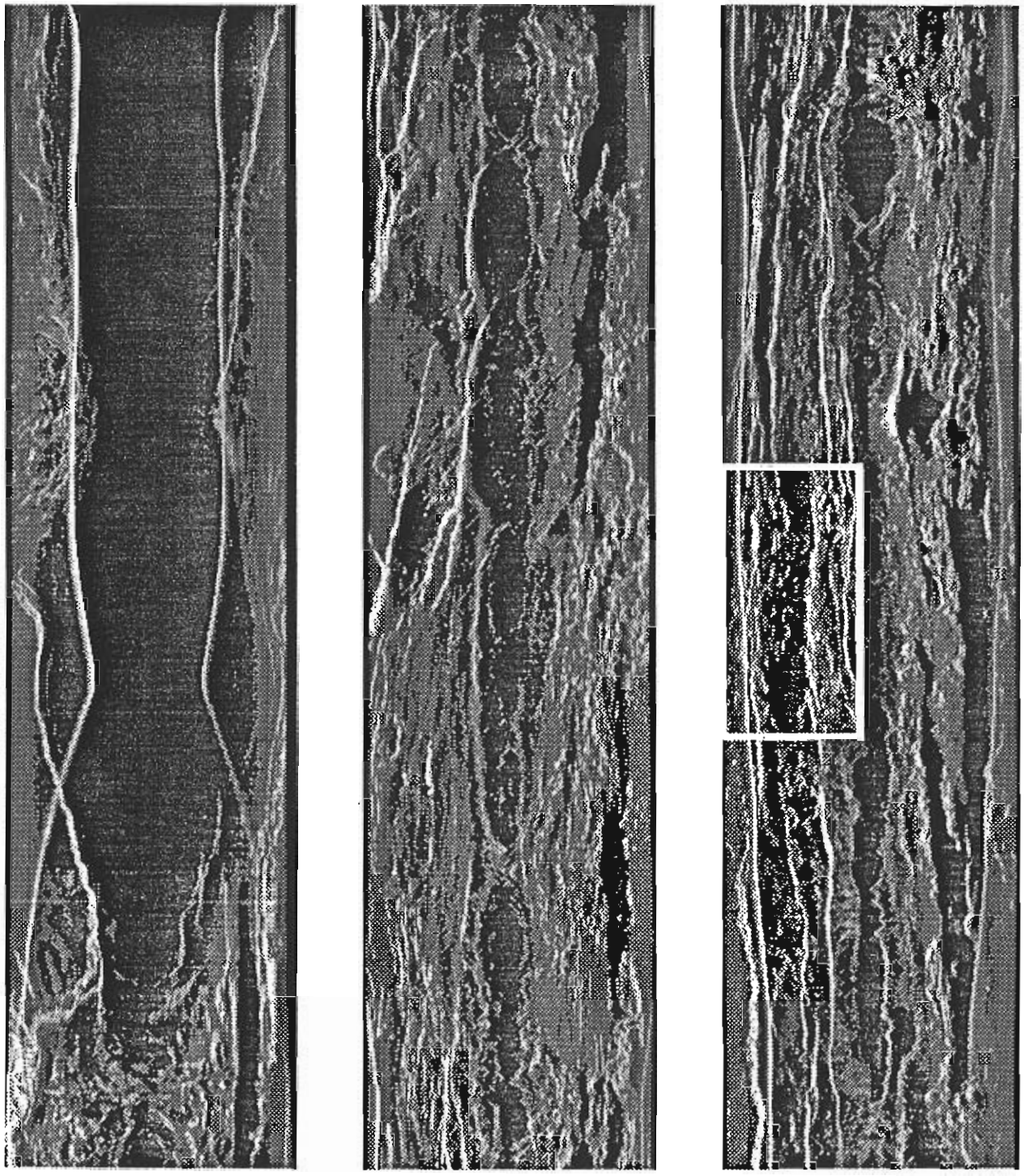

Figure 4.6 TOBI images starting 1243/040 Z.

The sedimented hummocky ridge enclosed in the white box is presented in detail below.

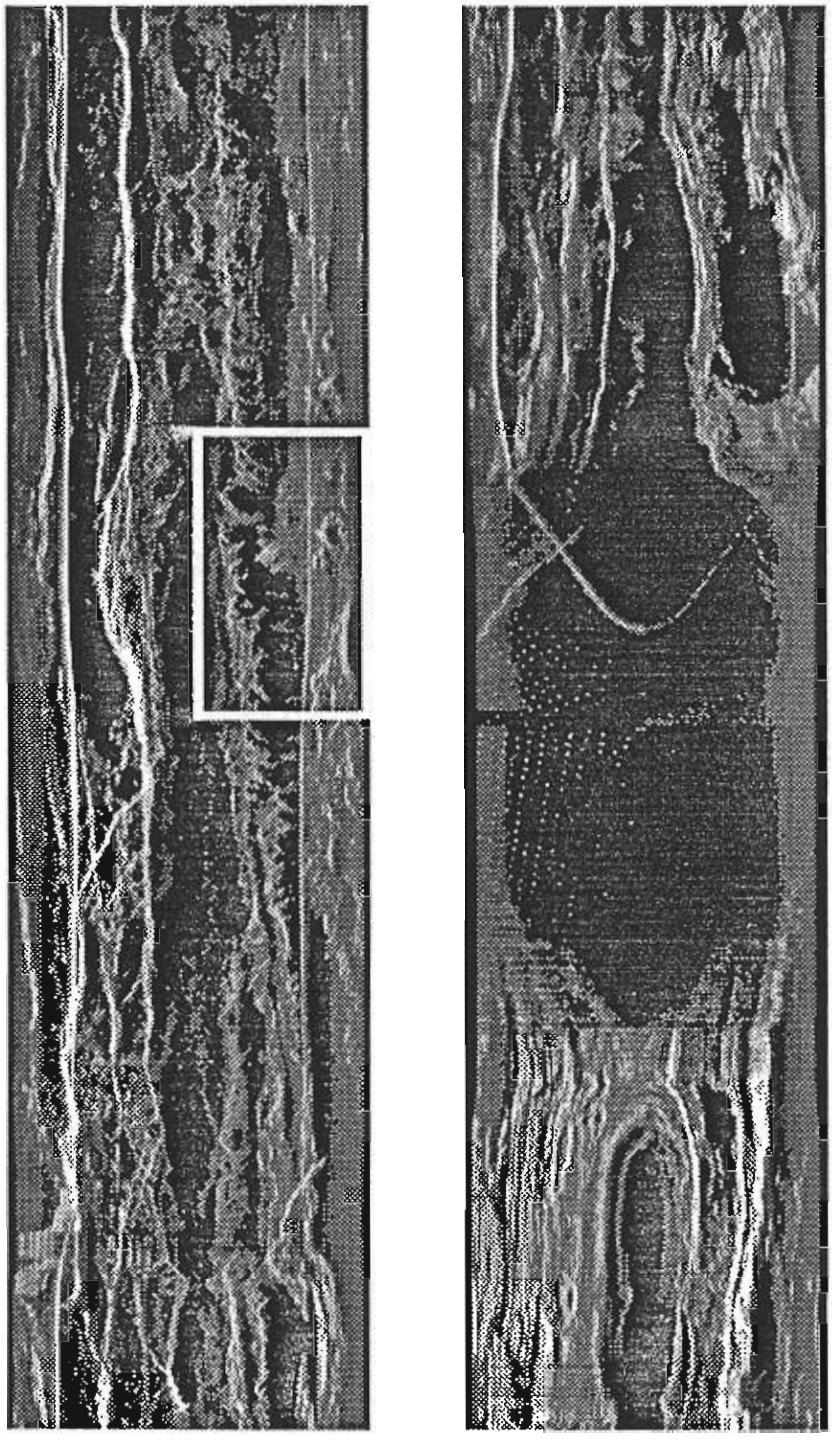

Figure 4.7 TOBI images starting 0200/041 Z.
A detailed image of the sedimented fault scarp (enclosed in white box) is presented below

4.4 TOBI Run, Detailed Images

4.4.1 Fault/flow area

The floor of the central part of segment 6 is largely covered with flat, smooth sheet flows, within which is a shallow central graben. These pictures show the sheet flows near the western bounding fault of the graben (the prominent fault near the center of both pictures). The subtle lobate patterning on the flow surfaces indicates separate flow units. Fissuring has affected the floor of the graben much more than the area outside it, though the dredge haul from outside the graben is more weathered than that from the fissured area within it.

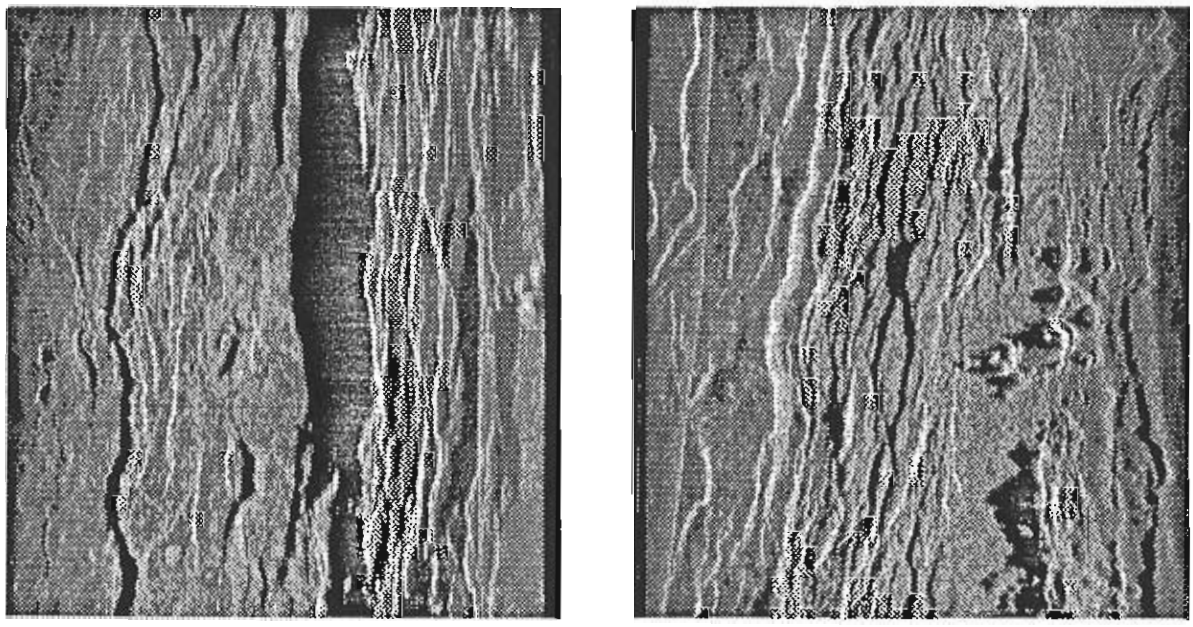

Figure 4.8 Dual-insonified fault/flow area.

This area has been insonified from the west (left hand image) and east (right hand image) directions. Dredges were obtained from the smoother flow area on the left of each image as well as the faulted area on the right of each image.

4.4.2 Mt. Doom

A few kilometers east of the fault/flow area is a single hummocky seamount rising 120 m. above the sheet flows, which are here only slightly fissured. The right hand image shows light-colored flow material from the seamount spreading out on the sheet flows, demonstrating that the sea-

mount is later than the sheet flows. Both are cut by later faults, throwing down to the west. Mount Doom is clearly the result of a small, single eruptive event.

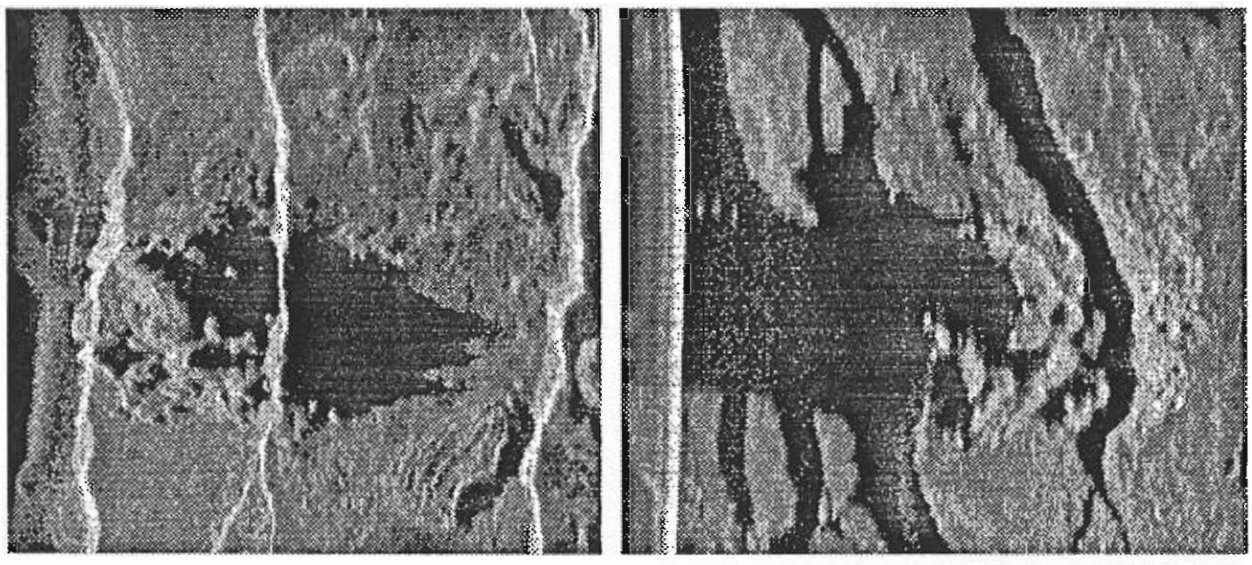

Figure 4.9 Dual-insonified Mt. Doom detailed images.
This hummocky mound has been insonified from the west (left hand image) and east (right hand image) sides.

4.4.3 Sombrero Seamount

An unexpected new class of seamounts, hat seamounts, was first imaged in Area 3. These have a central, raised, surrounded by a brim of similar flat lavas which is clearly related to the central crown. Here the lavas of the brim have apparently flowed out over pre-existing hummocky topography. Whether the flows come from the seamount or base of the central mound is not clear.

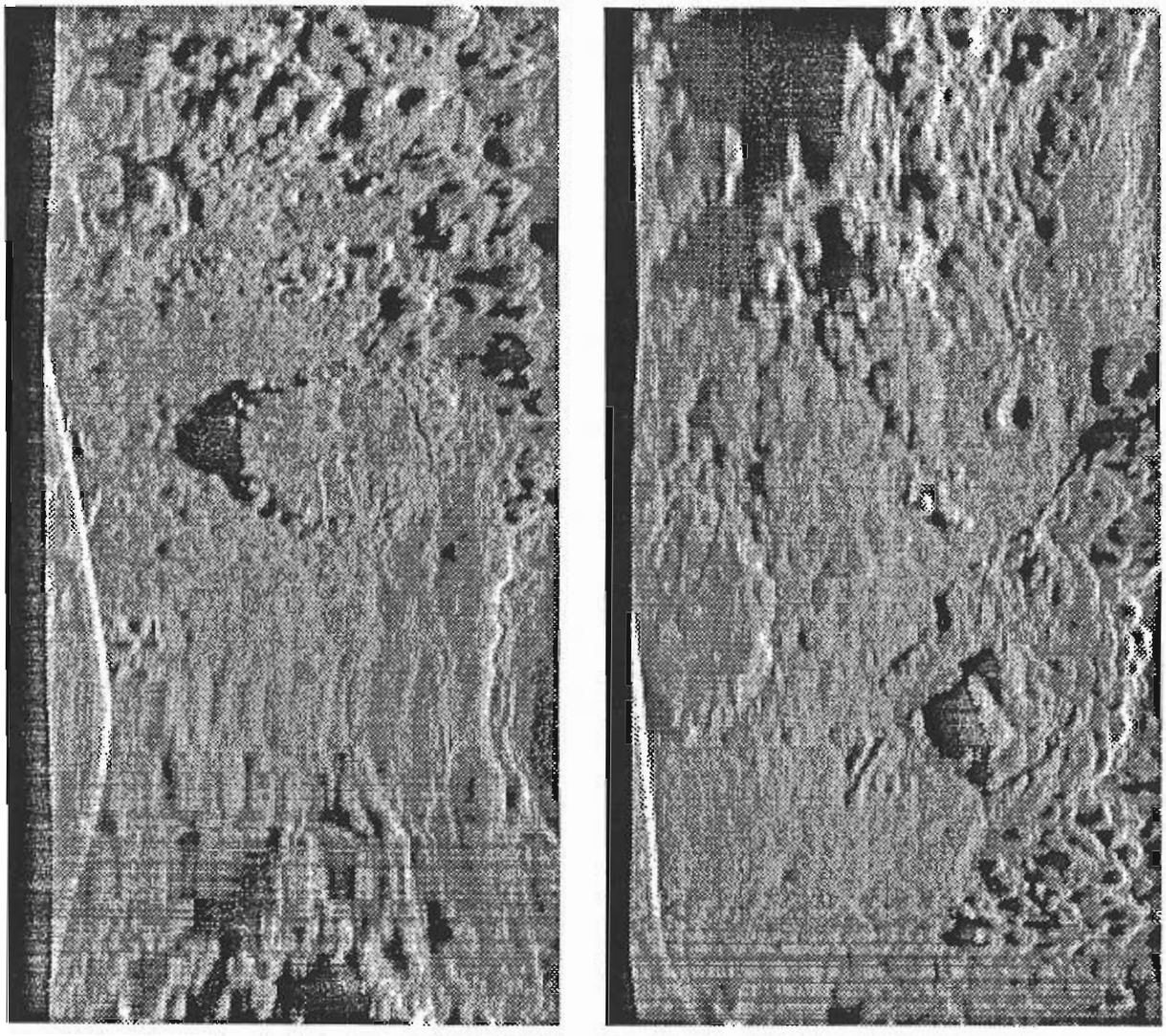

Figure 4.10 Dual-insonified Sombrero Seamount detailed images.

Hat shaped seamount with small flows and hummocks on its edges insonified from the west (left hand image) and east (right hand image) sides.

4.4.4 Tadpole Ridge

On the sheet flows in the center of segment 6 are a number of steep-sided ridges, apparently composed of a row of hummocks, often with a central fissure. Tadpole Ridge is one of these. Like the others it is sinuous, probably reflecting the sinuosity of the fissure from which it was fed, and paralleling fine sinuosity of nearby faults. Tadpole Ridge ends in a small seamount which may have been erupted at the same time. Such hummock ridges are a significant part of several AVR's in the MAR of this region.

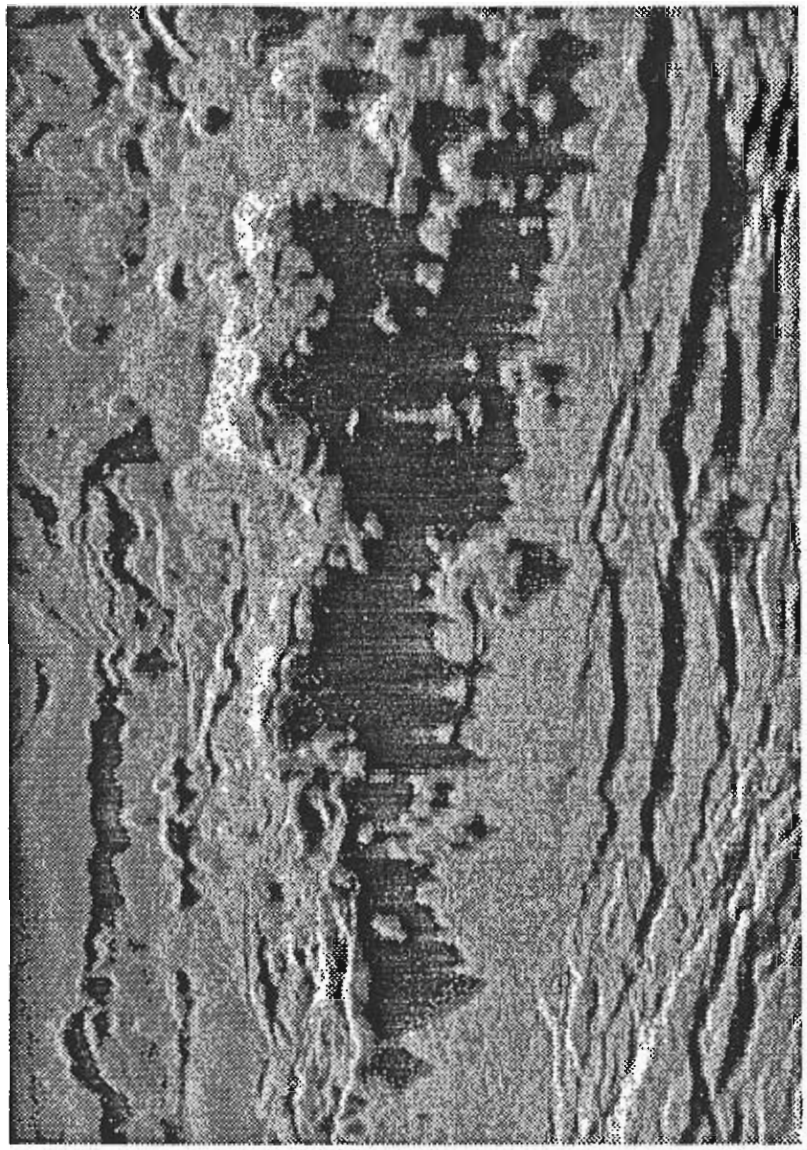

Figure 4.11 Tadpole Ridge

Detailed image of a fissure ridge eruption. The shape of the feature roughly follows fault patterns to the right of the ridge.

4.4.5 Sedimented hummocky ridge

The easternmost line in Area 3 was targeted on the first fault block above the median valley floor, where Sea Beam morphology suggests that there might be an faulted axial volcanic ridge. The fault block is surprisingly thickly sedimented, given its nearness to the median valley, but shows clear evidence that it was once an AVR. This image shows a hummocky ridge from the AVR, exactly similar in shape to those on active AVR's, and cut by similar faults to those that cut the active median valley.

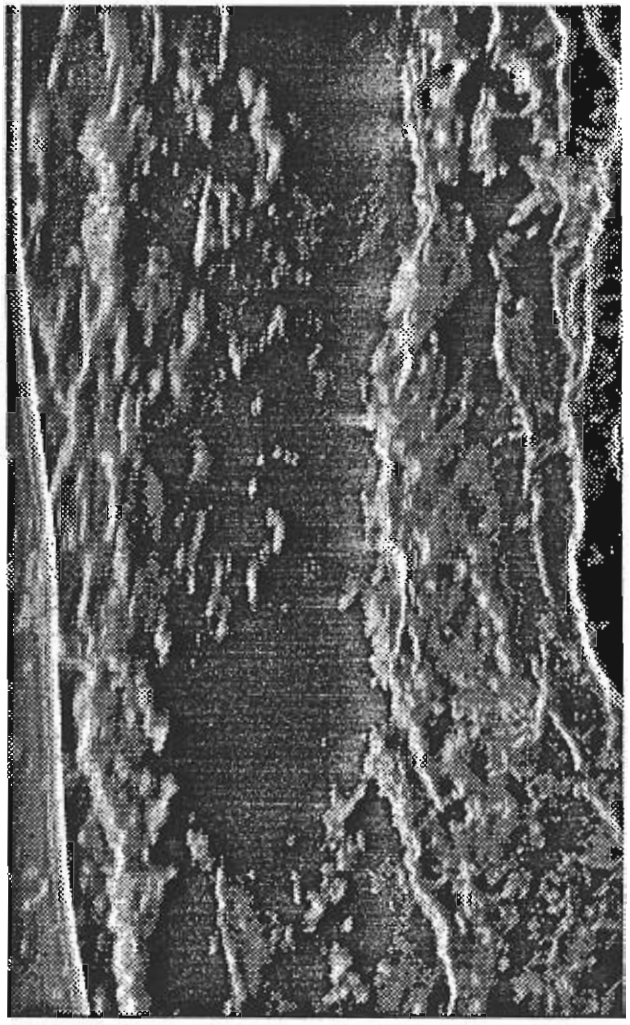

Figure 4.12 Sedimented hummocky ridge

This sediment covered hummocky ridge is found on the first fault block east of the median valley in Area 3.

4.4.6 Sedimented fault scarp

On the same TOBI line as imaged the sedimented hummocky ridge, the vehicle was towed for a while parallel to a fault scarp, imaging the scarp obliquely and showing by shadowing a range of features not normally seen in more direct images. Note the buttresses of rock along the scarp, and the stone chutes that feed into a complex talus ramp along the foot of the scarp. Pale colors are areas of talus that have moved recently, while darker colors are areas that have been covered with a blanket of sediment.

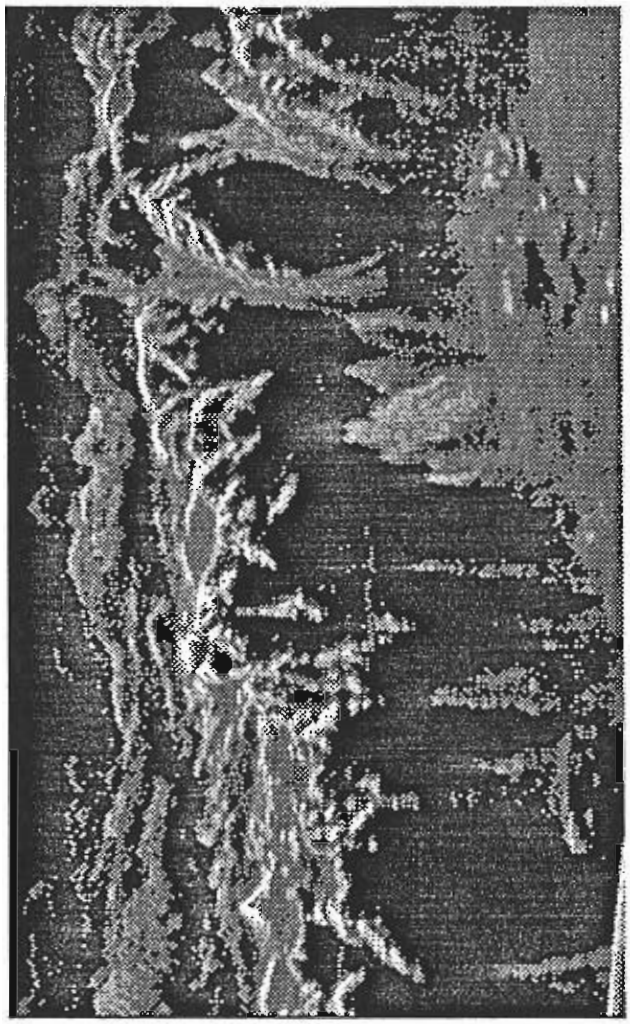

Figure 4.13 Sedimented fault block.

This sedimented secondary fault scarp is found on the first fault block east of the median valley in Area 3.

4.5 Geological map description

Detailed interpretation of the TOBI images of each area included the production of a geological map which can be found in the back pocket of this volume. These maps, although only preliminary interpretations and lacking bathymetric data, have been useful in underlining the spatial distribution of the volcanic edifices, faults and landslides that have been imaged. Description of individual features has already been included in the summaries, so the discussion here will be lim-

ited to the interaction observed between the different processes.

The geological map of area 3 focuses on segment 6 which is the only segment lacking a robust AVR. The volcanism in the centre of the segment is dominated by sheet flows, although a variety of hat seamounts, isolated hummocky heaps and linear ridges were imaged. Towards the southern end of the segment hummocky volcanism becomes dominant. Faulting within the area is extensive. The axial zone (between opposing fault dips) is restricted to as little as 500m in places, extending to a maximum of 2700m. As in area 2 the fault distribution is again related to segmentation. Large en echelon faults, locally displaying small lateral structures, dominate adjacent to the central parts of the segment. Towards the southern termination of the segment the concentration of smaller faults increases on the outer edge of the valley, and at the inner corner gives way to a landslide, which partially buries a large curvilinear fault. This relationship of faulting and landslips to segment termination is similar to that identified in area 2.

The offset zone between segments 5 and 6 is marked by a series of en echelon extensional faults oriented oblique to both the transfer zone and the ridge axis. This arrangement of faults is characteristic of patterns seen in zones of brittle shear which display a sinistral offset. Blocks within the zone are thus rotated in an anticlockwise manner about a vertical axis. Individual faults also display a component of rotation about a horizontal axis as shown by their association with back tilted-blocks. These back tilted-blocks comprise hummocky terrain, upon which the sedimentation is limited suggesting that the hummocks were generated within the transfer zone. The walls of the transfer zone are dissected by numerous large gullies which show extensive talus deposits at their base. Gullies and subsequent talus development is also a common feature of many of the larger faults in the area. As with area 2, sedimentation begins to be apparent outside the median valley as marked by the first of the large faults.

4.6 Dredge Sites

The sites dredged in this area are (see also figure 5.2 through

RD10) 25°07.059'N, 45°26.05'W, Depth 3520 m., 44 rocks

Flat and fissured smooth flows on the floor of the shallow central graben.

Hand specimens. Moderately altered (patchy palagonitic coatings on rock surfaces), aphyric, subangular to pillow-shaped, decimeter-sized, black glassy basalt. This dredge contained life forms: a white, ~2cm diam., "jelly ball;" and a fragmented, ~3cm diam., white sponge.

Thin section, RD 10.1. Microporphyritic pillow basalt. The thin section is of a glassy margin and the underlying variolitic pillow rind. The glass and variolitic basalt contain microlites of plagioclase and olivine. The plagioclase microlites show hollow box basal sections and rail track lath parallel sections, and are up to 0.5mm in length. The olivines are present as acicular crystals with a central boss, and as subrounded anhedral sections less than 0.1mm in size. Microphenocrysts are of plagioclase, up to 1.5mm long, with shape varying from euhedral to subhedral with acicular protrusions. Extinction angles range to 31 degrees.

RD11) 25°06.7N, 45°28.1'W, Depth 3554 m., 14 rocks + gravel

Flow lobes on the lip of the small axial graben which cover older fissures

Hand specimens. Manganese oxide-coated, aphyric, sub-angular, decimeter-sized, black-dark grey, pillow basalt.

Thin section of RD 11.15. Sparsely porphyritic pillow basalt. The thin section is taken of the pillow rind. The variolitic basalt contains microlites of acicular plagioclase and subrounded olivines. The plagioclase microlites have an aspect ratio of 5:1 to 10:1, are characterized by hollow box and rail track sections and are less than 0.2 mm in length. The olivines are subordinate to the plagioclase, representing 20% of the total groundmass. They are present as isolated subrounded crystals and clusters of acicular crystals. Phenocrysts represent only 5% of the whole rock and are hence rare in thin section. One identified in this section was a subhedral lath of 0.5 mm in length.

RD12) 24°05.54'N, 45°27.49'W, Depth 3618 m., 81 rocks

Curved fissure eruption, perhaps a seamount with a fissure flow tail.

Hand specimens. Moderately altered (patchy palagonitic and manganese-oxide coatings on rock surfaces), sparsely porphyritic (~5% plagioclase phenocrysts up to 4mm diam.) basalt with grey, coarse-grained interior and black, glassy rind. Rocks are angular to pillow-shaped, decimeter-sized, slightly vesicular (~1mm diam. vesicles) near the glassy rinds, and show possible flow lineations(?)/ devitrification features(?) near the glassy rinds. Some worm casts are present on the rock surfaces.

Thin section of RD 12.59 and 12.71. Highly porphyritic pillow basalt. The thin section is of a glassy margin and the underlying variolitic pillow rind. Both the glass and the variolitic basalt contain microlites of plagioclase. The plagioclase is acicular and displays the hollow box texture associated with rapid growth. The variolitic glass in this section shows a feathery dendritic growth. Phenocrysts are of plagioclase and subordinate olivine. The plagioclase are 0.5 to 3.5 mm in length and have an acicular to tabular form. The latter tends to show oscillatory zoning, while the former is characterized by simple albite and multiple twins. The extinction angle ranges potu 32 degrees. Olivines are euhedral to subhedral with subordinate anhedral forms. The size is commonly less than 0.5 mm, and the olivine tends to be isolated.

RD13) 25°06.2'N, 45°26.2'W, Depth 3415, 2 pieces of gravel + mud

Hummocky heap known as Mount Doom.

Hand specimens. a) Slightly Manganese oxide-coated, moderately porphyritic (~15% plagioclase phenocrysts, ~5mm diam.), angular, gravel-sized, dark grey basalt. Some of the "strange white coating "is on one side of one of the pieces of rock.

b) Beige, very fine-grained, mud with some evidence of calcareous material.

RD14) 24°58.6'N, 45°28.2'W, Depth 3641 m., 9 rocks + gravel

Cloche Seamount.

Hand specimens. Moderately altered (palagonitic and Manganese oxide-coated patches), moderately porphyritic (~15% plagioclase megacrysts), angular, gravel-sized, black glassy basalt. One glassy rind shows "strange white coating." A note in the rock log advises that

numbering on rocks is difficult to see and must be looked for carefully

RD15) 24°54.2'N, 45°29.5'W, Depth 3918 m., gravel

Sombrero Seamount.

Hand specimens. Highly altered (glassy rinds altered to palagonite), moderately porphyritic (~10-15% plagioclase and ~1% olivine megacrysts), angular, gravel-sized basalt with aphanitic groundmass and glassy rind. Phenocrysts occur in both the interior and glassy rind of these rocks.

RD16) 24° 55.5' N, 45° 29.17' W, Depth 3600m, Dredge empty

Hummocky heap between Cloche and Sombrero Seamounts

RD17) 24°54.14N, 45°42.1'W, Depth 4057 m., 2 rocks + gravel

North side of Possum Peak.

Hand specimens

a) 2 rocks and a small bag of gravel. Highly altered (palagonitic and Manganese oxide-coated glassy rind), moderately porphyritic (~20% round, black, micro-olivine phenocrysts), light-dark grey basalt with thin (<1cm) glassy rind. The rocks are subangular, gravel to decimeter-sized, and slightly vesicular. These samples are very different than any of the rocks in dredges 1-16.

b) small bag full of gravel. Very slightly altered (palagonitic patches), aphyric, rounded, gravel-sized, black glassy basalt.

Thin section of RD 17.1. Microporphyritic pillow basalt. The thin section is of variolitic pillow underlying the glassy margin. The pillow is dominated by microlites of plagioclase with minor amounts of olivine. Plagioclase show the hollow box and rail track morphology, they are up to 0.3 mm in length, with simple albite twinning. The extinction angle for the microlites is up to 40 degrees. Olivine represents only 5% of the groundmass and occurs in aggregated acicular forms. In contrast to all other sites the dominant phenocryst in this section is olivine. Only 10% of the phenocrysts are plagioclase. The olivines are euhedral to subhedral and contain inclusions of chrome spinel. Most of the crystals for in aggregates of 5-6 crystals. Epitaxial growth occurs on rare olivines. Plagioclase represents the subordinate phenocryst phase, they are up to 0.8 mm in length and are commonly show acicular protrusions. Simple albite twins are present.

RD18) 24° 53.6' N, 45° 41.7' W, Depth 3700 m., Dredge lost

South side of Possum Peak

RD19) 24°53.82'N, 45°29.69'W, Depth 3804 m., small bag of gravel

Sombrero Seamount.

Hand specimens. Moderately altered (palagonitic patches and Manganese-oxide coating),

slightly porphyritic (~ 5-10% plagioclase phenocrysts, <<1% olivine phenocrysts), subangular, gravel-sized, black basalt.

*Due to the rusty condition of the pipe dredge this dredge haul may contain some rust fragments in it! A separate bag of these fragments is included in this sample.

RD20) 24°55.5'N, 45°29.3'W, Depth 3730 m., 46 rocks + gravel

Hummocky heap between Cloche and Sombrero Seamounts.

Hand specimens. Highly altered (extensive palagonitic and Manganese-oxide coatings), slightly porphyritic (~10% plagioclase megacrysts), angular to pillow-shaped, decimeter to gravel-sized, black glassy basalt. These rocks are vesicular. One particularly pleasing sample seems to be a "part of a pillow where lava has settled leaving space." Unfortunately this sample has been broken into three bits. A reward of the kingdom of Wales will be made to any geologist/geophysicist who can satisfactorily re-assemble this lithic jigsaw puzzle.

Thin section of RD 20.31. Highly porphyritic pillow basalt. The thin section is take from the variolitic pillow. The variolitic basalt contains microlites of acicular plagioclase and olivine. These represent 30% of the whole rock. The plagioclases display the characteristic rapid growth textures, and all show preferred flow orientation, bending around the phenocrysts. Plagioclase microlites are around 0.2 mm in length and have a 6:1 aspect ratio. Olivines are subrounded to subhedral, 0.1 mm in diameter and isolated. The phenocrysts are plagioclase and olivine, with two types of plagioclase being identified. A sieve textured plagioclase, commonly lath shaped and a subrounded forms displaying oscillatory to simple smoothed circular zones. Extinction angles on the albite twins ranges up to 32 degrees.

4.7 Underway Geophysics

See Chapter 7 for summary of overall gravity and magnetics results.

4.8Camera Sites

Camera station 2: 'Sombrero' Seamount lat: 24° 53.8'N long: 45° 30.7'W

Operations. The BATHYSNAP camera was deployed at station 2 at 1930/043z. As at station 1, problems were found with winching, and the bottom was only reached at 0055/054z. This time we had rigged up an audio output to accompany the echosounder display (now cycling at 1 second intervals), and this device made it far easier to detect the double pings and to respond accordingly. For this deployment the winch was being driven from on deck, with instructions passed on by walkie-talkie from the echosounder interface in the main lab. This worked without problem for approximately 40 minutes, during which time we estimate that 42 pictures were taken. Unfortunately problems with interference on the radio led to our hitting the bottom with some vigor at 0137z, after which the double pinging became continuous and we presume that we lost the bob. We nevertheless continued the camera run, trying to keep the camera close to the bottom with reference to the echosounder record alone. At 0230z, however, we crashed into some unforeseen steeply-rising ground, and it was 3-4 minutes before we could bring the camera clear. Upon getting the BATHYSNAP on deck at 0430z we found the main aluminium cross-member of the camera frame to have been bent by 120°, and the reed switch assembly to have been smashed. Remarkably the camera, flash

and pinger were undamaged.

Results. Regrettably no images of the seafloor were recorded on the film from camera station 2. Analysis of the negatives shows some 400 photographs of the bob; accordingly we surmise that, although the reed probe between the switch and the pinger worked perfectly until its demise, that between the switch and the camera must have failed in the water. The camera was therefore triggered at a very early stage, and the film exhausted before the BATHYSNAP ever reached the bottom.

Camera station 3: 'Tadpole Ridge' lat: 25° 06.5'N long: 45° 27.7'W

Operations. Although we reconstructed the BATHYSNAP camera frame (adding weights so that it could be paid out more easily), we could not mend the reed switch in time for the third camera run. We therefore constructed a makeshift connection that allowed both pinger and camera to be triggered from a spare electromechanical bob-activated switch. The camera system was deployed at 0910/044z; however, at 0930z the new switch also short-circuited (at 450m water depth) and continuous double pinging started. The decision was made to continue the deployment as it was calculated that, with its improved winching characteristics, we could get the camera to the bottom and still have approximately 10-15 minutes worth of film left. We actually reached the bottom at 1043z, and used the echosounder display to keep the camera as close to it as possible until 1118z, when the run was aborted.

Results. Unfortunately no images were obtained from camera run 3, though why this is so is not obvious. It seems most likely that the camera again ran out of film just before we got it to the bottom; it appears that, by ill-fortune, somewhat more than half of the 100' roll of 35mm film had been used up for camera station 2, and that film for only 320-350 frames was carried on run 3.

4.9 Daily Log

February 07 (JD 38)

We completed the transit to waypoint C1 at about 0400. TOBI was put over the side at 0606, and the depressor weight followed at 0637. The TOBI survey began at 0826. As we began surveying down the eastern side of the inner valley floor, the eastern wall of the inner scarp was imaged as well as the center of the median valley floor. The valley floor was covered with lavas that alternated between being very smooth and being hummocky. Lobate edges of fissure flows were observed as well as flat pancake like seamounts. Rounding the corner into Segment 5, we imaged what looked like the base of a landslide. In fact, most of the south facing wall of the inner valley near the inside corner looked as if it is composed of large slump blocks. The volcanic morphology is more hummocky in the southern part of Segment 6 and into Segment 5 than in the center of Segment 6. Ridges oriented parallel to the strike of the axis cut the valley floor in Segment 5. Possum Peak is a smooth large feature oriented at an oblique angle to the tectonic fabric. The turn at way point C4 was begun at the end of the day.

Daily highlight was Harry's (peardrop) birthday party.

February 08 (JD 39)

Waypoint C5 was reached at approximately about 0400. The section of the survey between

waypoints C5 and C6 imaged Possum Peak on the north, and several ridges oriented parallel to the tectonic lineations. From the north these ridges surrounded by hummocky flows extend south into the large deep of Segment 5. One especially large ridge built of hummocks extends from the south into the deep. At waypoint C6, we turn north-northeast and started the run parallel to the axis in Segment 6. The morphology graduated from dominantly hummocky in the south to smoother faulted and fissured sheet flows. Single piles of hummocks and ridges of hummocks were observed. At the end of the day we began our turn south at waypoint C7.

The daily highlight was the Captain appearing in shorts for the first time on the trip.

February 09 (JD 40)

TOBI surveying of Segments 5 and 6 continues. Way point C8 was reached during the late hours of day 39, and the third track, this one running south, along the eastern side of the median valley floor was started. Just south of way point C8 a feature that looks like a faulted axial volcanic ridge being transported from the valley floor was imaged. The eastern bounding fault was also insonified. In the first half of the line, fissured and faulted flat terrain, as well as hummocky piles were seen. Progressively more hummocks occurred towards the south. Three flat-topped seamounts with large circular aprons were observed. At way point C9 we turned east for the last line to the north starting at C10. This track imaged the first fault block up from the median valley floor, and the entire way the image showed that the topography was blanketed by sediment.

February 10 (JD 41)

The day began near the end of the TOBI survey of Area 3. The track passed along the crest of a ridge on the first platform of the crestal mountains that may be an axial volcanic ridge faulted up and spread away from the axis. The surface of the ridge is sedimented, with hummocks of lava protruding through. Faults throwing down towards the median valley cast shadows to the west. TOBI imaged rock buttresses and talus slopes running down the western flank of the ridge towards the median valley. Bright streaks on the slopes showed continuing activity, presumably generated by earthquakes. At approximately 0730, we started hauling in on the cable, and the magnetometer was brought aboard.

After recovery the ship steamed to site DC1 for dredge RD10. This dredge site lies on what appears to be fissured sheet flows near the axis of Segment 6. We recovered abundant reasonably fresh lavas with much glass. This was followed by RD11 at site DC2, on the upper lip of a small fault throwing down towards the fissured area. Here flows can be seen clearly overlapping older fissures on TOBI images. The basalt from this dredge appears older than that from RD10, despite the stratigraphic relationships observed on the sidescan. A third dredge, RD12 at site DC3, was started on a fissure ridge standing above the sheet flows. By midnight this dredge was firmly stuck.

The seminar series continued with a discussion on the preliminary results of Area 2. A spectacular green flash was seen by many. Games of eye-hand coordination were plentiful. Jump rope was played after dinner.

February 11 (JD 42)

By 0030, the dredge was freed at site DC3, and recovered with a good haul of basalt. We then proceeded to site DC5 for RD13 on a hat seamount. A small but successful collection of fragments

of porphyritic basalts came up in the dredge. The rest of the day was not very successful from the dredging perspective, however. After dredging was completed at DC5 we proceeded to DC6 (RD15) the southern hat seamount. This time very few fragments of porphyritic basalts were recovered. RD16 at site DC6 was located on a hummocky heap between the two hat seamounts. This time the dredge was completely empty. After this it was decided to change to the dredge with teeth on it, and go back to DC6 the southern hat seamount. We did not arrive at the site before GPS went down in the evening, so we abandoned this idea and proceeded straight on to DC8 at the northern side of Possum Peak. The dredge was on the bottom for RD17 at the end of the day.

In our continuing seminar series, Rob Lloyd gave an overview of the computing system and data archiving on the ship, and Andy Hill gave an overview on the ship: its design, layout and capabilities. Jian Lin was mostly curious about accidents that have occurred during seagoing expeditions.

February 12 (JD 43)

RD 17 at site DC8 was brought aboard early in the morning of day 43. Two small blocks and some fragments were recovered. The ship then repositioned for RD18 at site DC9 on the south side of Possum Peak. We dredged to the north going up the flank. At the crest we stopped the ship and hauled in the dredge. Harry reported a loud grinding/straining noise and we began to haul and decided to leave the aft deck. After taking off the pinger and continuing to haul in the wire became more and more slack, and it was clear that the dredge was lost. The weak link at the start of the chain had given and all was gone. There was not evidence of these happenings on the tension graph. It is slightly disconcerting to think of Possum Peak littered with dredge bits.

Because it would take time to rig up another dredge it was decided we should steam back to DC6, the southern hat seamount. At about 0800 we slowed to open the hatch to the hold so that the new section of chain could be lowered down and cut. RD 19 at site DC6 was completely empty. We then reoccupied dredge site DC7, the hummocky heaps, and this time the dredge came back with a successful load of rocks, despite the fact that a weak link had gone and the bag was throttled. Many large porphyritic basalt blocks were in the haul

Camera runs were the next order of the day. We steamed to the southern hat seamount DC6 for camera deployment. Some problems with the camera were discovered when it was brought on deck, but these were dealt with in short order. When lowering the camera it was discovered that the wire meter on deck and the meter in the lab did not agree. The lab meter showed the camera at a depth 1000 m... below that of the meter on the deck. It was decided to proceed and use the pinger to find the bottom. When Dave Booth heard the double ping indicating that the camera had hit, he was unable to get the immediate attention of the deck crew, and therefore the camera trigger got messed up and snapshots started being taken continuously. The camera was towed along every once in a while touching bottom until suddenly the signal from the pinger disappeared. The ship kept moving and the pinger suddenly reappeared. It was determined that the camera had run into a wall, and that the pinger reappeared when it broke free. The camera was brought back on deck, and it was observed that one of the pieces of the frame was bent into a U shape.

The seminars today were by Marty Dougherty and Joe Cann. Marty described how the TOBI data were read from the optical disks written by IOS, and the image enhancement and image analysis he has been doing. Joe summarized the dredge sites in Area 3. A note of interest is that a large

dragon fly was spotted by Ben and Debbie flying around the aft deck. Also a seamount naming party was convened on the bow after sunset.

February 13 (JD 44)

The camera survived the impact, the frame was rebuilt, and the trigger repaired by John Wynar. At 0900 the camera was lowered over the site to picture the faulted and fissured sheet flows in the central graben, and move across to a hummocky fissure-fed flow. The trigger malfunctioned almost immediately, so that the camera was taking pictures continuously in the water column on its way to the bottom. It was determined that there would be about 15 minutes worth of film left when the camera reached the seafloor. Once on the seafloor it was towed for about 20 minutes and then hauled in.

After the camera was on deck, the ship steamed to Area 4 for the launching of TOBI which went over the side at 1410. At about 1600 a problem in the reception from the depth profiler was noted. The depressor weight was brought in and it was found that a loose connection at the weight was causing the problem. The depressor weight went in for the second time at 1827. The ship came back around to the track, and began surveying at about 2230. The 3.5 kHz echosounder and floating magnetometer were also deployed.

The seminar for today consisted of two talks. The first by Scott Garland was about combining TOBI images with bathymetric contours. The second by Eddie MacAllister and Jane Keeton was on how to use the image processing package Khoros. The day ended with a small celebration of hump day at the bow.

V. Area 4, Segments 7/8

5.1 Summary

Area 4 lies only a few miles north of Area 3 and consists of a large part of Segments 7 and 8, together with the septum that separates them, and a single TOBI swath that runs through the north end of Segment 8 into Segment 9 to insonify the southern half of that segment up to and including the TAG hydrothermal field.

Area 4 was selected because it gave the opportunity to image the two robust axial volcanic ridges of Segments 7 and 8. That of Segment 8 is especially large, and is crowned with a group of large seamounts. We took the opportunity to image the first fault block above the median valley floor on the west side, since that appeared from Sea Beam maps to contain an entire fossil axial volcanic ridge.

We also decided to continue the survey with a single line into Segment 9, to image the large valley that makes up the southern end of this segment (Segment 9 is the only other segment after Segment 6 not have a median valley). We then extended the line as far as the TAG hydrothermal field, so as to discover the response of the TOBI side scan and other instruments on the vehicle to the presence of a known major hydrothermal area. No dredging or camera work was conducted in Area 4.

The seamounts of Segments 7 and 8 are many and varied. The largest seamounts, and most of those visible on the upper parts of the AVRs, are of the hummocky type, rather irregular conical or flattened piles of hummocky lava. On the lower flanks of the AVRs smooth flattened seamounts are more common, and are often overlapped by later hummocky flows. One seamount in Segment 8 is similar to the large, low, flat-topped seamount in Area 2 (Segment 11), with a central crater and an irregular outline in plan.

Particularly striking on the AVR of Segment 7 are the numerous hummocky ridges which are several kilometers long, and often contain an axial fissure. Each is made up of a row of rather large hummocks, and must be the product of a single fissure eruption. These ridges are generally parallel to the AVR trend, and in places are piled on top of one another, so that locally areas of volcanic terrain are made up of superimposed ridges of this type.

Such ridges also occur on the AVR of Segment 8, but are not necessarily AVR parallel. In one part of the AVR hummock ridges occur in a reticulate pattern in two directions at right angles, one parallel to and the other normal to the AVR trend. In another part of this segment small ridges intersect in an irregular ramifying way.

In one or two places, and especially near the southern end of Segment 7, the volcanic stratigraphy that builds the AVRs is very well seen. Seamounts and hummocky flows overlap each other in clear sequence, and small faults can also be placed into the story.

Segment 9 was also imaged on the way the TAG hydrothermal area (see Chapter 6, Transits, for images of the TAG area). The spreading axis in Segment 9 turns out to be asymmetric relative to the topography. We had previously interpreted the axis of the deep in Segment 9 as the spreading

axis, but it is clear from the images that the neovolcanic zone lies at the east side of the deep, as was suggested by the crustal magnetization high, and that the deep is a flanking deep without its corresponding partner to the east.

As in other areas, tilted, plunging fault blocks play an important role in segment termination. The faults of these blocks throw down towards the spreading centre, and the blocks plunge down to meet the oblique boundary of the median valley floor. By means of these faults, which resemble en echelon tension gashes in their geometry, the wall of the median valley terminates Segment 7 without any axis normal faults.

Between Segment 7 and 8, and Segments 8 and 9 are two large septa, major topographic ridges which separate the two sections of median valley, and run oblique to the segment trend. Such septa are characteristic in this region of non-transform offsets of more than a few kilometers. We expected to find that the septa are complex, lying as they do between the ends of two active spreading cells. However the TOBI images of the septa showed no special structural features. The seafloor on the septum appears to be made up of young unsedimented volcanics, just as is the floor of the adjacent median valleys. The faults that cut the septa are ridge parallel faults of the usual type. The lack of any special tectonic fabric was itself very surprising.

At the south end of Area 4, we were very close to the Segment 6/Segment 7 boundary. The offset between these two segments is small, so that the transition is by simple overlap, as in Area 2. A patch of young volcanics in the SW corner of Area 4 probably is part of Segment 6 rather than Segment 7, occurring just within the overlap zone.

Landslides are a prominent feature of the images of Area 4, just as they are in the other areas studied. The most notable slides are at the northern end of Segment 8. There the Sea Beam maps show that the median valley suddenly narrows, and the TOBI images show that the narrowing is caused by two major landslides opposite to one another. These slides are complex features, as observed in other segments. That to the east has areas of gullying near the top of the slide front, the origin of which is obscure. If this were on land it would clearly be caused by running water, but that explanation is not obvious for features at the bottom of the ocean. A third important landslide narrows the median valley of Segment 9 just north of the TAG hydrothermal site, with the long tongue of a rockslide reaching far out into the median valley floor.

Our line to the west of the median valley in Segment 7 gave a very good image of a fossil AVR on the first fault block up from the median valley floor. The hummocky volcanic features are well preserved, and the block contains a large hummocky seamount of the same morphology as the large seamounts in the present median valley.

5.2 Waypoints

Waypoints and actual ship track for the TOBI survey in Area 4 are presented in Figure 5.1. Also in the figure are seamounts which have been previously identified from Sea Beam bathymetry (Smith and Cann, 1990, 1991), axial valley highs, and historical earthquakes in the region (relocated by Lin and Bergman, 1990).

The following way points defined the survey of Area 4.

D1) 25°21.0'N, 45°27.7'W

D2) 25°31.5'N, 45°24.75'W

D3) 25°49.0'N, 45°06.65'W

D4) 25°49.0'N, 45°02.9'W

D5) 25°30.0'N, 45°22.25'W

D6) 25°21.0'N, 45°24.85'W

D7) 25°21.0'N, 45o22.9'W

D8) 25°28.15'N, 45°20.85'W

D9) 25°43.8'N, 45°04.5'W

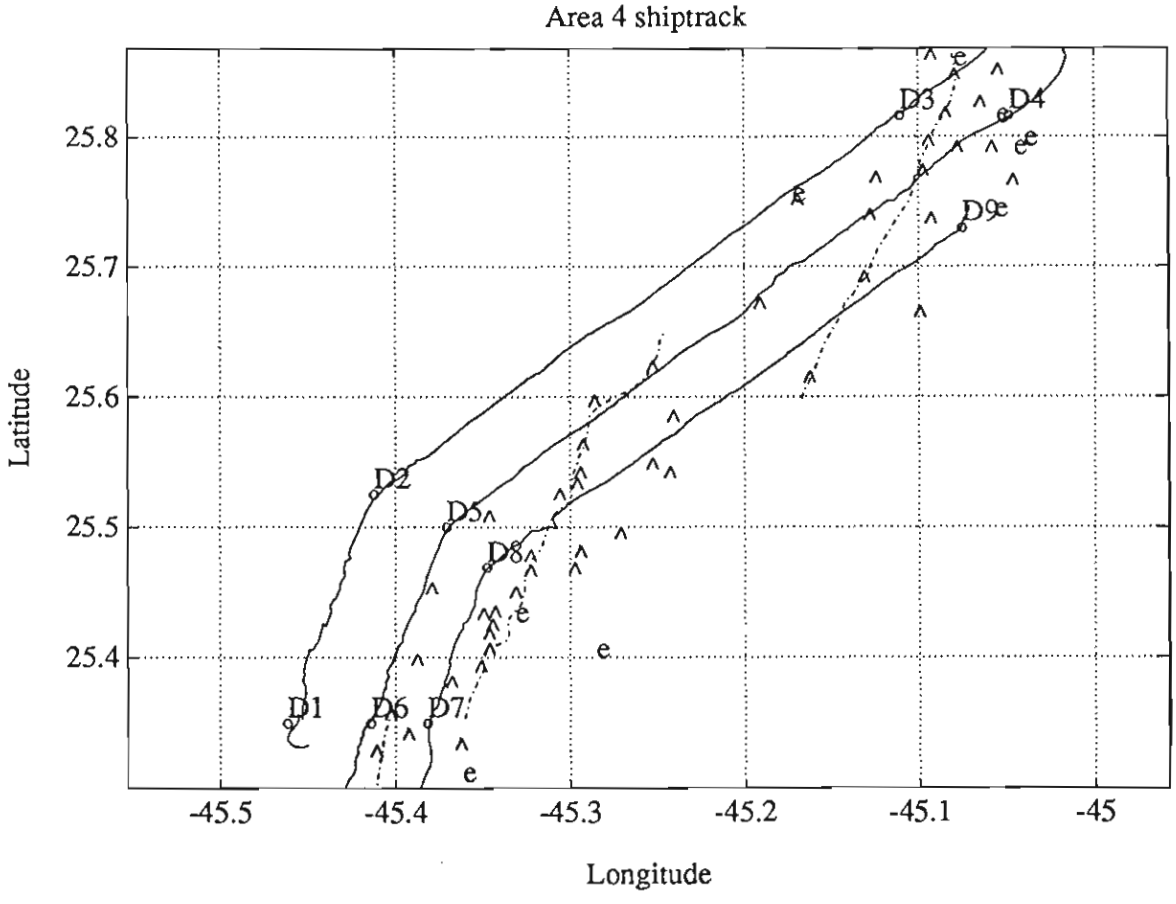

Figure 5.1 Area 4 shiptrack

Waypoints (text labels), shiptrack (solid line), axial volcanic highs (dashed lines), earthquakes (e's), and Sea Beam identified seamounts (^'s) for Area 4.

5.3 TOBI Run, Track line images

TOBI images for the entire Area 4 survey are shown in Figures 5.2 through 5.8. The images presented on these pages have been severely downsized from the original data. Each scanline of data (across track) in its original form contains 8000 pixels of information, 4000 to port and 4000 to starboard. Each pixel in the original data covers 0.75 meters of the seafloor. Distance from the TOBI sled and TOBI altitude affect this coverage so the 0.75 meter value should be taken as approximate. Along the ship track the original data contains a ping every 4 seconds for an along track pixel size of 4.0 meters. Again, as ship speed, distance from TOBI, and TOBI altitude affect this coverage, the 4.0 meter valued should be used as an approximation. In total, TOBI produces 8000 pixels of information every 4 seconds or 900 scanlines of 8000 pixels every hour.

The images in Figures 5.2 through 5.8 each represent approximately 4 hours, 27 minutes of information (4000 scanlines of 8000 pixels each in the original data) with time progressing from the top down in each frame. The original data has been reduced to 800 scanlines of 200 pixels each of the strips in the figures. Detailed images of certain interesting regions are outlined in white boxes and are presented in the next section. Rock dredge sites are also indicated on the images.

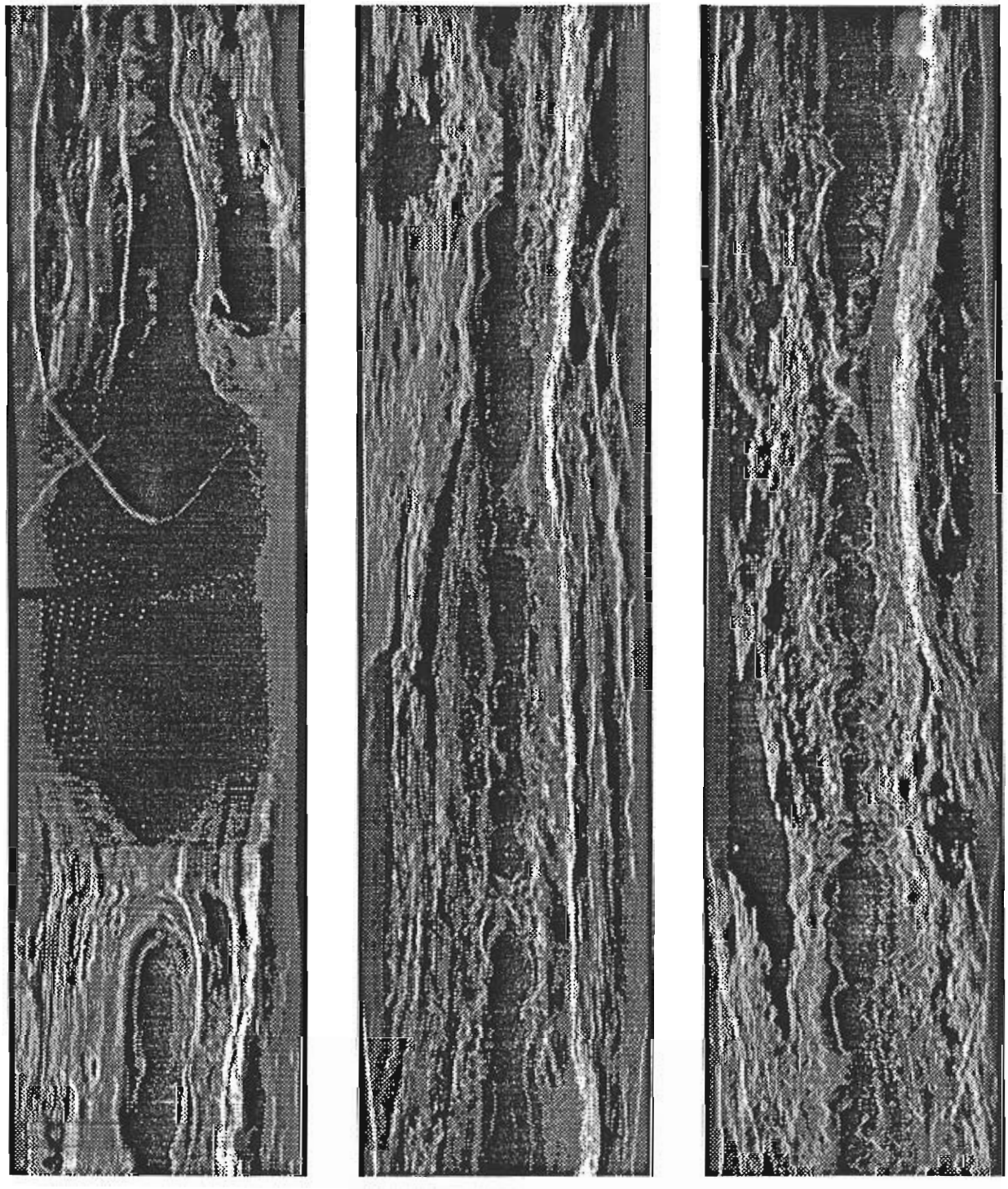

Figure 5.2 TOBI Images starting 2000/045 Z

Time progresses from left to right and from the top down in each frame. Each strip contains approximately 4000 TOBI pings for a total time of approximately 4.44 hours per strip. Area 4 starts at approximately 2000/045 Z, half way down the first strip on the left.

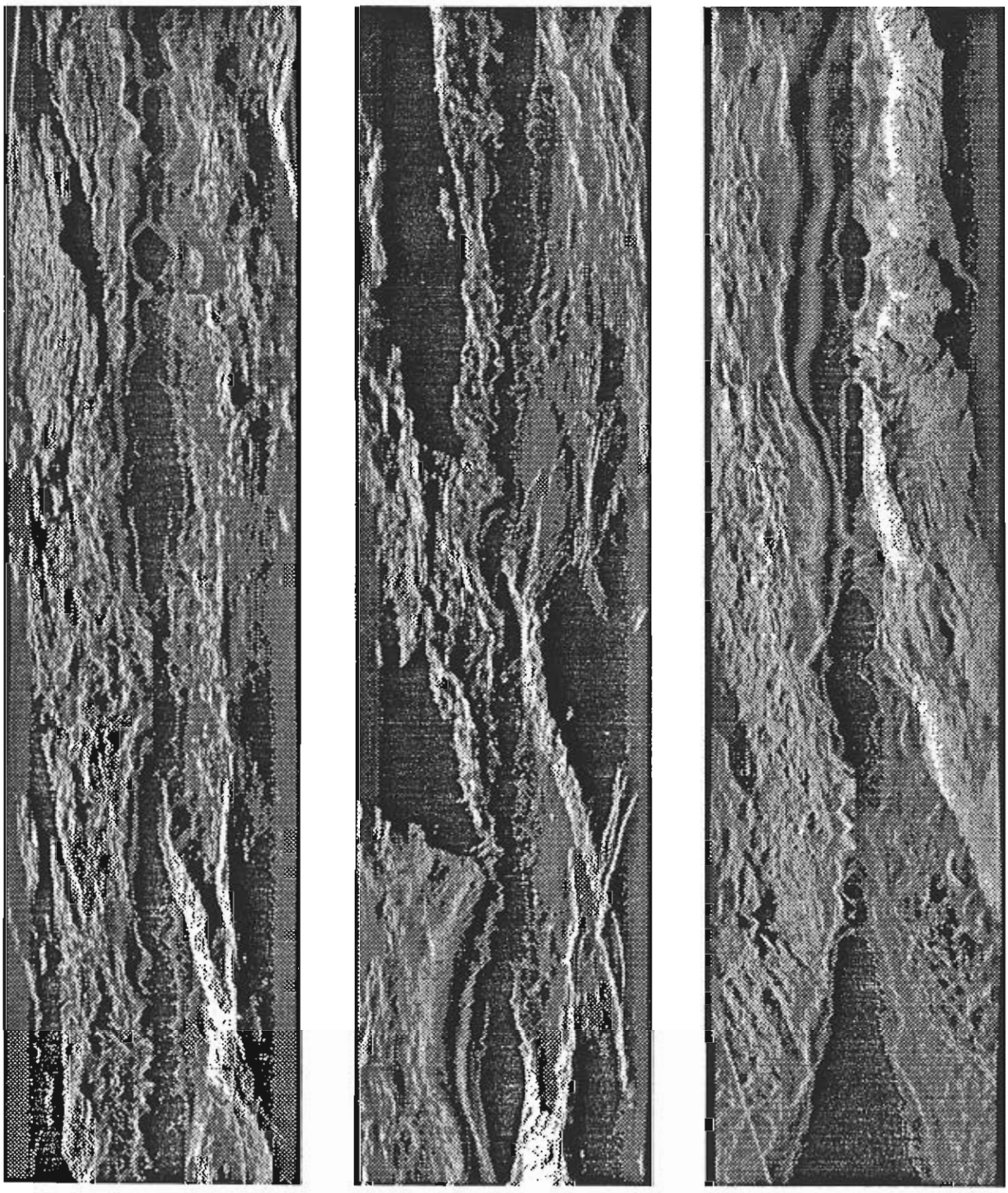

Figure 5.3 TOBI images starting at 0730./045 Z.

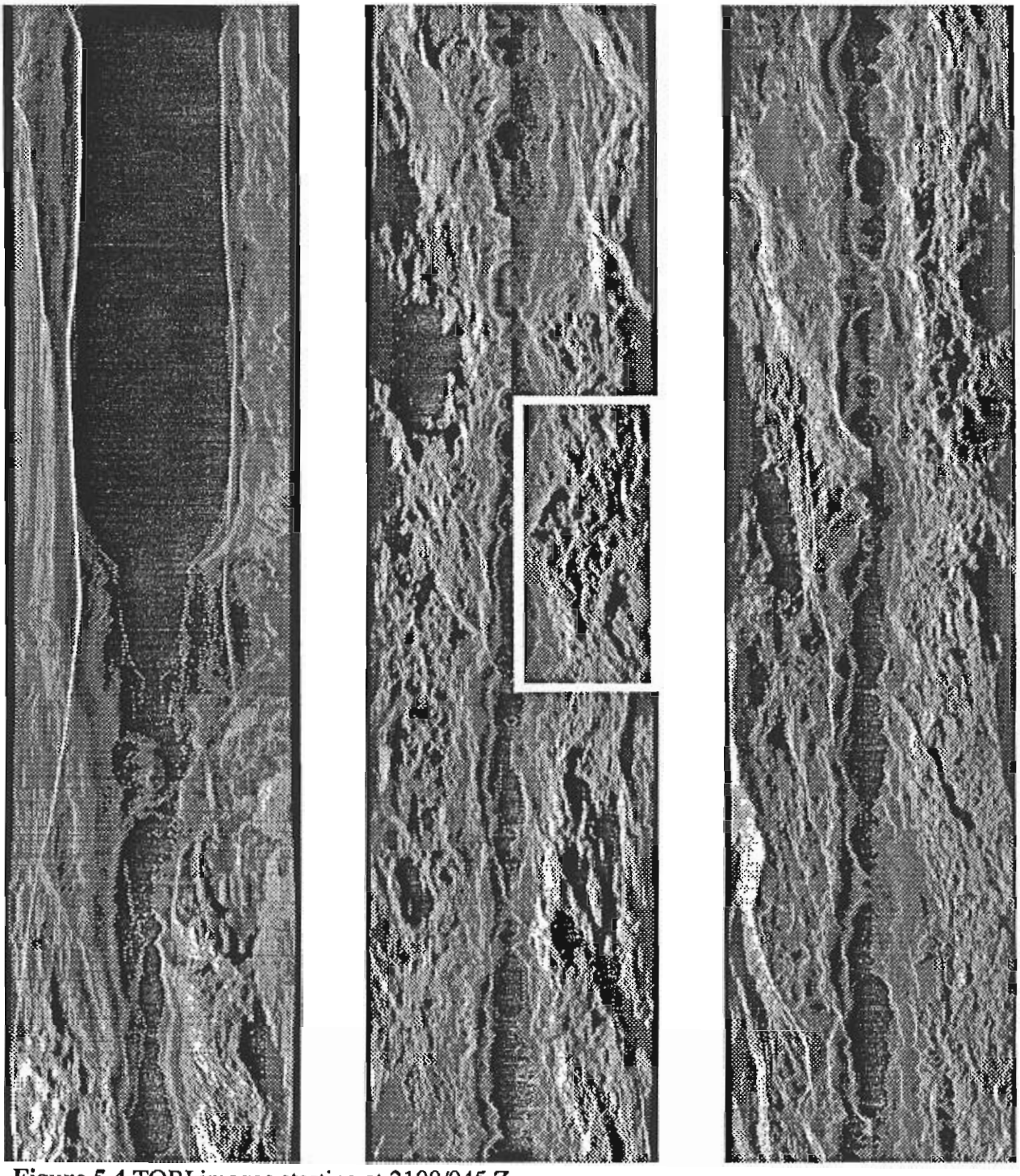

Figure 5.4 TOBI images starting at 2100/045 Z.

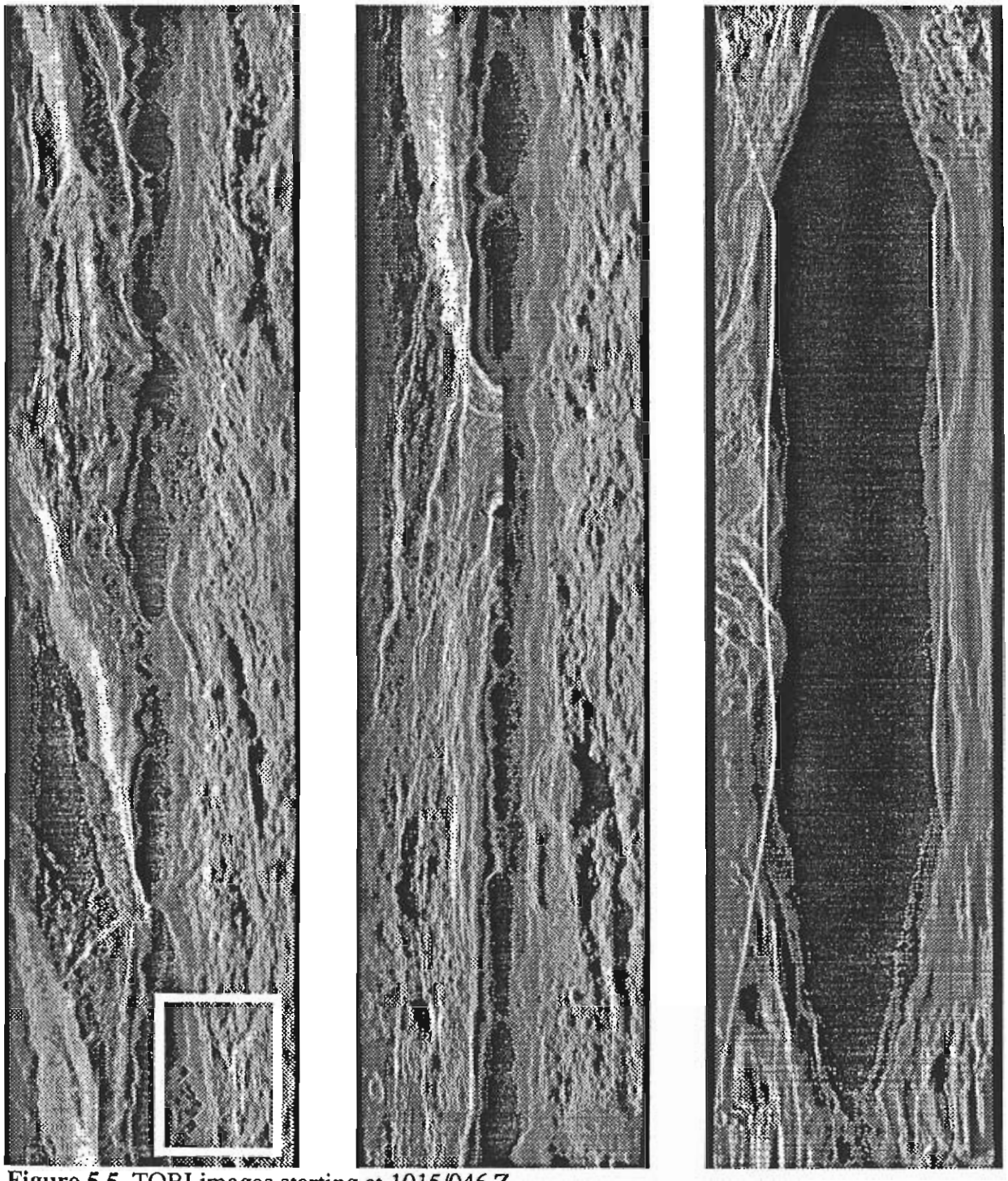

Figure 5.5 TOBI images starting at 1015/046 Z.

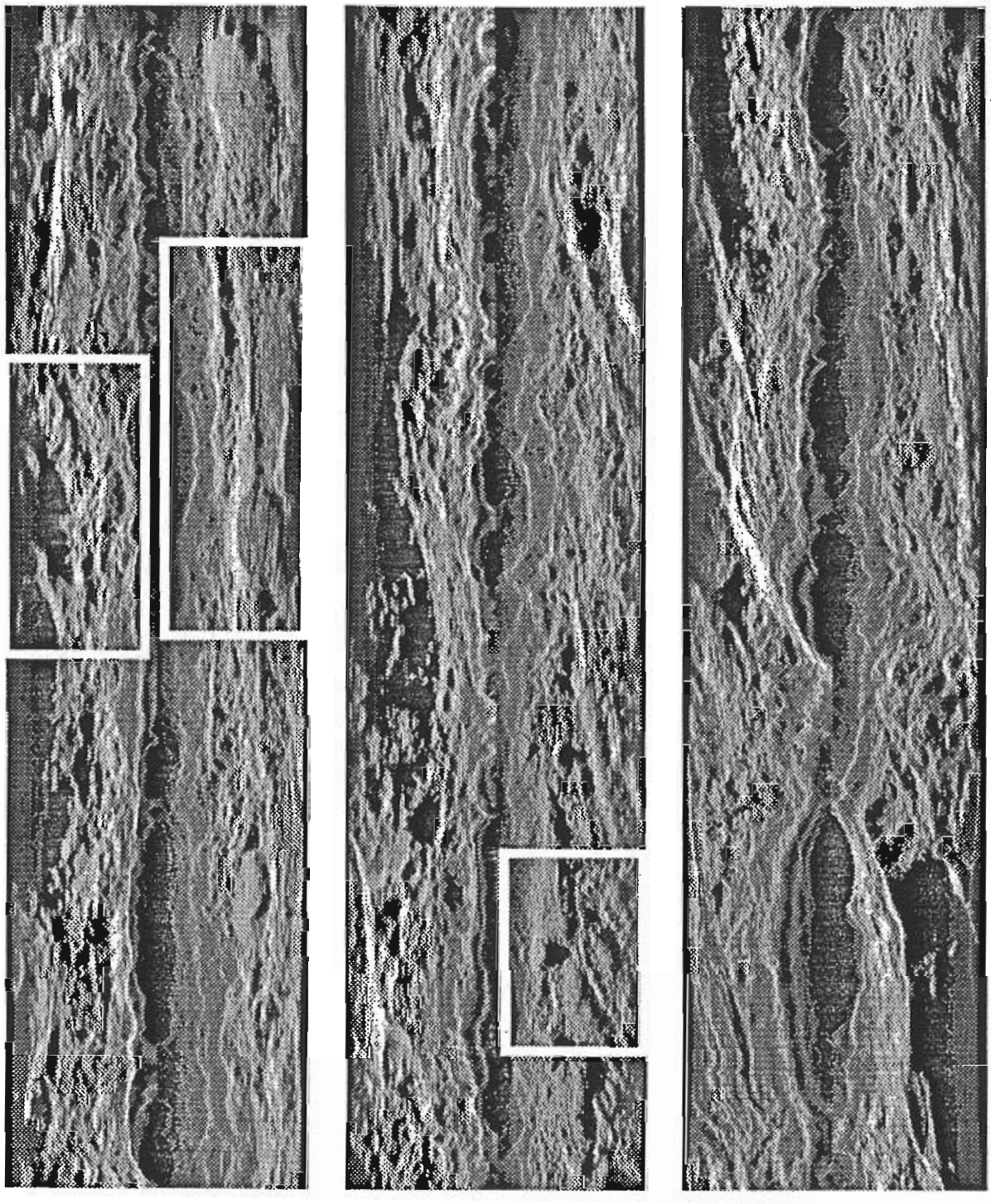

Figure 5.6 TOBI images starting at 2330/046 Z.

Hummocky seamount, stratigraphic relationships, and Caterpillar Ridges, outlined in white boxes, are described in detail below.

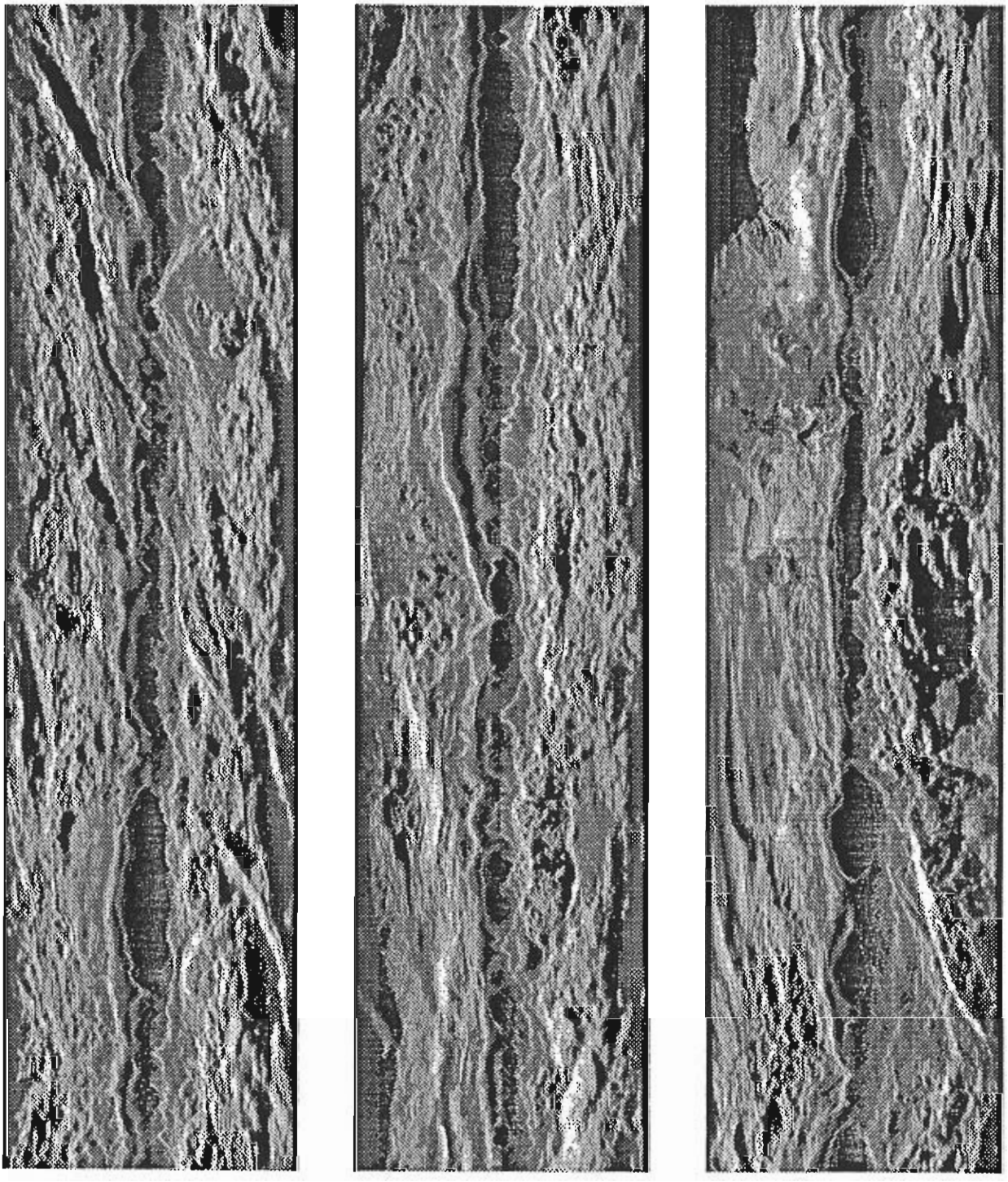

Figure 5.7 TOBI images starting at 1300/047 Z

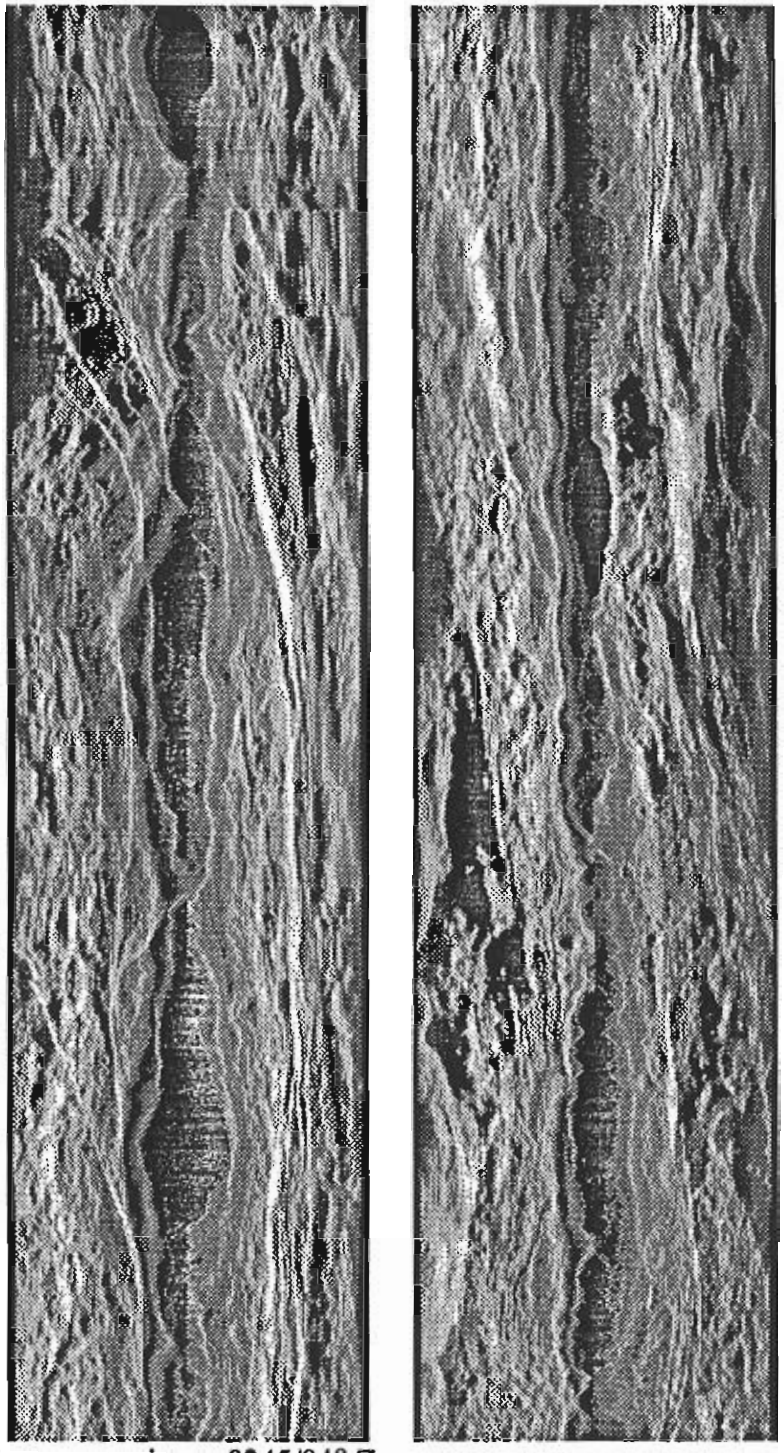

Figure 5.8 TOBI images starting at 0245/048 Z.

These images go slightly beyond Area 4 into the beginning of the transit to the TAG area (see Chapter 6).

5.4 TOBI Run, Detailed Images

5.4.1 Caterpillar Ridges

Caterpillar (or hummock) ridges, so called because of their resemblance to caterpillars, were first seen in Area 3. On the major AVR's of segments 7 and 8 in Area 4, they are particularly striking. The image show a group of caterpillar ridges erupted from fissures near the north end of the AVR of Segment 7. The run generally parallel to the ridge trend, and in places make up a large proportion of the ridge volcanism. The direction and angle of insonification affects the appearance of these features, but small faults and individual hummocks allow close correlation of the images.

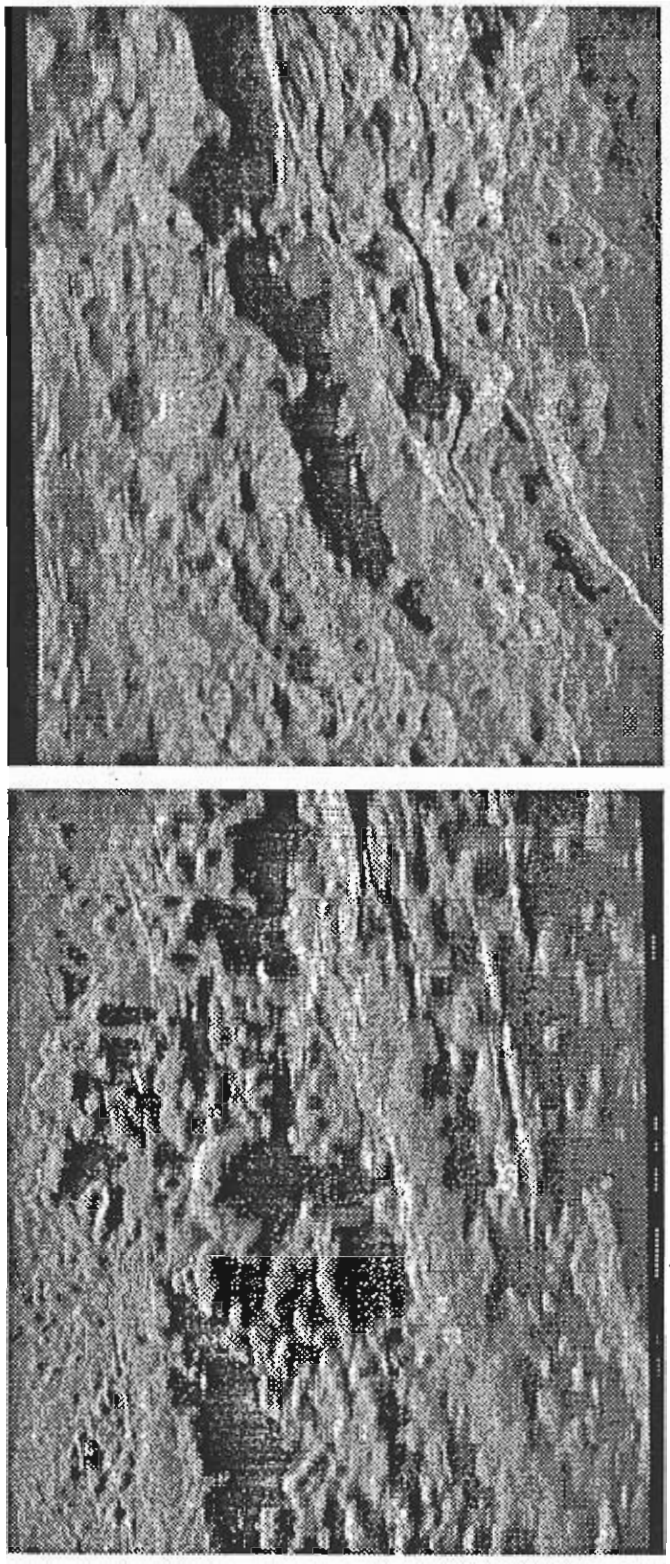

Figure 5.9 Caterpillar Ridges
East and west views of hummocky Caterpillar Ridges.

5.4.2 Hummocky seamount

Many of the seamounts identified from Sea Beam images prove in TOBI images conical or dome-shaped piles of hummocks. A small example of this type is Mt. Doom in Area 3. In Area 4 there were several fine larger examples. The seamount illustrated here is in the overlap zone between segments 6 and 7, and is a major pile of hummocks, probably analogous to the pillow volcanoes described from the extrusive part of the Troodos Ophiolite Complex in Cyprus.

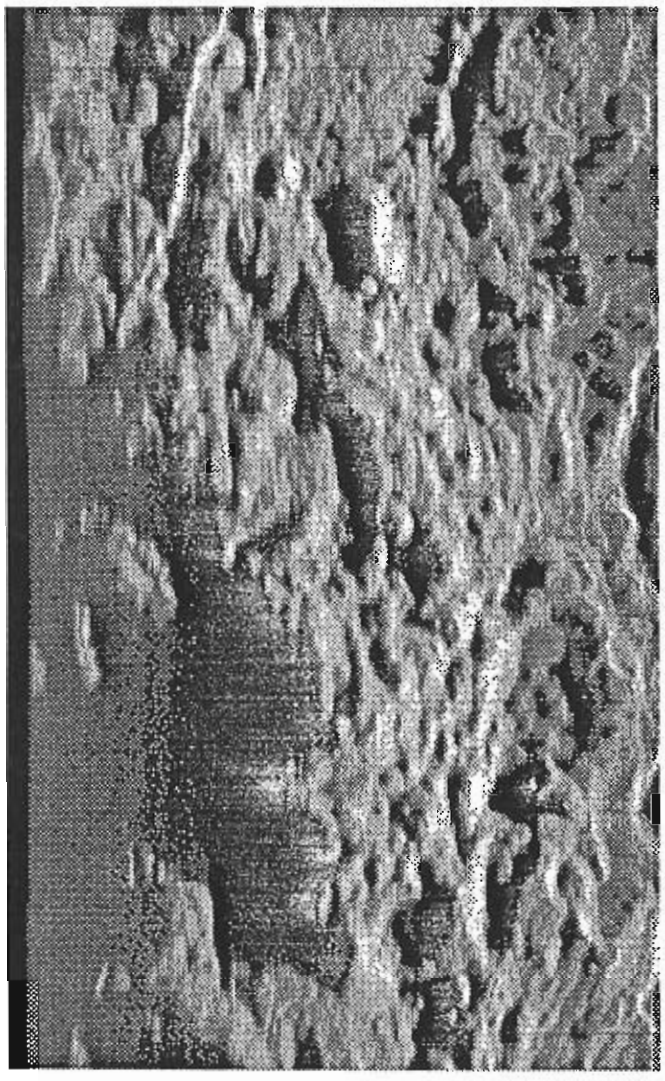

Figure 5.10 Hummocky seamount
A large hummocky seamount or pillow volcano.

5.4.3 Reticulated Ridges

Most areas of hummocky volcanics are organized into seamounts or into caterpillar ridges. A different organization appeared on the AVR of segment 8, imaged from a line running at 45 degrees to the AVR trend, which runs from the top left to bottom right in this image. Here the hummocks are organized into a pattern of reticulated ridges, with one trend parallel to the AVR axis and the other at right angles to it. The reason for this reticulation is not known. When this area was insonified from the opposite direction, and from a different height, the pattern was much less evi-

dent

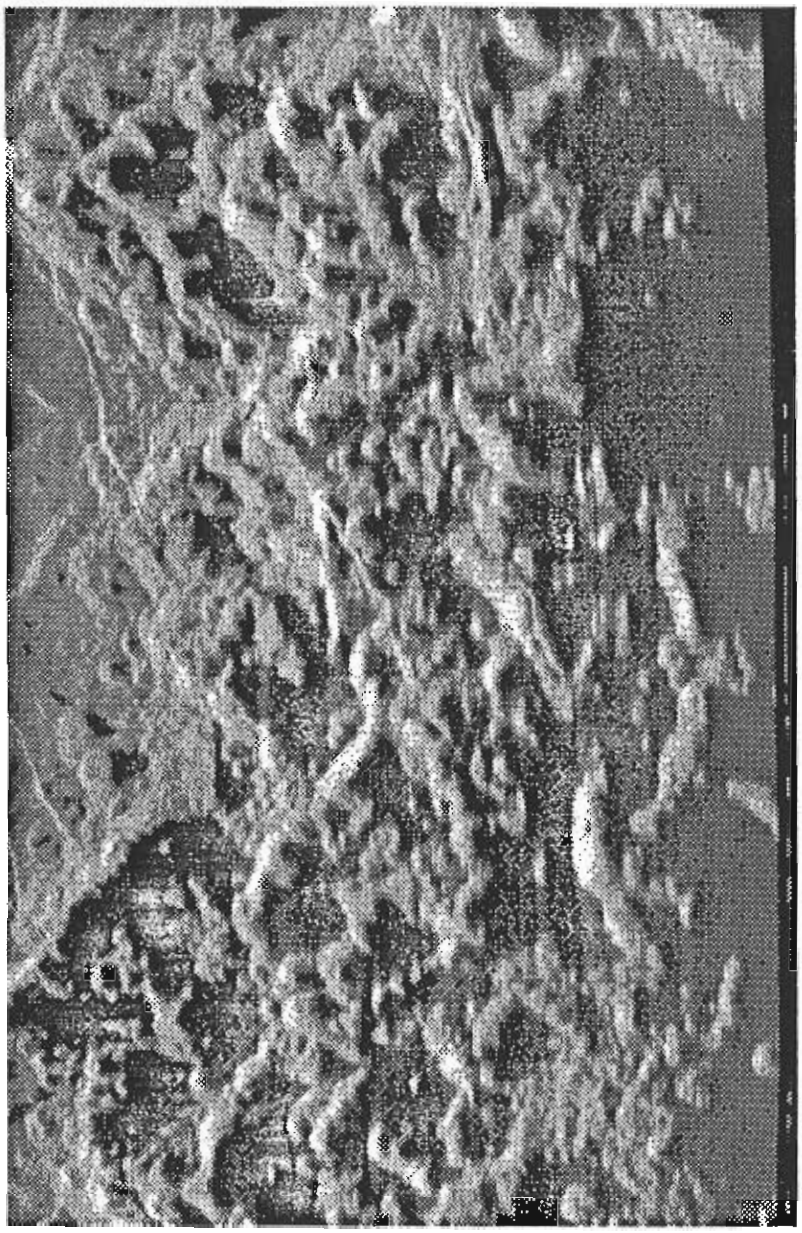

Figure 5.11 Reticulated Ridges

5.4.4 Stratigraphic relationships

An AVR is constructed by the superposition of many different volcanic elements. When these are all hummocky, the resulting stratigraphy is difficult to unravel, but when they are a mixture of smooth and hummocky forms, the picture is clearer. This image is of an area in the southern part of Segment 7 where stratigraphic relationships are very well seen. A low hat seamount (top right) has erupted onto early hummocky flows. This has been partly covered by three caterpillar

ridges, one of which is overlapped by a smooth, flat-topped seamount (bottom center) and then the whole sequence is cut by small faults and fissures.

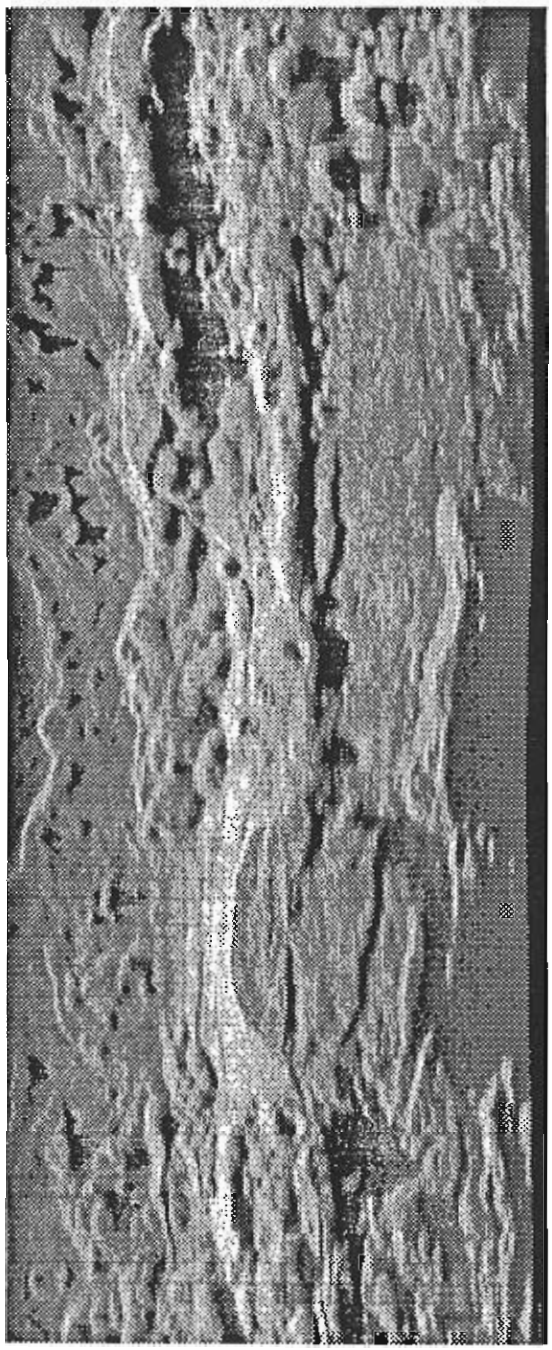

Figure 5.12 Stratigraphic relationships

5.5 Geological map description

Detailed interpretation of the TOBI images of each area included the production of a geological map which can be found in the back pocket of this volume. These maps, although only preliminary interpretations and lacking bathymetric data, have been useful in underlining the spatial distribution of the volcanic edifices, faults and landslides that have been imaged. Description of individual features has already been included in the summaries, so the discussion here will be limited to the interaction observed between the different processes.

Area 4 focuses on the overlap between segments 7 and 8. As in area 1, on the bathymetric data both segments are characterized by axial highs in a median valley separated by a septum (central high). The geological interpretation of the TOBI data supports this view. The AVRs are largely composed of hummocky terrain, which in this area is dominated by linear ridges (caterpillars) oriented subparallel to the ridge axis. Cross cutting linear ridges dominate towards the end of segment 8 and hummocky heaps are also seen throughout the area. Smooth seamounts have been identified sitting upon hummocks but more often they are at least partially buried.

Faulting within the neo-volcanic zone is limited to the few minor faults and fractures. Off-axis the proportion of faults increases. Faults adjacent to the central parts of the segment are curvilinear and show an en-echelon outcrop pattern. The large faults terminate in a myriad of smaller faults which form in dense concentrations giving a stepped (terraced) geometry. As described in the previous areas, a large concentration of minor faults appears to be coincidental with the ends of the segments although larger faults are still seen. Towards the end of the segment these larger faults cease to be en-echelon but are linked by a series of lateral ramps which parallel the non-transform offset.

The septum seen on the bathymetric data is not obvious on TOBI records, being marked by a few extensional faults cross cutting hummocky terrain. It would appear that most of the offset is taken up on the lateral ramps. The origin of the septum thus remains unsolved.

Two landslides occur in the area lying to the east and west of segment 8. Elsewhere sedimentation is limited to the development of minor talus slopes at the base of the larger faults and pelagic sedimentation off axis.

5.6 Dredging

No dredging was done in Area 4.

5.7 Underway Geophysics

See Chapter 7 for summary of overall gravity and magnetics results.

5.8 Camera Runs

No camera runs were made in Area 4.

5.9 Daily Log

February 13 (JD 44)

The ship steamed to Area 4 for the launching of TOBI which went over the side at 1410. At about 1600 a problem in the reception from the depth profiler was noted. The depressor weight was brought in and it was found that a loose connection at the weight was causing the problem. The

depressor weight went in for the second time at 1827. The ship came back around to the track, and began surveying at about 2230. The 3.5 kHz echosounder and floating magnetometer were also deployed.

The seminar for today consisted of two talks. The first by Scott Garland was about combining TOBI images with bathymetric contours. The second by Eddie MacAllister and Jane Keeton was on how to use the image processing package Khoros. The day ended with a small celebration of hump day at the bow.

February 14 (JD 45 - Valentine's Day)

The day began on the first survey line north in Area 4 collecting side-scan images of what may be a fossil axial volcanic ridge from Segment 7. Way point D2 was passed early on in the day. Images of the fossil ridge adjacent to Segment 7, the deeps at the ends of both Segment 7 and 8, as well as the septum separating the segment were obtained. The day was uneventful equipment wise. We began the turn to our southward line from way points D3 to D4 late in the day.

The seminar series was suspended because of the TOBI watches. The Valentine's Day BBQ started in the rain, but spirits remained high. Three of the crew (Joe, Martin, and Kevin) had severe haircuts; especially Joe.

February 15 (JD 46)

TOBI survey of Area 4 continued. In the early morning we turned south at way point D4 and imaged the axial volcanic ridge of Segment 8, the septum between the two segments, and continued down along the western deep of Segment 7. The septum separating Segments 7 and 8 appears to be volcanic in origin with hummocky surfaces on the discrete highs. Most of the volcanoes identified from Sea Beam data are found to be large masses of hummocks. At the edges of the deep at the southern end of Segment 7 several smooth textured flat-topped seamounts are seen. At the end of the day the turn from way point D6 to D7 was begun.

Radio contact was established with the KNORR which had just arrived on site to survey the wall of the Kane Fz with Scripp's Deep-Tow instrument. J. Delaney asked if we were going to tow over the TAG hydrothermal mounds. After considering the possibility it was decided that we should extend the final northward survey line of Area 4 to run over the TAG site. Way point D9 was changed, and 4 more way points were added to take us northward to Segment 9 and the TAG area.

The activities of the day included hacky sack and cricket. Scott offered to switch watches with Jane who celebrated Valentine's day in style.

February 16 (JD 47)

At the beginning of the day we were north of way point D7 on our way to way point D8 and then T1 (the first way point for the Tag Transit). Previous way point D9 was changed for the transit to the TAG region. We imaged the eastern side of Segment 7, and Segment 8. At T1 we turned northward towards Segment 9. A landslide similar to Tanner's Toe was imaged at the northeastern edge of Segment 8.

February 16 was noteworthy for its warm weather and calm seas. Marty produced a figure

for the cover of EOS ('Volcanic Features at the Mid-Atlantic Ridge'). Chris MacLeod was sick and others filled in for him on the TOBI watch.

VI. Transit Data

6.1 Area 2 - Area 3 Transit

6.1.1 Waypoints

During the approach from Area 2 to the north we ran a track designed to follow the spreading axes of Segments 10, 9, 8, and 7, to look at mantle Bouguer anomalies of each of these segments. We were able to extend this coverage during the TOBI runs through Segment 6 well into the offset zone. Each of the segments has a well defined mantle Bouguer anomaly centered near its mid point. The anomalies for Segment 11 (in Area 2) and Segment 6 are larger than any others.

The following way points were given to the bridge.

1) 26°14.4'N, 44°41.4'W

2) 26°15.5'N, 44°48.3'W

3) 25°58.0'N, 44°54.4'W

4) 25°58.0'N, 45°01.2'W

5) 25°37.3'N, 45°09.6'W

6) 25°37.2'N, 45°16.1'W

7) 25°20.0'N, 45°22.3'W

6.1.2 Daily Log

January 31

Weather deteriorated on the morning of 31 January. During the day winds reached speeds of 47-49 kts sustained out of the southeast. At 1600 the decision was made to sail directly south to survey Area 2 which consists of Segments 10 and 11. Estimated time of arrival was set at 1600 on 01 February, 1992. Weather began to moderate after dinner with wind speeds dropping to 20-25 kts. Seminars were given by Martin Dougherty, Jian Lin, Ben Brooks, and Rachel Pascoe in the main lab.

February 07 (JD 38)

We completed the transit to waypoint C1 at about 0400. TOBI was put over the side at 0606, and the depressor weight followed at 0637.

6.2 Area 3 -4 Transit

6.2.1 Waypoints

The transit to Area 4 was a short 15 miles from the northern boundary of Segment 6 to mid-way into Segment 7.

6.2.2 Daily Log

February 13 (JD 44)

After the camera was on deck, the ship steamed to Area 4 for the launching of TOBI which went over the side at 1410. At about 1600 a problem in the reception from the depth profiler was noted. The depressor weight was brought in and it was found that a loose connection at the weight was causing the problem. The depressor weight went in for the second time at 1827. The ship came back around to the track, and began surveying at about 2230. The 3.5 kHz echosounder and floating magnetometer were also deployed.

The seminar for today consisted of two talks. The first by Scott Garland was about combining TOBI images with bathymetric contours. The second by Eddie MacAllister and Jane Keeton was on how to use the image processing package Khoros. The day ended with a small celebration of hump day at the bow.

6.3 Area 4-TAG

6.3.1 Summary

The TAG hydrothermal site, containing probably several million tons of sulfides, is disappointingly small on the TOBI images (see Figure 6.1). It was well imaged as a circular domal structure, but the black smoker plume gave no identifiable signal. No temperature anomaly was recorded in the water column, and no transmissometer anomaly was found. Near the site, however, there was a local blanket of sediment visible on the images, which may be of hydrothermal sediment, and thus may be the best TOBI tracer for a major hydrothermal site.

6.3.2 Waypoints

After surveying Area 4 it was decided to extend the TOBI line to run across the TAG Hydrothermal mound. The following way points were given to the bridge for this run:

1) 25°43.8'N, 45°04.5'W

2) 25°55.9'N. 45°01.9'W

3) 25°58.2'N, 44°56.0'W

4) 26°15.0'N, 44°46.5'W

6.3.3 TOBI Run, Track line images

TOBI images for the Area 4 - TAG area survey are shown in Figure 6.1. The images presented on these pages have been severely downsized from the original data. Each scanline of data (across track) in its original form contains 8000 pixels of information, 4000 to port and 4000 to starboard. Each pixel in the original data covers 0.75 meters of the seafloor. Distance from the TOBI sled and TOBI altitude affect this coverage so the 0.75 meter value should be taken as approximate. Along the ship track the original data contains a ping every 4 seconds for an along track pixel size of 4.0 meters. Again, as ship speed, distance from TOBI, and TOBI altitude affect this coverage, the 4.0 meter valued should be used as an approximation. In total, TOBI produces 8000 pixels of information every 4 seconds or 900 scanlines of 8000 pixels every hour.

The image in Figure 6.1 each represent approximately 4 hours, 27 minutes of information

(4000 scanlines of 8000 pixels each in the original data) with time progressing from the top down in each frame. The original data has been reduced to 800 scanlines of 200 pixels each of the strips in the figures. Detailed images of certain interesting regions are outlined in white boxes and are presented in the next section.

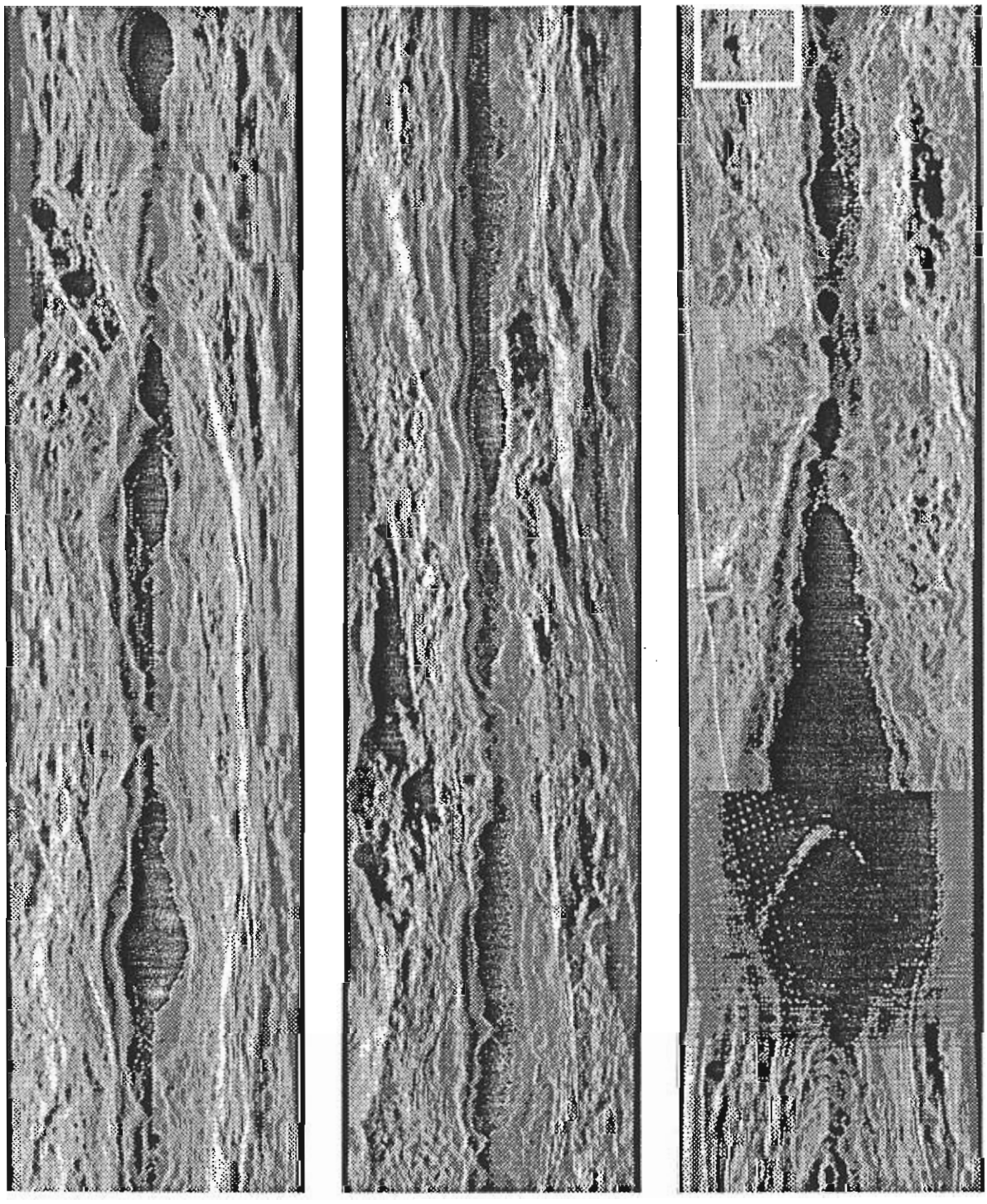

Figure 6.1 TOBI images starting 1245/047 Z
Transit to TAG hydrothermal area (outlined in white box).

6.3.4 Daily Log

February 16 (JD 47)

At the beginning of the day we were north of way point D7 on our way to way point D8 and then T1 (the first way point for the Tag Transit). Previous way point D9 was changed for the transit to the TAG region. We imaged the eastern side of Segment 7, and Segment 8. At T1 we turned northward towards Segment 9. A landslide similar to Tanner's Toe was imaged at the northeastern edge of Segment 8.

February 16 was noteworthy for its warm weather and calm seas. Marty produced a figure for the cover of EOS ('Volcanic Features at the Mid-Atlantic Ridge'). Chris MacLeod was sick and others filled in for him on the TOBI watch.

February 17 (JD 48)

On the morning of February 17 our position was off the TOBI scale bathymetry maps for Segments 7 and 8, and we were using a map produced by Jian and Rob Lloyd to plot TOBI positions. We transited across the boundary between Segments 8 and 9 and continued toward the position of the TAG hydrothermal mound. Segment 9 has no axial volcanic ridge, and the ship track ran along the middle of a deep. The hydrothermal mound is at the northeastern corner as you come out of the deep. The mound itself is about 200-300 m in diameter, and would appear on the TOBI records as a very small topographic high - about the same size as many hummocks that have been imaged. As we approached the TAG site we observed an area of lower reflectivity on the port side of the image. The hydrothermal mound is located to starboard of the ship. It was speculated that the dark patch was sediment covered, and may be associated with the hydrothermal activity.

A bump was tentatively identified as the TAG hydrothermal mound, and we steamed past it for about 1 hour. TOBI recovery was begun at approximately 1300, and the vehicle was on deck near 1445. We then began our transit to the final survey region: Area 1. The track was laid out to collect gravity data along the axis of the spreading segments.

A seminar was held at which the authorship of papers as well as the data distribution scheme were discussed. It was agreed in principle that papers that are written within a year of the cruise should include all participating scientist's names. Full moon causes restless spirits.

February 18 (JD 49)

We arrived on site at approximately 0400 to begin the survey of Area 1

6.4 TAG-Area 1 Transit

6.4.1 Waypoints

The transit northward from TAG to Area 1 was again based on getting good gravity lines along the axis of the magmatic segments. The following waypoints were made good during the ridge axis transit to Area 1:

1) 27°11'.0N, 44°22.5'W

2) 28°17.8'N, 43°48.0'W

3) 28°20.0'N, 43°44.0'W

4) 28°40.0'N, 43°37.0'W

6.4.2 Daily Log

For the daily log see February 17 and 18 above.

VII. Gravity and Magnetics

7.1 Gravity Survey - Overview

Gravity field was recorded on board RRS Charles Darwin by two gravitometers, S40 and S84. (A detailed description of these instruments were given at the beginning of this cruise report). Raw gravity data were archived both by the ship computer in digital values (the ABC system) and by paper recorders. The raw data were sampled at 10 second intervals, while the final free-air anomaly data were processed at 2 minute intervals. Both gravitometers performed well during the entire cruise, thanks to close attention of RVS personnel and our watch keepers.

The spreading segments of the Mid-Atlantic Ridge (MAR) between 28°-31° N were surveyed in a previous Sea Beam and gravity study (Lin et al., 1990). Although Sea Beam data were also collected between 24°-28° N, no complementary gravity data were available prior to this cruise. The gravity survey of CD65 mapped 11 previously unmapped spreading segments that stretches 370 km along the MAR axis. This survey filled a major gap in the MAR gravity data.

7.2 Free-Air Anomaly

The raw gravity data were reduced to free-air anomaly (FAA) by RVS Senior technician Robert Lloyd using software provided by the RVS. This EOTVOS reduction process corrects artificial gravity effects due to changes in ship course and speed. The RVS software for EOTVOS correction was based on theoretical formula provided by researchers at Cambridge University. The equation used are as follows:

EOTVOS correction (Worzel, 1959):

$$\Delta g = 7.487 \times S \times \sin(C) \times \cos(lat \times N) + S \times \frac{S}{240.8}$$

where S = speed-made-good in knots and C = course-made-good

International gravity formula (Jacobs, et al., 1959):

$$g(lat) = 978031.8 \times (1 + 0.0053024 \times (\sin(lat))^2 + 0.0000059 \times (\sin(2 \times lat))^2)$$

The accuracy of EOTVOS corrections depends on the smoothness of satellite navigation. During CD65 cruise, good GPS fixes (more than 2 satellites) were available 21 to 23 hours daily (see table 1). When the ship is on a steady course, the EOTVOS effect remains constant and perturbates little (less than 3 mgal). Even at large course changes, it is believed that good EOTVOS corrections can still be achieved. The gravitometers, however, require 10-15 minutes to stabilize after a major course change. This instrumental limitation may have caused some local spikes (up to 25 mgal) in the free-air anomaly (Figure 7.1). To yield a more meaningful free-air anomaly, we have removed manually all major artificial spikes in the free air anomaly, which are definitely associated with course changes. Fig. 7.1 shows a 4-day record of free-air anomaly between Day 34 and 38. In these four days, TOBI survey was carried out prior to Day 35.6, during which the free-air anomaly is relatively smooth. In the period after Day 35.6, rock dredging was carried out. Larger errors in the free-air anomaly were apparent during this period of frequent ship course and speed

changes.

The free-air anomalies recorded during TOBI surveys and transits (repeated tracks) between survey sites are shown in Figure 7.2a, as a function of latitude. The anomaly along these profiles varies in values from -50 to 20 mgal. More positive free air anomalies were observed over the elevated seafloor of each spreading segments. The close correlation between the free-air anomaly and seafloor depth (FIgure 7.2b) demonstrates that the gravity field is dominated by the seafloor topographic effects. Such topographic effects can be modeled and removed as discussed in the following section.

TABLE 1. GPS Data Gaps During Charles Darwin 65/92 Cruise
(Absence of logged data longer than 20 min)

from			to			total gap
92	031	23:19:49	to 92	032	08:06:08	(8.8 hrs)
92	032	10:00:50	to 92	032	11:07:46	(66.9 mins)
92	032	11:09:47	to 92	032	12:15:49	(66.0 mins)
92	032	12:20:51	to 92	032	13:06:32	(45.7 mins)
92	032	13:10:51	to 92	032	13:35:11	(24.3 mins)
92	032	16:10:50	to 92	032	16:46:19	(35.5 mins)
92	032	20:35:00	to 92	032	23:02:34	(2.5 hrs)
92	032	23:16:44	to 92	032	23:37:59	(21.2 mins)
92	033	11:38:16	to 92	033	12:09:39	(31.4 mins)
92	033	18:30:25	to 92	033	18:56:52	(26.4 mins)
92	033	20:45:19	to 92	033	22:41:43	(116.4 mins)
92	034	00:22:08	to 92	034	00:43:22	(21.2 mins)
92	034	09:20:52	to 92	034	09:44:10	(23.3 mins)
92	034	11:10:26	to 92	034	11:31:49	(21.4 mins)
92	034	20:29:19	to 92	034	22:28:20	(119.0 mins)
92	035	13:49:28	to 92	035	14:36:16	(46.8 mins)
92	035	20:19:32	to 92	035	22:43:17	(2.4 hrs)
92	035	22:50:20	to 92	035	23:16:42	(26.4 mins)
92	036	00:10:15	to 92	036	00:56:43	(46.5 mins)
92	036	19:40:26	to 92	036	20:01:39	(21.2 mins)
92	036	20:16:48	to 92	036	22:24:43	(2.1 hrs)
92	036	22:58:04	to 92	036	23:27:19	(29.2 mins)
92	037	00:04:42	to 92	037	00:52:13	(47.5 mins)
92	037	05:46:19	to 92	037	06:12:57	(26.6 mins)
92	037	06:50:26	to 92	037	07:14:55	(24.5 mins)
92	037	15:59:26	to 92	037	16:22:19	(22.9 mins)
92	037	21:10:13	to 92	037	22:07:43	(57.5 mins)
92	038	00:25:09	to 92	038	00:52:30	(27.4 mins)
92	038	21:00:58	to 92	038	21:47:22	(46.4 mins)
92	039	02:19:30	to 92	039	03:31:59	(72.5 mins)

92	039	20:59:25	to 92	039	21:52:36	(53.2 mins)
92	040	02:10:51	to 92	040	02:32:06	(21.2 mins)
92	040	20:00:52	to 92	040	20:25:09	(24.3 mins)
92	040	21:05:30	to 92	040	21:56:03	(50.5 mins)
92	041	13:39:36	to 92	041	13:59:55	(20.3 mins)
92	041	20:50:04	to 92	041	22:09:13	(79.2 mins)
92	042	20:50:43	to 92	042	21:11:54	(21.2 mins)
92	042	23:50:26	to 92	043	00:18:46	(28.3 mins)
92	043	01:50:26	to 92	043	02:47:17	(56.9 mins)
92	043	07:20:51	to 92	043	07:48:21	(27.5 mins)
92	043	09:00:24	to 92	043	09:32:08	(31.7 mins)
92	043	11:09:39	to 92	043	11:32:00	(22.4 mins)
92	043	18:10:26	to 92	043	18:40:50	(30.4 mins)
92	043	20:47:20	to 92	043	21:37:45	(50.4 mins)
92	043	23:58:53	to 92	044	00:26:14	(27.4 mins)
92	044	01:50:25	to 92	044	02:17:55	(27.5 mins)
92	044	09:40:25	to 92	044	10:01:49	(21.4 mins)
92	044	20:44:52	to 92	044	21:42:16	(57.4 mins)
92	044	23:55:47	to 92	045	00:24:12	(28.4 mins)
92	045	15:40:50	to 92	045	16:02:10	(21.3 mins)
92	045	20:37:31	to 92	045	21:10:49	(33.3 mins)
92	045	23:52:01	to 92	046	00:15:17	(23.3 mins)
92	046	20:27:30	to 92	046	21:38:10	(70.7 mins)
92	046	23:47:31	to 92	047	00:15:07	(27.6 mins)
92	047	07:09:33	to 92	047	07:31:59	(22.4 mins)
92	047	20:29:18	to 92	047	21:18:37	(49.3 mins)
92	047	23:44:05	to 92	048	00:12:20	(28.2 mins)
92	048	20:26:49	to 92	048	21:13:17	(46.5 mins)
92	049	07:08:54	to 92	049	07:32:16	(23.4 mins)
92	049	15:09:30	to 92	049	15:32:16	(22.8 mins)
92	049	20:23:51	to 92	049	21:06:29	(42.6 mins)
92	050	20:19:30	to 92	050	21:01:59	(42.5 mins)
92	051	20:15:08	to 92	051	20:48:41	(33.5 mins)
92	052	11:40:25	to 92	052	12:01:58	(21.6 mins)
92	052	20:10:27	to 92	052	20:47:48	(37.4 mins)
92	053	02:30:25	to 92	053	03:02:10	(31.8 mins)
92	053	19:49:41	to 92	053	20:37:07	(47.4 mins)

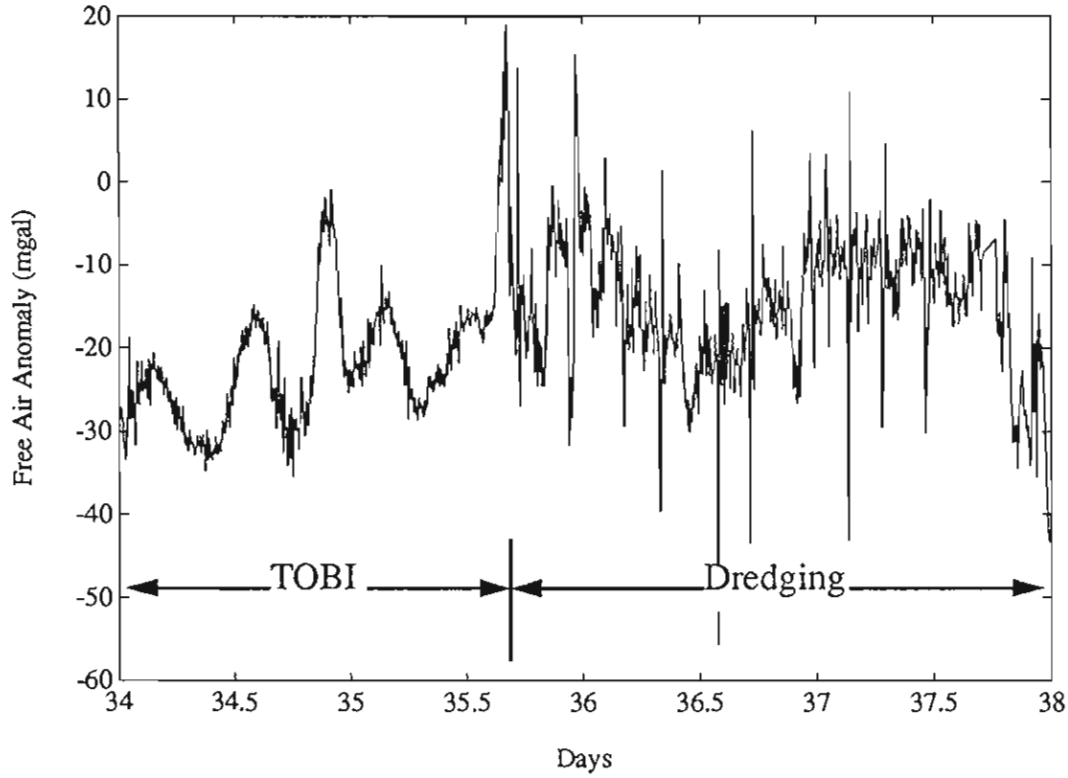

Figure 7.1 Free-air gravity anomaly, JD 034-038 Z

Free-air gravity anomaly recorded during JD 34 to JD 38, 1992. Note that the anomaly is relatively smooth during TOBI operation, but became noisy during rock dredging.

7.3 Mantle Bouguer Anomaly

The primary objective of the gravity survey is to determine the relative distribution of crustal and mantle density beneath offsetting spreading segments. To reveal the more interesting sub-seafloor density features, we reduced the free-air anomaly to the mantle Bouguer anomaly by removing the gravity effects of water/crust and crust/mantle interfaces. This modeling approach follows that of previous three-dimensional gravity mapping of Kuo and Forsyth (1988) and Lin et al. (1990).

The mantle Bouguer corrections were made based on Sea Beam bathymetry data collected previously by WHOI and University of Washington scientists (Purdy et al., 1991; Sempere et al., 1990). The sea surface gravity due to seafloor topographic reliefs were calculated using a Fourier Transformation spectrum method of Parker (1972). The initial model assumes a 6-km constant thickness crust and constant densities for water (1030 km/m^3), crust (2700 km/m^3), and mantle (3300 km/m^3). The resultant mantle Bouguer anomaly then reflects directly the deviations from this simple model. Digital bathymetry in a large region (46° to 42.5° W, 24.8° to 29.5° N) was refor-

matted into 512x512 grids, with longitude and latitude spacings of 0.68 and 1.02 km, respectively. Several test calculations were carried out, which show that the chosen spacings were adequate in modeling accurately the gravity effects at the sea surface.

For every free-air anomaly measurement **g_faa** at point **P (long,lat)**, we calculated a corresponding mantle Bouguer gravity correction **c (long, lat)**. The mantle Bouguer anomaly at point **P** is then obtained as

g_mb = g_faa - c (long,lat)

Approximately 10,000 measurements of good mantle Bouguer anomaly were obtained using the above method. These anomalies are shown in Figure 7.3 as a function of latitude. It is observed that the ridge-parallel gravity lines of the same areas show similar mantle Bouguer features. This indicates that our modeling has successfully removed local topographic effects, and that the mantle Bouguer anomalies indeed reflect sub-seafloor density structure. Detailed discussions on the geological implications of the gravity results are given in a later section.

Base station calibration

The mantle Bouguer gravity anomaly reflects only relative lateral density variations in the crust and mantle. We can also obtain absolute gravity values by calibrating ship board gravitometers with port measurements in Ponta Delgada. The first calibration was made on Day 24 (January 24), 1992 by RVS technician Chris Paulson. A second calibration will be carried out by Dave Booth and John Wynar on Day 61 (March 1) upon ship returning to Ponta Delgada. By comparing calibrations before and after the cruise, we can also determine the total drift of the gravitometers during the whole survey, which is expected to be less than 2 mgal.

Gravitometers S40:

Date: Day 24, 1992; Base station Mohlo Salazar, Ponta Delgada, Azores; g(absolute) = 980,116.08 mgal; G(obs) = 8462.0 divs; CAL =.9917 mgal/div
Date: Day 61, 1992; Returning to same base station; g(absolute)=980,116.69 mgal; G(obs) = 8460.0 divs; CAL=0.9917 mgal/div; Drift=-2.593 mgals (-0.07 mgal/day)

Gravitometer S84:

Date: Day 24, 1992; Base station Mohlo Salazar, Ponta Delgada, Azores; g(absolute) = 980,115.74 mgal; G(obs) = 11350.0 divs; CAL = 0.9967 mgal/div
Date: Day 61, 1992; Returning to same base station; g(absolute)=980,115.87 mgal; G(obs) = 1135.0* divs (*note: this value may in error and actually may be 11350.0 divs); CAL=0.9967 mgal/div; Drift=-0.17 mgals (-0.005 mgal/day)

In above values, g(absolute) and G(obs) were corrected to marine meter level.

7.4 Preliminary Results

The mantle Bouguer anomaly varies along axis with alternative highs and lows (Figure 7.3). Distinctive gravity lows were identified over the central portions of each spreading segment except segment 12. The gravity lows are the most negative over the mid-points of segment 17 (-20 mgal), segment 6 (-5 mgal), and segment 11 (-5 mgal). These lows are considerably more negative than those found over segment 8 (15 mgal) and segment 9 (15 mgal). Table 2 lists well defined gravity maxima and minima values and their relationship to the spreading segment geometry.

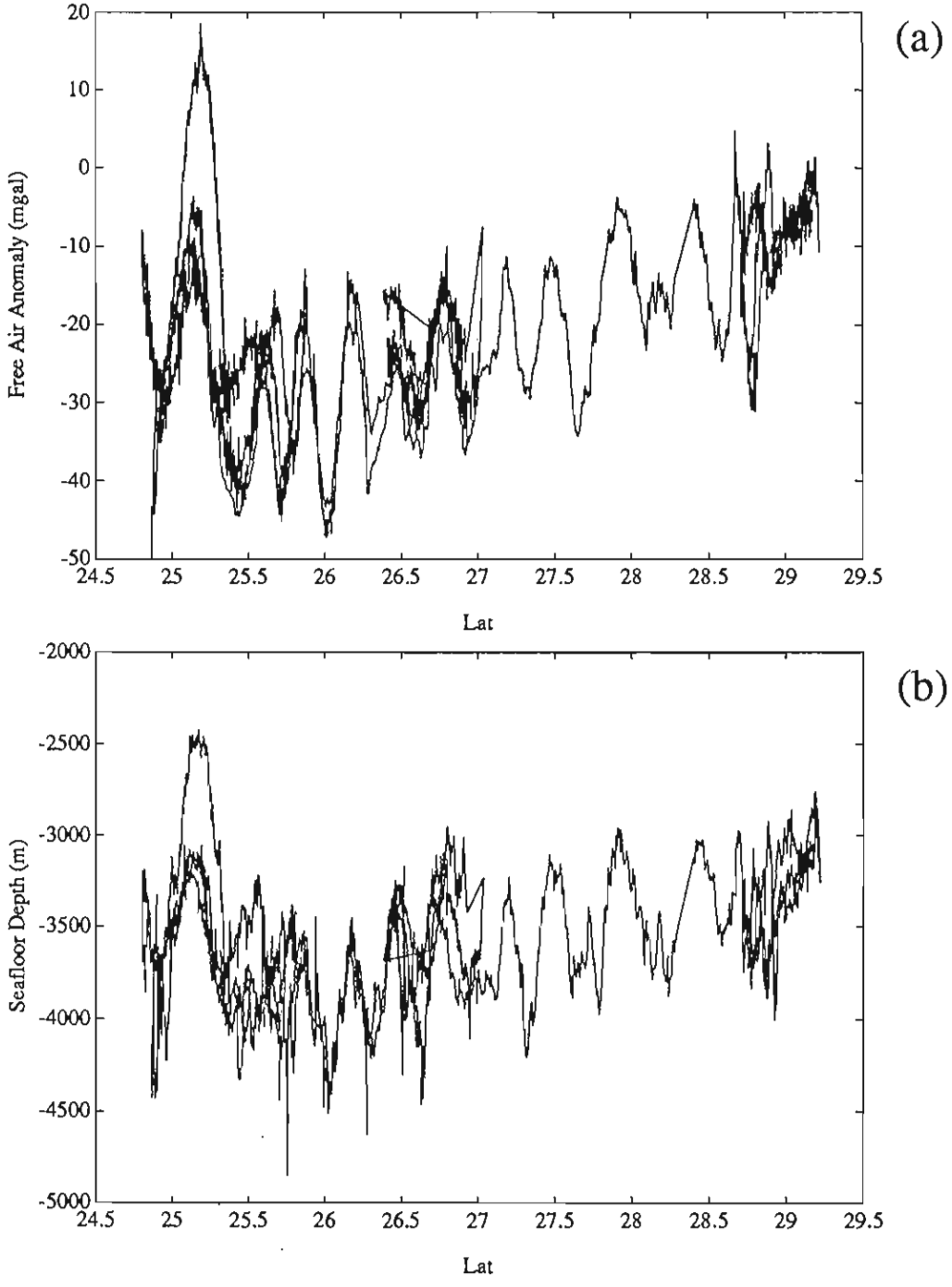

Figure 7.2 Free air anomaly and seafloor depth.

a). Free air anomaly recorded during TOBI surveys (repeated tracks) and transits between sites. Data recorded during rock dredging and camera runs were excluded. b). Axial seafloor depth in the same region as in 7.2a. The strong correlation between the free-air anomaly and seafloor depth demonstrates that the FAA is dominated by seafloor topographic effects.

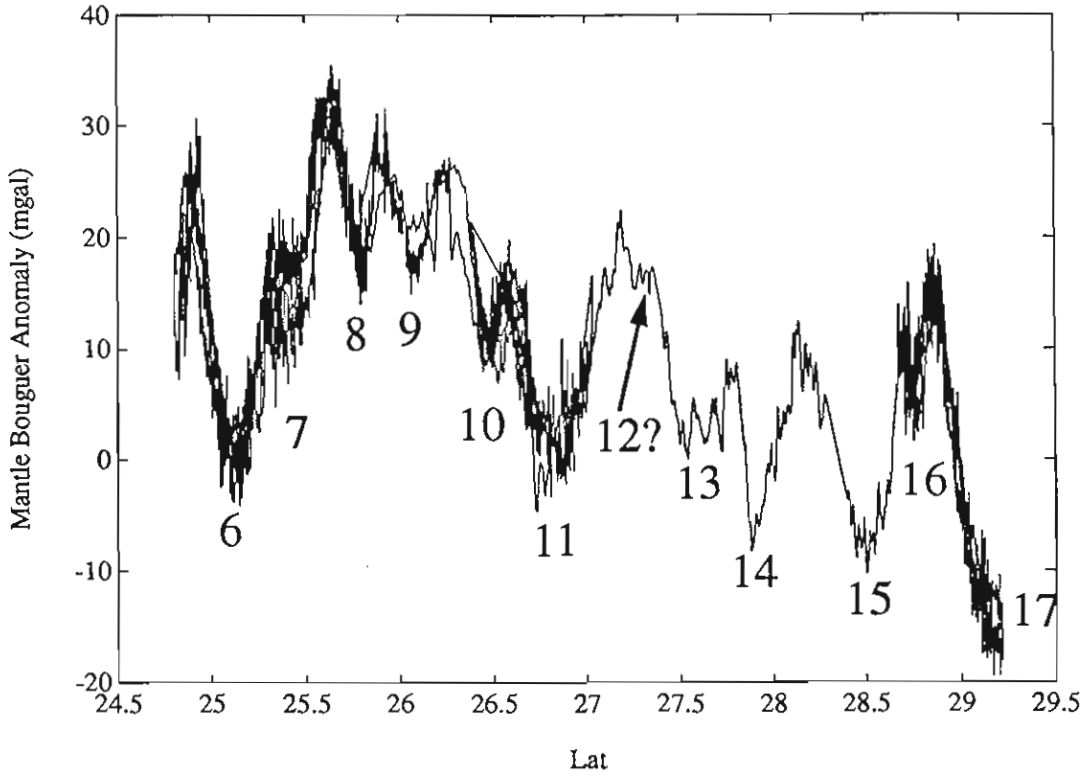

Figure 7.3 Calculated mantle Bouguer anomaly in the survey area.

Spreading segments are denoted by numbers. Note that well-defined gravity lows are centered over most segments. However, the magnitude of gravity lows varies dramatically among and within the segments.

Table 2. Along-Axis Mantle Bouguer Gravity Anomaly

High/Low	Latitude (deg, N)	Value (mgal)	Location
Low	25.14	0	segment 6
Low	25.45	2	segment 7
Low	25.81	8	segment 8
Low	26.10	8	segment 9
Low	26.48	10	segment 10
Low	26.81	1	segment 11
Low	27.55	0	segment 13
Low	27.91	-9	segment 14
Low	28.50	-11	segment 15
Low	28.76	5	segment 16
Low	29.24	-18	segment 17
High	24.90	23	seg 6 south end
High	23.33	15	seg 6&7 offset
High	30.00	30	seg 7&8 offset
High	25.90	26	seg 8&9 offset
High	26.28	26	seg 9&10 offset
High	26.58	18	seg 10&11 offset
High	27.19	21	seg 11&12 offset
High	27.79	8	seg 13&14 offset
High	28.17	9	seg 14&15 offset
High	28.69	10	seg 15&16 offset
High	28.87	15	seg 16&17 offset

7.4.1 Segment 6.

Detail gravity anomaly patterns for individual spreading segments are shown in Figs. 7.4-7.6. Segment 6, which stretches 48 km long, is associated with a profound low mantle Bouguer anomaly (Fig. 7.4a). The total change from segment ends to mid-point is about 20 mgals. While this anomaly magnitude is smaller than that of segment 17 (30 mgal), it is still the largest in comparison to other segments. From TOBI images we noted that sheet lava flows dominate the volcanic morphology of the central region of this segment. Whether the sheet lava morphology and low mantle Bouguer anomaly have their common origin in abnormally low mantle temperature awaits further investigation.

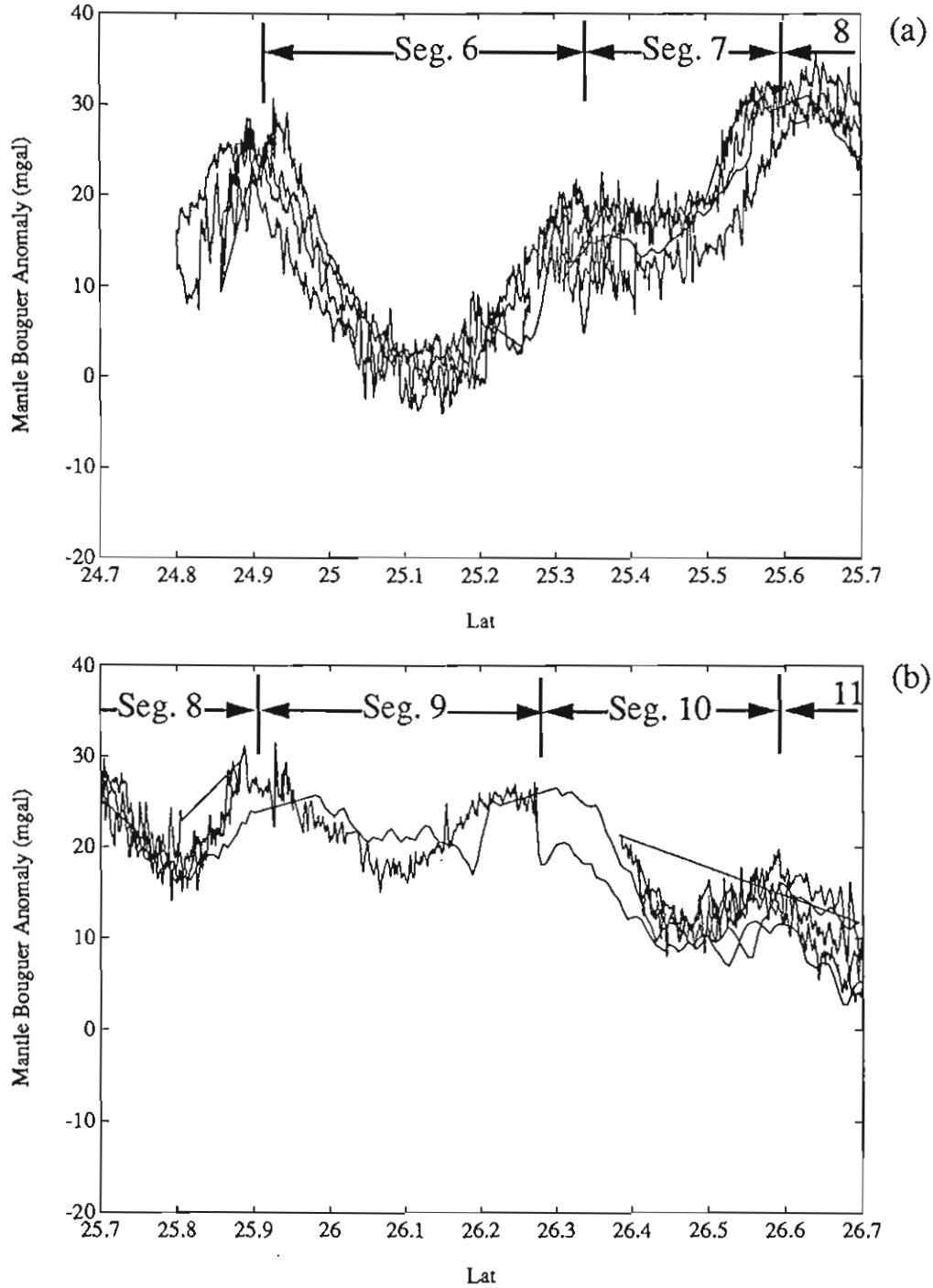

Figure 7.4 Mantle Bouguer anomaly between 24.7° - 26.7° N

Mantle Bouguer anomaly between a) 24.7° - 25.7° N, and b) 25.7° - 26.7° N. Segment numbers are indicated.

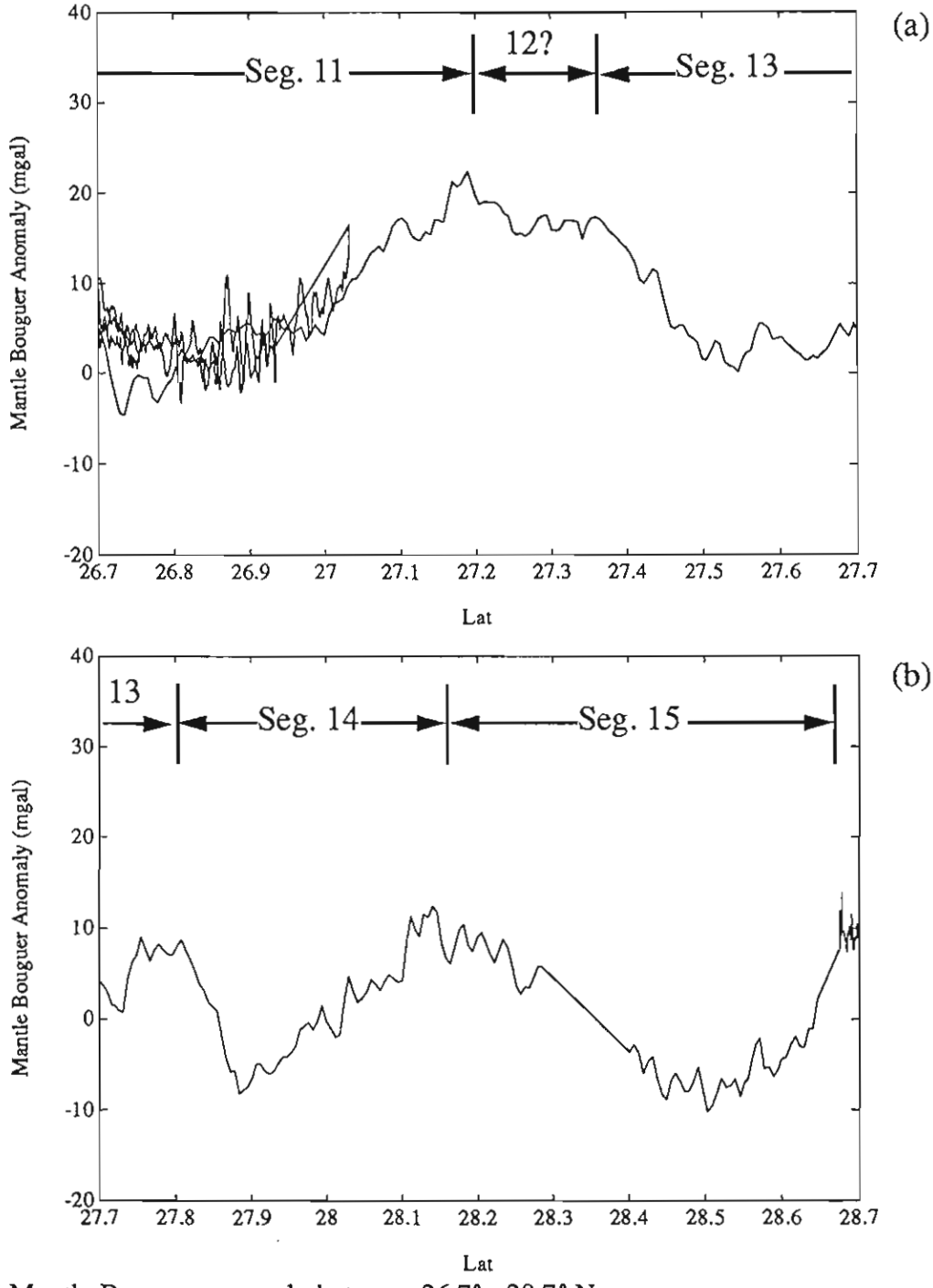

Figure 7.5 Mantle Bouguer anomaly between 26.7° - 28.7° N.

Mantle Bouguer anomaly between a) 26.7° - 27.7° N, and b) 27.7° - 28.7° N. Segment numbers are indicated.

7.4.2 Segment 7.

Segment 7 measures about 35 km in length (Figure 7.4 a). The overall anomaly of the whole segment is more positive than that of segment 6. The gravity anomaly is also asymmetric about the segment mid-point: the anomaly near the northern end is 15 mgal higher than that of the southern end. From Sea Beam data, we observed that a prominent volcanic ridge runs along the median floor of this segment.

7.4.3 Segments 8 and 9.

The overall gravity anomaly of these two segments is substantially more positive than those of the bounding segments 7 and 10, although the lengths of the four segments are comparable (Fig. 7.4 b). The peak-to-trough anomaly amplitudes of segments 8 and 9 are 18 and 13 mgal, respectively. We noted that the TAG hydrothermal vent field (26.17N) is not associated with a strong low gravity anomaly.

7.4.4 Segments 10 and 11.

The anomaly pattern of segments 10 and 11 mirror that of segments 7 and 6, respectively (Figs. 7.4 a and 7.4 b). A clear positive anomaly is found at the boundary of these two segments (26.58N), where TOBI data show overlapping axial volcanic ridges.

7.4.5 Segments 13, 14, and 15.

Transit gravity lines were obtained along the axis of these segments (Figs. 7.5 a and 7.5 b). The anomaly pattern of segments 14 and 15 are similar, both are more negative than that of segment 13.

7.4.6 Segments 16 and 17.

Both segments (Figure 7.6) were surveyed previously by three dimensional gravity mapping (Figure 4 of Lin et al., 1990). The along-axis profiles obtained in CD65 cruise compare well with the more completed survey of Lin et al., confirming the accuracy of present survey (Fig. 9).

Segment 16 is the shortest segment in this region (28 km), and is associated with a peak-to-trough anomaly of 8 mgal. Segment 17, on the other hand, is the longest spreading segment (60 km). It is associated with the most negative and strongest gravity anomaly.

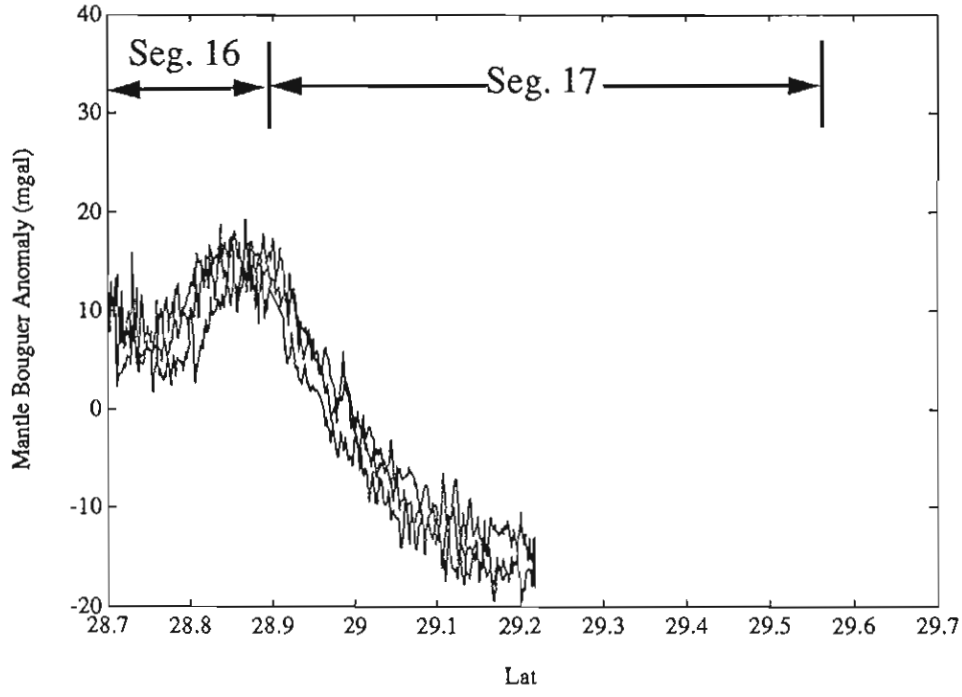

Figure 7.6 Mantle Bouguer anomaly between 28.7° - 29.7° N.

7.5 Magnetics

During CD65 cruise, magnetic data were collected by both the surface-towed RVS magnetometer and by the deep-towed TOBI magnetometer. (Description of these instruments were given in the beginning of this report.) TOBI magnetic data were recorded during all TOBI operations. Surface-towed magnetometer was deployed during TOBI surveys, as well as during some transit periods.

The TOBI vehicle is equipped with an IOS tri-axial fluxgate magnetometer. Unlike the surface-towed magnetometer, which measures only the total magnetic field, the TOBI magnetometer is capable of measuring individual (x,y,z) components accurately. It is estimated that the measurement uncertainty under normal operational condition (within a few degree TOBI vehicle pitch) is less than a few tens of nT.

The purpose of the TOBI magnetic survey is to determine the fine-scale variations in the oceanic crust magnetization. We are most interested in the variations associated with seafloor volcanic, tectonic, and hydrothermal features. Because the TOBI magnetometer locates only a few hundred meters above the seafloor, it can reveal magnetic anomaly features of a few hundred meters in size.

A comparison of TOBI magnetic data with surface data is shown in Fig. 7.7 for a three-day period. It is clear from this comparison that the long-wavelength TOBI magnetic anomaly agree well with the sea surface anomalies. These long-wavelength features have amplitudes of a few hundred nT. The TOBI data, however, also show very strong shorter wavelength variations of up to 3000 nt. Although some anomaly variations can be attributed to changes in TOBI towing altitude, a significant portion of the anomaly features might be caused by geological processes. To determine sources of these fine-scale magnetic anomaly and to understand their geological significance, we plan to analyze the TOBI data by removing the effects of uneven TOBI altitude and seafloor topography at WHOI.

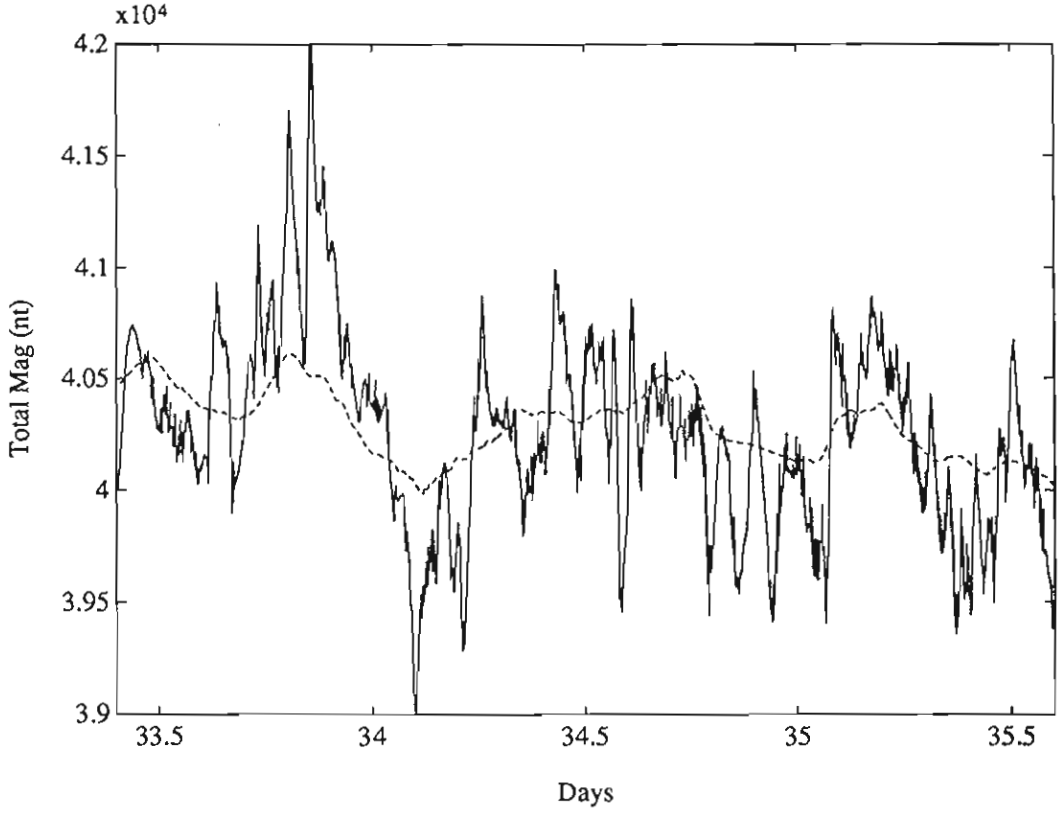

Figure 7.7 TOBI vs. surface magnetic anomaly, JD 33.5 - 35.5 Z.

TOBI (solid line) and surface (dashed line) magnetic anomaly, JD 33.5-35.5 Z. TOBI magnetic anomaly reveal both short and long wavelength features. The short wavelength features are largely absent in the surface anomaly.

Detailed examples of the three-component magnetic field observed over segments 10 and 11 during Day 33.5 to 35.5 Z are shown in Fig.7.8-7.11. The x direction is defined as the TOBI heading direction. The z component is positive facing downward. The positive y direction is defined below in map view:

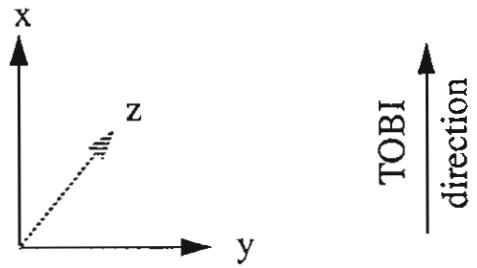

The following parameters can be extracted from the TOBI magnetic data files, see Chapter 8, TOBI Data Processing, for further details:

(1) Date and time (2) x,y,z magnetic field components, from which the horizontal and total field can be computed (3) TOBI vehicle altitude (4) Water depth at TOBI altitude, computed from measured water pressure (5) TOBI vehicle roll and pitch (6) TOBI compass direction

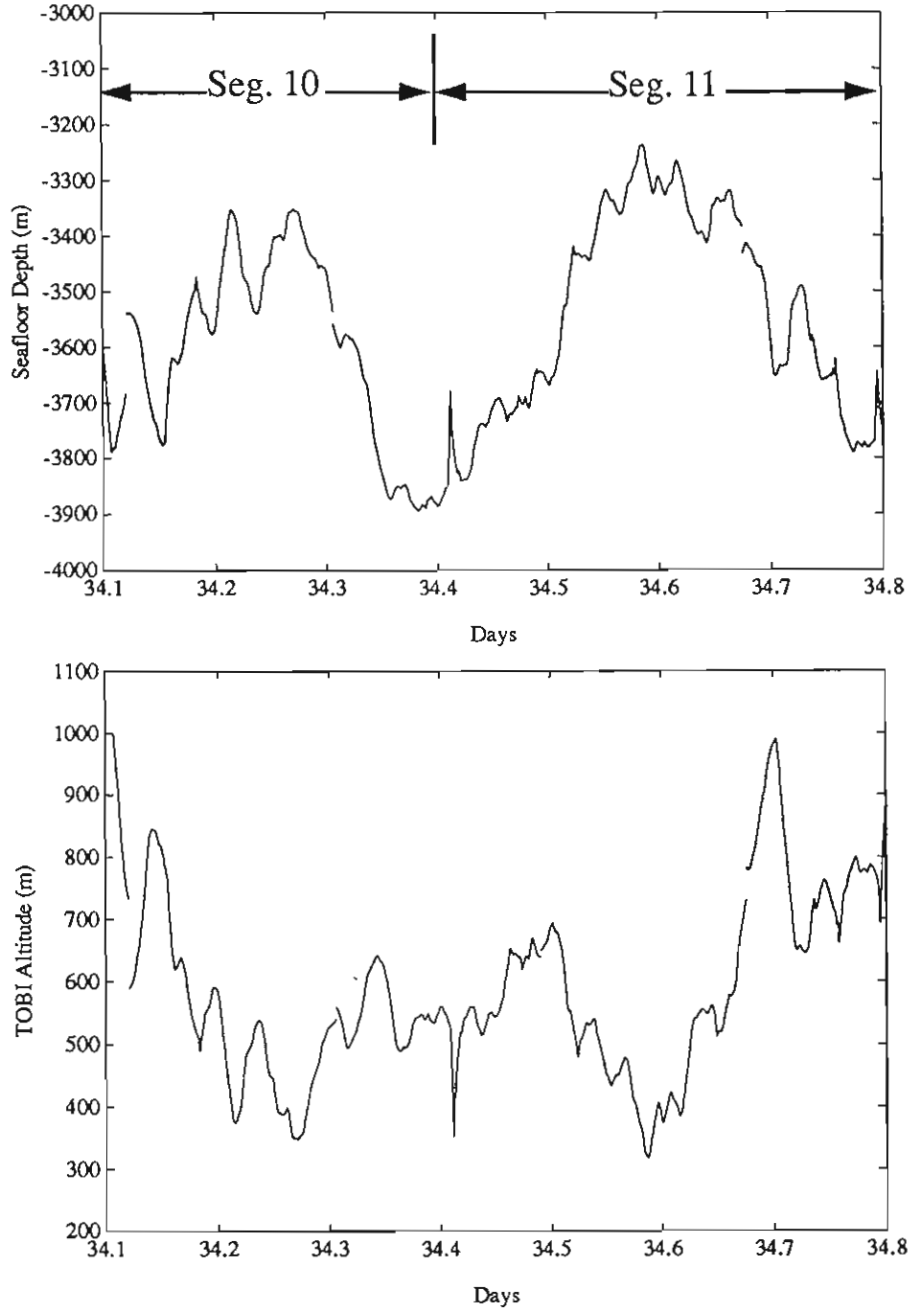

Figure 7.8 Three-component TOBI magnetic data, JD 34.1-34.8 Z

(a) Seafloor depth derived from TOBI altitude and vehicle water depth. (b) TOBI altitude recorded by TOBI depth profiler. Note that artificial spikes might develop, such as the one at 34.41 deg, when the profiler loses tracking of the seafloor.

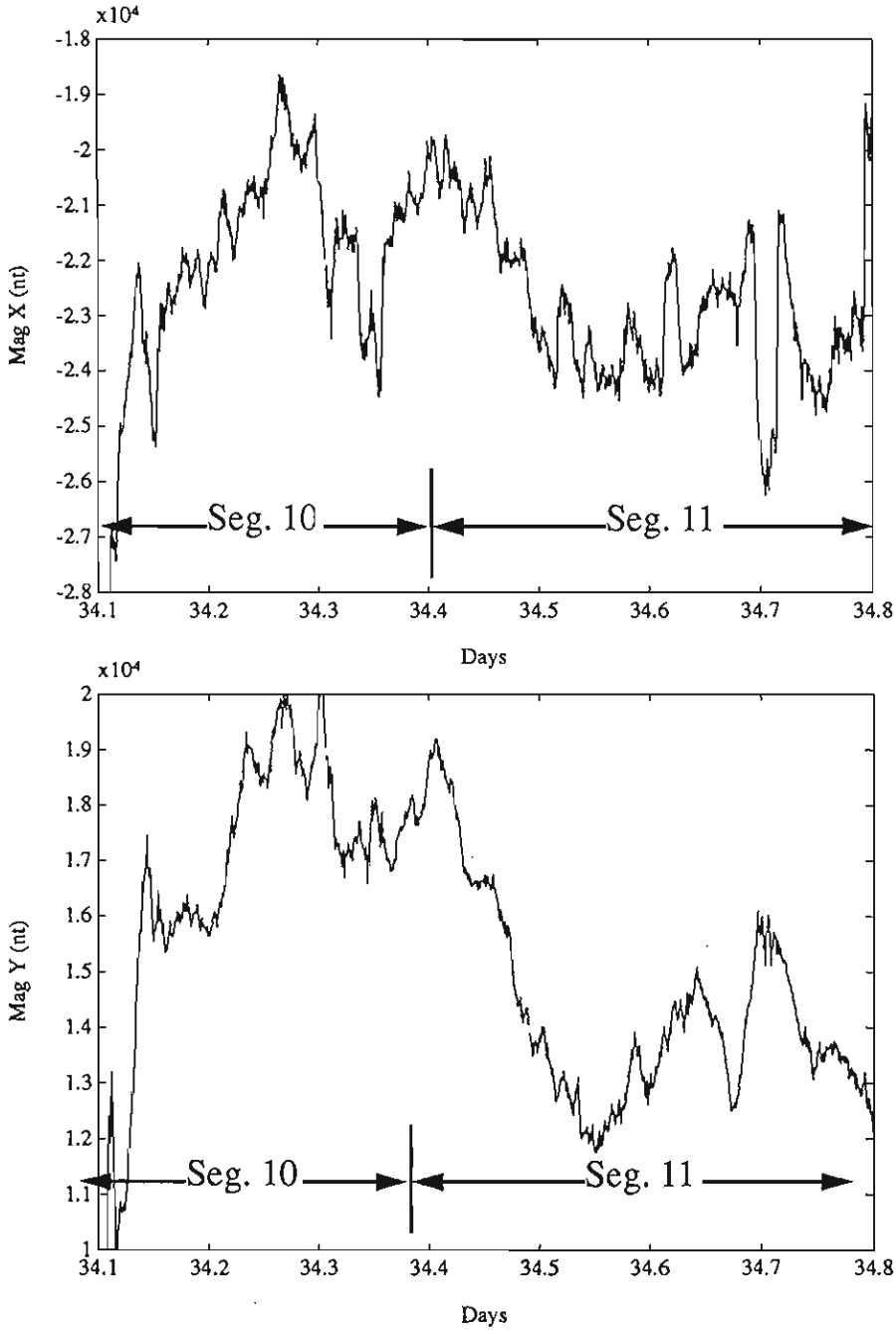

Figure 7.9 Three-component TOBI magnetic data, JD 34.1-34.8 Z (cont.)
Observed x component (a) and y component (b) of the magnetic field.

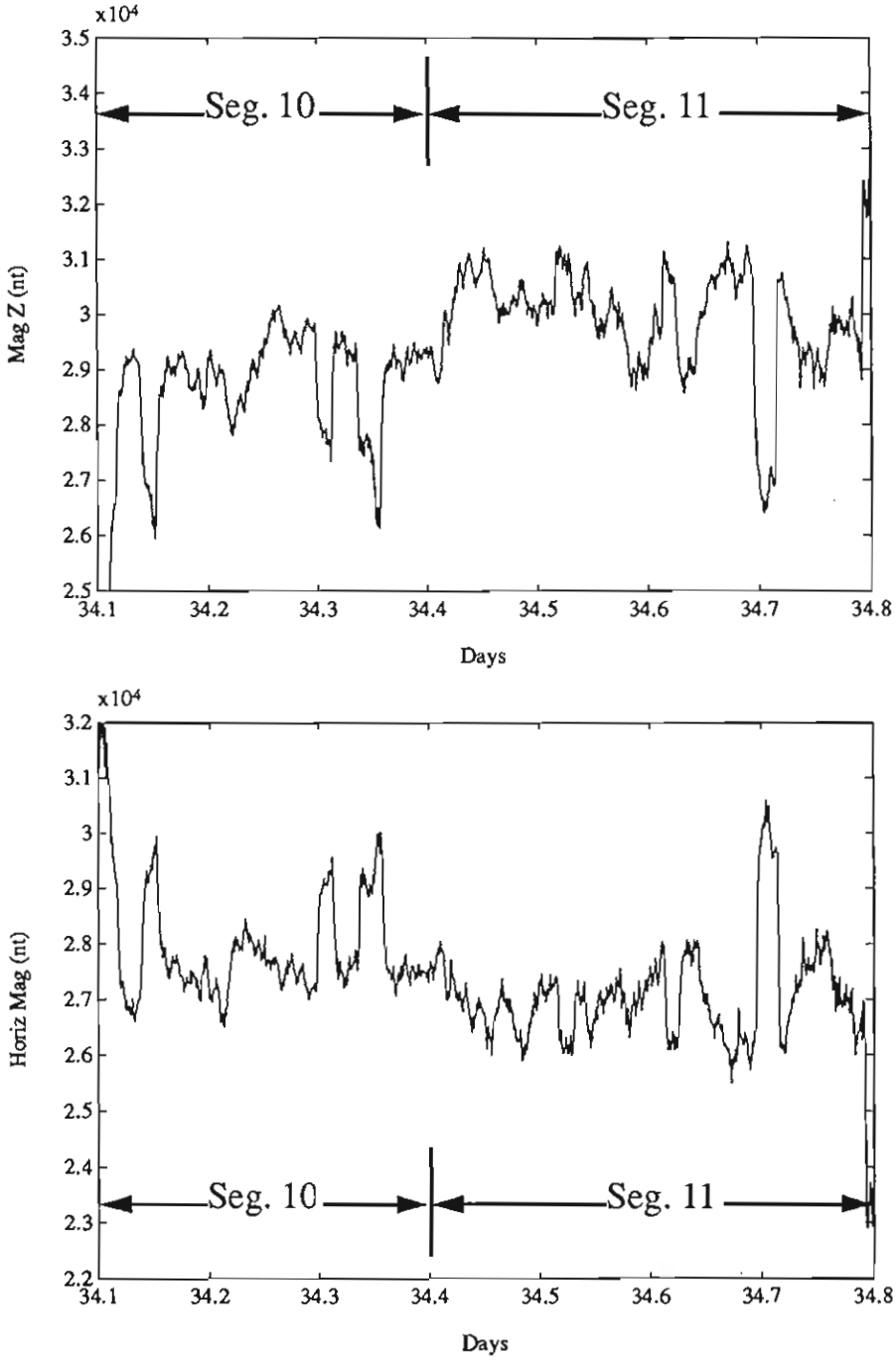

Figure 7.10 Three-component TOBI magnetic data, JD 34.1-34.8 Z (cont.)

(a) Observed z component of the magnetic field. (b) Horizontal field component calculated from data of Fig. 7.9.

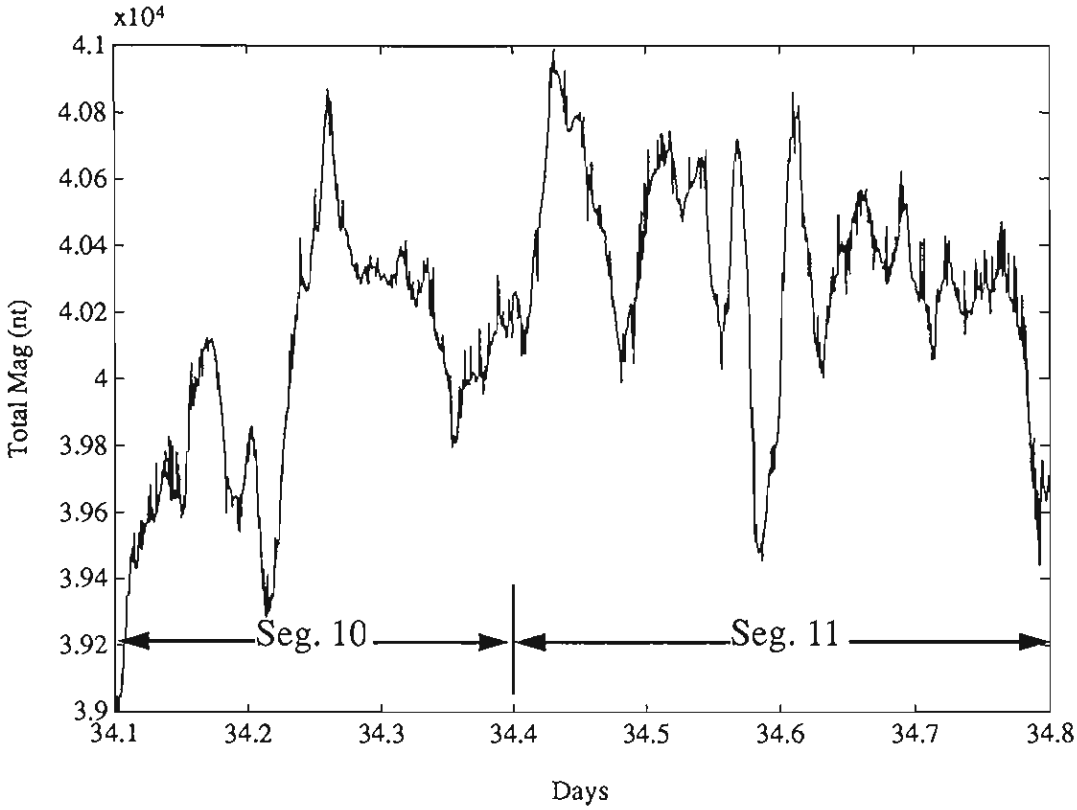

Figure 7.11 Three-component TOBI magnetic data, JD 34.1-34.8 Z (cont.)
Total TOBI magnetic anomaly calculated from the observed x,y, and z components.

VIII. TOBI Data Processing

8.1Computer systems on board

8.1.1 TOBI data acquisition

Overview of the TOBI logging system.

COMPONENTS:-

1) Keithley Data Acquisition box. This contains an 8 channel analogue to digital converter, 5 digital to analogue converters and 32 bits of digital input or output. The interface card in the IBM has a counter which provides the sampling clock.

2) Two Sony magneto-optical drive. They are single-sided drives but the cartridges are double-sided so they must be flipped over to write to the other side. In practice we use the A sides of a number of cartridges first so that after about 13 hours of logging the data can be transferred to the replay system.

3) Raytheon thermal recorder. This displays a slant_range corrected double-sided side-scan image with a profile derived from the side-scan.

4) Monitor 8513. Displays the same slant_range picture as appears on the thermal recorder'

5) Monitor 8514. Is the control monitor and shows disc usage and accepts commands to control for instance automatic altitude tracking, set display gain and gamma.

6) IBM PS2/80. This is a 16 Mhz. 80386 machine with 2Mbytes of memory, 110 Mbytes of hard disc and a math co-processor.

7) Profiler "stretcher box". The profiler is triggered at the same rate as the side-scan (4 sec. sweep) but only produces a few hundred milliseconds of useful data. The IBM produces a start pulse just before the bottom echo and the box samples rapidly for 200 mSecs. stores this data to be clocked out 20 times slower on the following sweep.

8) IBM PS2/50. This displays and processes digital data sent up from the vehicle. The display shows heading from the compass, pressure, the E-M Log components, resultant & direction, pitch & roll and magnetometer x,y & z and resultant.

9) The Orange Box. This contains vehicle power supply, digital data decoder and receivers for side_scan and profiler analogue signals.

10) Terminal. There is a two-way serial link between TOBI and the ship using modems at either end and the terminal allows communication with a micro-controller in the TOBI vehicle.

11) Dry paper recorder ie. EPC or Raytheon shows the profiler as received on one side at the expanded output from the stretcher box on the other.

Replay system

1) IBM PS2/80. This is a 20 Mhz. 80386 machine with 2Mbytes of memory, 300 Mbytes of hard disc and a math co-processor.

2) Raytheon thermal recorder.

3) Sony magneto-optical drive.

4) Printer.

8.1.2 TOBI data analysis, scientific computing

The computing system used for scientific purposes on board was a small network of UNIX workstations: a DECstation 5000, two Sun IPC's and a headless SPARC 2. The configuration for each workstation is as follows:

DECstation 5000/120 - 8 plane graphics, 48 megabytes of memory, approximately 1.5 gigabytes of disk storage, a SONY magneto optical disk drive, and a PostScript laser printer.

2 Sun IPC - 8 plane graphics, 12 (and 24) megabytes of memory, approximately 1 gigabyte of disk storage, an EXABYTE tape drive, a QIC tape drive, and a Tektronix color screen dump printer.

Sun SPARCstation 2 - no graphics, 32 megabytes of memory, 1 gigabyte of disk storages.

The TOBI image and magnetic data for the 4 survey areas occupied over a gigabyte of disk storage, we used NFS (Network File System) file systems to allow access from any of the workstations to the processed TOBI data. This networked environment allowed the raw TOBI magnetic disks to be processed on the DECstation and then moved to the publicly available NFS filesystems, with a minimum of administrative overhead.

8.1.3 RVS shipboard data logging and analysis

The RRS Charles Darwin is equipped with a standard data logging, archiving and processing system common to all NERC ships and also in use at NIOZ and SOZ in the Netherlands. It is a three layer system comprising firstly of a microprocessor associated with each data source, secondly a VME OS9 based system that acts as a data concentrator and archive and thirdly a network of three SUN UNIX workstations and an IBM PS2. RS232 is used between the instrument microprocessors and the concentrator and Ethernet between the concentrator and the processing network. Peripherals include a Zeta 836 drum plotter, a Tektronix 4693RGB screen dump printer, an A3 HPGL plotter and a HP LaserJet. Tape backup facilities are QIC150 and Exabyte.

All geophysical and computing equipment is supplied and supported by the NERC Research Vessel Services.

Daily processing is performed to derive the best navigation data from a number of sources, principally GPS, and to derive gravity and magnetic anomalies. Depths are corrected automatically using Carters Tables. Image processing of TOBI data and contouring of Sea Beam data are provided using ALV and UNIRAS. Navigation data is plotted on charts using a number of map pro-

jections; for this cruise exclusively Mercators projection. Also available are UTM, Orthographic Stereo, Albers,Snyder(Alaska) and Lamberts.

8.2 TOBI data stream

The primary recording system for the TOBI is an IBM PS/2, with an attached magneto optical disk. Records generated from TOBI are appended to the end of a MS-DOS file on the magneto-optical (MO) disk. To make the TOBI data available to the scientific computing network, the raw data on the MO disk is read, processed and stored in UNIX files.

This processing is a four stage operation: the disk is read, each record is processed, image files are written, and a file of magnetic data is produced.

Ptd will search the MO disk and find each record, perform slant range correction to the side scan sonar data and extract the magnetic data. Data files contain approximately 12000 records (or 295 megabytes) representing 11 to 12 hours of recording. Since the MO disk contains an MS-DOS filesystem that is not compatible with filesystems used by the UNIX workstations, *ptd* must read the entire disk and try to match on a user supplied string that is located at the beginning of each TOBI record. Finally, *ptd* writes the magnetic data to a user supplied data file and outputs the slant ranged corrected sonar data to the standard output, that will be connected via a UNIX pipe to the image conversion program.

The sonar data is read by another small C program, *side2pgm* that converts and reformats the data into an image format called *PGM (Portable Gray Map)*. The PGM format is a simple two dimensional array of binary (8-bit) pixels and a small header that supplies the dimensions of the image. This extremely simple format allows for easy manipulation and conversion. For example, KHOROS supplies a filter program the will allow one to convert PGM to it's native image format. A limitation of this image conversion process is that the original sidescan data is available with 12 bits of precision, but the PGM library is compiled with the ability to handle only 8 bit samples (recompilation of the PGM library with appropriate directive would remove this limitation, however most workstations can only display 8 bit pixel values anyway), therefore *side2pgm* arithmetically divides each pixel by 8, resulting in a 'darker' image. In practice, this darkening has not been a problem, a simple histogram equalization can easily correct the darkened image.

The processing stream discussed above is encapsulated in a UNIX shell script, thus an entire MO disk can be processed with minimal operator assistance. For each 4000 records three files are produced using the following file naming convention:

filetype_starttime_diskid_surveyarea.extension

where filetype is one of "**big**", "**small**", or "**mag**"; starttime is encoded as **julianday** '.' 24 hour time of the start of disk recording; **diskid** is the number on the outside of the disk, these numbers ranged from 90-113; survey area is one of **area1, area2, area3,** or **area4** followed by a letter indicating which of the three segments (a, b, or c); and an file name extension that can be either "**pgm**" or "**dat**". As an example, **small_048.1045_107_area4a.pgm**, is the first small PGM file from disk 107 that was produced from area4 on 048 day at 1045.For further details see the *mkimages* manual page.

Other programs are available to allow one to extract ASCII information from the magnetic data file, index the records on the TOBI MO disk, read the disk, and some PGM utility programs.

The manual pages for *ptd, side2pgm* and these other programs are included in this report and on the EXABYTE tape produced on board the Charles Darwin.

8.3 TOBI data analysis

8.3.1 PGM

Figures in this report were processed and converted to POSTSCRIPT format using *PBMPlus* image processing software. The *PBMPlus* software library is a freely available software package written by Jef Poskanzer. The original motivation for this package was to supply many different image and bitmap conversion programs that would allow a user to easily convert from one format to another. The current version (included on the cruise data tape) contains support for most "standard" image processing filters.

All of the programs included with *PBMPlus* follow the well defined UNIX paradigm of a pipeline, where many different programs can be connected to transform the source image. For example, this short pipeline will scale a large TOBI image file into a more manageable size and normalize the new small image:

pnmscale -width 200 -height 800 big_image_file.pgm | pgmnorm > smaller_image_file.pgm

See the PGM manual pages for further information.

8.3.2 Khoros

Khoros is a software environment dedicated to the visualization of scientific data. This software was available on the scientific Sun systems used onboard the RRS Darwin. The software was developed at the University of New Mexico; the version used on the ship is release 1.0, 1991. Khoros is available in the public domain.

The Khoros infrastructure is based on 3 interface styles: (1) command line interface; (2) graphical, menu-driven interface (cantata); and (3) the basic operations of a visual programming language.

Cantata allows specified routines to be iconized as 'glyphs' and displays the flow between a succession of routines. Procedures created within cantata may be archived and restored for a subsequent work session. Menus that can be brought down within cantata include:

In order to discover how to execute a command outside of cantata, type '<routine name> -U' for help. To execute the interactive display procedure, editimage, for example, type 'editimage -i <input VIFF filename>'. Manual pages are located in khoros/manual.

The data exchange format required for Khoros is the VIFF format. A routine, 'pbm2viff', is available to re-format our TOBI pgm files.

The principle image display routines are 'putimage', 'editimage' and 'viewimage'. 'putimage' is a simple image viewing routine with no associated features. 'editimage' is an interactive viewing tool, which has the ability to alter an image's lut, colour table and allows zooming through pixel replication. 'viewimage' enables the 3-dimensional display of images or elevation data using

contour, mesh or surface plots, with corresponding interactive perspective views; as well as conventional 2-dimensional image and contour displays.

'xprism2' and 'xprism3' provide a graphical display capability. 'xprism3' is again able to display 3-dimensional data in a similar manner to 'viewimage'.

One task that we have accomplished using Khoros is a 3-dimensional combination of Seabeam bathymetry and TOBI sidescan using 'viewimage'. The required input data are 2 VIFF files of corresponding image and elevation data with equal dimensions.

The bathymetry data are selected using 'Matlab' and interpolated to a grid size equivalent to a 'small' pgm file, i.e. 200 columns by 800 rows. 'asc2viff' within Khoros converts this to the appropriate VIFF format. The bathymetry and TOBI data are loaded into 'viewimage' as respective elevation and image files. Using a surface plot and the 'use imagery' option in the attributes menu, 'viewimage' presents a 3-dimensional display where the bathymetry is represented by the xyz plot and the grey scale imagery is draped over the surface, filling in the appropriate grid cells.

We have found an introduction to Khoros is best sought through the cantata environment. This, however, can appear deceptively simple and command lines can thus prove to be more explanatory.

8.3.3 ALV

The ALV toolkit is designed to aid image processing work on Sun workstations. This software was available on the RVS Sun systems aboard the RRS Darwin. It is intended to be easy to use, though not restrictive to experienced users, user-configurable, extensible and flexible. For example the toolkit will work on both black and white and colour workstations and in either case will transparently, to the user, display an image to the best of its ability on the screen.

The toolkit is made up of a number of tools. These include programs to display an image on the screen, to display a histogram, to perform histogram equalization, to threshold, to print an image on an Apple Laserwriter, to invert an image and to convolve an image with a user-supplied linear filter. Currently, there are 47 such programs.

The toolkit uses the standard Sun rasterfile format to store its images allowing multiple depth images to be processed by the same toolkit and easy migration of data between pack- ages.

8.4 TOBI data backup and distribution

An EXABYTE tape was produced on board to distribute all the TOBI images, magnetic data, underway geophysics, TOBI log positions, *PBMPlus* software package, and other software developed during the cruise.

The table was written using the UNIX *tar* command and files on the tape can be extracted using *tar*. For example, to extract the area1_big directory:

tar xvf /dev/exebyte_device_name "area1_big"

Below is the table of contents of the *tar* tape:

```
rw-rw-r--282/1514583739 Feb 24 06:08 1992 area1_big/big_049.1803_108_area1a.pgm.Z
rw-rw-r--282/1512447704 Feb 24 07:00 1992 area1_big/big_049.1803_108_area1b.pgm.Z
```

rw-rw-r--282/1512534819 Feb 24 07:37 1992 area1_big/big_049.1803_108_area1c.pgm.Z
rw-rw-r--282/1512792023 Feb 24 08:43 1992 area1_big/big_050.0722_109_area1a.pgm.Z
rw-rw-r--282/1514498567 Feb 24 09:35 1992 area1_big/big_050.0722_109_area1b.pgm.Z
rw-rw-r--282/1513955489 Feb 24 10:17 1992 area1_big/big_050.0722_109_area1c.pgm.Z
rw-rw-r--282/1514629425 Feb 24 04:17 1992 area1_big/big_048.1045_107_area4b.pgm.Z
rw-rw-r--282/1510502655 Feb 24 04:54 1992 area1_big/big_048.1045_107_area4c.pgm.Z
rw-rw-r--282/1514603729 Feb 24 12:06 1992 area1_big/big_050.2041_110_area1a.pgm.Z
rw-rw-r--282/1512886316 Feb 24 13:03 1992 area1_big/big_050.2041_110_area1b.pgm.Z
rw-rw-r--282/1511686749 Feb 24 10:06 1992 area1_big/big_051.1000_tobi111_area1b.pgm.Z
rw-rw-r--282/158586687 Feb 24 10:44 1992 area1_big/big_051.1000_tobi111_area1c.pgm.Z
rw-rw-r--282/157462079 Feb 24 20:33 1992 area1_big/big_051.2319_112_area1a.pgm.Z
rw-rw-r--282/156143209 Feb 24 21:21 1992 area1_big/big_051.2319_112_area1b.pgm.Z
rw-rw-r--282/158207651 Feb 24 21:54 1992 area1_big/big_051.2319_112_area1c.pgm.Z
rw-rw-r--282/1516461687 Feb 24 09:16 1992 area1_big/big_051.1000_tobi111_area1a.pgm.Z
rw-rw-r--1005/2014359163 Feb 24 13:40 1992 area1_big/big_050.2041_110_area1c.pgm.Z
rw-rw-r--282/158692438 Feb 24 22:52 1992 area1_big/big_052.1238_113_area1a.pgm.Z
rw-rw-r--282/1511269903 Feb 25 00:06 1992 area1_big/big_052.1238_113_area1b.pgm.Z
rw-rw-r--282/15 24 Feb 25 00:38 1992 area1_big/big_052.1238_113_area1c.pgm.Z
rw-rw-r--282/157308465 Feb 15 15:35 1992 area4_big/big_041.0200_tobi100_area3b.pgm.Z
rw-rw-r--282/1512418114 Feb 24 03:27 1992 area4_big/big_048.1045_107_area4a.pgm.Z
rw-rw-r--282/1511486029 Feb 15 23:57 1992 area4_big/big_045.0251_tobi101_area4b.pgm.Z
rw-rw-r--282/1510021003 Feb 16 00:38 1992 area4_big/big_045.0251_tobi101_area4c.pgm.Z
rw-rw-r--282/1518343169 Feb 16 02:28 1992 area4_big/big_045.1610_tobi102_area4a.pgm.Z
rw-rw-r--282/1510825234 Feb 16 03:42 1992 area4_big/big_045.1610_tobi102_area4b.pgm.Z
rw-rw-r--282/1517109967 Feb 16 04:22 1992 area4_big/big_045.1610_tobi102_area4c.pgm.Z
rw-rw-r--282/1517594209 Feb 16 18:58 1992 area4_big/big_046.0529_tobi103_area4a.pgm.Z
rw-rw-r--282/1518315091 Feb 16 20:13 1992 area4_big/big_046.0529_tobi103_area4b.pgm.Z
rw-rw-r--2000/2018496540 Feb 16 20:50 1992 area4_big/big_046.0529_tobi103_area4c.pgm.Z
rw-rw-r--282/158049581 Feb 18 06:58 1992 area4_big/big_046.1848_tobi104_area4a.pgm.Z
rw-rw-r--282/1517880753 Feb 18 08:24 1992 area4_big/big_046.1848_tobi104_area4c.pgm.Z
rw-rw-r--287/1517732426 Feb 18 17:23 1992 area4_big/big_047.0807_tobi105_area4a.pgm.Z
rw-rw-r--287/1518253875 Feb 18 18:35 1992 area4_big/big_047.0807_tobi105_area4b.pgm.Z
rw-rw-r--287/1519710990 Feb 18 19:59 1992 area4_big/big_047.0807_tobi105_area4c.pgm.Z
rw-rw-r--287/1518401332 Feb 19 06:40 1992 area4_big/big_047.0807_tobi106_area4a.pgm.Z
rw-rw-r--287/1519353815 Feb 19 07:50 1992 area4_big/big_047.0807_tobi106_area4b.pgm.Z
rw-rw-r--287/1519338923 Feb 19 08:31 1992 area4_big/big_047.0807_tobi106_area4c.pgm.Z
rw-rw-r--1005/2010591523 Feb 15 16:09 1992 area4_big/big_041.0200_tobi100_area3c.pgm.Z
rw-rw-r--282/1511660035 Feb 15 22:57 1992 area4_big/big_045.0251_tobi101_area4a.pgm.Z
rw-rw-r--282/1518172145 Feb 18 07:45 1992 area4_big/big_046.1848_tobi104_area4b.pgm.Z
rw-rw-r--282/15 160015 Feb 24 04:17 1992 area1_small/small_048.1045_107_area4b.pgm
rw-rw-r--282/15 160015 Feb 24 04:58 1992 area1_small/small_048.1045_107_area4c.pgm
rw-rw-r--282/15 160015 Feb 24 06:08 1992 area1_small/small_049.1803_108_area1a.pgm
rw-rw-r--282/15 160015 Feb 24 07:00 1992 area1_small/small_049.1803_108_area1b.pgm
rw-rw-r--282/15 160015 Feb 24 07:40 1992 area1_small/small_049.1803_108_area1c.pgm
rw-rw-r--282/15 160015 Feb 24 08:29 1992 area1_small/small_050.0722_109_area1a.pgm
rw-rw-r--282/15 160015 Feb 24 08:29 1992 area1_small/small_050.0722_109_area1c.pgm
rw-rw-r--282/15 160015 Feb 24 08:29 1992 area1_small/small_050.0722_109_area1b.pgm
rw-rw-r--282/15 160015 Feb 24 08:29 1992 area1_small/small_050.2041_110_area1a.pgm
rw-rw-r--282/15 160015 Feb 24 08:29 1992 area1_small/small_050.2041_110_area1c.pgm
rw-rw-r--282/15 160015 Feb 24 09:16 1992 area1_small/small_051.1000_tobi111_area1a.pgm
rw-rw-r--282/15 160015 Feb 24 10:06 1992 area1_small/small_051.1000_tobi111_area1b.pgm
rw-rw-r--282/15 160015 Feb 24 10:49 1992 area1_small/small_051.1000_tobi111_area1c.pgm
rw-rw-r--282/15 160015 Feb 24 21:21 1992 area1_small/small_051.2319_112_area1b.pgm
rw-rw-r--282/15 160015 Feb 24 21:57 1992 area1_small/small_051.2319_112_area1c.pgm

rw-rw-r--282/15 160015 Feb 24 08:29 1992 area1_small/small_050.2041_110_area1b.pgm
rw-rw-r--282/15 160015 Feb 24 20:33 1992 area1_small/small_051.2319_112_area1a.pgm
rw-rw-r--282/15 160015 Feb 24 22:52 1992 area1_small/small_052.1238_113_area1a.pgm
rw-rw-r--282/15 0 Feb 24 22:59 1992 area1_small/small_052.1238_113_area1b.pgm
rw-rw-r--282/15 160015 Feb 25 00:38 1992 area1_small/small_052.1238_113_area1c.pgm
rw-rw-r--282/15 160015 Feb 15 15:35 1992 area4_small/small_041.0200_tobi100_area3b.pgm
rw-rw-r--282/15 160015 Feb 15 16:12 1992 area4_small/small_041.0200_tobi100_area3c.pgm
rw-rw-r--282/15 160015 Feb 15 22:57 1992 area4_small/small_045.0251_tobi101_area4a.pgm
rw-rw-r--282/15 160015 Feb 15 23:57 1992 area4_small/small_045.0251_tobi101_area4b.pgm
rw-rw-r--282/15 160015 Feb 16 00:41 1992 area4_small/small_045.0251_tobi101_area4c.pgm
rw-rw-r--282/15 160015 Feb 16 02:28 1992 area4_small/small_045.1610_tobi102_area4a.pgm
rw-rw-r--282/15 160015 Feb 16 03:42 1992 area4_small/small_045.1610_tobi102_area4b.pgm
rw-rw-r--282/15 160015 Feb 16 04:28 1992 area4_small/small_045.1610_tobi102_area4c.pgm
rw-rw-r--282/15 160015 Feb 16 18:59 1992 area4_small/small_046.0529_tobi103_area4a.pgm
rw-rw-r--282/15 160015 Feb 16 20:13 1992 area4_small/small_046.0529_tobi103_area4b.pgm
rw-rw-r--282/15 160015 Feb 16 20:54 1992 area4_small/small_046.0529_tobi103_area4c.pgm
rw-rw-r--282/15 160015 Feb 18 06:58 1992 area4_small/small_046.1848_tobi104_area4a.pgm
rw-rw-r--282/15 160015 Feb 18 07:45 1992 area4_small/small_046.1848_tobi104_area4b.pgm
rw-rw-r--282/15 160015 Feb 18 08:29 1992 area4_small/small_046.1848_tobi104_area4c.pgm
rw-rw-r--287/15 160015 Feb 18 17:23 1992 area4_small/small_047.0807_tobi105_area4a.pgm
rw-rw-r--287/15 160015 Feb 18 18:35 1992 area4_small/small_047.0807_tobi105_area4b.pgm
rw-rw-r--287/15 160015 Feb 18 20:04 1992 area4_small/small_047.0807_tobi105_area4c.pgm
rw-rw-r--287/15 160015 Feb 19 06:40 1992 area4_small/small_047.0807_tobi106_area4a.pgm
rw-rw-r--287/15 160015 Feb 19 07:50 1992 area4_small/small_047.0807_tobi106_area4b.pgm
rw-rw-r--287/15 160015 Feb 19 08:35 1992 area4_small/small_047.0807_tobi106_area4c.pgm
rw-rw-r--282/15 160015 Feb 24 03:27 1992 area4_small/small_048.1045_107_area4a.pgm
rw-rw-r--282/15 472000 Feb 24 06:08 1992 area1_mag/mag_049.1803_108_area1a.dat
rw-rw-r--282/15 472000 Feb 24 07:00 1992 area1_mag/mag_049.1803_108_area1b.dat
rw-rw-r--282/15 470112 Feb 24 07:37 1992 area1_mag/mag_049.1803_108_area1c.dat
rw-rw-r--282/15 472000 Feb 24 04:17 1992 area1_mag/mag_048.1045_107_area4b.dat
rw-rw-r--282/15 470230 Feb 24 04:54 1992 area1_mag/mag_048.1045_107_area4c.dat
rw-rw-r--282/15 472000 Feb 24 08:27 1992 area1_mag/mag_050.0722_109_area1a.dat
rw-rw-r--282/15 472000 Feb 24 08:27 1992 area1_mag/mag_050.0722_109_area1b.dat
rw-rw-r--282/15 470112 Feb 24 08:27 1992 area1_mag/mag_050.0722_109_area1c.dat
rw-rw-r--282/15 472000 Feb 24 08:27 1992 area1_mag/mag_050.2041_110_area1a.dat
rw-rw-r--282/15 472000 Feb 24 08:27 1992 area1_mag/mag_050.2041_110_area1b.dat
rw-rw-r--282/15 472000 Feb 24 09:16 1992 area1_mag/mag_051.1000_tobi111_area1a.dat
rw-rw-r--282/15 472000 Feb 24 10:06 1992 area1_mag/mag_051.1000_tobi111_area1b.dat
rw-rw-r--282/15 470112 Feb 24 10:44 1992 area1_mag/mag_051.1000_tobi111_area1c.dat
rw-rw-r--282/15 472000 Feb 24 21:21 1992 area1_mag/mag_051.2319_112_area1b.dat
rw-rw-r--282/15 470112 Feb 24 21:54 1992 area1_mag/mag_051.2319_112_area1c.dat
rw-rw-r--282/15 470112 Feb 24 08:27 1992 area1_mag/mag_050.2041_110_area1c.dat
rw-rw-r--282/15 472000 Feb 24 20:33 1992 area1_mag/mag_051.2319_112_area1a.dat
rw-rw-r--282/15 472000 Feb 24 22:52 1992 area1_mag/mag_052.1238_113_area1a.dat
rw-rw-r--282/15 469640 Feb 25 00:06 1992 area1_mag/mag_052.1238_113_area1b.dat
rw-rw-r--282/15 0 Feb 25 00:14 1992 area1_mag/mag_052.1238_113_area1c.dat
rw-rw-r--282/15 472000 Feb 15 15:35 1992 area4_mag/mag_041.0200_tobi100_area3b.dat
rw-rw-r--282/15 470230 Feb 15 16:09 1992 area4_mag/mag_041.0200_tobi100_area3c.dat
rw-rw-r--282/15 472000 Feb 15 22:57 1992 area4_mag/mag_045.0251_tobi101_area4a.dat
rw-rw-r--282/15 472000 Feb 15 23:57 1992 area4_mag/mag_045.0251_tobi101_area4b.dat
rw-rw-r--282/15 470112 Feb 16 00:38 1992 area4_mag/mag_045.0251_tobi101_area4c.dat
rw-rw-r--282/15 472000 Feb 16 02:28 1992 area4_mag/mag_045.1610_tobi102_area4a.dat
rw-rw-r--282/15 472000 Feb 16 03:42 1992 area4_mag/mag_045.1610_tobi102_area4b.dat
rw-rw-r--282/15 470112 Feb 16 04:22 1992 area4_mag/mag_045.1610_tobi102_area4c.dat

rw-rw-r--282/15 472000 Feb 16 18:58 1992 area4_mag/mag_046.0529_tobi103_area4a.dat
rw-rw-r--282/15 472000 Feb 16 20:13 1992 area4_mag/mag_046.0529_tobi103_area4b.dat
rw-rw-r--282/15 470112 Feb 16 20:50 1992 area4_mag/mag_046.0529_tobi103_area4c.dat
rw-rw-r--282/15 472000 Feb 18 06:58 1992 area4_mag/mag_046.1848_tobi104_area4a.dat
rw-rw-r--282/15 472000 Feb 18 07:45 1992 area4_mag/mag_046.1848_tobi104_area4b.dat
rw-rw-r--282/15 470112 Feb 18 08:24 1992 area4_mag/mag_046.1848_tobi104_area4c.dat
rw-rw-r--287/15 472000 Feb 18 17:23 1992 area4_mag/mag_047.0807_tobi105_area4a.dat
rw-rw-r--287/15 472000 Feb 18 18:35 1992 area4_mag/mag_047.0807_tobi105_area4b.dat
rw-rw-r--287/15 470112 Feb 18 19:58 1992 area4_mag/mag_047.0807_tobi105_area4c.dat
rw-rw-r--287/15 472000 Feb 19 06:40 1992 area4_mag/mag_047.0807_tobi106_area4a.dat
rw-rw-r--287/15 472000 Feb 19 07:49 1992 area4_mag/mag_047.0807_tobi106_area4b.dat
rw-rw-r--287/15 470112 Feb 19 08:31 1992 area4_mag/mag_047.0807_tobi106_area4c.dat
rw-rw-r--282/15 472000 Feb 24 03:27 1992 area4_mag/mag_048.1045_107_area4a.dat
rw-r--r-- 0/112488617 Feb 17 15:54 1992 area2_big/big_032.1840_tobi90_area2a.pgm.Z
rw-r--r-- 0/112742081 Feb 17 15:55 1992 area2_big/big_032.1840_tobi90_area2b.pgm.Z
rw-r--r-- 0/19288991 Feb 17 15:55 1992 area2_big/big_032.1840_tobi90_area2c.pgm.Z
rw-r--r-- 0/116608763 Feb 17 15:56 1992 area2_big/big_033.0858_tobi91_area2a.pgm.Z
rw-r--r-- 0/117401570 Feb 17 15:58 1992 area2_big/big_033.0858_tobi91_area2b.pgm.Z
rw-r--r-- 0/117641105 Feb 17 15:59 1992 area2_big/big_033.0858_tobi91_area2c.pgm.Z
rw-r--r-- 0/114015673 Feb 17 15:59 1992 area2_big/big_033.2222_tobi92_area2a.pgm.Z
rw-r--r-- 0/115640055 Feb 17 16:00 1992 area2_big/big_033.2222_tobi92_area2b.pgm.Z
rw-r--r-- 0/116211261 Feb 17 16:01 1992 area2_big/big_033.2222_tobi92_area2c.pgm.Z
rw-r--r-- 0/115051858 Feb 17 16:02 1992 area2_big/big_034.1147_tobi93_area2a.pgm.Z
rw-r--r-- 0/112625782 Feb 17 16:03 1992 area2_big/big_034.1147_tobi93_area2b.pgm.Z
rw-r--r-- 0/18230009 Feb 17 16:03 1992 area2_big/big_034.1147_tobi93_area2c.pgm.Z
rw-r--r-- 0/111239038 Feb 17 16:04 1992 area2_big/big_035.0103_tobi94_area2a.pgm.Z
rw-r--r-- 0/117057866 Feb 17 16:05 1992 area2_big/big_035.0103_tobi94_area2b.pgm.Z
rw-r--r-- 0/111850267 Feb 17 16:06 1992 area2_big/big_035.0103_tobi94_area2c.pgm.Z
rw-r--r-- 0/1 160015 Feb 18 06:13 1992 area2_small/small_032.1840_tobi90_area2a.pgm
rw-r--r-- 0/1 160015 Feb 18 06:13 1992 area2_small/small_032.1840_tobi90_area2b.pgm
rw-r--r-- 0/1 160015 Feb 18 06:13 1992 area2_small/small_032.1840_tobi90_area2c.pgm
rw-r--r-- 0/1 160015 Feb 18 06:13 1992 area2_small/small_033.0858_tobi91_area2a.pgm
rw-r--r-- 0/1 160015 Feb 18 06:13 1992 area2_small/small_033.0858_tobi91_area2b.pgm
rw-r--r-- 0/1 160015 Feb 18 06:13 1992 area2_small/small_033.0858_tobi91_area2c.pgm
rw-r--r-- 0/1 160015 Feb 18 06:13 1992 area2_small/small_033.2222_tobi92_area2a.pgm
rw-r--r-- 0/1 160015 Feb 18 06:13 1992 area2_small/small_033.2222_tobi92_area2b.pgm
rw-r--r-- 0/1 160015 Feb 18 06:13 1992 area2_small/small_033.2222_tobi92_area2c.pgm
rw-r--r-- 0/1 160015 Feb 18 06:13 1992 area2_small/small_034.1147_tobi93_area2a.pgm
rw-r--r-- 0/1 160015 Feb 18 06:13 1992 area2_small/small_034.1147_tobi93_area2b.pgm
rw-r--r-- 0/1 160015 Feb 18 06:13 1992 area2_small/small_034.1147_tobi93_area2c.pgm
rw-r--r-- 0/1 160015 Feb 18 06:13 1992 area2_small/small_035.0103_tobi94_area2a.pgm
rw-r--r-- 0/1 160015 Feb 18 06:13 1992 area2_small/small_035.0103_tobi94_area2b.pgm
rw-r--r-- 0/1 160015 Feb 18 06:13 1992 area2_small/small_035.0103_tobi94_area2c.pgm
rw-r--r-- 0/1 472000 Feb 18 06:09 1992 area2_mag/mag_032.1840_tobi90_area2a.dat
rw-r--r-- 0/1 472000 Feb 18 06:09 1992 area2_mag/mag_032.1840_tobi90_area2b.dat
rw-r--r-- 0/1 470348 Feb 18 06:09 1992 area2_mag/mag_032.1840_tobi90_area2c.dat
rw-r--r-- 0/1 472000 Feb 18 06:09 1992 area2_mag/mag_033.0858_tobi91_area2a.dat
rw-r--r-- 0/1 472000 Feb 18 06:09 1992 area2_mag/mag_033.0858_tobi91_area2b.dat
rw-r--r-- 0/1 470230 Feb 18 06:09 1992 area2_mag/mag_033.0858_tobi91_area2c.dat
rw-r--r-- 0/1 472000 Feb 18 06:09 1992 area2_mag/mag_033.2222_tobi92_area2a.dat
rw-r--r-- 0/1 472000 Feb 18 06:09 1992 area2_mag/mag_033.2222_tobi92_area2b.dat
rw-r--r-- 0/1 470230 Feb 18 06:09 1992 area2_mag/mag_033.2222_tobi92_area2c.dat
rw-r--r-- 0/1 472000 Feb 18 06:09 1992 area2_mag/mag_034.1147_tobi93_area2a.dat
rw-r--r-- 0/1 472000 Feb 18 06:09 1992 area2_mag/mag_034.1147_tobi93_area2b.dat

rw-r--r-- 0/1 470112 Feb 18 06:09 1992 area2_mag/mag_034.1147_tobi93_area2c.dat
rw-r--r-- 0/1 472000 Feb 18 06:09 1992 area2_mag/mag_035.0103_tobi94_area2a.dat
rw-r--r-- 0/1 472000 Feb 18 06:09 1992 area2_mag/mag_035.0103_tobi94_area2b.dat
rw-r--r-- 0/1 455244 Feb 18 06:09 1992 area2_mag/mag_035.0103_tobi94_area2c.dat
rw-r--r-- 0/111966809 Feb 23 20:47 1992 area3_big/big_038.0635_tobi95_area3a.pgm.Z
rw-r--r-- 0/117026277 Feb 23 20:52 1992 area3_big/big_038.0635_tobi95_area3b.pgm.Z
rw-r--r-- 0/117169123 Feb 23 20:48 1992 area3_big/big_038.0635_tobi95_area3c.pgm.Z
rw-r--r-- 0/111686355 Feb 23 20:48 1992 area3_big/big_038.0635_tobi96_area3a.pgm.Z
rw-r--r-- 0/117737613 Feb 23 20:50 1992 area3_big/big_038.0635_tobi96_area3b.pgm.Z
rw-r--r-- 0/119920189 Feb 23 20:51 1992 area3_big/big_038.0635_tobi96_area3c.pgm.Z
rw-r--r-- 0/117820105 Feb 23 20:53 1992 area3_big/big_039.1005_tobi97_area3a.pgm.Z
rw-r--r-- 0/117638983 Feb 23 20:54 1992 area3_big/big_039.1005_tobi97_area3b.pgm.Z
rw-r--r-- 0/112141970 Feb 23 20:55 1992 area3_big/big_039.1005_tobi97_area3c.pgm.Z
rw-r--r-- 0/112010285 Feb 23 20:56 1992 area3_big/big_039.2324_tobi98_area3a.pgm.Z
rw-r--r-- 0/114374491 Feb 23 20:56 1992 area3_big/big_039.2324_tobi98_area3b.pgm.Z
rw-r--r-- 0/114575122 Feb 23 20:57 1992 area3_big/big_039.2324_tobi98_area3c.pgm.Z
rw-r--r-- 0/15097571 Feb 23 20:58 1992 area3_big/big_040.1243_tobi99_area3a.pgm.Z
rw-r--r-- 0/18251687 Feb 23 20:58 1992 area3_big/big_040.1243_tobi99_area3b.pgm.Z
rw-r--r-- 0/18709112 Feb 23 20:58 1992 area3_big/big_040.1243_tobi99_area3c.pgm.Z
rw-r--r-- 0/18310332 Feb 23 20:59 1992 area3_big/big_041.0200_tobi100_area3a.pgm.Z
rw-r--r-- 0/1 160015 Feb 23 21:06 1992 area3_small/small_038.0635_tobi95_area3a.pgm
rw-r--r-- 0/1 160015 Feb 23 21:06 1992 area3_small/small_038.0635_tobi95_area3b.pgm
rw-r--r-- 0/1 160015 Feb 23 21:06 1992 area3_small/small_038.0635_tobi95_area3c.pgm
rw-r--r-- 0/1 160015 Feb 23 21:06 1992 area3_small/small_038.0635_tobi96_area3a.pgm
rw-r--r-- 0/1 160015 Feb 23 21:06 1992 area3_small/small_038.0635_tobi96_area3b.pgm
rw-r--r-- 0/1 160015 Feb 23 21:06 1992 area3_small/small_038.0635_tobi96_area3c.pgm
rw-r--r-- 0/1 160015 Feb 23 21:06 1992 area3_small/small_039.1005_tobi97_area3a.pgm
rw-r--r-- 0/1 160015 Feb 23 21:06 1992 area3_small/small_039.1005_tobi97_area3b.pgm
rw-r--r-- 0/1 160015 Feb 23 21:06 1992 area3_small/small_039.1005_tobi97_area3c.pgm
rw-r--r-- 0/1 160015 Feb 23 21:06 1992 area3_small/small_039.2324_tobi98_area3a.pgm
rw-r--r-- 0/1 160015 Feb 23 21:06 1992 area3_small/small_039.2324_tobi98_area3b.pgm
rw-r--r-- 0/1 160015 Feb 23 21:06 1992 area3_small/small_039.2324_tobi98_area3c.pgm
rw-r--r-- 0/1 160015 Feb 23 21:06 1992 area3_small/small_040.1243_tobi99_area3a.pgm
rw-r--r-- 0/1 160015 Feb 23 21:06 1992 area3_small/small_040.1243_tobi99_area3b.pgm
rw-r--r-- 0/1 160015 Feb 23 21:06 1992 area3_small/small_040.1243_tobi99_area3c.pgm
rw-r--r-- 0/1 160015 Feb 23 21:07 1992 area3_small/small_041.0200_tobi100_area3a.pgm
rw-r--r-- 0/1 472000 Feb 23 21:06 1992 area3_mag/mag_038.0635_tobi95_area3a.dat
rw-r--r-- 0/1 472000 Feb 23 21:06 1992 area3_mag/mag_038.0635_tobi95_area3b.dat
rw-r--r-- 0/1 470230 Feb 23 21:06 1992 area3_mag/mag_038.0635_tobi95_area3c.dat
rw-r--r-- 0/1 472000 Feb 23 21:06 1992 area3_mag/mag_038.0635_tobi96_area3a.dat
rw-r--r-- 0/1 472000 Feb 23 21:06 1992 area3_mag/mag_038.0635_tobi96_area3b.dat
rw-r--r-- 0/1 470112 Feb 23 21:06 1992 area3_mag/mag_038.0635_tobi96_area3c.dat
rw-r--r-- 0/1 472000 Feb 23 21:06 1992 area3_mag/mag_039.1005_tobi97_area3a.dat
rw-r--r-- 0/1 472000 Feb 23 21:06 1992 area3_mag/mag_039.1005_tobi97_area3b.dat
rw-r--r-- 0/1 470112 Feb 23 21:06 1992 area3_mag/mag_039.1005_tobi97_area3c.dat
rw-r--r-- 0/1 472000 Feb 23 21:06 1992 area3_mag/mag_039.2324_tobi98_area3a.dat
rw-r--r-- 0/1 472000 Feb 23 21:06 1992 area3_mag/mag_039.2324_tobi98_area3b.dat
rw-r--r-- 0/1 470112 Feb 23 21:06 1992 area3_mag/mag_039.2324_tobi98_area3c.dat
rw-r--r-- 0/1 472000 Feb 23 21:06 1992 area3_mag/mag_040.1243_tobi99_area3a.dat
rw-r--r-- 0/1 472000 Feb 23 21:06 1992 area3_mag/mag_040.1243_tobi99_area3b.dat
rw-r--r-- 0/1 470112 Feb 23 21:06 1992 area3_mag/mag_040.1243_tobi99_area3c.dat
rw-r--r-- 0/1 472000 Feb 23 21:06 1992 area3_mag/mag_041.0200_tobi100_area3a.dat
rw-r--r-- 0/1 622279 Feb 24 19:34 1992 geophys/pbmplus.tar.Z
rw-r--r-- 0/1 29675 Feb 24 20:38 1992 geophys/scott.tar.Z

```
rw-r--r-- 0/1 6156 Feb 24 19:09 1992 geophys/tobi.dat.Z
rw-r--r-- 0/1 358999 Feb 24 20:39 1992 geophys/underway.dat.Z
```

The file pbmplus.tar.Z is a compressed tar archive of the original PGM distribution software. To extract and compile this software the following commands should be executed (if you have problems consult your system administrator or the documentation in the each archive):

```
$ mkdir pbmplus
$ cd pbmplus
$ zcat pbmplus.tar.Z | tar xvf -
$ make
```

The same procedure, with appropriate name substitutions (scott for pbmplus), should be done to compile the programs in scott.tar.Z

The files tobi.dat.Z and underway.dat.Z are compressed ASCII data files of the TOBI logging positions and underway geophysics respectively.

Errata: The last disk of the cruise was improperly processed (disk 113 contain only 7986 records, the processesing command assumed there would be at least 11000). To fix the problem, execute the following commands from the csh:

```
% uncompress area1_big/big_052.1238_113_area1b.pgm.Z
%side2pgm -fix area1_big/big_052.1238_113_area1b.pgm
% pnmscale -width 200 -height 800 area1_big/big_052.1238_113_area1b.pgm |\
    pgmnorm | pnmgamma 2.0 > area1_small/small_052.1238_113_area1.pgm
```

You may now re-compress the file area1_big/big_052.1238_113_area1b.pgm. The file big_052.1238_113_area1c.pgm.Z should not be present on the tape, it contains no information and should be removed.

8.5 Unix manual pages

The following are manual pages of TOBI reading and processing software used on the ship. These man pages are also provided on the TOBI data tape in Unix man page format.

8.5.1 ITD

ITD(2)

NAME

itd - index a magneto-optical disk of TOBI records

SYNOPSIS

itd [-v] [-o offset] [-s rec# | -t time] [-n #rec] [-c 'Clue'] [device]

DESCRIPTION

itd indexes the records generated from the TOBI (Towed Ocean Bottom Instrument) and stored on a magneto optical disk drive.

The output of itd is a ASCII decimal pairing of record byte offsets and binary time (actually printed in decimal of the binary encoding).

A primitive string matching algortihm is used to locate each record, options exist to precisely locate those records that are of interest.

OPTIONS

A non-existent or illegal command line option specification will cause itd to display a usage statement and terminate

-v Turn on verbose output. A message is generated as each record is found, and a brief total record statistic is printed at successful completion.

-o offset To specify a byte offset to begin searching for TOBI records.

-c 'Clue' A 48 character string is present at the beginning of each TOBI record. If you don't know the precise byte offset (and the records are not contiguous), then by specifying this clue the program will locate each record for you. The TOBI record are not always contigu- ous, although they seems to be only one break. If you don't know the header string, use strings(2) to search the disk. See itd(2) for an explanation of indexing. Only six characters are significant

-n number_of_records Specifys the number of TOBI records to find. The TOBI disks we have had access to contain 11985 records, approximately 12 hours of data.

-s starting record Specifys the record number skipped from the first record in the file.

-t starting time The starting record time, in integer format as encoded from ANSI standard C struct tm. See time(2).

SEE ALSO

dd(2), itd(2), ptd(2), tobi(5).

BUGS

Knows absolutely nothing about MS-DOS file systems. In particular, if the TOBI data file on the disk was not allocated in complete records rtd will not be able to process then. When I get off this ship and get some MS-DOS file system documentation I should be able to correct this (I can't off the top of my head remember how the FAT and clustering worked).

AUTHOR

Scott Garland, Boise State University, scg@kanaha.idbsu.edu.

8.5.2 MKIMAGES

MKIMAGES(2)

NAME

mkimages - process TOBI data disk, generate pgm images and magnetics data files

SYNOPSIS

mkimages tobi_id time survey_area [directory]

DESCRIPTION

mkimages is a shell script to process an entire TOBI optical disk, pro- duce both large and small pgm images, and a magnetics data file. Due to the large size of each magnetic disk, mkimages produces three sets of files from a single disk, each representing approximately 4 hours and 4 thousand TOBI records.

For each of the three processing intervals, these files are created:

big_"tobi_id"_"time"_"survey_area".pgm.Z, a large (8000x4000) pgm(5) file of the sidescan sonar data.

small_"tobi_id"_"time"_"survey_area".pgm, a 200x800 scaled version of the "big" file.

mag_"tobi_id"_"time"_"survey_area".dat, the magnetics data file, see rmag(2).

mkimages uses ptd(2) to read the TOBI data disk and pipes the output to side2pgm(2) to pro- duce the pgm(5) files. After each of the three data sets the "big" data file is compressed using compress(2).

This script will most certainly have to be modified for local configura- tions before use on land.

OPTIONS

A non-existent or illegal command line option specification will cause mkimages to display a usage statement and terminate.

tobi_id	Specifys an id string used to identify the data disk number, for example "tobi90".
time	The field is the date and time (ex. 043.1840), represented as a string, when the optical cartridge began recording data.
survey_area	Specifys a string key to the survey area. On CD/65 these values ranged from "area1" to "area4".
directory	An optional directory that the data files will be written into.

USAGE

To process an entire disk ("tobi90"), and create the files in /home/tobi/data, the following command execution:

mkimages tobi90 041.0800 area2 /home/tobi/data

SEE ALSO

dd(2), itd(2), ptd(2), pgm(5), tobi(5). The "Extended Portable Bitmap Toolkit", by Jef Poskanzer (jef@well.sf.ca.us or {apple, ucbvax}!well!jef).

BUGS

This is a simple shell script, which should allow easy modification. Any of which may cause the script to stop working.

Suffers the same byte swapping limitations as that of ptd(2).

AUTHOR

Scott Garland, Boise State University, scg@kanaha.idbsu.edu.

8.5.3 PGM

PGM(2)

NAME

pgm - faster access to large PGM files

SYNOPSIS

rtd x y width height file

DESCRIPTION

rtd is a tiny program that uses fseek(2s) to access image data in a PGM file. It's especially suited for access to very large files that are not practical to be contained in primary memory.

OPTIONS

A non-existent or illegal command line option specification will cause pgm to display a usage statement and terminate.

x y width height Specifys the dimensions of the subimage that is to be cut from a larger image.

file This is a PGM(5) image file.

SEE ALSO

dd(2), itd(2), ptd(2), pgm(5).

The "Extended Portable Bitmap Toolkit", by Jef Poskanzer (jef@well.sf.ca.us or {apple, ucb-vax}!well!jef).

BUGS

This is a very simple program, therefore it probably has lot's of them.

AUTHOR

Scott Garland, Boise State University, scg@kanaha.idbsu.edu.

8.5.4 PTD

PTD(1)

NAME

ptd - read and process a magneto-optical disk of TOBI records

SYNOPSIS

ptd [-v] [-o offset] [-s rec# | -t time] [-n #rec] [-m file] [-c 'Clue'] [device]

DESCRIPTION

ptd reads each record generated from the TOBI (Towed Ocean Bottom Instrument) on a SONY magneto optical disk drive, and performs a slant range correction on the port and starboard data and outputs the combined port and starboard data as a binary record of 8000 16 bit integers.

TOBI magneto optical disks often contain more than 11,000 records, thus it was necessary to perform some minimal processing to extract those data items that were requested, without having to copy the entire TOBI data file to local disk space before processing, or reprocess the mag- netic disk multiple times.

The TOBI processing system writes records to a single file on IBM/PC under a MS-DOS file system. Since a single file is used and data is con- tinually recorded, one can extract the complete TOBI record without hav- ing to deal with the MS-DOS file system on the disk.

A primitive string matching algorithm is used to locate each record, other options exist to precisely locate those records that are of interest.

This program may be used on any TOBI record file, therefore one may copy the data from the magnetic disk, using rtd(1), to a UNIX file and then run ptd on the UNIX file.

OPTIONS

A non-existent or illegal command line option specification will cause ptd to display a usage statement and terminate.

-v Turn on verbose output. A message is generated as each record is processed, and a brief total record statistic is printed at suc- cessful completion.

-o offset To specify a byte offset to begin searching, or processing, of TOBI records.

-c 'Clue' A 48 character string is present at the beginning of each TOBI record. If you don't know the precise byte offset (and the records are not contiguous), then by specifying this clue the program will locate each record for you. The TOBI record are not always contigu- ous, although they seems to be only one break. If you don't know the header string, use strings(2) to search the disk. See itd(2) for an explanation of indexing. The length of this string is limited to 6 characters, a simple code modification would be required to increase this number. This option is not necessary if the source data file has already been read from the disk.

-n number_of_records The number of TOBI records to process. The TOBI disks we have had access to, contain approximately 12000 records for about 12 hours of data.

-s starting record Specifys the number of records skipped from the first record in the file.

-t starting time The starting record time, in integer format as encoded some what like ANSI standard C struct tm; however, the year is offset from 1980, which is different from ctime(3) that is offset from 1900.

-m file The name of the file to which the magnetic data should be written, if this option is omitted no magnetic data file is created. The format for this file is a binary sequential flat file using the following record structure:

```
struct magnetic {
        short           time;
        short           date;
        short           magx[NSAMPLES];
        short           magy[NSAMPLES];
        short           magz[NSAMPLES];
        short           roll[NSAMPLES];
        short           pitch[NSAMPLES];
        short           compass[NSAMPLES];
        short           press[NSAMPLES];
        short           altitude;
        };
```

Where NSAMPLES is 8.

RECORD FORMAT

The record format of the data recorded by TOBI is represented below, where NSAMPLES is 8, NSONAR is 4000, and a record is generated every 4 seconds. The fields lonminutes and latminutes are written as floats on the IBM PS/2 that is the primary data recorder; however, because of alignment restrictions on MIPS RISC I've changed them to 4 byte arrays. The latitude and longitude fields are approximate positions at the start of recording and don't change during the recording of a single file.

```
struct tobi {
        char header[48];
        short version;
        short time;
        short date;
        short londegrees;
        char lonminutes[4];
        short latdegrees;
        char lonminutes[4];
        short           magx[NSAMPLES];
        short           magy[NSAMPLES];
        short           magz[NSAMPLES];
        short           roll[NSAMPLES];
        short           pitch[NSAMPLES];
        short           emlog_fa[NSAMPLES];
        short           emlog_ps[NSAMPLES];
        short           compass[NSAMPLES];
        short           press[NSAMPLES];
        short           altitude;
        short           wapath;
        short           temp[NSAMPLES];
        short           trans[NSAMPLES];
        char            padding[330];
        short           port_sonar[NSONAR];
        short           starboard_sonar[NSONAR];
        short           profile[NSONAR];
        };
```

It should be noted that some of the fields, in particular the altitude, may be modified by the operator during the TOBI run. We have occasion- ally encountered accidental data entry mistakes that were corrected dur- ing the recording process (for example, the date changed abruptly after a couple of hundred records).

USAGE

SEE ALSO

dd(2), itd(2), ptd(2), tobi(5).

BUGS

Knows absolutely nothing about MS-DOS file systems. In particular, if the TOBI data file on the disk was not allocated in complete records ptd will not be able to process then. When I get off this ship and get some MS-DOS file system documentation I should be able to correct this (I can't off the top of my head remember how the FAT and clustering worked. Plus, since these disks have such a large capacity it appears there are multiple volumes on the disk).

No byte swapping occurs, this is not a problem on the DECstation, how- ever, for the SPARC based architectures the output data will have to be swapped (obviously, this doesn't apply to the character header, but the header isn't of much use anyway). See the dd(2) command for easy way to swap binary data files.

AUTHOR

Scott Garland, Boise State University, scg@kanaha.idbsu.edu.

Chris Flewellen and Peter Slootweg, both from NERC's Institute of Oceanographic Sciences Deacon Laboratory, wrote the slant range correction algorithm.

8.5.5 RMAG

RMAG(1)

NAME

rmag - read and print data from TOBI magnetics files.

SYNOPSIS

rmag [-v] [-avg] [-swap] [-DTXYZMRICPAW] [files...]

DESCRIPTION

rmag reads the magnetics (and other information) in a magnetics data file produced by ptd(2), formats the data into ASCII and writes the requested fields to the standard output. Run time options exist to allow the user to average, swap and compute simple values from the data file.

OPTIONS

A non-existent or illegal command line option specification will cause rmag to display a usage statement and terminate.

-v Turn on verbose output.

-swap Swaps the bytes in each record before processing. The magnetics file data byte ordering

is that of a IBM/PC and DECstation. If this program is being used on a SPARC based Sun the user should specify this option.

-avg Averages the data fields over the 8 samples provided by TOBI. A TOBI record is generated every 4 seconds, and for certain fields each 4 second record contains 8 samples. This option will perform a simple average off the 8 samples for the following data fields: magx, magy, magz, roll, pitch compass.

-DTXYZMRICPAW A key specifying the indicated data that the user wishes to be printed. Each letter indicates an individual data field or combi- nation of data fields. The following lists each key letter and the corresponding data field:

F - Fixed date and time A composite time and date calculation (yday + (hr + ((min + sec/60)/60)/24).

T - Time Time of each record printed as "hr min sec" all as integer fields

D - Date Date of each record printed as number of days since January 1, 1992. Printed as an integer field.

X - Magnetic X X coordinate of the magnetics.

Y - Magnetic Y

Y coordinate of the magnetics.

Z - Magnetic Z Z coordinate of the magnetics. This field is multiplied by 1.5.

M - Total magnetic field Calculated as follows: sqrt(magx**2 + magy**2 + magz**2).

R - Roll roll.

P - Picth pitch.

C - Compass compass.

P - Pressure pressure.

A - Altitude altitude of the TOBI.

W - Water Depth Calculated using: depth = ((pressure)/(1.028)) + altitude.

USAGE

To print the X,Y,Z coordinates of the magnetic data and the total magnetic field one would specify

rmag -avg -XYZM datafile > magnetic.dat

SEE ALSO

dd(2), ptd(2), tobi(5).

BUGS

No byte swapping occurs, this is not a problem on the DECstation, how- ever, for the SPARC based architectures the data will have to be swapped. See the dd(2) command for easy way to swap binary data files.

Each field is printed on the standard output in a predefined order, it should print the fields using the order specified in the key.

AUTHOR

Scott Garland, Boise State University, scg@kanaha.idbsu.edu.

With many helpful suggestions from Jian Lin, Woods Hole Oceanographic Insitution.

8.5.6 RTD

RTD(2)

NAME

rtd - read a magneto-optical disk of TOBI records

SYNOPSIS

rtd [-v] [-o offset] [-s rec# | -t time] [-n #rec] [-m file] [-c 'Clue'] [device]

DESCRIPTION

rtd finds and prints the records generated from the TOBI (Towed Ocean Bottom Instrument), that are stored in a single file using a MS/DOS file system on a magneto optical disk drive.

A primitive string matching algorithm is used to locate each record, options exist to precisely locate those records that are of interest.

OPTIONS

A non-existent or illegal command line option specification will cause rtd to display a usage statement and terminate

-v Turn on verbose output. A message is generated as each record is processed, and

a brief total record statistic is printed at suc- cessful completion.

-o offset To specify a byte offset to begin searching, or processing, of TOBI records.

-c 'Clue' A 48 character string is present at the beginning of each TOBI record. If you don't know the precise byte offset (and the records are not contiguous), then by specifying this clue the program will locate each record for you. The TOBI record are not always contigu- ous, although they seems to be only one break. If you don't know the header string, use strings(2) to search the disk. See itd(2) for an explanation of indexing. Only six characters are signifi- cant.

-n number_of_records Specifys the number of TOBI records to process. The TOBI disks we have had access to contain 11985 records, approximately 12 hours of data.

-s starting record Specifys the record number skipped from the first record in the file.

-t starting time The starting record time, in integer format as encoded from ANSI standard C struct tm. See time(2).

RECORD FORMAT

The record format of the data recorded by TOBI is represented below, where NSAMPLES is 8, NSONAR is 4000, and a record is generated every 4 seconds. The fields lonminutes and latminutes are written as floats on the IBM/PC that is the primary data recorded; however, because of align- ment restrictions on MIPS RISC I've changed them to 4 byte arrays. The latitude and longitude fields are approximate positions at the start of recording and don't change during the recording of a single file.

```
struct tobi {
        char            header[48];
        short           version;
        short           time;
        short           ate;
        short           londegrees;
        char            lonminutes[4];
        short           latdegrees;
        char            lonminutes[4];
        short           magx[NSAMPLES];
        short           magy[NSAMPLES];
        short           magz[NSAMPLES];
        short           roll[NSAMPLES];
        short           pitch[NSAMPLES];
        short           emlog_fa[NSAMPLES];
        short           emlog_ps[NSAMPLES];
        short           compass[NSAMPLES];
        short           press[NSAMPLES];
```

```
short       altitude;
short       wapath;
short       temp[NSAMPLES];
short       trans[NSAMPLES];
char        padding[330];
short       port_sonar[NSONAR];
short       starboard_sonar[NSONAR];
short       profile[NSONAR];
};
```

It should be noted that some of the fields, in particular the altitude, may be modified by the operator during the TOBI run. We have occasion- ally encountered accidental data entry mistakes that were corrected dur- ing the recording process (for example, the date changed abruptly after a couple of hundred records).

SEE ALSO

dd(2), itd(2), ptd(2).

BUGS

Knows absolutely nothing about MS-DOS file systems. In particular, if the TOBI data file on the disk was not allocated in complete records rtd will not be able to process then. When I get off this ship and get some MS-DOS file system documentation I should be able to correct this (I can't off the top of my head remember how the FAT and clustering worked).

No byte swapping occurs, this is not a problem on the DECstation, how- ever, for the SPARC based architectures the data will have to be swapped. See the dd(2) command for easy way to swap binary data files.

AUTHOR

Scott Garland, Boise State University, scg@kanaha.idbsu.edu.

8.5.7 SIDE2PGM

SIDE2PGM(2)

NAME

side2pgm - convert TOBI side-scan data to PGM image format

SYNOPSIS

side2pgm [-v] [-fix file | [-swap] [-h height] [file]]

DESCRIPTION

side2pgm converts TOBI side scan sonar data to PGM (portable graymap) image format. Since the images generated by side2pgm are consistently greater than 30 megabytes, side2pgm can rescan the PGM file and correct the file header which could have been left incomplete when side2pgm was reading from a pipe.

The TOBI port and starboard data is scaled to 8 bits (input values are signed 16 bit quantities, with 12 bits significant) by simply dividing by 8.

A P5, binary 8 bit, PGM image format is produced. If the local installa- tion of PBMPlus was compiled using the BIGBITS option, then a P5 12 bit image could be output, and the 4 bit loss could be avoided. This possi- bility is ignored in this implementation.

OPTIONS

A non-existent or illegal command line option specification will cause side2pgm to display a usage statement and terminate.

-v	Turn on verbose output. A message is generated as each record is processed, and a brief total record statistic is printed at suc- cessful completion.
-fix file	side2pgm will open the file, calculate the height of the image, and rewrite the header. The PGM header must have been written using side2pgm. This option is provided because side2pgm does not always know the height of the image until after it has processed the file, and when reading from a pipe, fseek'ing to the beginning is prohi- bited.
-swap	Swap the TOBI data before conversion. The TOBI data is generated using IBM/PC byte ordering.
-h height	If the height (number of records) is known prior to running side2pgm, it will allow the program to generate a correct PGM header. When using this option, side2pgm will only process height records, regardless of how many are avail- able.
file	The TOBI input file. Records of length 8000, 2 byte shorts, with 4000 values per port and starboard side.

USAGE

To convert from a data file, input.dat, of 4000 records:

side2pgm -height 4000 input.dat > output.pgm

To convert a data input from the standard input, and then fix the header, the following two executions are required:

ptd tobi.dat | side2pgm > output.pgm

side2pgm -fix output.pgm

SEE ALSO

dd(2), itd(2), ptd(2), pgm(5), tobi(5). The "Extended Portable Bitmap Toolkit", by Jef Poskanzer (jef@well.sf.ca.us or {apple, ucbvax}!well!jef).

BUGS

The algorithm (dividing by 8) for conversion from 12 bits to 8, demon- strates a particularly pathetic effort. Thus, the output from side2pgm is frequently corrected using a PBMPLUS pipeline "pgmnorm | pnmgamma 2.0".

No byte swapping occurs, this is not a problem on the DECstation, how- ever, for the SPARC based architectures the data will have to be swapped. See the dd(2) command for easy way to swap binary data files.

AUTHOR

Scott Garland, Boise State University, scg@kanaha.idbsu.edu.

8.5.8 TOBI

TOBI(5)

NAME

TOBI - Towed Ocean Bottom Instrument data recording format

DESCRIPTION

TOBI magneto optical disks often contain more than 11,000 records, gen- erated at 4 second intervals. These records are stored in a single file using an MS/DOS file system on and IBM PS/2.

Since most of the computer based analysis and image processing occur on UNIX based workstations, it was necessary to be able to directly read the magneto optical disks. However, we had only limited recall of MS-DOS file system structures, so a more direct approach to reading the UNIX device was applied.

RECORD FORMAT

The record format of the data recorded by TOBI is represented below, where NSAMPLES is 8, NSONAR is 4000, and a record is generated every 4 seconds. The fields lonminutes and latminutes are written as floats on the IBM/PC that is the primary data recorded; however, because of align- ment restrictions on MIPS RISC I've changed them to 4 byte arrarys. The latitude and longitude fields are approximate positions at the start of recording and don't change during the recording of a single file.

```
struct tobi {
        char                    header[48];
```

```
short       version;
short       time;
short       date;
short       londegrees;
char        lonminutes[4];
short       latdegrees;
char        latminutes[4];
short       magx[NSAMPLES];
short       magy[NSAMPLES];
short       magz[NSAMPLES];
short       roll[NSAMPLES];
short       pitch[NSAMPLES];
short       emlog_fa[NSAMPLES];
short       emlog_ps[NSAMPLES];
short       compass[NSAMPLES];
short       press[NSAMPLES];
short       altitude;
short       wapath;
short       temp[NSAMPLES];
short       trans[NSAMPLES];
char        padding[330];
short       port_sonar[NSONAR];
short       starboard_sonar[NSONAR];
short       profile[NSONAR]; };
```

It should be noted that some of the fields, in particular the altitude, may be modified by the operator during the TOBI run. We have occasion- ally encountered accidental data entry mistakes that were corrected dur- ing the recording process (for example, the date changed abruptly after a couple of hundred records).

For "short" data type in the above 'C' structure is a 16 bit integer, or FORTRAN fans an "integer*2".

FIELD DESCRIPTIONS

header	A 48 character character string, entered by the TOBI operators. On CD/65 the header was "Charles Darwin", another that I've seen is "Maurice Ewing".
version	A version number of the reporting software.
time	An unsigned bit encoding of the time that the record was recorded. This 16 bit field is encoded as follows:
date	An unsigned bit encoding of the data that the record was recorded. This 16 bit field is encoded as follows:
londegrees	This is the approximate longitude, in degrees, at the start of the TOBI recording. Don't use.

lonminutes This is the approximate longitude, in minutes, at the start of the TOBI recording. Don't use.

latdegrees This is the approximate latitude, in degrees, at the start of the TOBI recording. Don't use.

latminutes This is the approximate latitude, in minutes, at the start of the TOBI recording. Don't use.

magx Magnetometer X coordinate. Trixial fluxgate; 10nT resolution. Eight samples every four seconds. This field should be multiplied by 10.0.

magy Magnetometer Y coordinate. Eight samples every four seconds. This field should be multiplied by 10.0.

magz Magnetometer Z coordinate. This value is always multiplied by 15.0. Eight samples every four seconds.

roll Roll on the TOBI, accuracy 0.15 degrees. Eight samples every 4 seconds.

pitch Pitch on the TOBI, accuracy 0.15 degrees. Eight samples every 4 seconds.

emlog_fa Electro-magnetic log fore/aft velocity. Eight samples every 4 seconds.

emlog_ps Electro-magnetic log port/starboard velocity. Eight samples every 4 seconds.

compass Compass heading, accuracy 0.35 degrees. Eight samples every 4 seconds.

press Pressure.

altitude TOBI altitude in meters.

profile_path Profiler path, in milli-seconds.

temp Temperature, cccuracy 0.01 degrees.

trans Transmissometer.

padding 330 bytes of padding. I think this is where the scatterometer data will eventually be placed.

port_sonar Data returned from the port sidescan sonar, 4000 samples of 16 bi, shorts (12 significant). Swath width is 6 km with resolution of 2m.

starboard_sonar Data returned from the starboard sidescan sonar, 4000 samples of 16 bit shorts (12 significant). Swath width is 6 km with resolution of 2m.

profile Data returned from the profiler, 4000 samples of 16 bit shorts. Beam width 15 degrees, up to 50 meters of penetration.

DISK FORMAT

The TOBI records are stored in a MS-DOS file named TOBI.DAT (at least it was on every disk we received on CD/65).

I barely recall MS-DOS filesystem data structures, but what I surmised from the MO disks I looked at was the following: The MO disks contain a "few" volume headers; followed by what looks like the file allocation table (FAT); immediately after was the first directory entry, from which you should be able to see the file name the TOBI records were stored.

So much for MS-DOS filesystems, within the next couple of hundred bytes you should see the TOBI record header field (on CD/65 this was "Charles Darwin"). The first character of this header is the first byte of the TOBI record. Since the file was stored sequentially, nearly all the records follow each other; however, at what I think was a volume boun- dary, there was an approximatly 100 byte gap before the next record.

This gap necessitates the record hunting scheme's employed in the TOBI processing programs, a match must occur on the TOBI record header before a record can be considered found.

SEE ALSO

dd(2), itd(2), ptd(2), rmag(2), rtd(2). "TOBI A New Development in Deep-Ocean Geological Mapping", Dr. Douglas G. Masson and Nick W. Mil- lard, Natural Envirnment Research Council, Insitute of Oceanographic Sciences Deacon Laboratory.

IX. References

Jacobs, et al., 1959, "Physics and Geology", McGraw Hill.

Kuo, B. Y. and Forsythe, D. W., 1989, Gravity anomalies of the ridge-transform system in the south Atlantic between 31 and 34.5 S: Upwelling centers and variations in crustal thickness, Mar. Geophys. Res., 10, 205-232.

Lin, J., G. M. Purdy, H. Schouten, J.-C. Sempere and C. Zervas, 1990, Evidence from gravity data for focussed magmatic accretion along the Mid-Atlantic Ridge, Nature, v. 344, 627-632.

Lin, J., and E. A. Bergman, 1990, Rift grabens, seismicity, and volcanic segmentation of the Mid-Atlantic Ridge: Kane to Atlantis Fracture Zones, EOS Trans. AGU, 71, 1572.

Parker, R. L., 1972, The rapid calcuation of potential anomalies, Geophys. J. R. Astro. Soc., 31, 447-455.

Purdy, et al., 1991

Sempere, J.-C.., G.M. Purdy, and H. Schouten, 1990, Segmentation of the Mid-Atlantic Ridge Between 24° and 30° 40' N, Nature, 344, 427-429.

Smith and Cann, 1990

Smith and Cann 1992

Tucholke, 1992

Worzel, J.L., 1959, J. Geophys. Res., v. 64, p. 1299-1315